GENETIC ENGINEERING OF *Pseudomonas fluorescens* FOR ENHANCED CITRIC ACID SECRETON

A THESIS SUBMITTED TO

THE MAHARAJA SAYAJIRAO UNIVERSITY OF BARODA

FOR THE DEGREE OF

DOCTOR OF PHILOSOPHY IN BIOCHEMISTRY

BY

HEMANTA ADHIKARY

DEPARTMENT OF BIOCHEMISTRY

FACULTY OF SCIENCE

THE MAHARAJA SAYAJIRAO UNIVERSITY OF BARODA

VADODARA – 390 002, GUJARAT, INDIA

SEPTEMBER 2012

STATEMENT UNDER O. Ph.D. 8/ (iii) OF

THE M. S. UNIVERSITY OF BARODA, VADODARA

This is to certify that the work presented in this thesis is original and was obtained from the studies undertaken by me under the supervision of **Dr. G. Naresh Kumar.**

Vadodara Hemanta Adhikary

Date: Candidate

This is to certify that the work presented in the form of a thesis in fulfillment of the requirement for the award of the Ph. D. degree of The M. S. University of Baroda by **Mr. Hemanta Adhikary** is his original work. The entire research work and the thesis have been built up under my supervision.

Dr. G. Naresh Kumar
Research Supervisor
Department of Biochemistry
Faculty of Science
The M. S. University of Baroda
Vadodara- 390 002.

Dedicated to my beloved Maa and Deuta....

ACKNOWLEDGEMENTS

Submission of my thesis puts a cessation to a struggling phase of an altogether different learning process and rememinds me about the beautiful quote "Perseverance is the key to success".When my journey began I had never imagined that I would be able to reach the stage where I am at present. In my long quest of some scientific answers I was immensely been supported by many people in their unique ways for which this became a lifetime experience. When I sit back and reminisce about those people I would like to extend my gratefulness towards them and acknowledge them from the bottom of my heart.

First of all I would like to extend my gratitude to my Research Guide Prof. G. Naresh Kumar. From the very inception I am indebted towards him as he undertook me in his wing when I was a callow and was struggling hard to earn a pat of appreciation, self confidence and encouragement on my back when I was in real need. He bestowed immense faith in me which strengthened my confidence and boosted up my morale. I was smitten by his candor and candidness and appreciated the freedom he gave me to work in the Lab as I want. During our various discussions his cognizance of scientific insight made me bow with respect and made me feel very proud that I got an opportunity to work under such a wonderful personality.Few people in the world would be lucky enough to work with sucsh an excellent guide as well a good human being. Thank you very much Sir.

I would like to express my deep gratitude to Prof. Sarita Gupta, for being a constant source of encouragement.Time to time healthy criticism and suggestions of yours really helped making me intellectually stronger. Also thank you for allowing me to use the lab facilities whenever I required.

I am sincerely grateful to Dr.G Archana, Dept of Microbiology and biotechnology Centre for her timely guidance and excellent suggestions at annual seminars which helped me a lot in improving my experiments. Thanks a lot for being so supportive as and when required. Above all, I will always remember your mouth watering dishes during group meet at home. Than you mam for being so caring.

My heartfelt gratitude towards Prof. Rasheedunnisa Begum for her constant encouragement and support. Your extensive comments and suggestions during annual seminars really helped me a lot to improve myself.

Dr. S. Acharya needs a special mention for his instant motivation and healthy discussions everywhere in the department as well as in tea sessions. I also got the opportunity to interact with him during my teaching assistantship in the department. Thank you Sir for guiding me whenever I approached to you.

I would like to thank Dr. C. Ratnaprabha for her support and allowing me to use her lab facilities. Thanks to Dr. Jayshree Pohnerkar who were always silent but a constant source of encouragement for me. Thanks to Dr. Puspa Robin for her support all the time.

Dr. LaxmiPriya and Dr. Devesh Suthar has been a special figure during my teaching assistantship in the department through which I got an opportunity to interect with them and come closure . I will always

admire the punctuality and passion of Dr. LaxmiPriya mam towards for any kind of work.There are a lot to learn from both of you. Thank you mam and thank you, Sir.
Thanks to Dr. Mrinalini Nair, Department of microbiology and Biotechnology Centre for her initial training. I also extend my deep gratitude to Prof. Anjana Desai for patiently hearing my seminars and for her expert comments that really helped.

I would also like to show appreciation to the the Office Staff including Pethe Sir, Akshitaben, Rameshbhai Shaileshbhai, Manishbhai, Balwant bhai, Sandeep and all other staff members for their standing help and guidance in all the official matters. Thank you so much Bhartiben, for settling the project accounts smoothly and ensuring timely payment of the fellowship and also for your sisterly care all the time. Thanks to Anilbhai for helping me out with lab maintenance and make it an organized place to work in. I specially thank Mr. Jeetendra Dave, Mr. Ansul and all the corporate people for patiently listening to our sudden but urgent demands for chemicals/fine-chemicals and trying their levels best to deliver the order in time.

I sincerely acknowledge the Department of Biotechnology (DBT), Govt of India for the JRF and SRF.

I wish to express my warm and sincere thanks to Dr. Sanjay Jha, Asst prof. Navsari Agricultural University (NAU), without whome, I definitely would not have completed this tough journey and left bag and baggage for home. Platinum confidence glowing anytime in his face really gave energy to work hard. Thanks a lot Sir, for allowing me to use the HPLC and Green house facility without which my last objective would not have completed by now. Thanks to Dr. Sumant Jha and Dr. M.K,Mahatma (NAU) for their extreme guidance during the experiments. Thanks to Ms Raina, Mr. Vanraj for their support whenever I required.

I deeply acknowledge Prof. H. Duckworth, university of Manitoba, Canada for providing me the NADH insensitive plasmids, also thanks to Prof. Lynda Thomashow and Prof Mark Sylvi, USA, for providing me Pseudomas strains.

Well, can not wait more to write about my lab, my second home.It was a real pleasure and lifetime learning experience to work with so many people with different individual identity and interect with them, the maxmum time in a day.I was lucky enough to have wonderful seniors in the lab including Dr. Vikash Sharma, Dr. Gopith Shah, Dr. Divya Patel, Dr. Jisha Elias, Dr. Adity Buch. I was always a follower of Jisha mam and Aditi mam whose dedication towards their work inspired me a lot. Would like to extend my heartfelt thanks to our lab Alumni Dr. Karunakaran (KK), Dr. Prasant Kunjariya with whome I was in constant touch. It was a pleasure having seniors cum colleague like Dr. Prasant Kumar, Mr Chanchal Kumar and Mr. Jitendra wagh. Thanks for all your support without which this journey would have been really difficult. Thaks to Ms Kavita Yadav (battchi) for her help and support during my stay in the lab. The Lab is really blessed with juniors like Sumit, Asish, Archana Ujwal and neonate Roma. Thanks to all for your support and makimg M.M.B.L. a workable place. I wish you all the best and hope you all take M.M.B.L to the top and sky should be the limit.

I would like to express heartfelt thanks all the MSc. dissertation students who worked with me including Ketan, kedar, Silvia, Paulomi, Hitharth and Ajeeta.Thanks to Kisu, Riddhi, Sneha,Sriram, Ayush,

Deepak, Jyoti for your contribution to the lab and making it a healthy place to work . Thanks to Sonika and Anad for constant inspiration and support all the time.

This mammoth journey would not have completed without the support of my comrades, friends and Research colleagues. It was a pleasure having seniors like Dr. Sajil M, Dr, Hemandra V., Dr. Keyur D., Dr. Maulik Thakkar, Dr. Hiren Modi , Dr. Jyotika Rajawat, Dr. Heena Mir,Dr. Iqbal V., Dr. Vijay M., Dr. Shirayu Pandya ,Dr Niraj Bhatt, Dr Pradeep Mishra, Dr. Prakash Pillai and Dr. Sanket Soni who guided all the time and encouraged for systematic research that helped a lot. Thanks for sharing the most fun-filled moments with us which will be always cherised.

My buddies Mrinal (Bhai), Nidheech (Betu) and Rusikesh (Chotu) been a backbond to me.They were always available to me in difficult times and provided immense support, whether its about requirement of chemicals, instruments, experimental planning, late night stay in the lab and been a constant support. You guys rock and simply awesome.

Thanks to Naresh (Baba) and Mitesh for their constant help and support all the time.Heartfelt thanks to Mrs. Purna and 'The Swapnalis' , I find no words to thank both of you for moral support and specially Swapnali for her grand salute throughout. Thanks to Tusar, Akhilesh, Anubha, Muskan,Sucheta, Krisma, Radha, Abhay, Komal, Ankita varsha, Bhrinda, Shoaib for being supportive all the time. Special thanks to Ankita for her constant help and support all the time .I am thankful to the beginners in the department for making the department a perect place to work.

Friends like Prasant, Jagat and Chandraprakash made the journey easy going. Thanks Prasant for guidance and help all the time. Thanks Jagat for supporting me and being with me like a shadow in difficult moments. Thanks to Chandraprakash (Guruji) for his support and guidance.

My heartfelt thanks Mahima, Soshina and Santosh. Words become few to express thanks to u guys.
Thanks to Dr. Bishnu Prasad and Mr. Harshuk Tank for constantly encouraging me and givin me guidance whenever I approach. Thanks to Dr. Arif Khan, Dr. Kuldeep patel, Dr. marpe Bam, Dr. Sandeep Godowana, Priya Mam, Ruchi mam, Murli Sir, Dr. Sumant, Subramaniyam(Subbu), Anup, .Sohail bhai,Vikash, Gaurav, Akhil, Abhik, Akhilesh, Hasim for time to time support and encouragement. Thanks to Dr. Ansarullah for his support.

Thanks to Dr. Ananta Madhab Barua, Assoc. prof. Assam Agricultural University and family for constantly supporting me to go ahead and do well. Thanks to Manisha Chodhury, Deepali Dutta, Nabajyoti Deka for their constant encouragement.Thanks to all my teachers of Tezpur University Assam who gave me a real trining during MSc. and made me capable to reach up to here. Thanks to Digants baishya, Ameet Verma, Ravi, Yash, Amit, Ranjan, Mayuri, Aurelia, Rakesh Abhishek all were my classmate during MSc. Thank you all for constant encouragement till now.

My sincere thanks to Dr. U. M. upadhyai, Sigma Institute of Pharmacy, for providing financial support by appointing me as a visiting lecturer during my PhD tenure. Thank you so much Sir.

Thanks to Dr. Sudhir K.Rai for sending me research papers any time I ask for. Thanks to Aunty for serving me tiffin and keeping me healthy.

Sincere thanks to Basu bhai and Kirit bhai faculty of Science for the help in clearing bills and office related matters. Special thanks to Milin bhai, Head office, M.S. University for his tremendous help all the time.

My heartfelt thank also goes to Prof. J. Y. Masson, Quebec, Canada for listening to my presentation and critically analyzing my work during his visit to the department.

Gives me immense pleasure to introduce Dr. Sunil Ch. Sharma, Dr. Krishna Sharma, Mr. Alakesh Parasor (Papu da) and Ms. Anindita Parasor (My fiancé) which have been a incessent source of support and encouragement Thanks to them.You all are a part of my success .

Above all, I owe all my success to my family: my parents, Dada and Bou, Baideu-Bhindeu and nephew Ayan. They have constantly been a source of inspirations no matter whatever situation befall me they stood behind me to support and encourage me. The word "Thank You" would be too small to define their hard work and sacrifices to see me in this state as of today. Seeing their zeal I could keep on going in my Research life and complete the journey successfully.

And the list goes on... I apolozise to all whose name I missed here but that does not mean ignorance but unintentional. Hence, thanks to each and everyone.

Last but not the least I would like to thank Almighty God for giving me the strength to stand up to all the expectations of my parents and teachers

Hemanta Adhikary

ABBREVIATIONS

ATCC	American type culture collection
X-Gal	5-Bromo-4-chloro-3-indolyl-β-D galactopyranoside
IPTG	Isopropyl β-D thio galactopyranoside
LB	Luria broth
SDS	Sodium Dodecyl Sulphate
APS	Ammonium persulfate
Ori	Origin of replication
WT	Wild type
PPC	Phosphoenolpyruvate carboxylase
CS	Citrate synthase
PYC	Pyruvate carboxylase
ICL	Isocitrate lyase
ICDH	Isocitrate dehydrogenase
GDH	Glucose dehydrogenase
G-6-PDH	Glucose-6-phosphate dehydrogenase
GADH	Gluconate dehydrogenase
PPC	Phosphoenolpyruvate carboxykinase
PYC	Pyruvate carboxylase
PYK	Pyruvate kinase
ME	Malic enzyme
MDH	Malate dehydrogenase
LDH	Lactate dehydrogenase
POX	Gluaicol peroxidase
APX	Ascorbate peroxidase
SOD	Superoxide dismutase

NR	Nitrate reductase
PDH	Pyruvate dehydrogenase
PFK	Phosphofructokinase
PTS	Phosphotransferase system
GFP	Green fluorescent protein
PQQ	Pyrolloquinoline quinone
G-6-P	Glucose-6-phosphate
6-PG	6-phosphogluconate
PEP	Phosphoenolpyruvate
OAA	Oxaloacetate
ATP	Adenosine triphosphate
DNA	Deoxyribonucleic acid
cAMP	Cyclic adenosine monophosphate
NADH	Nicotinamide adenine dinucleotide (reduced)
NADP(H)	Nicotinamide adenine dinucleotide phosphate (reduced)
DTT	1, 4-Dithiothreitol
EMP	Embden–Meyerhof–Parnas pathway
TCA	Tricarboxylic acid
PPP	Pentose phosphate pathway
ETC	Electron transport chain
ED	Entner-Doudoroff
PSM	Phosphate solubilizing microorganisms
P/Pi	Phosphate / inorganic phosphate
HPLC	High performance liquid chromatography
BLAST	Basic local alignment search tool
PCR	Polymerase Chain Reaction
PAGE	Polyacrylamide Gel Electrophoresis
EDTA	Ethylene diamine tetra acetic acid

Tris	Tris (hydroxymethyl) aminomethane buffer
CTAB	Cetyl trimethylammonium bromide
PGPR	Plant Growth Promoting Rhizobacteria
RE	Restriction Endonuclease
nm	Nanometer
ng	Nanogram
kb	kilobase (s)
bp	base pair (s)
kDa	Kilodalton
rpm	Revolutions per minute
OD	Optical Density
DCW	Dry cell weight
mM/M	Millimolar/Molar
µl/ml	Microlitres/millilitres
Amp	Ampicillin
Km	Kanamycin
Str	Streptomycin
Tmp	Trimethoprim

Note: The full forms of several rarely used abbreviations have been described within the text.

CONTENTS

CONTENT OF TABLES

CONTENT OF FIGURES

INTRODUCTION AND REVIEW OF LITERATURE

CHAPTER 1

1 INTRODUCTION

"*Recall the face of the poorest and the weakest man whom you have seen, and ask yourself, If the steps you contemplate are going to be of any use to him. Will he gain anything by it? Will it restore to him control over his own life and destiny?"*

Mahatma Gandhi

1.1 Metabolic engineering

Metabolic engineering can be defined as purposeful modification of cellular metabolism using recombinant DNA and other molecular biological techniques (Bailey 1991; Lee et al. 2009). Metabolic engineering considers metabolic and cellular system as an entirety and accordingly allows manipulation of the system with consideration of the efficiency of overall bioprocess, which distinguishes itself from simple genetic engineering (Stephanopoulos et al., 1998; Lee, S.Y. et al., 1999). Furthermore, metabolic engineering is advantageous in several aspects, compared to simple genetic engineering or random mutagenesis, since it allows defined and directed engineering of the cell, thus avoiding unnecessary changes to the cell and allowing further engineering if necessary.

1.1.1 Modern metabolic engineering: converting microbes to a chemical factory

Development of recombinant DNA technology in the post genomic era has accumulated staggering volume of gene, protein and metabolite data. The cost of oligonucleotide synthesis has exponentially declined and more precise techniques for studying cellular metabolism have been developed. Empowered by these developments the focus of metabolic engineering research has gradually been shifted from perturbing individual pathways to manipulating the entire cell itself giving rise to the concept of system metabolic engineering converting microbes to a chemical factory (Yadav et al., 2012).

Microbes have naturally evolved enzymes and pathways that can convert biomass into hundreds of unique chemical structures, a property that can be effectively exploited for

their engineering into Microbial Chemical Factories (MCFs). The first step in engineering novel or natural pathways for MCFs is to identify potential natural cell metabolites or biomass derived feedstock's that can serve as starting materials and the series of biochemical reactions required to convert these into the desired product. Martin et al., (2009) have reviewed some of the computational tools available for identifying and selecting from the multiple possible pathways connecting different starting materials to a product of interest. Once a pathway is selected, appropriate natural enzymes expected to catalyze pathway reactions need to be selected using enzyme information from various databases. *In silico* approaches such as protein BLAST searches and molecular docking may help in such enzyme selection. Further pathway optimization to enhance product titers relies on an integrated approach composed of (1) metabolic engineering to enhance precursor metabolite availability using gene knockouts and enzyme expression level manipulation, (2) protein engineering to enhance pathway enzyme specificity and activity and (3) cofactor balancing via effective cofactor (NADH/NADPH) recycling (**Fig. 1.1**).

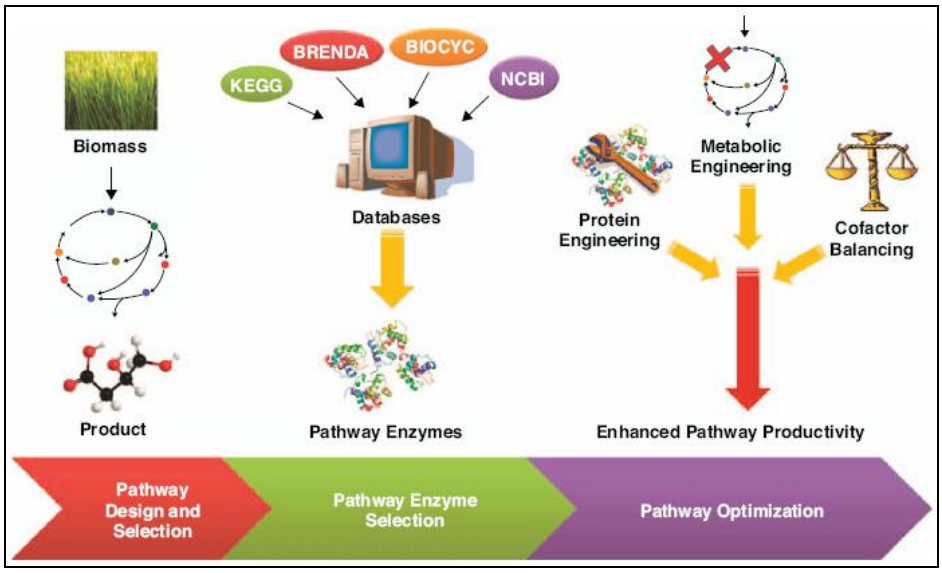

Figure 1.1: Design and engineering of pathways for microbial chemical factories (MCFs) (Dhamankar et al., 2011).

A number of research groups have employed combinations of these strategies towards developing novel pathways and enhancing productivities of already established pathways for the microbial synthesis of a number of value added biochemicals to name few

polymer and pharmaceutical building blocks putrescine, Cadaverine, succinic acid (Raab et al., 2010; Blankschien et al., 2010; Qian et al.,2009; 2011), 3-hydroxybutyric acid and 3-hydroxyvaleric acid (Tseng et al.,2009; 2010), native silk protein, the high value flavoring agent natural vanillin (Hansen et al., 2009; Lee et al., 2009; Xia et al., 2010), pharmaceutical drug precursors such as taxadiene, amorpha-4,11-diene and D-glucaric acid (Anthony et al., 2009; Ajikumar et al., 2010; Moon et al., 2010) and plant secondary metabolites such as flavanoids, stilbenoids and isoprenoids (Trantas et al., 2009; Asadollahi et al., 2010; Stephanopolous et al., 2011).

1.1.2 Strategies of Metabolic engineering for Strain improvement

Productivity of microbes isolated from nature is generally low. Genetic and metabolic engineering strategies have been used increasingly to modify or introduce new cellular or metabolic capabilities. Conventional metabolism-oriented engineering strategies often fail to obtain expected phenotypes owing to focusing narrowly on targeted metabolic capabilities while neglecting microbial physiological responses to environmental stresses. To meet the new challenges posed by the biotechnological production of fuels, chemicals and materials, microbes should exert strong physiological robustness and fitness, in addition to strong metabolic capabilities, to enable them to work efficiently in actual bioprocesses or in various environmental conditions.

Before 1970, microbes were used mainly in the traditional brewing and fermentation industries, such as the production of soy sauce, cheese, alcohol, antibiotics and other natural products. The production strains used were either selected from nature or mutated physically and chemically. Since the 1970s, with the development of recombinant DNA technology, scientists began to engineer microbes to meet desired requirements using genetic engineering, which enabled the introduction of novel microbial metabolic pathways. Among the products produced biotechnologically were recombinant pharmaceuticals and their precursors, antibiotics, amino acids and enzymes. Since the 1990s, the concept of metabolic engineering has enabled further improvements in microbial engineering and facilitated the broadening of substrates spectra, enabling improved titers and yields, heterologous protein production, engineering pathways for xenobiotic degradation, as well as the synthesis of

new bioproducts (Zhang et al., 2009). Metabolically engineered microbes have driven the rapid development of the biotechnological production of fine-chemicals, amino acids and biodegradable polymers. More recently, increasing food demands together with impending energy crises and environmental pollution, have driven the application of microbes for the production of biofuels, bulk-chemicals and biomaterials from renewable non-food biomass, which requires further improvements of the microbes used to increase product titer and productivity and to decrease the incurring production cost (Zhang et al., 2010). Since the 1990s, metabolically engineered microbes have been applied extensively in the production of organic acid, amino acids (Wendisch et al., 2006), sugar alcohols (Akinterinwa et al., 2008), biofuels (Atsumi et al., 2008; Lawrence et al., 2011; Zhang et al., 2011) and pharmaceuticals (Chartrain et al., 2000). Recent developments in '-omics' technologies have powered metabolic engineering strategies from the level of a local pathway to that of the global metabolic network (**Fig. 1.2**).

Advances in metabolic engineering combined with various '-omics' approaches (Park et al., 2008) have contributed to improving cellular metabolic activities to achieve a more efficient biotechnological production of target products (Lee et al., 2005; 2006; Park et al., 2007).

The term 'physiological engineering' was first used by Jens Nielsen in 1997 in relation to penicillin production by Penicillium chrysogenum (Nielsen et al., 1997). At that time, physiological engineering referred to understanding the function of important pathways in microorganisms by using an integrated approach of microbial physiology and bioreaction engineering. It involved metabolic flux analysis, metabolic control analysis and kinetic modeling to generate fundamental knowledge for metabolic engineering that was based on reproducible cultivation experiments and reliable measurements. During the past decade, metabolic engineering has become the central approach for strain improvement, mainly targeted at improving specific metabolic capabilities. However, the main physiological characteristics related to industrial and agriculture applications including microbial metabolic capability, insensitivity of pathway key enzymes to end-

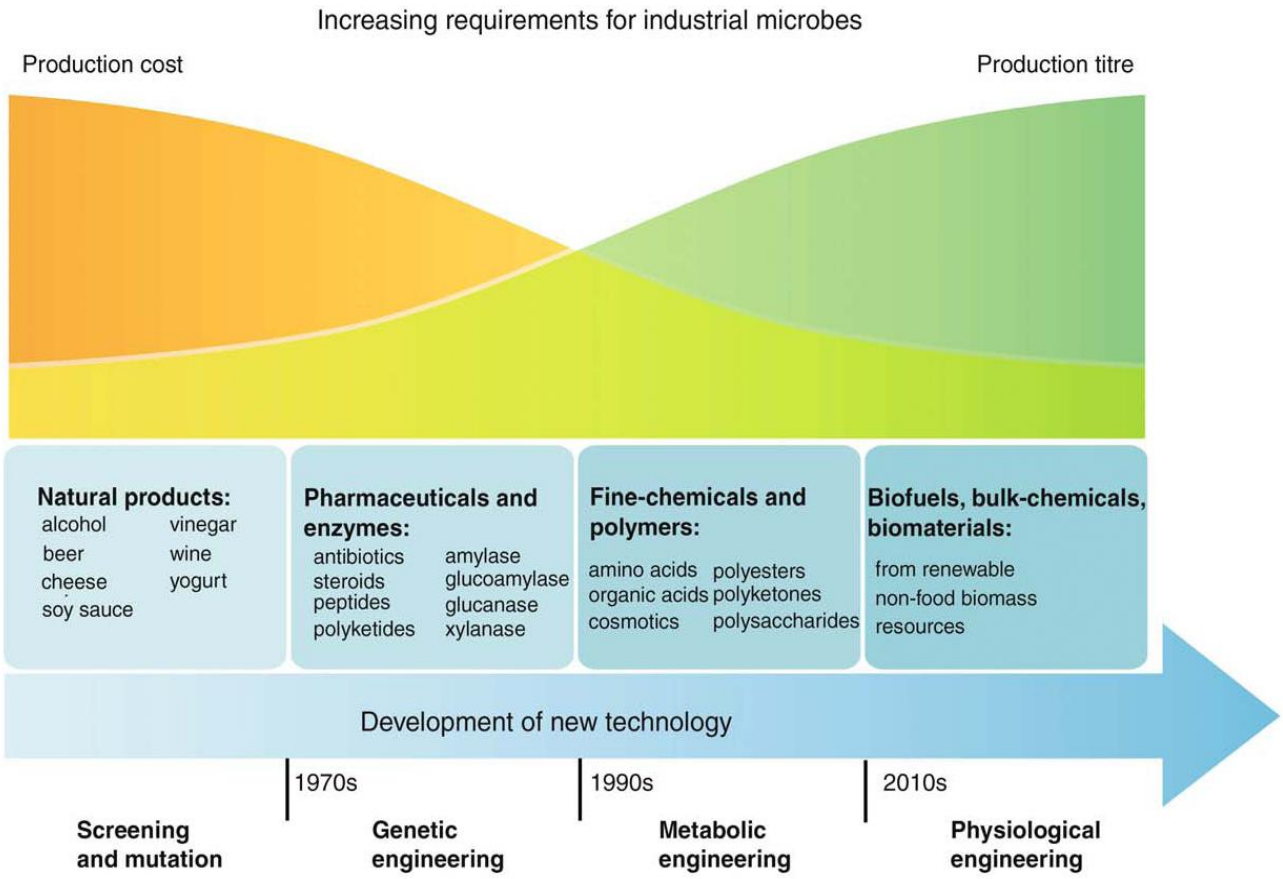

Figure 1.2: Recent advances in the engineering of microbes (Zhang et al., 2009).

1.1.3 Physiological engineering: New evolving technology for strain improvement

product inhibition or feedback repression, robustness under adverse environmental perturbations, tolerance of high concentration substrates or metabolites, and fitness throughout the entire biological cycle are also important for efficient biotechnological production of fuels, chemicals, materials and performance in ecohabitats. In this context, an evolved concept of physiological engineering comes into picture which refers to a strategy of strain improvement with the aim of either improving existing or engineering novel functionalities into microbes (Tyo et al., 2009). Different from the conventional metabolism-oriented engineering strategy, such a strategy focuses primarily on the physiological status of microbial cells and on the physiological functionality related to the actual biotechnological production processes. Therefore, this strategy aims not only to improve microbial metabolic activities at a specific physiological status, but also to further

investigate the molecular mechanisms underpinning the desired physiological characteristics.

1.1.4 Successful examples of metabolic engineering: Recent reports

Recent advances in system biology and synthetic biology approaches are providing support to metabolic engineering to become a growing tree of chemical diversity (**Fig. 1.3**) at the whole cell level particularly of microorganisms. Systems biology merged with metabolic engineering principles is quickly expanding the chemical palate of cells. Our capacity to engineer cells is becoming a competing force against traditional synthetic organic chemistry and heterogeneous catalysis. These new microbial factories have the capability to produce countless products, with new ones being added constantly. Synergies with the fields of synthetic biology have enabled new-found technologies for *de novo* design of enzymes, altering gene expression and creating novel network regulation completely unrelated to the native cellular regulatory network (Jiang et al., 2008; Young and Alper, 2010; Zastrow et al., 2012).

1.2 Engineering the central carbon metabolism

The term "central carbon metabolism" (CCM) describes the integration of pathways of transport and oxidation of main carbon sources inside the cell. In most bacteria, the main pathways of the CCM are those of the phosphotransferase system (PTS), glycolysis, gluconeogenesis, pentose phosphate (PP) pathway, and the tricarboxylic acid cycle (TCA) with the glyoxylate bypass. As a whole, the system has a complex structure and it is regulated by complex networks of reactions. The knowledge about regulation in CCM has great industrial relevance as it may allow the engineering of selected metabolic steps to reroute carbon fluxes toward precursors for industrially important metabolites (Nielsen, 2011). This kind of metabolic engineering however is a difficult task as the knowledge is incomplete regarding the regulation of central carbon metabolism flux for many industrially and agriculturally important bacteria.

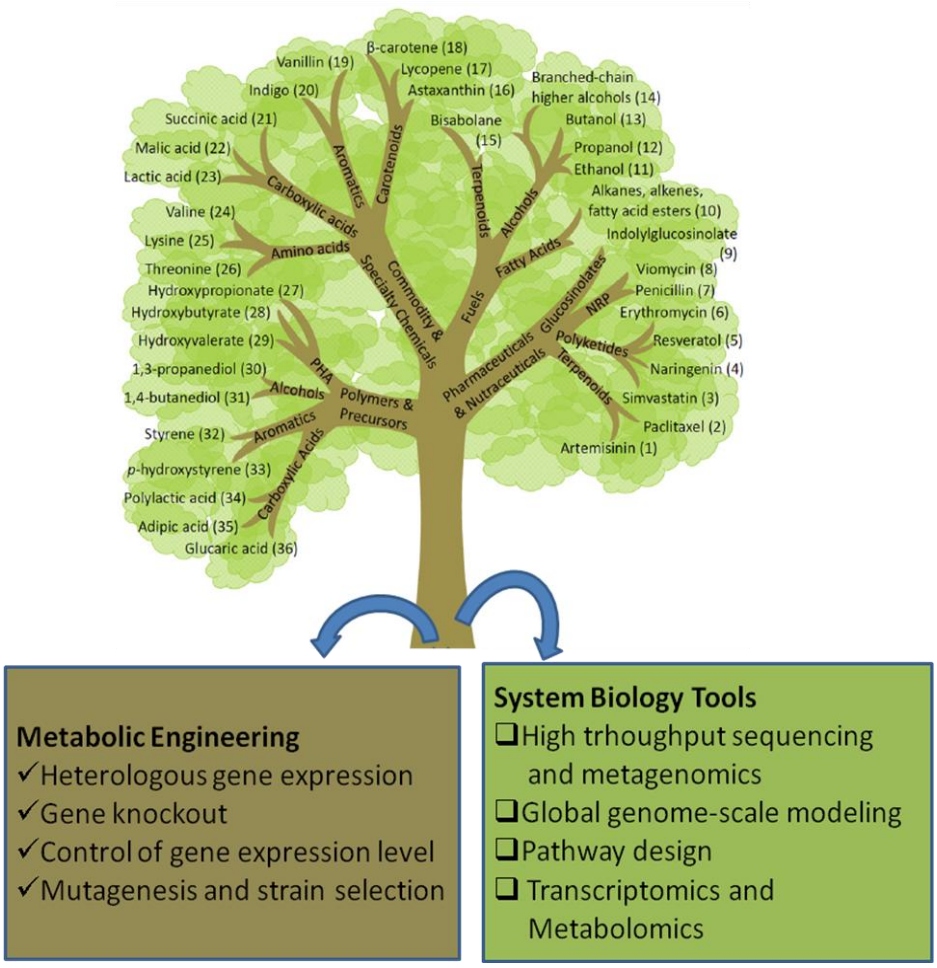

Figure 1.3: Metabolic engineering and system biology converting microbes as cell factory. Numbers correspond to the list of references. Abbreviations: NRP; nonribosomal peptide, PHA; polyhydroxyalkanoate (Modification of the figure from Curran et al., 2012).

1.2.1 *Escherichia coli*

E. coli, a Gram-negative bacterium, is being used widely today in a large number of biotechnological processes. The ease of cultivation as it grows quickly in minimal medium, as well as its ability to metabolize both pentoses and hexoses (Zaldivar et al., 2001), have made it the bacterium of choice for research and over the years the wealth of information in genomics, proteomics and metabolism have led it to be regarded as the prime prokaryotic model (Kadir et al., 2010). The CCM of *E. coli* and specifically the metabolism of glucose are intensively studied and well known topics (Sauer et al., 2005); Shiloach et al., 2009). Glucose metabolism starts with its uptake via the PTS and proceeds with several interconnected pathways with the major being: glycolysis, gluconeogenesis, the pentose-

monophosphate bypass with the Entner-Dudoroff pathway, the TCA cycle with the glyoxylate bypass, anaplerotic reactions and acetate production and assimilation and shikimic acid pathway (**Fig. 1.4**).

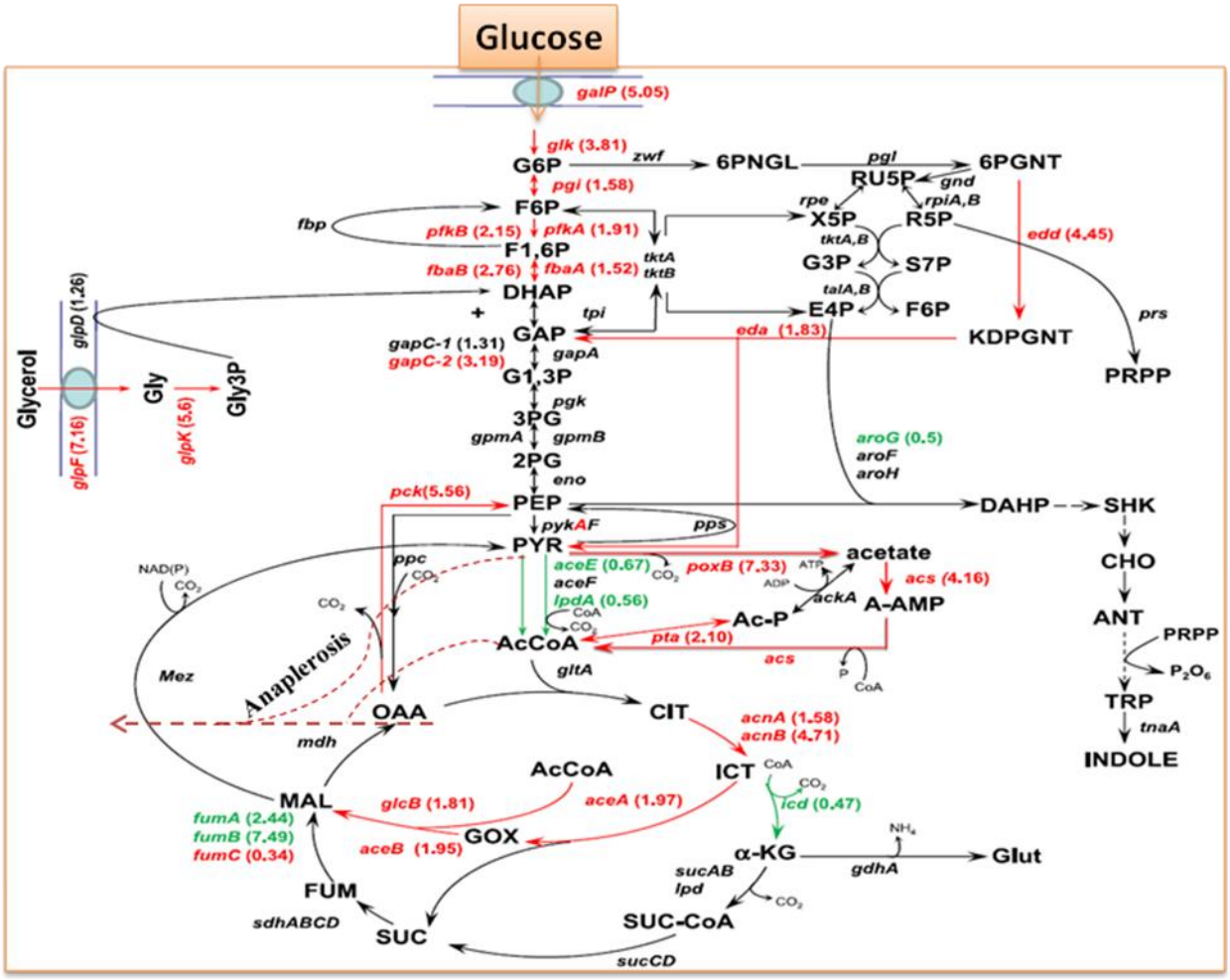

Figure 1.4: Central Carbon metabolism of *E. coli* JM101 grown on glucose and glycerol (Modification from Martínez-Gómez et al 2012). Relative transcription values are highlighted with colors when grown on glycerol as c source compared to glucose. **Genes in red: overexpressed. Genes in green: underexpressed. Genes in black: no change.** Metabolite abbreviations: Gly – glycerol; Gly3P - glycerol-3-phosphate; G - glucose; G6P - glucose-6-phosphate; F6P - fructose-6-phosphate; F1,6P - fructose-1,6-biphosphate; DHAP - dihydroxyacetone phosphate; G3P, glyceraldehydes 3-phosphate; G1,3P, 1,3-bisphosphoglycerate; 3PG, 3-phosphoglycerate; 2PG, 2-phophoglycerate; PEP, phosphoenolpyruvate; PYR, pyruvate;6PGLN, 6-phosphoglucono-δ-lactone; 6PGNT, 6-phophogluconate; Ru5P, ribulose-5-phosphate; R5P, ribose-5-phosphate; Xu5P, xylulose-5-phosphate;S7P, seudoheptulose-7-phosphate; E4P, erythrose-4-phosphate; Ac-CoA, acetyl coenzyme A; Ac-P, acetyl phosphate; A-AMP, acetyl-AMP; CIT, citrate; ICT,isocitrate; GOX, glyoxylate; α-KG, α-ketoglutarate; SUC-CoA, succinyl-coenzyme A; SUC, succinate; FUM, fumarate; MAL, malate; OAA, oxaloacetate;KDPGNT, 2-keto-3-deoxy-D-gluconate-6-phosphate; PRPP, 5-phospho-D-ribosyl-

α-1-pyrophosphate; DAHP, 3-deoxy-D-arabino-heptulosonate-7-phosphate; SHK, shikimate; CHO, chorismate; ANT, anthranilate; TRP, L-tryptophan (Papagianni, 2012).

The network controlling the carbon uptake integrates metabolism, signal transduction and gene expression (Baldazzi et al., 2010). In addition to the glycolytic metabolism, a gluconeogenic carbon recycling process that involves acetate is occurring simultaneously in *E. coli* JM101 when growing on glycerol. Glycerol, an energy-poor carbon source, has enhanced its biotechnology importance as carbon source since it is a byproduct of the biodiesel synthesis, whose production is expected to increase in the future (Dharmadi et al., 2006; Vasudevan et al., 2008; Bisen et al., 2010). *E. coli* growing aerobically on glycerol incorporates this molecule into central metabolism as dihydroxyacetone phosphate (DHAP), a metabolite which can participate in both gluconeogenic and glycolytic processes (Frankel et al., 1996; Martínez-Gómez et al., 2012). A balanced aerobic growth on glycerol depends on three global regulators: cAMP-CRP as the principal inducer of the glycerol catabolic regulon (including *glp*F, *glp*K *and glp*D); Cra(FruR) as regulator of some gluconeogenic genes, and ArcA as regulator of several central metabolic genes including the TCA cycle and others involved in respiration (Weissenborn et al., 1992; Iuch et al., 1995). Several genes are upregulated (*pyk*A, *pck*A, *glt*A, *fum*ABC, *sdh, mdh* and *acn*A) while *ackA* is downregulated when grown in glycerol as compared to glucose (Oh et al., 2000). It appears that when glycerol is used as the sole carbon source in addition to the glycolytic metabolism, a carbon stress response occurs that includes acetate scavenging and gluconeogenesis mediated by RpoS and Crl through indole. Interestingly, when JM101 was grown on a mixture of glycerol plus acetate, the μ of this strain was not enhanced but both compounds are utilized (**Table 1.1; Figure 1.5**).

Table 1.1: Specific growth rates (μ) and stoichiometric parameters of *E. coli* JM101 strain grown on single or mixtures of carbon sources (Martínez-Gómez et al., 2012).

Condition	μ(h-1)	Yx/s (g/mmolC)	Qs (mmolC /gdcw h)	mmolC of acetate produced(+) or consumed(-)
Glucose	0.69	0.013	51.8	+28.2
Glycerol	0.49	0.014	34.3	Not detected
Glucose+Glycerol	0.72(0.45)	0.017(0.006)	43.1	+4.1
Glycerol+acetate	0.43	0.011	39.5	-11.0
Glucose+acetate	0.72(0.1)	0.013(0.017)	55.4(6.55)	+6.0

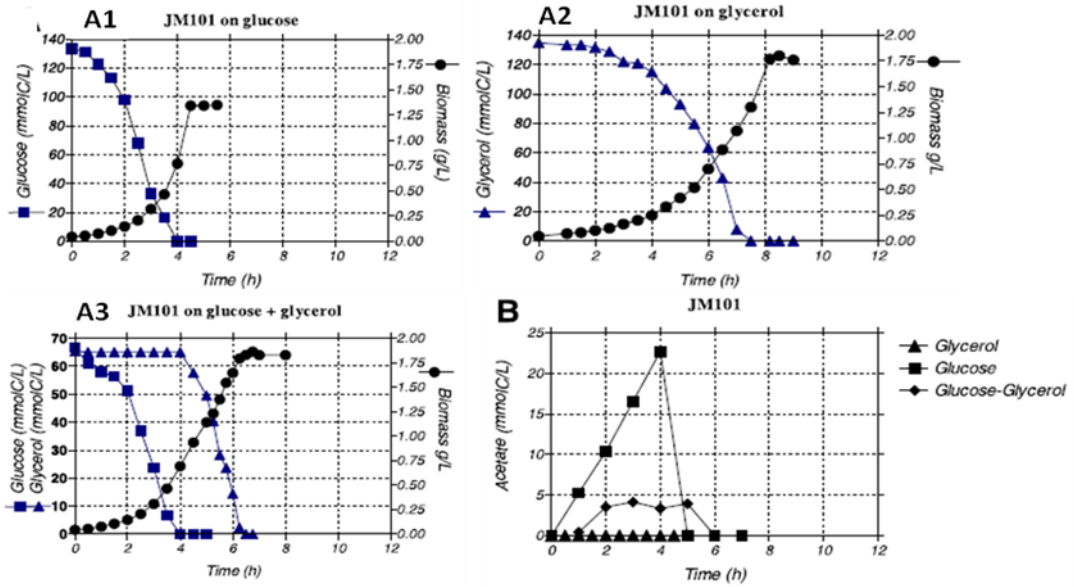

Figure 1.5: Growth profiles and substrate utilization (mmolC/L) of strain JM101 grown on glucose (A1) or glycerol (A2) and in the mixture glucose plus glycerol (A3). Acetate levels (mmolC/L) of strain JM101 grown on glucose, or glycerol and on a mixture of glucose plus glycerol (B) (Martínez-Gómez et al., 2012).

1.2.2 *Bacillus subtilis*

Bacillus subtilis is a gram positive spore forming bacterium and is the second most intensively studied bacteria after *E. coli.* Glucose is internalized via PTS *and* metabolizes a large proportion of it to pyruvate and acetyl CoA, and subsequently converts these compounds to lactate, acetate and acetoin as by-products of metabolism which are excreted into the extracellular environment . The enzymes of glycolysis depend on the cofactor NAD+ to take up electrons and hydrogen atoms that are released by substrate oxidation; the conversion of pyruvate to lactate has the advantage of regenerating NAD+ from its reduced form, NADH, which is a step that is essential for continued glycolysis. The conversion of acetyl CoA to acetate is coupled to the synthesis of ATP by the activities of the enzymes phosphotransacetylase and acetate kinase. Thus, these overflow pathways enable the cell to maintain redox balance and generate ATP without using the cytochrome system. When the glucose has been fully consumed, the cells reintroduce the by-products into central metabolism (using lactate dehydrogenase, acetoin dehydrogenase and acetyl CoA synthetase) and metabolize them further through the citric acid cycle, so generating additional ATP and reducing power. The genes that encode the enzymes that are involved in overflow metabolism are regulated by proteins that sense the nutritional status of the cell. In *B. subtilis*, CcpA activates the expression of the genes that are required for the synthesis of acetate, lactate and acetoin.The uptake of PTS sugar lead to an increase in FBP concentration in the cell which triggers ATP dependent HPr kinase/phosphatase-catalyzed phosphorylation o Hpr and Crh at Ser-46.The seryl phosphorylated complex with CcpA forming P-Ser-Hpr/CcpA and P-Ser-Crh/CcpA, now binds to cre to cause CCR or CCA depending upon the position of cre by transcriptional repression of the gene involved in the overflow metabolism.(Sonenshein 2007;Gorke and Stulke 2008; Fujita 2009) (**Fig. 1.6**).

The overall flux distribution done by ^{13}C metabolic flux analysis suggested glycolysis as the main catabolic pathway for glucose, acetate secretion, significant anaplerosis, and absent gluconeogenesis (**Fig. 1.7**) (Martin et al., 2011). The TCA cycle is one of the major routes of carbon catabolism in *B. subtilis* (Blenke et al., 2006).

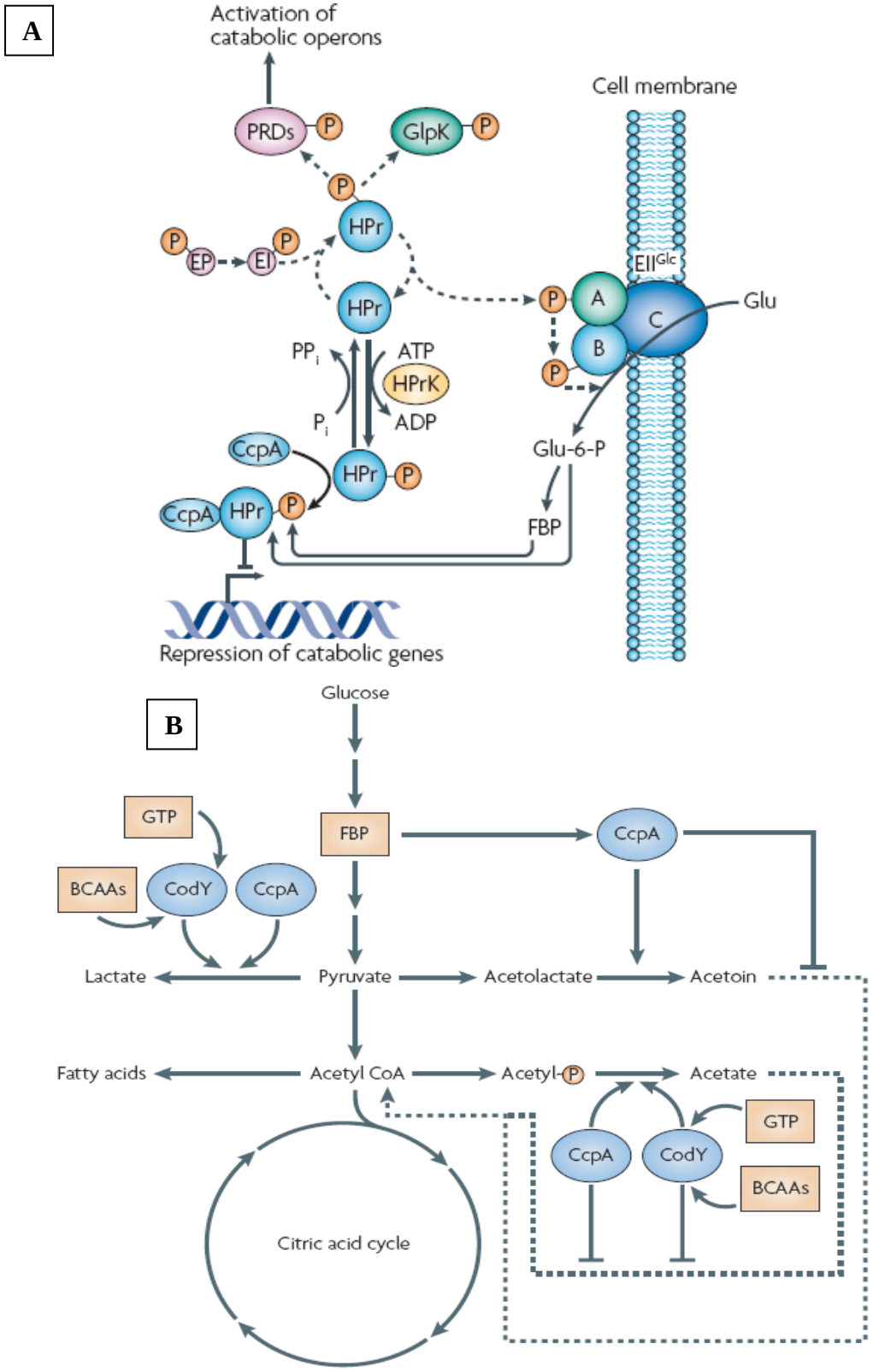

Figure 1.6: Glucose uptake and contribution of global CCR regulators for nutritional intersections in *B. subtilis* (A and B) (Sonenshein, 2007; Gurke and Stulke, 2008).

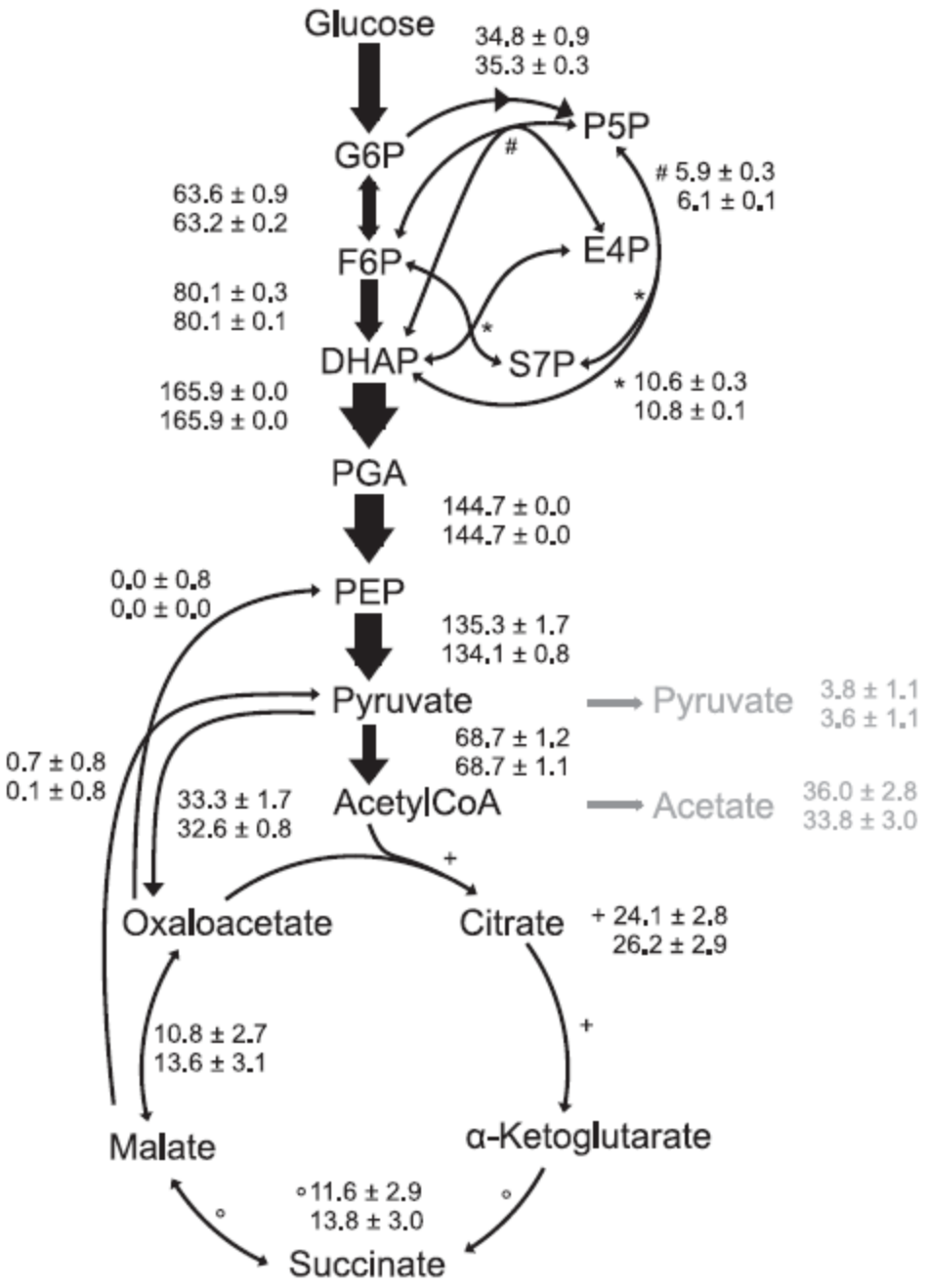

Figure 1.7: Intracellular flux distribution of *B. subtilis* wild-type during exponential growth on 20% (w/w) [U-13C] and 80% [1-13C] glucose derived from ^{13}C-patterns of solely intact metabolic intermediates (top values), or intact and fragmented carbon backbones of metabolic intermediates (bottom values) of the same culture. Shown are relative flux values normalized to the glucose uptake rate of 8.2mmol g^{-1} h^{-1}. Black arrows depict maximum and inner white arrows the minimum estimated flux value based on the Monte Carlo bootstrap error estimates with a confidence interval of 95%. (Martin et al., 2011).

Acetoin (3-hydroxy-2-butanone, AC) is an extensively used flavor compound as well as an important metabolic product produced by various microorganisms. It is classified as one of the 30 platform chemicals which were given priority to their development and utilization by the U.S. Department of Energy (Werpy and Petersen 2004). Production of acetoin can be achieved by chemical or biological synthesis. Compared to chemical synthetic and enzyme conversion methods, the microbial fermentation route has advantages of being more environmentally friendly and cost-effective. In a recent study, *B. subtilis* BSUW06 strain yields high levels of acetoin by disruption of *bdhA*, *acoA*, and *pta* genes involved in acetoin catabolic and competing pathways (Wang et al., 2012). The overexpression of *alsSD* increased pyruvate availability to acetoin biosynthesis, redirecting carbon flux towards the desired pathway (**Fig. 1.8**)

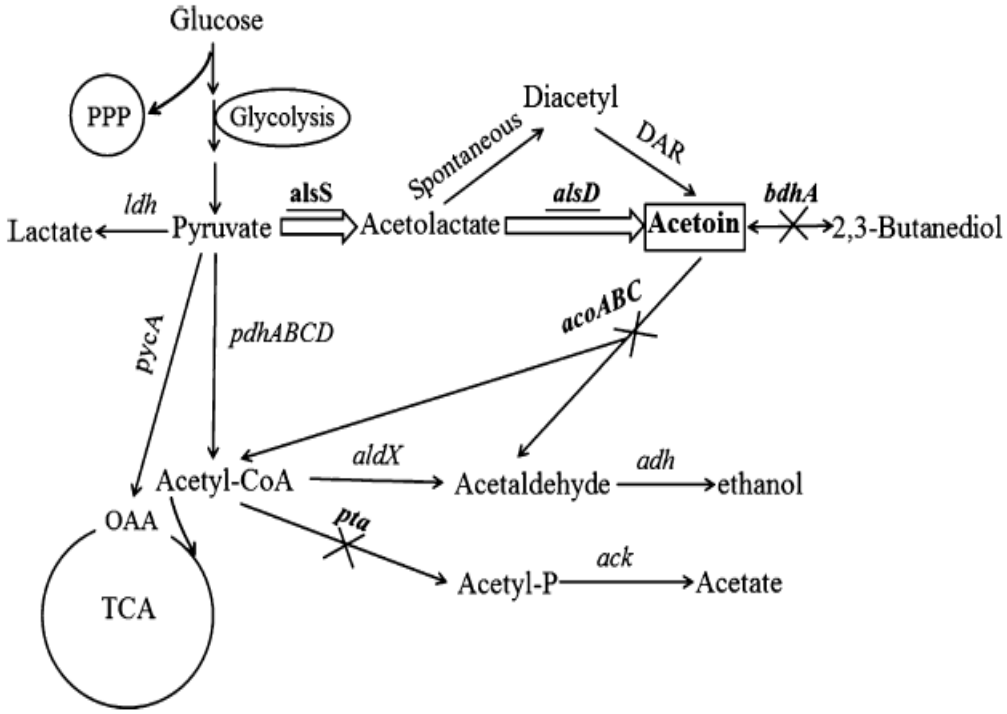

Figure 1.8: The acetoin biosynthetic pathway and other overflow metabolism pathways in *B. subtili* .Genes *alsS, alsD, bdhA, acoABC, ldh, pdhABCD, pycA, pta, ack, aldx* and *adh* encode acetolactate synthase, acetolactate decarboxylase, 2,3-butanediol dehydrogenase, acetoin dehydrogenase, lactate dehydrogenase, pyruvate dehydrogenase, pyruvate carboxylase, phosphotransacetylase, acetate kinase, aldehyde dehydrogenase and alcohol dehydrogenase. PPP pentose phosphate pathway, TCA tricarboxylic acid cycle, DAR diacetyl reductase. Overexpressed genes are underlined. Disrupted pathway steps are indicted by arrow breaks (Wang et al., 2012).

B. subtilis emerged an important model microorganism in the field of metabolic engineering for the production of riboflavin (Sauer et al., 1998). The PP pathway and the pyruvate shunt were identified as major pathways of glucose catabolism in a recombinant riboflavin-producing *B. subtilis* strain (Sauer et al., 1997). *B. subtilis* metabolism has an unusually high capacity for the reoxidation of NADPH. Riboflavin formation in *B. subtilis* is limited by the fluxes through the biosynthetic rather than the central carbon pathways. Therefore overexpression of enzymes (e.g. G6PDH and 6PGDH) that facilitate the route of carbon flow towards the PP pathway increased the pool of ribulose-5P which is a precursor for riboflavin biosynthesis and led to increased riboflavin yields (Zhu, Chen et al. 2007; Duan et al., 2010; Wang et al.,2011).

1.2.3 *Corynobacterium glutamicum*

A species of the class Actinobacteria *C. glutamicum* was discovered 50 years ago as a natural overproducer of glutamate. Today, it is used for the industrial production of more than 2 million tons of amino acids (glutamate, lysine and tryptophan) per year (Wittmann et al., 2010; Nešvera et al., 2011). Genetic manipulations in *C. glutamicum* were initiated in 1984, after isolation of small native plasmids. Progress in the genetic analysis of *C. glutamicum* accelerated after the determination of the complete genome sequences of two *C. glutamicum* strains (Yukawa et al., 2007).

The central metabolism of *C. glutamicum* involving glycolysis, pentose phosphate pathway (PPP), TCA cycle as well as anaplerotic and gluconeogenetic reactions (**Fig. 1.9**). Different enzymes are involved in the interconversion of carbon between TCA cycle (malate/oxaloacetate) and glycolysis (pyruvate/phosphoenolpyruvate). For anaplerotic replenishment of the TCA cycle, *C. glutamicum* exhibits pyruvate carboxylase and phosphoenolpyruvate (PEP) carboxylase as carboxylating enzymes. Malic enzyme and PEP carboxykinase catalyze decarboxylation reactions from the TCA cycle. Gluconeogenetic enzymes, oxaloacetate decarboxylase and PEP synthetase around the anaplerotic node is involved in the regeneration of excess ATP. The major enzymes, glucose 6-phosphate dehydrogenase and 6-phosphogluconate dehydrogenase in the oxidative part of the PPP and the TCA cycle enzyme isocitrate dehydrogenase are linked to supply NADPH.

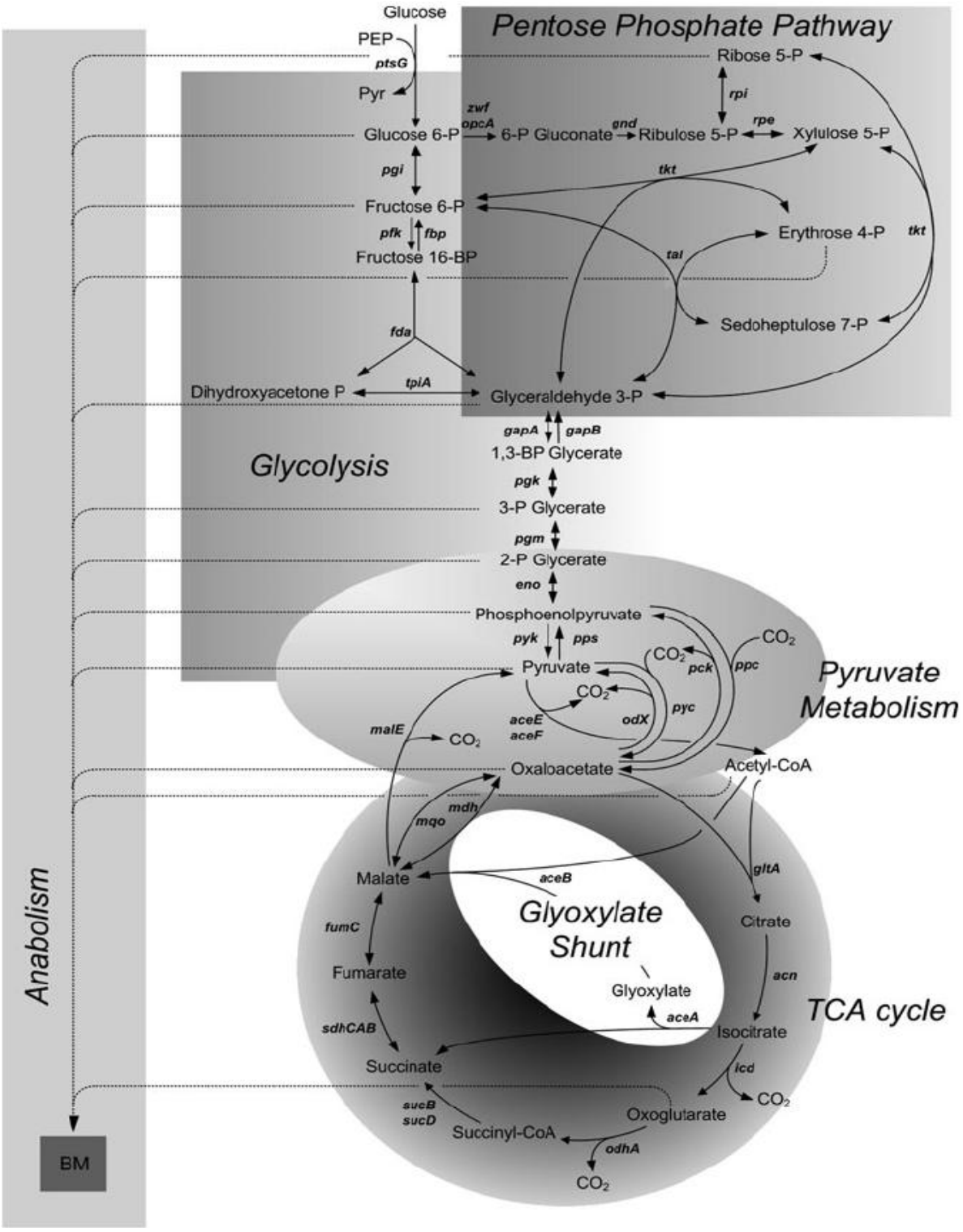

Figure 1.9: Central carbon metabolism in *C. glutamicum* (Wittmann, 2010).

High carbon loss through CO_2 formation by the TCA cycle is generally undesired with respect to carbon yield for the desired product. Hence, targeted down regulation of

TCA cycle is employed for improved lysine production (Becker et al., 2011). Upon replacement of the start ATG codon of *icdh* gene in *C. glutamicum* by GTG, the enzyme activity was reduced by 70% (Becker et al., 2009). This modification redirected the flux from the TCA cycle towards anaplerosis which enhanced lysine production by more than 40%.

1.2.4 *Streptomyces spp.*

Bacteria of the genus *Streptomyces* is very efficient producer of antibiotics. The Embden-Meyerhof-Parnas (EMP) pathway, the PP pathway and the TCA cycle are present in a number of *Streptomyces* species (Hodgson et al., 2000). Secondary metabolic pathways have been extensively studied in these bacteria for strain and yield improvement. The productivity of secondary metabolites is mainly determined by the availability of biosynthetic precursors (e.g. acetyl-CoA and malonyl-CoA). The carbon fluxes into the PPP or the glycogen synthetic pathway were reduced by deleting genes for G6PDH isozymes and 6PGDH, respectively. Since acetyl-CoA and/or malonyl-CoA is a precursor for the biosynthesis of actinorhodin (Act), a gene complex for acetyl-CoA carboxylase (ACCase) when overexpressed resulted in more rapid utilization of glucose and increased the efficiency of Act biosynthesis (**Fig. 1.10**) (Ryu et al., 2006).

Genetic engineering of glycolytic pathway in *Streptomyces clavuligerus* was carried out for improving clavulanic acid production (Li and Townsend, 2006). Clavulanic acid is a potent β-lactamase inhibitor used to combat resistance to penicillin and cephalosporin antibiotics. Clavulanic acid biosynthesis is initiated by the condensation of L-arginine and D-glyceraldehyde-3-phosphate (G3P). The limited G3P pool was overcome by targeted disruption of *gap1* genes which doubled production of clavulanic acid. Addition of arginine to the cultured mutant further improved clavulanic acid production.

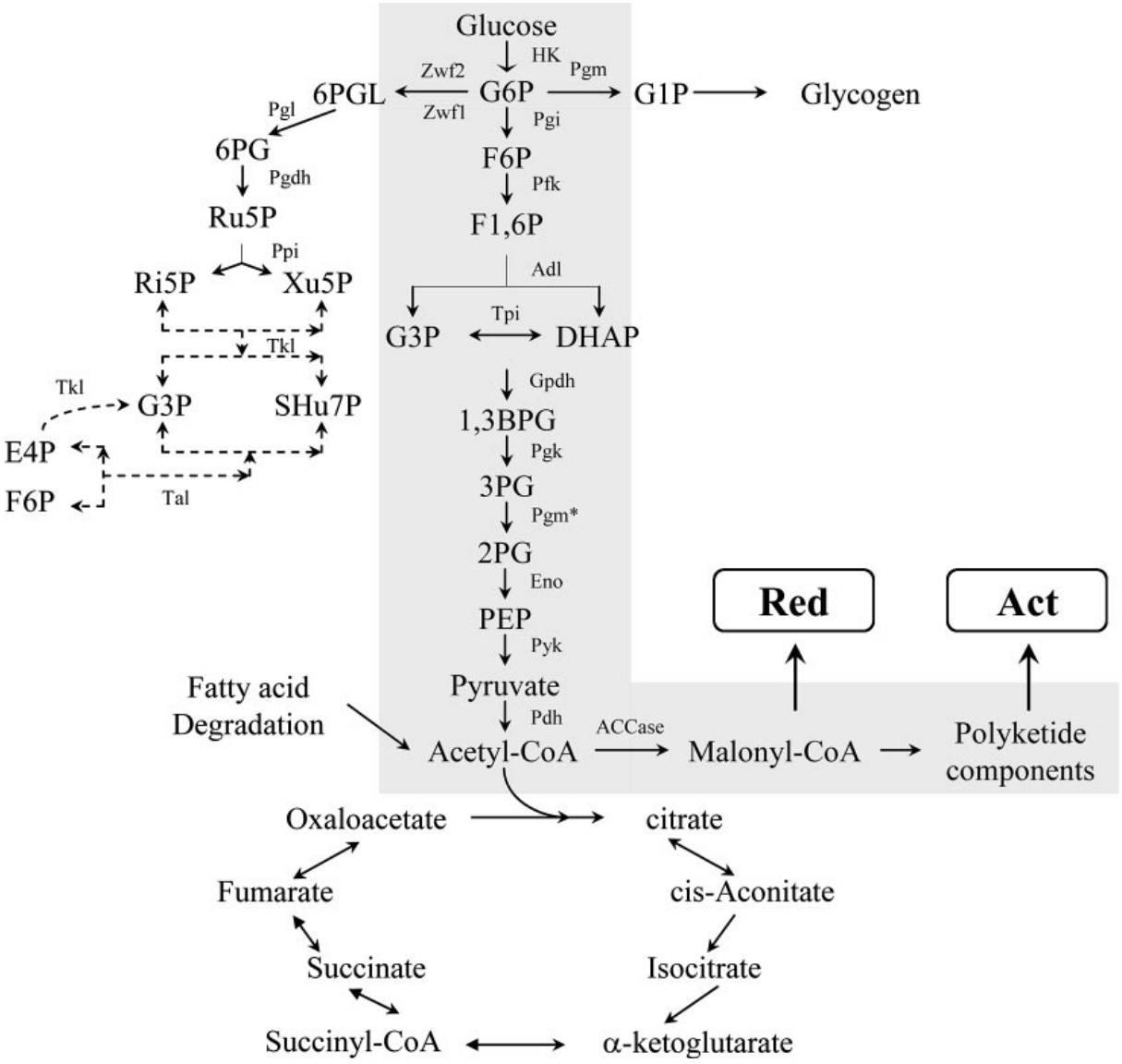

Figure 1.10: Central carbon metabolism and intermediates from primary metabolism for Act production in *S. coelicolor* (Ryu et al., 2006). G6P, glucose-6-phosphate;F6P, fructose-6-phosphate; F1,6DP, fructose-1,6-diphosphate; GAP, glyceraldehyde-3-phosphate; 1,3 BPG, 1,3-diphosphoglycerate; 3PG, 3-phosphoglycerate; 2PG, 2-phosphoglycerate; PEP, phosphoenolpyruvate; 6PGL, 6-phosphoglucolactone; 6PG, 6-phosphogluconate; Ru5P, ribulose-5-phosphate; Ri5P, ribose-5-phosphate; Xu5P, xylulose-5-phosphate; SHu7P, sedoheptulose-7-phosphate; E4P, erythrose-4-phosphate; HK, hexokinase;*Pfk*, phosphofructokinase; *Adl*, aldolase; *Tpi*, triose phosphate isomerase; *Gpdh*, glyceraldehyde-3-phosphate dehydrogenase; *Pgk*, phosphoglycerate kinase; *Pgm**, phosphoglycerate mutase; *Eno*, enolase; *Pyk*, Pyruvate kinase; *Pdh*, pyruvate dehydrogenase; *ACCase*, acetyl-CoA carboxylase; *Zwf*, glucose-6-phosphate dehydrogenase; *Pgm*, phosphoglucomutase; *Pgl*, phosphoglucolactonase; *Pgdh*, phosphogluconate dehydrogenase;*Ppi*, phosphopentose isomerase; *Tkl*, transketolase; *Tal*, transaldolase.

1.2.5 *Lactococcus lactis* and other lactic acid bacteria

Small genome size (~2-3 Mb) and simple energy and carbon metabolism that converts sugars to pyruvate via glycolytic pathway (**Fig. 1.11**) make lactic acid bacteria a promising targets of metabolic engineering strategies. *L. lactis* shows homolactic metabolism when growing in rapidly metabolized sugars with more than 90% of the metabolized sugar being converted to lactic acid. Deviation from homolactic fermentation is observed under aerobic conditions or during the metabolism of galactose or maltose. PFK was identified as the key regulatory enzyme of the glycolytic flux .The control of the glycolytic flux also resides to a large extend in processes outside the glycolytic pathway itself, like glucose transport and the ATP consuming reactions (Papagini et al., 2007; 2011, 2012).

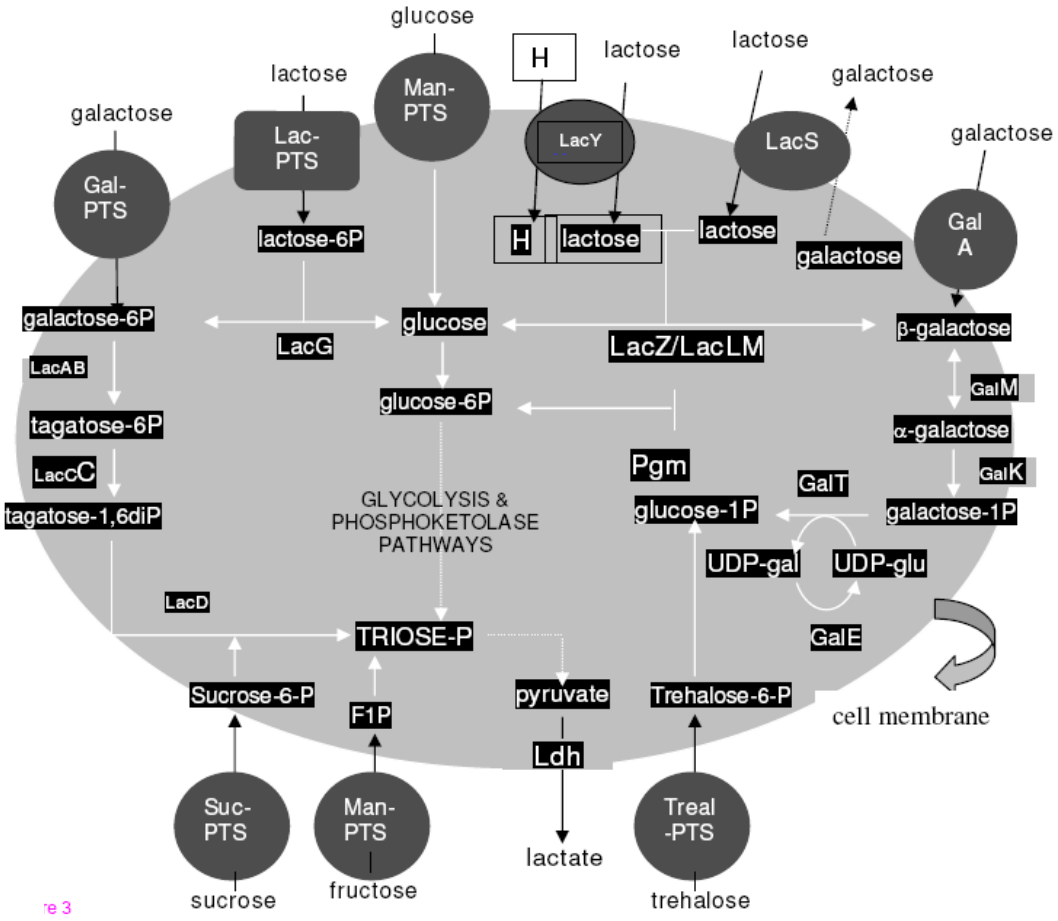

Figure 1.11: Central carbon metabolic pathway of *Lactobacillus lactis* (Papagini, 2012).

Cloning of *pfk*A gene from *Aspergillus niger* in *L. lactis* resulted in a two-fold increase in PFK specific activity (from 7.1 to 14.5 U/OD600) with a proportional increase of the maximum specific rates of glucose uptake (from 0.8 to 1.7 μMs^{-1} g CDW^{-1}) and lactate formation (from 15 to 22.8 g lactate (g $CDW)^{-1}$ h^{-1}) (Papagianni and Avramidis, 2009; 2011). Glycolytic flux in *L. lactis* is also affected by the carbon catabolite protein (CcpA) which besides its role in catabolite repression also regulates sugar metabolism through activation of the *las* operon encoding the glycolytic enzymes PFK and PYK, and LDH (Luesink et al., 1998).

1.2.6 *Pseudomonas spp.*

The genus *Pseudomonas* comprises of a large group of highly diverse Gram negative bacteria that are found abundantly as free-living organisms in soils, fresh water and marine environments, and in many other natural habitats. According to the microbial classification based on rRNA similarities, the largest group comprises of fluorescent species including *P. aeruginosa*, *P. fluorescens* (several biovars), *P. putida*, *P chlororaphis*, *P. syringae* (many pathovars), *P. cichorii*, *P. stutzeri*, *P. mendocina*, *P. alcaligenes*, *P. pseudoalcaligenes*, *P. agarici*, etc., (predicted according to Palleroni et al.1973). The great catabolic versatility of pseudomonads has conferred an important ecological advantage which has allowed them (i) to colonize new habitats, including those toxic for most micro-organisms, (ii) to acquire and develop the specific mechanisms responsible for their natural resistance to harmful compounds and adaptations against metal stresses (Schleissner et al., 1997; Hamel et al, 2001), (iii) to promote plant growth and (iv) control plant pathogens by secretion of several antibiotics and antifungal molecules (Preston, 2004).

1.2.6.1 Glucose metabolism in *Pseudomonas* sp.

A common characteristic of Pseudomonas is their considerable metabolic versatility, being able to assimilate a wide range of compounds and environmental conditions (Palleroni and Moore, 2004). Some species, as for example *Pseudomonas aeruginosa*, can behave as severe opportunistic pathogens. Other species, such as *Pseudomonas fluorescens or*

Pseudomonas putida, can be beneficial for plants and thrive in the plant rhizosphere (Molina et al., 2000; Martins dos Santos et al., 2004).

Compared to facultative anaerobe *E. coli*, the glucose metabolism of *Pseudomonas* differs chiefly in the following aspects - (i) Absence of PTS mediated glucose uptake and Entner–Doudoroff (ED) pathway being almost exclusive catabolic route; (ii) Most Pseudomonas species (*P. aeruginosa, P. putida*, *P. fluorescens, Pseudomonas syringae, Pseudomonas mendocina* and *Pseudomonas entomophyla*, but not *Pseudomonas stutzeri*) lack phosphofructokinase which impedes the assimilation of glucose through the glycolytic pathway. (iii) PP pathway exhibiting completely biosynthetic functions; (iv) The respiratory mechanisms being highly efficient with very low overflow metabolism; (v) Significantly functional pyurvate bypass instead of the malate dehydrogenase (MDH) in TCA cycle; (vi) Glucose is extracellualrly converted to gluconate and 2-ketogluconate and simultaneously is also internalized by an active mechanism; and (vii) Absence of cAMP dependent glucose mediated catabolite repression (Mac Gregor et al., 1992; del Castillo and Ramos, 2007).

Glucose crosses the outer membrane into the periplasmic space through the OprB-1 porin (**Fig. 1.12**). Thereafter, glucose can be directly transported into the cell, or converted to gluconate or to 2-ketogluconate in the periplasmic space catalyzed by a membrane-bound PQQ-GDH and gluconate dehydrogenase (GADH), respectively, via direct oxidative pathway. Gluconate and 2-ketogluconate are then internalized using specific transporters into the cell and are acted upon by ATP dependent gluconokinase and 2-ketogluconokinase, respectively and 2-keto-6-phosphogluconate reductase finally producing 6-phosphogluconate (6-PG) which is further oxidized through the ED pathway to enter the central metabolism (Swanson et al., 2000; Fuhrer et al., 2005; Buch et al., 2009, 2008). 6-PG dehydratase (encoded by *edd*) and 2-keto-3-deoxy-6-phosphogluconate (KDPG) aldolase (encoded by *eda*) are the two enzymes comprising the ED pathway This complex mechanism for glucose uptake has been demonstrated earlier for *P. aeruginosa* PAO , *P. aeruginosa* M60 and *P. fluorescens* A3.12 (Williams et al., 1996). Generally, the genes responsible for direct oxidation of glucose and subsequent intracellular metabolism of gluconate and 2-KG occur variably among as evident from **Table 1.2** (Nelson et al., 2002; Joardar et al., 2005; Lee et al., 2006). Alternately, pseudomonads can also accumulate

glucose *via* an active transport mechanism (Midgley and Dawes, 1973; Eisenberg et al., 1974; Guymon and Eagon, 1974) which is induced by glucose and transports glucose in the form of free sugar; requiring a periplasmic glucose binding protein in *P. aeruginosa* (Lessie and Phibbs, 1984; Cuskey, 1985). Thus, direct oxidation is not the obligatory step for glucose metabolism. Intracellular glucose is rapidly phosphorylated by glucokinase (*glk*) followed by oxidation to 6-PG by glucose-6-phosphate dehydrogenase (*zwf*). These reactions comprise of the intracellular phosphorylative pathway.

Table 1.2: Distribution of the essential glucose catabolism genes across the partially and completely sequenced genomes of *Pseudomonas* spp. (Stover et al., 2000)

Pseudomonas strain	GDH	GAD	GLK	6-PGDH	GNK	KGK	KGR
P. aeruginosa PAO1	+	+	+	-	+	-	-
P. aeruginosa UCBPP-PA14	+	+	+	-	+	-	+
P. putida KT2440	+ *	putative	+	+	+	-	+
P. putida F1	+	+	+	+	-	-	-
P. putida GB-1	-	-	+	+	-	-	-
P. fluorescens Pf5	putative	putative	+	-	putative	-	putative
P. fluorescens PfO-1	-	-	+	+	-	-	-
P. syringae pv. phaseolicola 1448A	+	-	+	putative	putative	-	-
P. stutzeri A1501	+	-	+	-	-	-	-
P. mendocina ymp	+	-	+	+	-	-	-
P. syringae pv. tomato DC3000	putative	-	+	+	+	-	-
P. entomophila L48	+	-	+	putative	+	-	-

GDH, glucose dehydrogenase;GAD, gluconate dehydrogenase; GLK, Glucokinase; GNK, gluconokinase; KGK, 2-ketogluconokinase; KGR, 2-ketogluconate-6-phosphate reductase; 6-PGDH, 6-phosphogluconate dehydrogenase. *GDH in *P. putida* KT2440 remains controversial as genome sequence reveals presence of *gcd* gene while Fuhrer et al (2005) demonstrated absence of the GDH mediated direct oxidation pathway in the same strain.

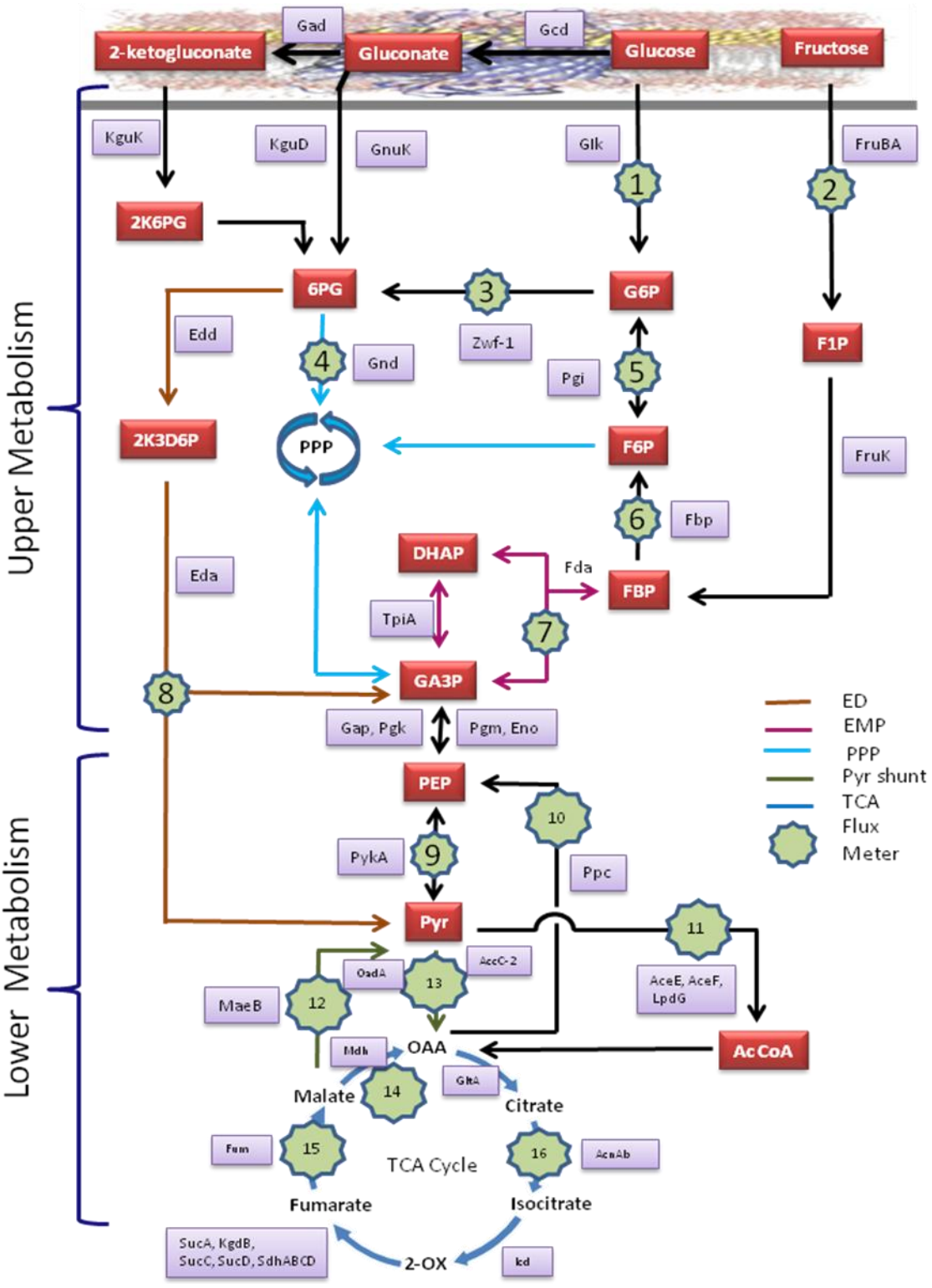

Figure 1.12: Glucose and fructose metabolism in *Pseudomonas* sp. (Modification from Chavarría et al., 2012).

In most pseudomonads, both the glucose oxidation pathways are operative with few exceptions. Contribution of periplasmic and intracellular pathways in the glucose catabolism varies in pseudomonads according to the physiological conditions and nature of substrate utilized. At least in *P. putida*, the direct import of gluconate into the cell normally accounts for only 10% of glucose metabolism, the remaining 90% occurring by direct uptake of glucose and of the 2-ketogluconate generated in the periplasmic space from glucose (del Castillo et al., 2007) (**Fig. 1.12**). *P. putida* C5V86 (Basu and Phale, 2006) and *P. citronellolis* (Fuhrer et al., 2005) exclusively catalyze glucose by intracellular phosphorylative oxidation as they lack the GDH and GADH activities whereas *P. acidovorans* lacks GLK as well as GDH thereby failing to assimilate glucose (Lessie and Phibbs, 1984). Glucose does not play central role in *Pseudomonas* as it does in *E. coli, B. subtilis* or lactic acid bacteria. In fact, the preferred carbon sources for *Pseudomonas* are some organic acids or amino acids, rather than glucose. For example, in the presence of succinate and glucose, the expression of enzymes of the *P. aeruginosa* central pathway for glucose catabolism such as G6PDH or 2-keto-3-deoxy-6-phosphogluconate (KDPG) aldolase is repressed until succinate is consumed (Rojo, F., 2010). The expression of genes for the assimilation of other sugars such as gluconate, glycerol, fructose and mannitol is also inhibited by succinate or acetate. Glucose, however, has a repressing effect on the expression of several genes, for example on the *P. aeruginosa* regulons for mannitol or histidine utilization, on the *P. aeruginosa* amidase genes, on the *P. putida* pWW0 plasmid genes for the degradation of toluene (del Castillo and Ramos, 2007), on the *P. putida* genes involved in the assimilation of methylphenol) and phenylacetic acid or on the genes required to degrade styrene in *P. fluorescens* ST (Rampioni et al., 2008).

1.2.6.2 Growth of fluorescent pseudomonads on PTS versus non-PTS sugars

Fructose is the only carbohydrate which is uptaken in fluorescent pseudomonads *via* PEP:fructophosphotransferase system, except in *P. cepacia* and certain strains of *P. saccharophila* which accumulate fructose by active transport (Lessie and Phibbs, 1984). Fructose is imported through a typical PTS permease (FruA) consisting of a fusion of EIIBFru and EIICFru domain and is then converted to fructose 1-phosphate (F1P) and fructose 1,6-bisphosphate (F1,6BisP) (Nogales et al., 2008; Puchalka et al. 2008). F1,6BisP can enter the ED pathway and/or a standard glycolytic Embden-Meyerhof-Parnas (EMP)

route (**Fig. 1.12**). Despite these differences in the earlier stages of their metabolism, glucose and fructose ultimately converge into the production of phosphoenolpyruvate (PEP) and pyruvate as the point of entry into the TCA cycle. Interestingly the carbon flux of the cell is totally different when grown on glucose as compared to fructose. The central biochemical landscape following the uptake of carbohydrate as shown in the **Fig. 1.12** divided into an upper domain (i.e., the EMP, ED, and PP pathways) for the breakdown of the hexoses into C3 compounds (pyruvate and phosphoenolpyruvate) and a lower domain that encompasses the phosphoenolpyruvate-pyruvate-oxaloacetate (PEP-Pyr-OAA) checkpoint node and the TCA cycle. In a recent study, carbon fluxes of *P. putida* were high upper metabolic domain and get reduced significantly in the lower metabolism (Chavarría et al., 2012). Bulk (~96%) of glucose was metabolized via the ED pathway to pyruvate, while the other ~4% of the sugar was channeled into the PP route (**Fig. 1.13 & 1.14**). The fate of fructose was, however, altogether different in which channeling to ED pathway occurs at ~52% whereas ~34% and ~14% are diverted into EMP and PPP, respectively.

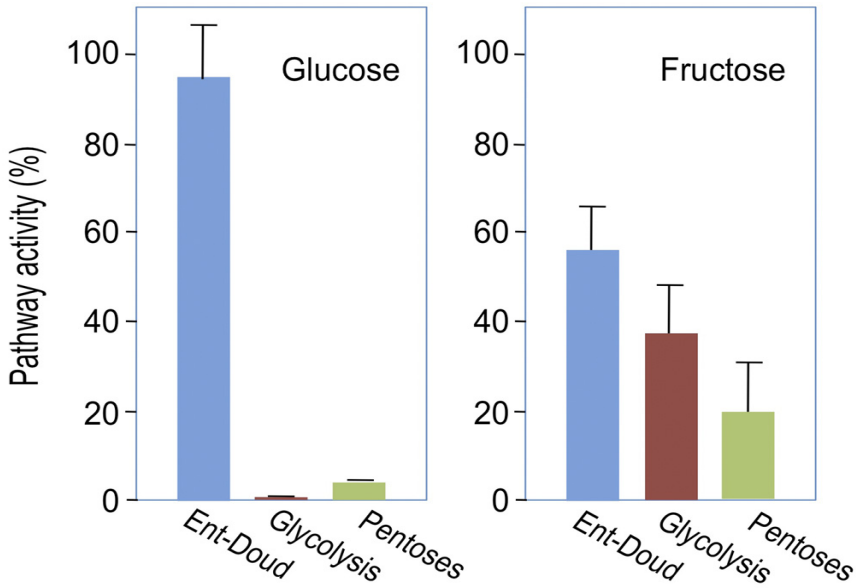

Figure 1.13: Channeling of glucose and fructose through each of the upstream sugar-catabolic pathways. The activities on the *y* axes represent the net fluxes of carbon through each of the routes calculated using metabolic flux analysis of *P. putida* MAD2 grown on the compound indicated in each case.Note that *P. putida* degrades glucose mainly through the Entner-Doudoroff (ED) pathway (~96%). Fructose is also catabolized mostly by the ED route (52%) but with an important contribution from standard glycolysis (the Embden-Meyerhof-Parnas (EMP) pathway), which accounts for ~34% of the corresponding flux (Chavarría et al., 2012).

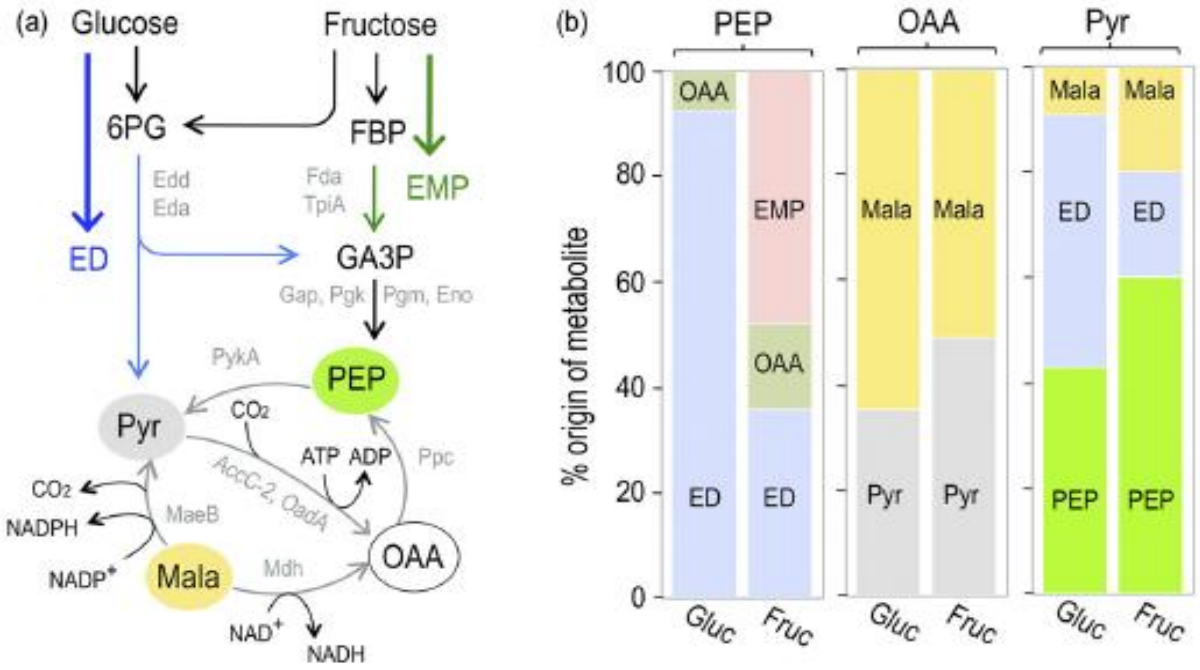

Figure 1.14: The origin of the components of the phosphoenolpyruvate-pyruvate-oxaloacetate (PEP-Pyr-OAA) node. (a) Major biochemical reactions that connect the ED and EMP routes with the malate and oxaloacetate components of the Krebs cycle (Chavarría et al., 2012). The routes necessary for the conversion of glucose and fructose into metabolic currency (Pyr and PEP) are illustrated on top along with the enzymes that belonging to the ED or the EMP pathways. The bottom highlights the reactions at the boundary between the upper and the lower metabolic domains, including the PEP-Pyr-OAA node and the Pyr shunt. (b) A breakdown of the route of key metabolites (PEP, OAA, and pyruvate) through each of the connecting reactions of the upper and lower metabolic boundaries for either glucose or fructose. The percentage of each precursor compound or pathway is indicated in every case.

1.2.6.3 Anaplerotic node in fluorescent pseudomonads

The central glycolytic/gluconeogenic pathways and the TCA cycle are metabolically linked by the crucial junction represented by the phosphoenolpyruvate–pyruvate–oxaloacetate node also referred to as *anaplerotic node* (**Fig. 1.15**) (Sauer and Eikmanns, 2005). This node comprises a set of reactions that direct the carbon flux into appropriate directions and thus, it acts as a highly relevant switch point for carbon flux distribution within the central metabolism. Under glycolytic conditions, the final products of glycolysis PEP and pyruvate enter the TCA cycle via acetyl-CoA (oxidative pyruvate decarboxylation and fueling of the cycle) and via formation of oxaloacetate by carboxylation (C3-

carboxylation). Under gluconeogenic conditions the TCA cycle intermediates oxaloacetate or malate are converted to pyruvate and PEP by decarboxylation (C4-decarboxylation) and thus, the PEP–pyruvate–oxaloacetate node provides the direct precursors for gluconeogenesis.

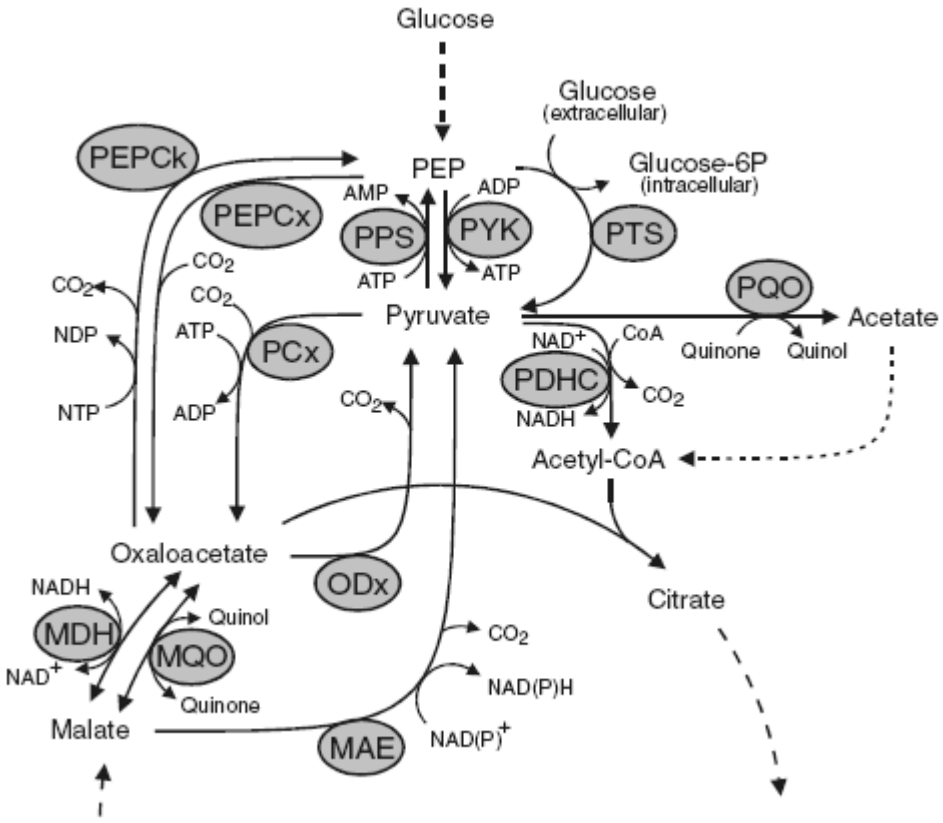

Figure 1.15 The enzymes at the PEP–pyruvate–oxaloacetate node in aerobic bacteria (Sauer and Eikmanns, 2005)). Abbreviations: MAE, malic enzyme; MDH, malate dehydrogenase; MQO, malate: quinone oxidoreductase; ODx, oxaloacetate decarboxylase; PCx, pyruvate carboxylase; PDHC, pyruvate dehydrogenase complex; PEPCk, PEP carboxykinase; PEPCx, PEP carboxylase; PPS, PEP synthetase; PQO, pyruvate: quinone oxidoreductase; PTS, phosphotransferase system; PYK, pyruvate kinase.

The anaplerotic node in pseudomonads involves PYC for oxaloacetate biosynthesis in addition to phosphoenolpyruvate carboxylase (PPC); however, the distribution of these two enzymes in *Pseudomonas* sp. varies from strain to strain (Sauer and Eikmanns, 2005). Additionally, the metabolite balance at the anaplerotic node in fluorescent pseudomonads could also be influenced by malic enzyme of the TCA cycle as well as differential metabolic regulations attributed to the general lack of a PTS for glucose uptake and the key glycolytic

enzyme phosphofructokinase. Understanding the metabolic flexibility at the anaplerotic node in fluorescent pseudomonads could be significant since oxaloacetate at the node is not only a key anabolic precursor but also is intermediate in the biosynthesis of organic acids like citric, malic, succinic, pyruvic and acetic acids, which could be implicated in P-solubilization (Khan et al., 2006). Moreover, P-limitation has been shown to affect the anaplerotic node in *Pseudomonas fluorescens* ATCC 13525 by causing a decrease in PYC activity; thereby having an adverse effect on growth (Buch et al., 2008). Buch et al (2010) showed an enhancement in P solubilization ability by manipulating the enzymes at the anaplerotic node. Heterologous overexpression of *S. elongatus* PCC 6301 *ppc* gene in *P. fluorescens* ATCC 13525 lead to 12–14-fold higher PPC activity both in M9 and TRP minimal media as compared to the control without *ppc* gene. Improved biomass yield and unaltered growth rate of *ppc* overexpressing strain along with reduced glucose consumption (80% from 89%) and decreased yields of the metabolic by-products like pyruvate and acetate, indicated efficient carbon utilization and decreased carbon overflow probably due to diversion of the carbon units towards anabolic processes. Thus, a physiological level of PYC activity at the anaplerotic node of *P. fluorescens* ATCC 13525 was apparently not optimal for efficient carbon tilization and PPC served the anaplerotic function.The enhanced direct oxidation pathway counterbalanced the reduced glucose consumption under P-sufficient condition, as demonstrated by increased gluconic acid yield and GDH activity. On TRP medium, ppc transformants of Fp315 showed faster growth, media acidification and rock-phosphate solubilization as compared to its control. Elevating the flux through the anabolic pathways in *P. fluorescens* by enhancing the biosynthesis of precursor oxaloacetate, could benefit the cellular growth under P-limitation.

1.3 Global phosphate resources and the potential of fluorescent pseudomonads as P Biofertilizers

P fertilizers are essential for maintaining and increasing the world food production. Phosphorous is completely produced from large scale mining of rock phosphate which is non renewable resources. In ancient times P was applied to agricultural soil by recycling animal manure, crushed animal bones, human and bird excreta, city waste and ash. Industrial revolution replaced this by phosphate material from non renewable resources. According to

the International Fertilizer Industry Association (IFA), in 2008, close to 53.5 million tonnes (Mt) of P_2O_5 (i.e. 175 Mt of phosphate concentrates, averaging 30.7% P_2O_5 content) was mined (IFA, 2009a). Hence there is a gradual depletion of global high-grade P resources (USGS, 2008), (Vuuren et al., 2010**;** Childers et al., 2011).

1.3.1 Depleting global P resources

According to the reports, about 40–60% of the current resource base would be extracted by 2100. At the same time, production will concentrate in Asia, Africa and West Asia, and production costs will likely have increased.

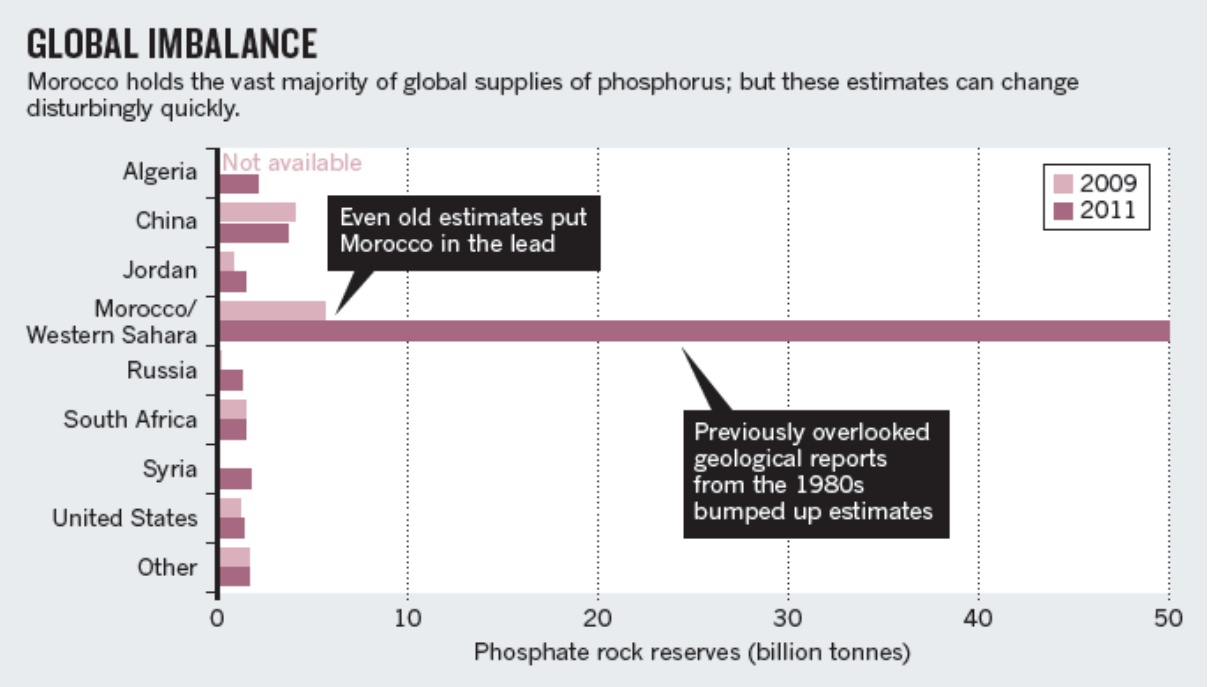

Figure 1.16: Global imbalance of P resources (Elser and Bennett, 2011).

Most of the current resource base is concentrated in Africa (Morocco) (**Fig. 1.16**). The depletion of resources outside Africa may lead to a high share of African production in world phosphate rock supply which is more than half the global production, unless new important resources are identified and exploited in other regions. Short-term focus on domestic resources may lead to higher prices and in the long run to even higher imports.

Depletion is also likely to increase phosphate production costs by about a factor of 3–5, during this century (**Fig. 1.17-1.19**).

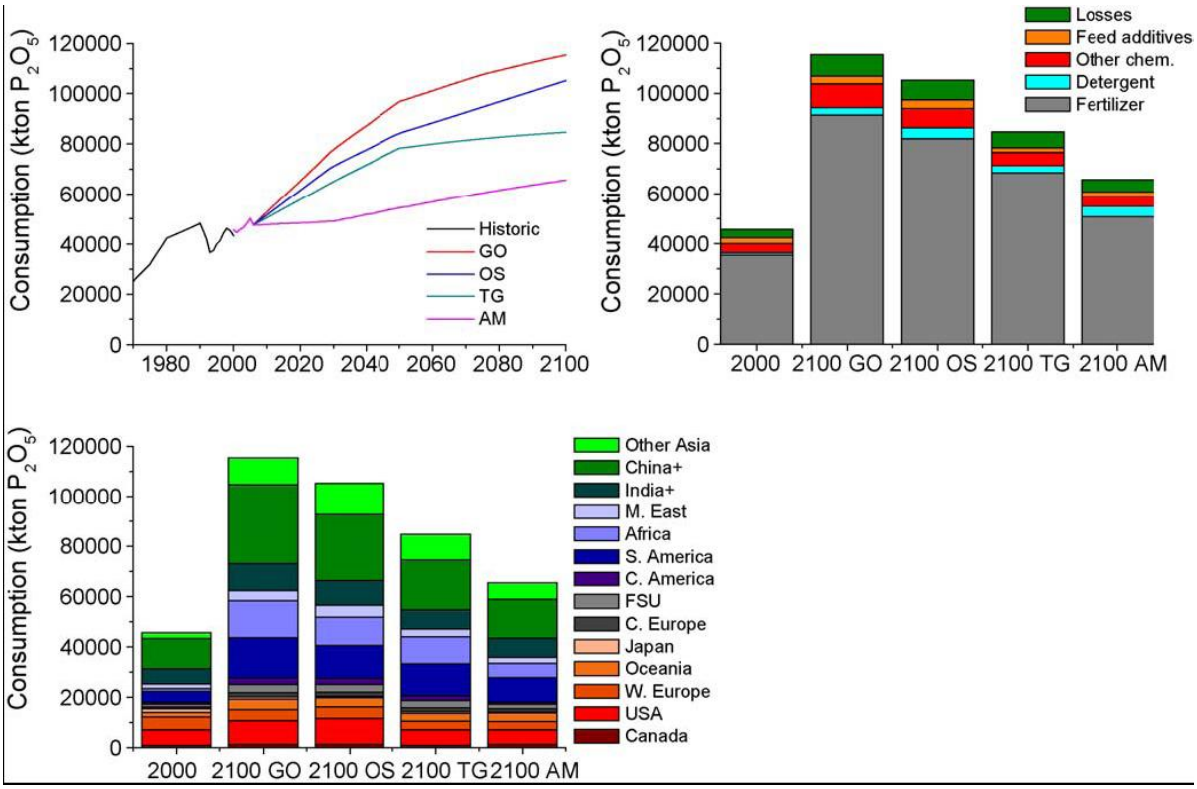

Figure 1.17: Total global P consumption (a), P use per use category (b), and P use per world region (c), for the four Millennium Ecosystem Assessment (MA) scenarios (Vuuren et al., 2010).

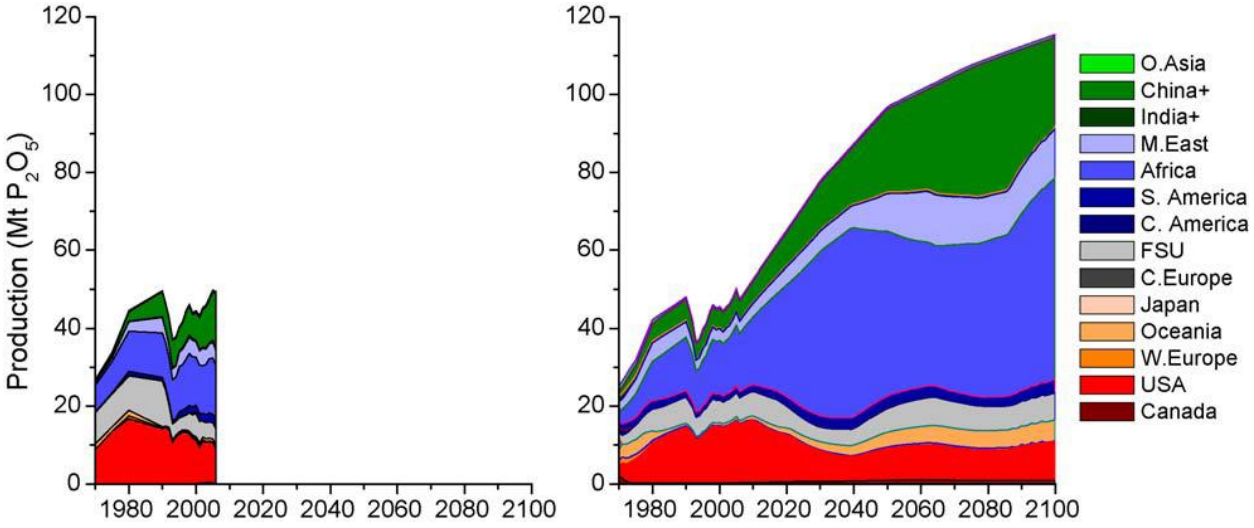

Figure 1.18: P production for the 1970–2006 period (historical data; left panel) and for the 2000–2100 period, in the Global Orchestration (GO) scenario (Vuuren et al., 2010).

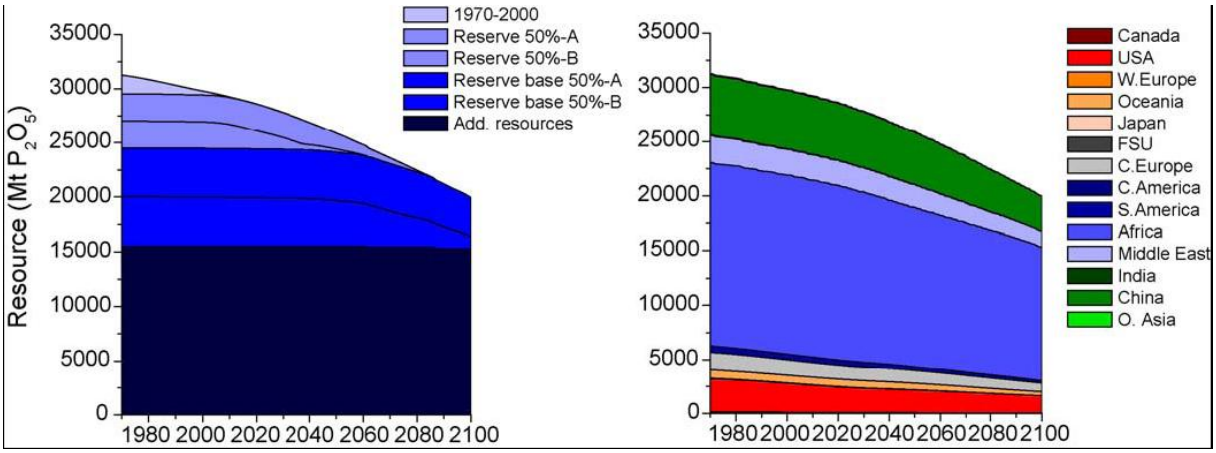

Figure 1.19: Depletion of resource base (reserves, reserve bases and additional resources) of phosphate rock under the GO scenario (default estimate) (Vuuren et al., 2010). The 1970–2000 category represents the cumulative production in this period (thus creating a best-guess resource e base estimate for 1970).

Increasing the efficiency of P application seems to be an urgent need to mitigate the increasing global P imbalance and fulfil the phosphorous requirement of crop and livestocks**.** In this context mineral phosphate solubilization by microbes like *P. fluorescens* holds tremendous importance. Exploitation of phosphate solubilizing bacteria through biofertilization has enormous potential for making use of ever increasing fixed P in the soil, and natural reserves of phosphate rocks. (Elser and Bennet, 2011).

1.3.2 Phosphate solubilization by fluorescent pseudomonads

Phosphorous is one of the major nutrient limiting plant growth.70% of the phosphate present in the soil is in the complexed form which is unavailable to plants. Soluble P-ion oncentration in most soils varies from 0.1 to 10µM while P required for optimal growth ranges from 1 to 60 µM. Thus, inspite of abundant phosphate in the soil the plants show phosphate deficient conditions. Phosphate solubilizing microorganisms (PSM) are the most promising bacteria among the plant growth promoting rhizobacteria (PGPR); which may be used as biofertilizers for plant growth and nutrient use efficiency in phosphate deficient soil. Rhizospheric microorganisms including bacteria like few *Pseudomonas* sp., *Serratia*,

Bacillus sp, *Rhizobium* sp., *Azotobacter*, *Azospirullum* and fungi like *Aspergillus*, *Penicillium*, etc. (Archana et al., 2012) are now known to act as powerful PSMs.

Fluorescent pseudomonads act as one of the promising plant growth promoting rhizobacteria. These PSMs dissolve the soil P through production of low molecular weight organic acids including the mono-, di- and tri-carboxylic acids like acetic, lactic, oxalic, tartaric, succinic, citric, gluconic, 2-ketogluconic, formic, malic, pyruvic and glyoxalic acid (**Table 1.3**).

Table 1.3: Organic acid secreted by phosphate solubilizing pseudomonads (Reframmed from Archana et al 2012).

Fluorescent pseudomonads	Organic acid secreted
Pseudomonas cepacia	Gluconic and 2-ketogluconic
P. fluorescens	Gluconic, Citric, Formic, Lactic, Oxalic
P. fluorescens RAF15	Gluconic,2-ketogluconic, Tartaric
Pseudomonas corrugata NRRL B-30409	Gluconi, 2-ketogluconic
Pseudomonas sp	Lactic
P. trivialis	Gluconic,2-ketogluconic,lactic,formic, oxalic, citric
P. poae	Gluconic,formic,lactic,oxalic acid,Citric
P. fluorescens AF15	Formic
P. aeruginosa	Gluconic
P. corrugata	Gluconic
P. striata	Oxalic, succinic, Tartaric Fumaric, glyoxalic, isovaleric, isobutyric,Itaconic, ketobutyric, malonic, propionic
P. aerogenes	Fumaric, Lactic,acetic glyoxalic, isovaleric, isobutyric, Itaconic, ketobutyric, malonic, propionic

The hydroxyl and carboxyl groups of these acids chelate cations (Al, Fe, Ca) and make the P available for plants. in addition to lowering the pH of rhizosphere (Deubel *et al.*, 2000; Stevenson, 2005). The pH of rhizosphere is lowered through biotical production of proton/bicarbonate release (anion/cation balance) and gaseous (O_2/CO_2) exchanges.

Inorganic acids e.g. hydrochloric acid can also solubilize phosphate but they are less effective compared to organic acids at the same pH (Kim *et al.*, 1997). In certain cases phosphate solubilization is induced by phosphate starvation (Gyaneshwar *et al.*, 1999). A general sketch of P solubilisation and mechanisms in soil by bacteria is shown in **Fig. 1.20** and **Fig. 1.21**.

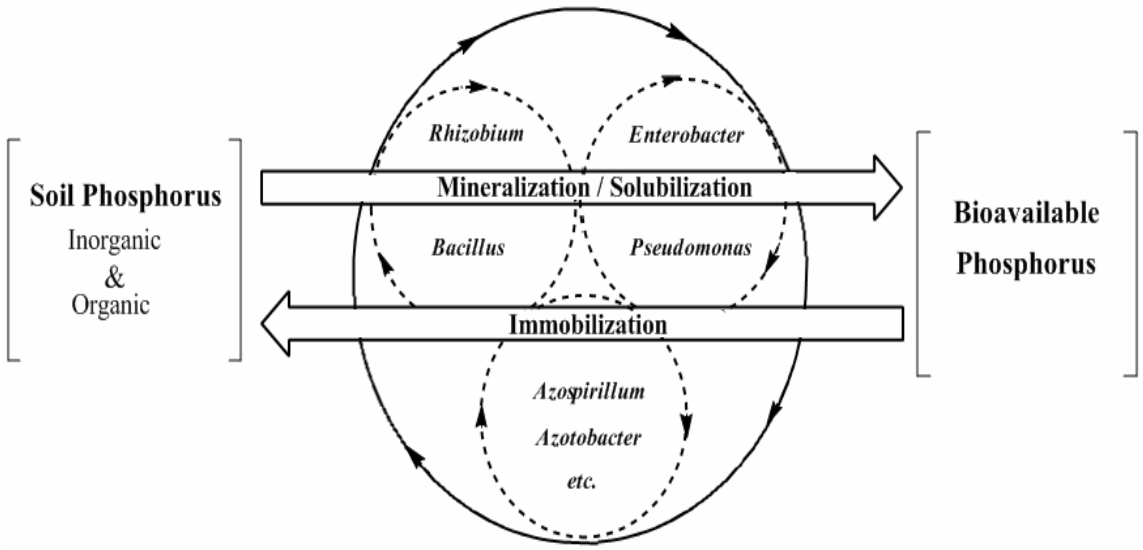

Figure 1.20: Schematic diagram of soil phosphorus mobilization and immobilization by bacteria (Khan et al., 2009).

Plant inoculation experiments resulted in variable effects on P supply, plant growth and crop yields (Gyaneshwar et al., 2002). These varied effects are attributed to the nature of the soil and survival of inoculated microbes in the rhizosphere and their colonizing ability. Also, the nature and amount of organic acids limit the efficacy of PSM in soils and in field conditions (Gyaneshwar *et al.*, 2002; Khan *et al.*, 2007; Srivastava *et al.*, 2006). High buffering capacity of soil reduces the effectiveness of PSB in releasing P from bound phosphates.

Insertion of P-solubilizing genes in agriculturally important microorganisms lacking P-solubilizing ability or enhancing the microbial activity of weak PSMs has been an attractive approach to develop beneficial microbes with improved utility as soil inoculants (Rodriguez et al., 2006). Goldstein and Liu (1987) cloned a gene from *Erwinia herbicola*

that is involved in mineral phosphate solubilization by screening the antibiotic-resistant recombinants from a genomic library in a medium containing hydroxyapatite as the source of P. The expression of this gene allowed production of gluconic acid and mineral phosphate solubilization activity in *E. coli* HB101. Sequence analysis of this gene (Liu et al., 1992) suggested its probable involvement in the synthesis of the enzyme pyrroloquinoline quinone (PQQ) synthase, which directs the synthesis of PQQ. Several Gram-negative bacteria are capable of producing organic acids by such direct oxidation of aldehydes, which then get diffused in surroundings and help in the acidification of poorly soluble mineral phosphates (Goldstein 1986; Sashidhar and Podile, 2010). Glucose dehydrogenase (GDH) requires PQQ as a redox cofactor for direct oxidation of glucose to gluconic acid, which then diffuses in the soundings of bacterial niche and helps in acidic solubilization of insoluble phosphates in soil. Both membrane-bound and soluble forms of GDH, in spite of having different substrate specificity, use PQQ as a cofactor.

The role of PQQ as a redox coenzyme has been reported for several dehydrogenases, including methanol dehydrogenase, ethanol dehydrogenase and GDH. There are plant growth-promoting bacteria that use GDH-PQQ holoenzyme for solubilization of inorganic phosphates in soil (Han et al. 2008). These studies suggest that microbes producing PQQ can increase the phosphate availability in soil for the growth and development of crop plants, which in turn increase crop productivity (Mishra et al., 2012). Following a similar strategy, a mineral phosphate solubilization gene from *Pseudomonas cepacia* was isolated (Babu-Khan et al., 1995). This gene (*gabY*), whose expression also allowed the induction of the mineral phosphate solubilization phenotype via gluconic acid production in *Escherichia coli* JM109, showed no apparent homology with the previous cloned PQQ synthetase gene (Goosen et al., 1989), but it did with a permease system membrane protein. The *gabY* gene could play an alternative role in the expression and/or regulation of the direct oxidation pathway in *P. cepacia*, thus acting as a functional mineral phosphate solubilization gene *in vivo*.

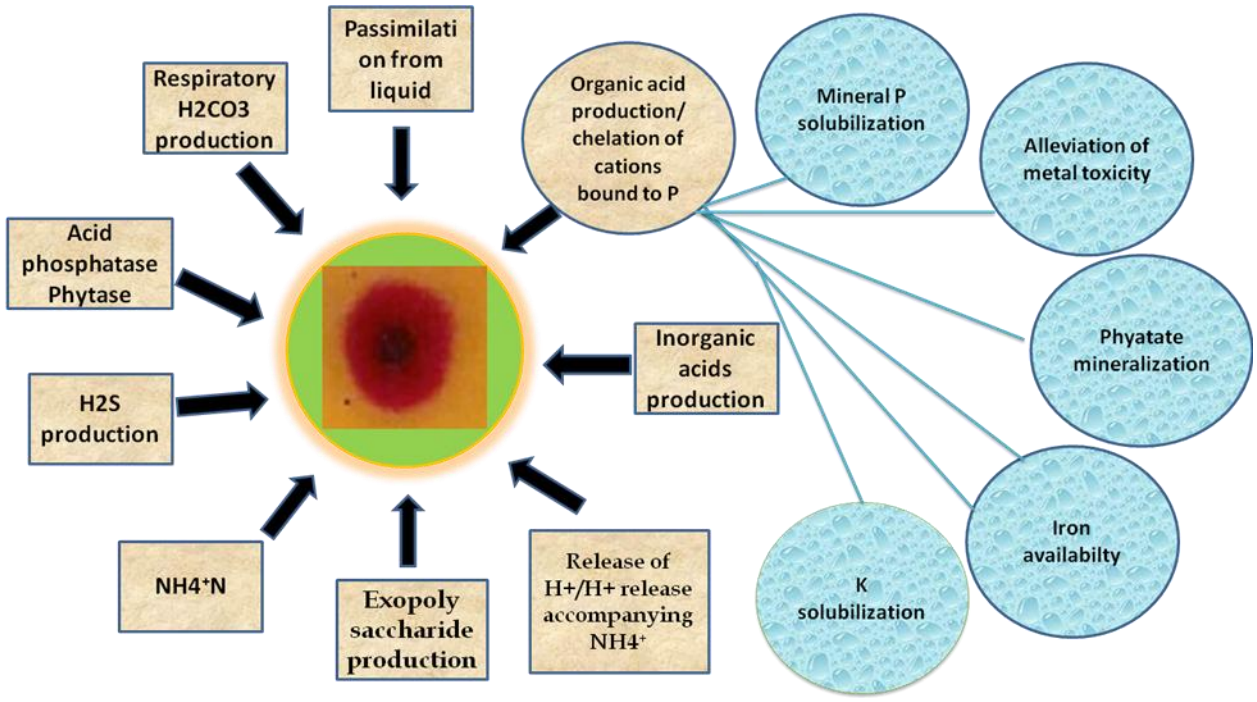

Figure 1.21: Mechanism of p solubilization by phosphate solubilizing bacteria and role of organic acid secretion in plant growth promotion (Redrawn from Archana et al., 2012).

Fluorescent pseudomonads are efficient biocontrol PGPR which also find application in bioremediation. Beneficial effects of the inoculation with *Pseudomonas* sp. to many crop plants have been well established (Brundrett, 2009; Gianinazzi *et al*., 2010). Additional mineral phosphate solubilizing ability would help enhancing the efficacy of these pseudomonads as a phosphate biofertilizer.

1.3.3 Role of citric acid in P solubilization

The secretion of gluconic acid is the major mechanism of P-solubilization by gram negative bacteria (Goldstein 1995; Kim et al., 1998). The acidification of soil by organic acids depends on both the nature and quantity of the organic acid for e.g. acetic, lactic and succinic at 100 mM bring about a drop in pH of a soil solution from around 9.0 to about 6.0; a similar drop is brought about by only 20 mM of gluconic acid, 10 mM of oxalic acid and even lesser amount of citric and tartaric acids (Gyaneshwar et al. 1998; Srivastava *et al.*, 2006) (**Table 1.4**). Addition of organic acids decreases the pH of the alkaline vertisol soil solution in the order Acetic = Succinic = Lactic < <Gluconic < <Oxalic < Tartaric = Citric

and results in P release in a similar order. *Penicillium billai* secretes 10 mM each of citric and oxalic acids (Cunningham & Kuiack, 1992) and has been shown to be effective in releasing P in the field conditions (Asea et al., 1988). On the other hand, *C. koseri* and *B. coagulans* were found to secrete various organic acids in the range 1-5 mM whereas as the concentration of these acids required to reduce the pH of the soil was 20-50 times more.

Table 1.4: Organic acids for phosphate solubilisation in different soil types (Srivastava *et al*.,2006).

Organic acid	**Alkaline vertisol pH > 7**	**Acidic alfisol supplemented with RP pH < 7**
Citric acid	10 mM	10-20Mm
Oxalic acid	10 mM	5-10 mM
Gluconic acid	20mM	50mM
Tartaric acid	10mM	20mM

Citric acid has better chelation properties due to presence of its three –COOH group's having pKa values of 3.15, 4.77, and 6.40, respectively. Hence, fluorescent pseudomonads producing citric acid could be effective as P biofertilizers in alkaline soils.

1.3.4 Metabolic engineering strategies in fluorescent pseudomonads for P solubilization by citric acid.

Secretion of oxalic acid and citric acid is a well reported phenomena in *Pseudomonas fluorescens* exposed to Al toxicity.CS, an enzyme that condenses oxaloacetate and acetylCoA to citrate, experienced a two-fold increase activity in the Al-stressed cells, compared to the control cells. While a six fold increase in fumarase activity and five fold decrease malate synthase activity was found in the Al-stressed cells compared to the controls (Apanna et al., 2003). Excretion of citric acid by anamorphic fungi *viz*., *Aspergillus* and *Penicillium* is a frequent phenomenon in natural habitats and in laboratory cultures (Wolfgang 2006). Naturally pseudomonads do not secrete any citric acid. The role of citrate synthase (CS) in citric acid biosynthesis and glucose catabolism in pseudomonads was investigated by overexpressing the *Escherichia coli gltA* gene in *Pseudomonas*

fluorescens ATCC 13525 (Buch et al., 2009.). Approximately, 2-fold increase in CS activity in the *gltA* overexpressing strain was observed with an enhanced intracellular and extracellular citric acid yields during the stationary phase, by about 2- and 26-fold, respectively, as compared to the control, without affecting the growth rate, glucose depletion rate or biomass yield. This is in contrast to the earlier reports from the known citric-acid producing bacteria, in which increase in CS activity is either the result of a TCA block in the form of *icd* mutation or is in response to aluminium toxicity **(**Barone et al., 2008). Increasing CS activity in *P. fluorescens* for citric acid overproduction from glucose is a better strategy than *icd* mutation in *E. coli*, which reduces biomass and growth (Aoshima et al., 2003).

1.4 Rationale of thesis

Fluorescent pseudomonads are well known for the biochemical and metabolic diversity. Genome sequence of several *Pseudomonas* sp. and metabolic data reveals that there are lot of interspecies diversity in terms of occurrence and regulation of enzymes at the central metabolism and PEP-Pyruvate-OAA node. This study is an effort to genetically engineer a stable system for phosphate biofertilizer and to examine its applicability amongst diverse fluorescent pseudomonads. Present study describes improvement in citric acid secretion in fluorescent pseudomonads to the required amount for P release from soils. Additionally, the genetic manipulations need be directed to the chromosomal integration as it would lead not only to increased stability but also decrease the metabolic load caused by the presence of the plasmids in the bacterial cell (Buch et al., 2010; Sharma et al., 2011).The overall strategy of the present study is depicted in **Fig. 1.22**.

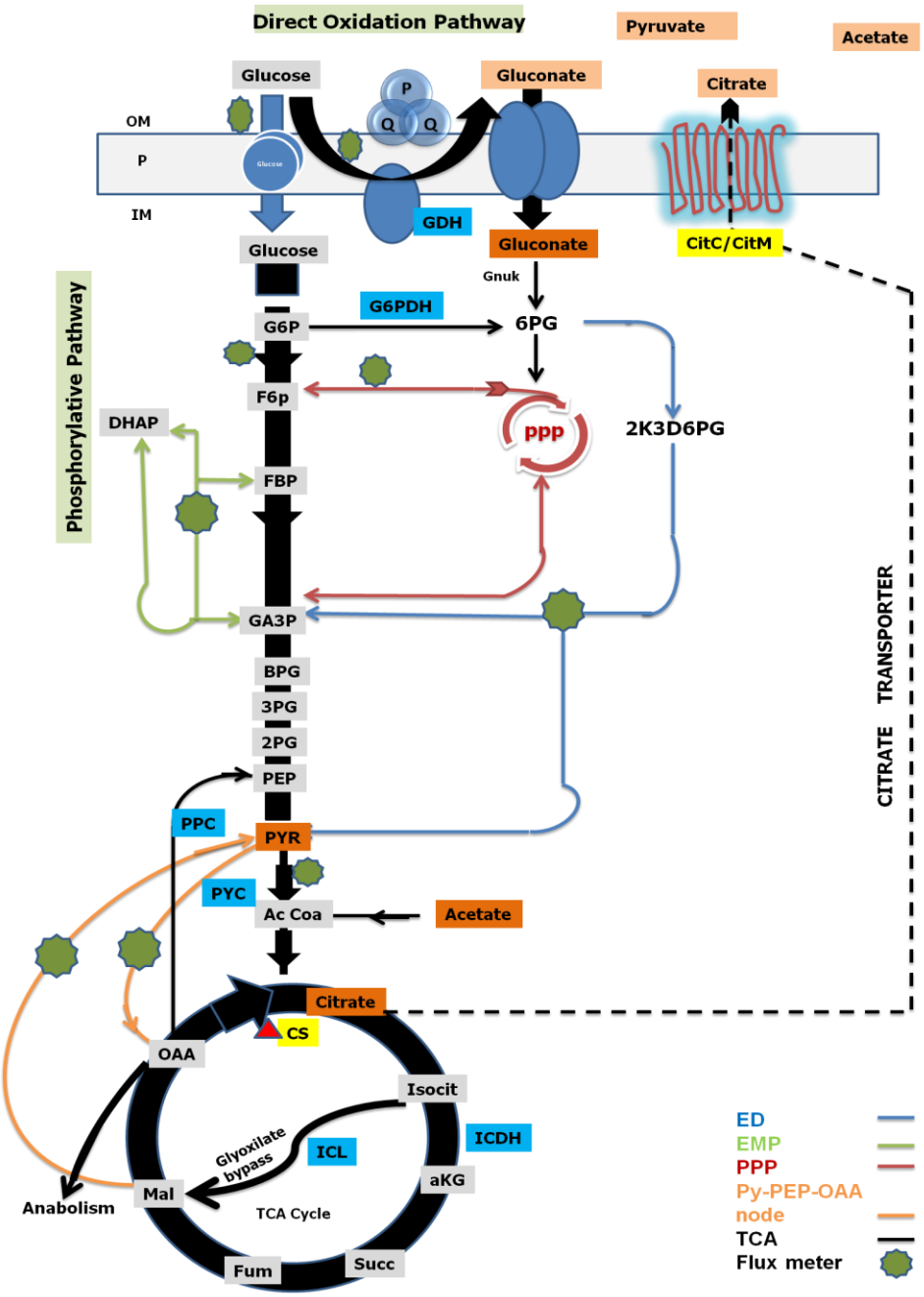

Figure 1.22: Design and analysis of genetic modification in fluorescent pseudomonads. Yellow boxes indicate the gene heterologously overexpressed, red triangle attached to the CS indicate NADH insensitivity.Blue bosex indicate those enzymes whose fluctuations are reported due to genetic modification. Orange boxes indicate the metabolite whose change is being monitored both intracellular and extracellular. Abbreviations: *ppc*, phosphoenolpyruvate carboxylase; *cs*, citrate synthase; *pyc*, pyruvate carboxylase; *pyk*, pyruvate kinase; *icl*, isocitrate lyase; *icd*, isocitrate dehydrogenase; *pdh*, pyruvate dehydrogenase complex, *glt*, glucose transporter; *glk*, glucokinase; *zwf*, glucose-6-phosphate dehydrogenase; *edd*, 6-phosphogluconate dehydratase and *eda*, 2-keto-6-phosphogluconate aldolase

1.5 Objectives

The objectives of the present study were defined as follows-

1. Effect of constitutive heterologous overexpression of *E. coli* NADH insensitive *cs* in *Pseudomonas fluorescens* Pfo-1

2. Metabolic characterization of engineered *Pseudomonas fluorescens* Pfo1coexpressing *E. coli* NADH insensitive CS and *Salmonella typhimurium* sodium citrate transporter or *Bacillus subtilis* magnesium dependent citrate transporter operon.

3. Evaluation of the effect of engineered genetic modifications on P-solubilizing ability of plant growth promoting rhizospheric fluorescent pseudomonads.

4. Genomic integration of *E. coli* NADH insensitive CS and *Salmonella typhimurium* Na^{+}/*Bacillus subtilis* Mg^{+2}–dependent citrate transporter operon in the genome using a Mini-Tn7 transposon and study their effects on P solubilisation and plant growth promotion.

MATERIALS and METHODS

CHAPTER 2

2 Materials and Methods

2.1 Bacterial strains / Plasmids

All the plasmids use in the present study and their restriction maps are given in **Table 2.1** and **Fig. 2.1**.The wild type and genetically modified *E. coli* and *Pseudomonas* strains are listed in **Table 2.2 and 2.3**. *E. coli* DH5α was used for all the standard molecular biology experiments wherever required. The NADH insensitive *cs* mutant plasmid was a generous gift from Prof Harry Duckworth, University of Manitoba, Canada. The *glt*A (citrate synthase gene) mutant of *E. coli* was obtained from *E. coli* Genetic Stock Center. The mini Tn7 delivery and helper plasmid for genomic integration was a generous gift from Prof. Soren Molin, Technical University of Denmerk.

Table 2.1: List of plasmids used in the present study.

Plasmids	Features	Reference
pUCPM18	pUC18 derived Broad-Host-Range vector; Ap^r	Hester et al., 2000
pUCPM18 Gm	pUC18 derived Broad-Host-Range vector; Ap^r Gm^r	Ch 3
pAB8	pUCPM18 with *kan*^{r} gene; Amp^r, Km^r	Buch et al., 2009
pBluescript/KS	Cloning vector for *E. coli*; Ap^r	Sambrook et al, 2000
pTZ57R/T	T vector	MBI Fermentas
pTZ57R/T *R163L*	T vector with *E. coli* NADH insensitive gene R163L	Ch 3
pTZ57R/T *K167A*	T vector with *E. coli* NADH insensitive gene R163L	Ch 3
pTZ57R/T *Y145F*	T vector with *E. coli* NADH insensitive gene R163L	Ch 3
pTZ57R/T *CitM*	T vector with *E. coli* NADH insensitive gene R163L	Ch 4

pCS-Ec	pBluescript with *cs* gene of *E. coli*; Ap^r	Delhaize, E
pAB7	pUCPM18 with *E. coli cs* gene under P_{lac} and kan^r gene; Ap^r, Km^r	Buch et al., 2009
R163L	NADH insensitive cs gene	Duckworth, H., 2003
K167A	NADH insensitive cs gene	Duckworth, H., 2003
Y145F	NADH insensitive cs gene	Duckworth, H., 2003
pR163L	pUCPM18 with NADH insensitive cs gene, Amp^r, Km^r	Ch3
pK167A	pUCPM18 with NADH insensitive cs gene, Amp^r, Km^r	Ch3
pY145F	pUCPM18 with NADH insensitive cs gene, Amp^r, Km^r	Ch3
pCitC	pUCPM18 with *CitC* gene, Amp^r, Gm^r	Ch4
pCitM	pUCPM18 with *CitM* gene, Amp^r, Gm^r	Ch4
pYC	pUCPM18 with Y145F and CitC gene under p*lac*, Amp^r, Gm^r	Ch4
AKN68	pUXBF-13 , Helper plasmid providing the Tn7 transposase proteins	Lambertsen et al., 2004
AKN69	Mini Tn7(Gm)$P_{A1/04/03\text{-}eyfp}$, plasmid Amp^r,Gm^r, Cm^r	Lambertsen et al., 2004
pYC Int	p*lac yc* operon cloned into AKN69 plasmid, Amp^r,Gm^r, Cm^r	Ch5

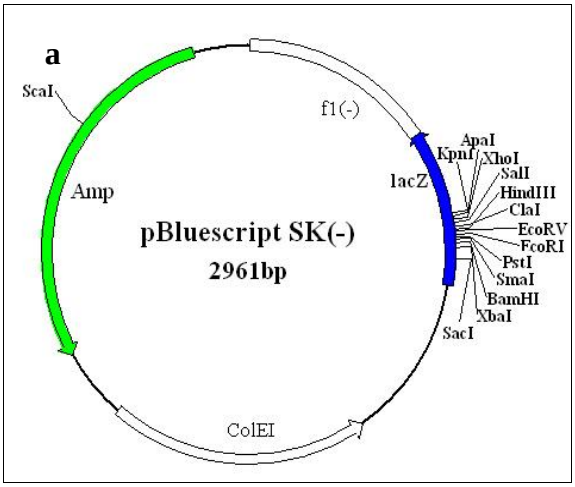

pBluescript KS: cloning vector Amp^r

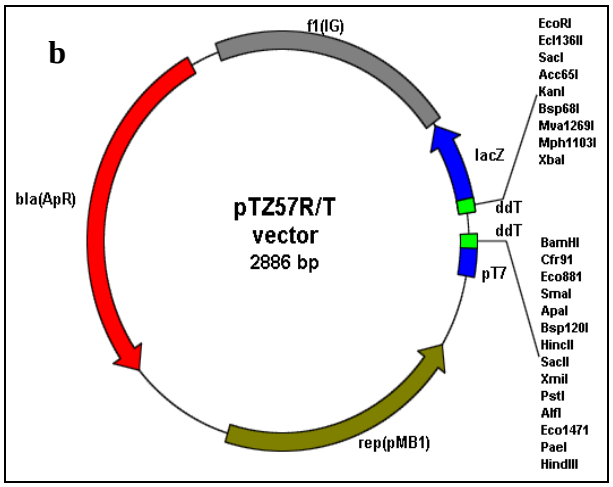

pTRZ57/R: TA cloning vector Amp^r

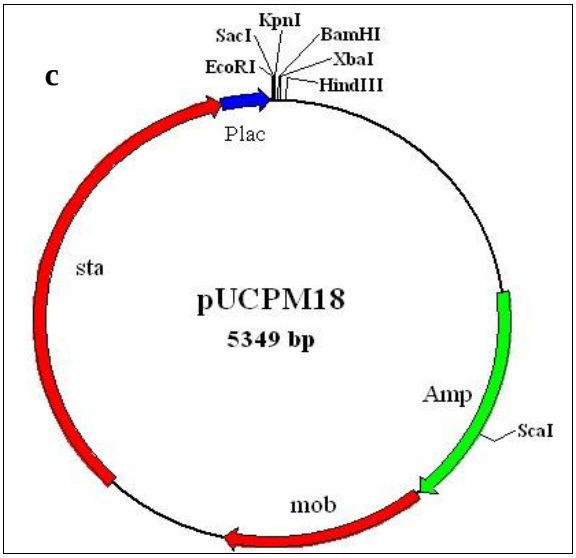

Generous gift from Dr. J. R. Sokatch, University of Oklahoma Health Sciences

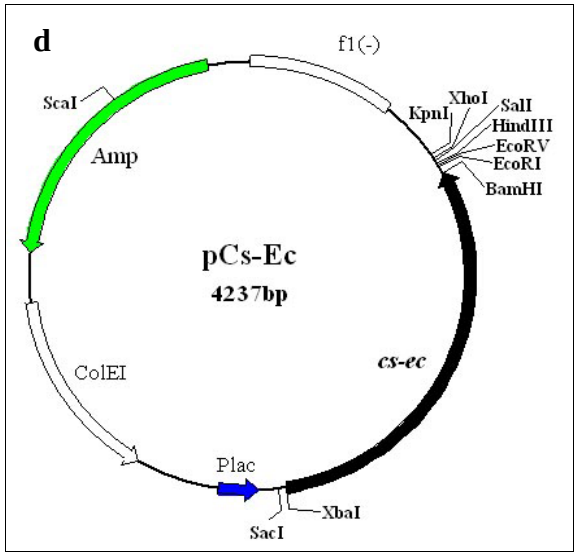

Generous gift from Dr. Delhaize, E., CSIRO Plant Industry, Australia

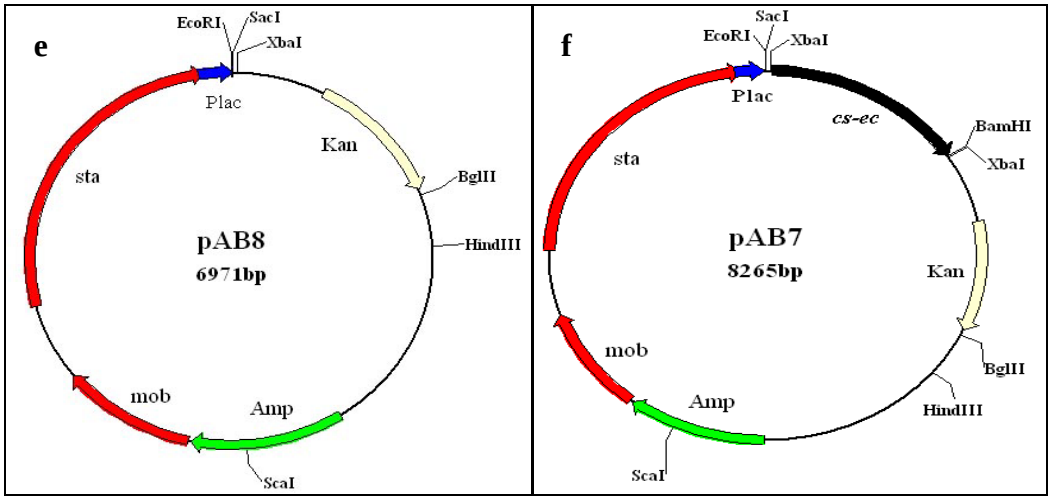

pUCPM18 plasmid containing kanamycin resistance gene (Buch et al., 2008)

pUCPM18 plasmid containing wild type *E. coli* citrate synthase gene, Km^r (Buch et al., 2008)

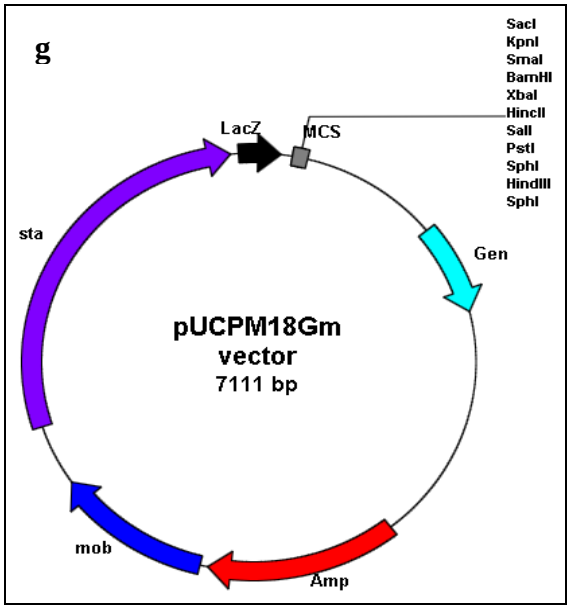

pUCPM18 plasmid containing gentamycin resistance gene (Buch et al., 2008)

Fig. 2.1: Restriction maps of the plasmids used in this study. (a) and (b) are standard pBluescript and TA plasmid used for conventional cloning in *E. coli*.,(c),(e) and (g), are the broad-host-range vectors used for expression of heterologous genes under *lac* promoter in *P. fluorescens*., (d) and (f) are plasmids used to obtain *cs*, genes.

Broad host range, multicopy plasmid vectors, pUCPM18 and pBBR1MCS-2, were selected for expression in pseudomonads on account of their small size and versatile multiple cloning sites. **pUCPM18** plasmid is derived from a pUC-derivative, pUCP18 plasmid which is stably maintained in both *E. coli* and *Pseudomonas* species (Schweizer, 1991). pUCPM18 was developed from pUCP18 (GenBank accession number: U07164) by incorporating a 750bp mob fragment from pLAFRI (broad host range vector used for genetic analysis of gram-negative bacteria; Vanbleu et al., 2004), in order to enable convenient mobilization within *Pseudomonas* species (Hester et al, 2000). It replicates in *E. coli* using ColE1 origin of replication (*ori*) while in *Pseudomonas* it replicates owing to a pRO1614 derived DNA fragment encoding a putative *ori* and a replication-controling protein (West et al., 1994).

Table 2.2: List of *E. coli* strains used in the present study

Bacterial Strains	Genotype	Reference
E. coli DH5α	*lacI*^{q} *rrnBT14 DlacZWJ16 hsdR514 DaraBADAH33,DrhaBADLD78* ***ppc****::Km*; Km^{r}	Peng et al., 2004
E. coli W620	CGSC 4278 - *glnV44* ***gltA6*** *galK30 LAM- pyrD36 relA1 rpsL129 thi*$^{-1}$; Str^{r}	*E. coli* Genetic Stock Center
E. coli S17.1	*thi pro hsdR recA RP4-2* (Tet::Mu) (Km::Tn7); Tmp^{r}	Simon et al., 1983
DH5α (pAB8)	*E. coli* DH5α with pAB8 plasmid; Ap^{r}, Km^{r}	Buch et al
DH5α (pAB7)	*E. coli* DH5α with pAB7 plasmid; Ap^{r}, Km^{r}	Buch et al
DH5α (pR163L)	*E. coli* DH5α with pR163L plasmid; Ap^{r}, Km^{r}	Ch 3
DH5α (pK167A)	*E. coli* DH5α with pK167A plasmid; Ap^{r}, Km^{r}	Ch 3
DH5α (pY145F)	*E. coli* DH5α with pY145F plasmid; Ap^{r}, Km^{r}	Ch 3

W620 (pAB8)	*E. coli* W620 with pAB7 plasmid; Str^r, Ap^r, Km^r	Ch 3
W620 (pAB8)	*E. coli* W620 with pAB8 plasmid; Str^r, Ap^r, Km^r	Ch 3
W620 (pR163L)	*E. coli* W620 with (pR163L) plasmid; Str^r, Km^r	Ch 3
W620 (pK167A)	*E. coli* W620 with (pK167A)plasmid; Str^r, Km^r	Ch 3
W620 (pY145F)	*E. coli* W620 with (pY145F) plasmid; Str^r, Km^r	Ch 3
S17.1 (pAB7)	*E. coli* S17.1 with pAB7 plasmid; Tmp^r, Amp^r, km^r	Ch 3
S17.1 (pAB8)	*E. coli* S17.1 with pAB8 plasmid; Km^r, Amp^r,	Ch 3
S17.1 (p R163L)	*E. coli* S17.1 with pAB8 plasmid; Km^r, Amp^r,	Ch 3
S17.1 (p K167A)	*E. coli* S17.1 with pAB8 plasmid; Km^r, Amp^r,	Ch 3
S17.1 (p Y145F)	*E. coli* S17.1 with pAB8 plasmid; Km^r, Amp^r,	Ch 3
E.coli JM105 AKN69	*E. coli* JM105 with AKN69 plasmid Gm^r, Cm^r	Klausen et al., 2003
E.coli SM10λpir AKN68	*E. coli* SM10λpir with AKN68 plasmid	Bao et al., 1991

Amp=Ampicillin; Km=Kanamycin; Gm=Gentamycin; Str^r =Streptomycin; Cm= Chloramphenicol;

^{r} = resistant.

Table 2.3: List of *Pseudomonas* strains used in the present study

P. fluorescens **Strains**	**Genotype/Relevant characteristics**	**Reference**
ATCC 13525	Wild Type	Ch5, Ch6
PfO-1	Wild Type	Ch3-Ch6
Pf-5	Wild Type	Ch5,Ch6
CHAO-1	Wild Type	Ch5,Ch6
P109*	Wild Type	Ch5,Ch6
Fp315*	Wild Type	Ch5,Ch6
PfO-1 (AB7)	*P. fluorescens* PfO-1with pAB7 plasmid; Tc^r	Ch3
PfO-1 (pAB8)	*P. fluorescens* PfO-1with pAB8 plasmid; Tc^r	Ch3
PfO-1 (pR163L)	*P. fluorescens* PfO-1with pR163L plasmid; Km^r	Ch3
PfO-1 (pK167A)	*P. fluorescens* PfO-1with pK167A plasmid; Km^r	Ch3
PfO-1 (pY145F)	*P. fluorescens* PfO-1with pY145F plasmid; Km^r	Ch3
PfO-1 (pYFpCitC)	*P. fluorescens* PfO-1with pY145F and pCitC plasmid; Amp^r,Km^r Gm^r	Ch4
PfO-1 (pYFpCitM)	*P. fluorescens* PfO-1with pY145F and pCitM plasmid; Amp^r,Km^r Gm^r	Ch4
PfO-1 (pYC)	*P. fluorescens* PfO-1with pYC plasmid; Gm^r	Ch4
PfO-1 (Int)	*P. fluorescens* PfO-1 genomic integrant Amp^r, Gm^r	Ch5
ATCC 13525 (pYC)	*P. fluorescens* ATCC 13525 with *pYC* plasmids;Amp^r, Gm^r	Ch6
ATCC 13525 (Int)	*P. fluorescens* ATCC 13525 genomic integrant Amp^r, Gm^r	Ch5,Ch6

Pf-5(pYC)	*P. fluorescens* Pf-5 with *pYC* plasmids; Amp^r, Gm^r	Ch6
Pf-5 (Int)	*P. fluorescens* Pf-5 genomic Integrant Amp^r, Gm^r	Ch5, Ch6
CHAO-1(pYC)	*P. fluorescens* CHAO-1 with *pYC* plasmids; Amp^r,Gm^r	Ch6
CHAO (Int)	*P. fluorescens* CHAO-1 genomic Integrant Amp^r, Gm^r	Ch5, Ch6
P109 (pYC)	*P. fluorescens* P109 with *pYC* Amp^r, Gm^r	Ch6
P109 (Int)	*P. fluorescens* P109 genomic Integrant Amp^r, Gm^r	Ch5, Ch6
Fp315(pYF)	*P. fluorescens* Fp315with *pYF* Amp^r, Km^r	Ch5
Fp315(pYC)	*P. fluorescens* Fp315with *pYC* Amp^r, Gm^r	Ch6
. Fp315(Int)	*P. fluorescens* Fp315 genomic Integrant Amp^r, Gm^r	Ch5, Ch6

Km^r = Kanamycin; Gm^r = Gentamycin; resistant. *P. fluorescens* strains including native isolates were used to incorporate genetic modifications and for further physiological studies.*Fluorescent pseudomonads isolated from wheat rhizosphere were a generous gift from **Prof. B. N. Johri, Pantnagar University**. These isolates were already characterized with respect to P-solubilization ability on Pikovaskya's (PVK) Agar and ACC Deaminase activity as a marker for plant growth promoting ability

2.2 Media and Culture conditions

The *E. coli* strains and pseudomonads were cultured and maintained on Luria Agar (LA) and Pseudomonas Agar respectively (Hi-Media Laboratories, India). *E. coli* cultures were grown at 37ºC while all *Pseudomonas* cultures were grown at 30ºC. For growth in liquid medium, shaking was provided at the speed of 200rpm. The plasmid transformants of both *E. coli* and pseudomonads were maintained using respective antibiotics at the final concentrations as mentioned in **Table 2.4** as and when applicable. Both *E. coli* and *Pseudomonas* wild type strains and plasmid transformants grown in 3ml Luria broth (LB) containing appropriate antibiotics were used to prepare glycerol stocks which were stored at -20ºC.

Table 2.4: Recommended dozes of antibiotics used in this study (Sambrook et al 2000).

Antibiotic	Rich medium	Minimal medium
Tetracycline	30µg/ml	**7.5µg/ml**
Kanamycin	50µg/ml	**12.5µg/ml**
Streptomycin	10µg/ml	**2.5µg/ml**
Trimethoprim	60µg/ml	**15µg/ml**
Ampicillin	50µg/ml	**12.5µg/ml**
Erythromycin	100µg/ml	-
Chloramphenicol*	20µg/ml	-
Spectinomycin	50µg/ml	-
Gentamycin*	20µg/ml	-

The antibiotic dozes were maintained same for both *E. coli* and pseudomonads. All the antibiotics were prepared in sterile distilled water at the stock concentrations of 1000x or 2000X (for antibiotics marked with *) and were used accordingly to have the desired final concentrations.

The compositions of different minimal media used in this study are as described below. Antibiotic concentrations in all the following minimal media were reduced to 1/4th of that used in the above mentioned rich media (**Table 2.4**).

2.2.1 Koser's Citrate medium

Composition of the Koser's Citrate medium included magnesium Sulphate, 0.2g/L; monopotassium phosphate, 1.0g/L; sodium ammonium phosphate, 1.5g/L; sodium citrate, 3.0g/L and agar, 15g/L. The readymade media was obtained from Hi-Media Laboratories, India, and was used according to manufacturer's instructions.

2.2.2 M9 minimal medium

Composition of M9 minimal broth was according to Sambrook et al (2000) including Na_2HPO_4 $7H_2O$, 34g/L; KH_2PO_4, 15g/L; NH_4Cl, 5g/L; NaCl, 2.5g/L; 2mM $MgSO_4$; 0.1mM $CaCl_2$ and micronutrient cocktail. The micronutrient cocktail was constituted of $FeSO_4.7H_2O$, 3.5 mg/L; $ZnSO_4.7H_2O$, 0.16 mg/L; $CuSO_4.5H_2O$, 0.08 mg/L; H_3BO_3, 0.5 mg/L; $CaCl_2.2H_2O$, 0.03 mg/L and $MnSO_4.4H_2O$, 0.4 mg/L. Carbon sources used were glucose, xylose, fructose and lactose as and when required. For solid media, 15g/L agar was added in addition to above constituents.

5X M9 salts, micronutrients (prepared at 1000X stock concentration) and carbon source (2M stock) were autoclaved separately. Fixed volumes of these were added aseptically into pre-autoclaved flasks containing distilled water to constitute the complete media with the desired final concentrations. Volume of water to be autoclaved per flask was calculated by subtracting the required volumes of each ingredient from the total volume of the media to be used.

2.2.3 Tris buffered medium

The media composition included Tris-Cl (pH=8.0), 100mM; NH_4Cl, 10mM; KCl, 10mM; $MgSO_4$, 2mM; $CaCl_2$, 0.1mM; micronutrient cocktail; Glucose, 100mM and phosphate (P) sources (Sharma et al., 2005). 1mg/ml Senegal Rock phosphate (RP) or KH_2PO_4 were used as insoluble and soluble P sources respectively. Each ingredient was separately autoclaved at a particular stock concentration and a fixed volume of each was added to pre-autoclaved flasks containing sterile distilled water (prepared as in Section 2.2.3) to constitute complete media.

2.2.4 Pikovskaya's (PVK) Agar

The media composition included Ammonium sulphate, 0.5g/L; Calcium phosphate, 5.0g/L; Dextrose, 10.0g/L; Ferrrous sulphate, 0.0001g/L; Magnesium sulphate, 0.1g/L; Manganese sulphate, 0.0001g/L; Potassium chloride, 0.2g/L; Yeast extract, 0.5g/L and agar, 15.0g/L. Dextrose was substituted by same amount of xylose and fructose as and when

mentioned. The readymade media was obtained from Hi-Media Laboratories, India, and was used according to manufacturer's instructions.

2.3 Morphological characterization and antibiotic sensitivity profile

Primary fluorescence of the native isolates and the *P. fluorescens* 13525 transformants was checked on Pseudomonas agar (for fluorescein production) plates. The antibiotic sensitivity profile was obtained for all the above 10 native isolates by checking the growth of these cultures by streaking on LA plates containing antibiotics. The same was also confirmed by inoculating single colonies of all the strains independently in 3ml LB containing recommended dose of antibiotics (Sambrook et al., 2000) and checking the growth after overnight shaking at 30ºC. The antibiotics used were erythromycin, ampicillin, kanamycin, spectinomycin, chloramphenicol, gentamycin, trimethoprim and tetracycline at the final concentrations as described in **Table 2.4**.

2.4 Molecular biology tools and techniques

The routine molecular biology experiments were carried out following the standard protocol of Sambrook et al.(2004) with modifications as when necessary

2.4.1 Isolation of plasmid and genomic DNA

2.4.1.1 Plasmid DNA isolation from *E. coli* and *P. fluorescens* 13525

The plasmid DNA from *E. coli* was isolated by the boiling lysis method using CTAB while that from *P. fluorescens* 13525 was isolated using standard alkali lysis method (Sambrook et al., 2000).

2.4.1.2 Isolation of large size plasmid DNA from native pseudomonads

The native plasmids in the soil isolates of fluorescent pseudomonads, which are generally known to be of large size, were isolated by the protocol described for the isolation of ~117kb TOL plasmid (Ramos-Gonzalez et al., 1991). Single colonies of the pseudomonads were inoculated in 3ml of LB and were allowed to grow at 30ºC under shaking conditions (200rpm). 0.5ml of freshly grown cultures was centrifuged at 9, 200x *g*

for 2 minutes and the pellet was re-suspended homogenously in 200µl of sterile STE [20% sucrose in 25mM Tris-Cl containing 25mM EDTA (pH=8.0) and 1mg/ml lysozyme]. Complete lysis of the cells was achieved by adding 100µl of alkaline SDS [0.3N NaOH containing 2% SDS]. After gentle mixing, the resulting viscous solution was incubated at 55ºC for 5 minutes to minimize the chromosomal DNA contamination. Following this the solution was treated with equal volume of phenol-chloroform and after gentle mixing was subjected to centrifugation at 9, 200x *g* for 10 minutes. The aqueous layer recovered was subjected to chloroform extraction, centrifugation at 9, 200x *g* for 10 minutes, recovery of the aqueous phase and finally DNA precipitation using 0.6 volumes of isopropanol. The DNA was allowed to precipitate at room temperature for ~30-40 minutes, washed with 70% ethanol and finally dissolved in 30µl Tris-EDTA (TE) buffer (Sambrook et al., 2000). Of this, 15µl DNA solution was subjected to agarose gel electrophoresis using 1% agarose (Section 2.4.4).

2.4.1.3 Genomic DNA isolation from *Pseudomonas*

Fresh *Pseudomonas* culture obtained by growing a single colony inoculated in 3ml LB under shake conditions at 30ºC was dispensed in 1.5ml sterile centrifuge tubes, pelleted at 9, 200x *g* and washed twice with sterile normal saline. Following this, the cells were used for genomic DNA isolation performed using genomic DNA extraction kit (Cat.# FC46, Bangalore Genei, India) according to the manufacturer's instructions. The DNA was finally re-suspended in 40µl of sterile double distilled water.

2.4.2 Transformation of plasmid DNA

2.4.2.1 Transformation of plasmid DNA in *E. coli*

The transformation of plasmids in *E. coli* using $MgCl_2$-$CaCl_2$ method and blue-white selection of the transformants using IPTG and X-Gal (as and when applicable) was carried out according to Sambrook et al (2000).

2.4.2.2 Transformation of plasmid DNA in *P. fluorescens* 13525

Plasmid transformation in *P. fluorescens* 13525 was done using the NaCl-$CaCl_2$ method (Cohen et al., 1972) with slight modifications which are as follows. *P. fluorescens* 13525 was grown at 30ºC in LB broth to an O.D. $_{600}$ of 0.6-0.8. At this point, the cells were chilled for about 10minutes, centrifuged at 5000rpm for 5 minutes and washed once in 0.5 volume 10mM NaCl (chilled). After centrifugation (5000rpm for 5 minutes), bacteria were re-suspended in half the original volume of chilled 0.1M $CaC1_2$, incubated on ice-bath for 1hr, centrifuged (5000rpm for 5 minutes) and then re-suspended in $1/10^{th}$ of the original culture volume of chilled 0.1M $CaC1_2$. 0.2ml of competent cells treated with $CaCl_2$ was used per vial (micro-centrifuge tube) to add DNA samples (minimum 0.8-1.0µg is required) and were further incubated on ice-bath for 1hr. Competent cells were then subjected to a heat pulse at 42°C for 2 min to enable DNA uptake, immediately chilled for 5 minutes and then were supplemented with 1.8ml of sterile LB broth followed by incubation for 1hour at 30°C under shake conditions. These cells were then centrifuged and plated on Pseudomonas Agar plates containing appropriate antibiotics. The colonies obtained after overnight incubation of the plates at 30°C were then subjected to fluorescence check and plasmid DNA isolation.

2.4.3 Transfer of plasmid DNA by conjugation

The plasmids were transformed in *E. coli* S17.1, for mediating the conjugal transfer of the plasmids used (Section 2.4.2.1) and the resultant transformant strain was used as the donor strain. *E. coli* S17.1 harboring the plasmid and the recipient pseudomonad strain were separately grown in 3ml LB broth with respective antibiotics at 30°C under shake conditions for approximately 16h. The freshly grown cultures of recipient and the donor strains were aseptically mixed in 1:1 ratio (v/v) in a sterile centrifuge tube and the cells were centrifuged at 5000rpm for 5 minutes. The media supernatant was discarded to remove the antibiotics and the pellet was re-suspended in 0.2ml of fresh sterile LB and the bacteria were allowed to mate at 30°C. After 16h, the bacterial culture mix was centrifuged at 5000rpm for 5 minutes and the resultant pellet was re-suspended in 0.2ml of sterile normal saline. About 30µl of this cell suspension were plated on Pseudomonas agar containing the appropriate antibiotics

for selection (antibiotic dose was as described in **Table 2.4**) to obtain the transconjugants. Conjugation mediated plasmid transfer was employed only for the native isolates of fluorescent pseudomonads.

2.4.4 Agarose gel electrophoresis

The DNA samples were mixed with appropriate volume of 6X loading buffer (0.25% bromophenol blue, and 40% sucrose in water) and subjected to electrophoresis through 0.8% agarose (containing 1µg/ml ethidium bromide) gel in Tris-acetate-EDTA (TAE) buffer at 5v/cm for 0.5-2h. The DNA bands were visualized by fluorescence under the UV-light using UV transilluminator.

2.4.5 Restriction enzyme digestion analysis

0.5-1.0µg DNA sample was used for each restriction enzyme digestion. 1-3U of the restriction enzymes (RE) was used with the appropriate 10X buffers supplied by the manufacturer in a final reaction volume of 10µl. The reaction mixture was incubated overnight at 37°C. The DNA fragments were visualized by ethidium bromide staining after electrophoresis on 0.8% agarose gels and were subsequently photographed. In case of double digestion, a compatible buffer for the two REs was essentially checked. If not available, digestion with one enzyme is performed followed by purification and subsequent digestion with the other enzyme, using respective buffers.

2.4.6 Gel elution and purification

The DNA fragments of desired sizes were recovered from the gel by cutting the agarose gel slab around the DNA band. The agarose piece was weighed in a sterile microcentrifuge tube and was solubilized in 2.5 volumes of 6M sodium iodide (NaI, freshly made) [e.g. for 200mg of agarose piece, 500µl of NaI was added]. Once completely dissolved, 15µl of silicon dioxide suspension (50% w/v, stored at 4°C) was added and was incubated at room temperature for 15-20 minutes. The DNA bound to silica was recovered by centrifuging at 9, 200x *g* for 2 minutes; the pellet was washed twice with 70% ethanol,

dried and finally re-suspended in 20-30µl sterile double distilled water. The microcentrifuge tube was incubated at 55°C for 10 minutes to allow complete dissociation of DNA from silica beads into the solution and then was subjected to centrifugation at 9, 200x *g* for 2 minutes. The resultant supernatant was gently recovered using sterile micropipette tip and was transferred to fresh sterile tube. The purification efficiency was checked by subjecting 2µl DNA solution to gel electrophoresis and visualizing the sharp DNA band of desired size. The purified DNA was used for ligation experiments only if >50ng/µl DNA was recovered after purification.

2.4.7 Ligation

The ligation reaction was usually done in 10µl volume containing the following constituents: Purified vector and insert DNA (volume varied depending on the respective concentrations); 10X T4 DNA Ligase buffer, 1µl; T4 DNA ligase (MBI Fermentas), 0.5-1.0U and sterile double distilled water to make up the volume. The cohesive end ligation reaction was carried out at 16°C for 12-16h. The vector to insert molar ratio (molar concentrations calculated by the under mentioned formula) of 1:4 was maintained, with a total of 50-100ng of DNA in each ligation system.

$$\text{pmoles of DNA} = \frac{\text{Amount of DNA (µg) x 1, 515}}{\text{Size of the DNA fragment (no. of base pairs)}}$$

2.4.8 SDS-PAGE

Table 2.5: Composition of SDS-PAGE reagents (Sambrook et al, 2000)

(A) Monomer solution (30%) (Store at 4°C in dark)		**(B) Resolving gel buffer-1.5M Tris (pH 8.8)** Adjust pH with HCl		**(C) Stacking gel buffer 1.0M Tris (pH 6.8)** Adjust pH with HCl	
Acrylamide	14.6 gm	Tris base	9.1 gm	Tris	3.02 gm
Bisacrylamide	0.4 gm	SDS	0.2 gm	SDS	0.20 gm
D. H_20	Till 50 ml	D. H_20	Till 50 ml	D. H_20	Till 50ml

(D) Tank Buffer (pH 8.3)		**(E) Sample Loading buffer (2X)**		**(F) Other reagents**	
Tris base	6.0 gm	SDS	4%	APS	10% (fresh)
Glycine	28.8 gm	Glycerol	20%	TEMED	2-3 µl
SDS	2.0 gm	Tris-Cl (pH6.8)	0.125M	Water saturated n-butanol	
D. H_20	Till 2 L	Bromophenol blue	0.05%w/v	Sigma protein molecular weight marker SDS6H2-(30,000-200,000).Used 14µg total protein/well	
Adjust the pH with HCl		β-mercapto ethanol	10mM		
		D. H_20	Till 10ml		
(G) Separating Gel (8%, 10ml)		**(H) Stacking Gel (3.9%, 5ml)**		**(I) Staining Solution**	
30% Monomer	2.7 ml	30% Monomer	0.65 ml	0.025% Commassie Blue R- 250 in 40% Methanol and 7% Acetic acid	
Separating gel buffer (pH 8.8)	2.5 ml	Stacking gel buffer (pH 6.8)	1.25 ml		
D. H_20	2.3 ml	D. H_20	3.05 ml	**(J) De-staining solution**	
10% APS	50 µl	10% APS	25 µl	(10% methanol and 10% Acetic acid)	
TEMED	2 µl	TEMED	3 µl		

SDS-PAGE slab gel electrophoresis was carried out using 8% acrylamide gel by following the procedures described by Sambrook et al (2000). After electrophoresis the gel was stained using the staining solution (**Table 2.5**) for approximately 1h and then de-stained with de-staining solution (**Table 2.5**) by incubating overnight under mild shaking conditions. Result was recorded by direct scanning of gel.

2.4.9 Polymerase Chain Reaction (PCR)

The PCR reaction set up was based on the guidelines given in Roche Laboratory Manual. The assay system and the temperature profile used are described in **Table 2.6.**

Assay system used		**Temperature Profile**	
Sterile DDW	38 µl	Initial denaturation	94°C- 5 min
dNTP (10mM with 2.5mM each)	3 µl	Denaturation	94°C- 30 sec
Reverse Primer 20pmoles	1 µl	Annealing	Varies from 55-62°C for 30sec.
Forward Primer 20pmoles	1 µl		
Template DNA (100ng/µl)	1 µl	Elongation	72°C for 45sec-2.5min
Taq PCR buffer (10X)	5 µl	Final Elongation	72°C- 10 min
Taq DNA Polymerase (1 unit/µl)[#]	1.0 µl	For plasmid	(30 cycles)
Total System	**50 µl**	For genomic DNA	(40 cycles)

Table 2.6: PCR conditions used in the present study.

PCR amplifications were performed in Techne TC-312 thermal cycler. *Exact primer annealing temperature and primer extension time varied with primers (designed with respect to different templates) and has been specified in the text as and when applicable. # Processivity of Taq polymerase is ~1000 bases per min. Taq DNA polymerase and its buffer, dNTPs and primers were obtained respectively from Bangalore Genei Pvt. Ltd., India, Sigma Chemicals Pvt. Ltd. and MWG Biotech. Pvt. Ltd, India, respectively and were used according to manufacturer's instructions.

The theoretical validation of the primers with respect to absence of intermolecular and intramolecular complementarities to avoid primer-primer annealing and hairpin structures and the appropriate %G-C was carried out with the help of online primer designing software Primer 3. The sequence, length and %G-C content of primers are subject to variation depending on the purpose of PCR and will be given as and when applicable in the following chapters. The PCR products were analyzed on 1.0% agarose gel along with appropriate molecular weight markers (Section 2.4.4)

2.4.10 DNA sequencing

The DNA sequencing service was obtained from MWG Biotech. Pvt. Ltd. (India) for ~1.1kb *Pseudomonas* genomic DNA and ~750bp of 16SrDNA (details in Chapter 8.)

2.4.11 BLAST Search

The online computational tool "BLAST" for the DNA sequence alignments and homology search was used for microbial classification of a *Pseudomonas* isolate P4 and for characterization of a genomic integration event in the same (details in Chapter 8).

These molecular biology tools were collectively applied, as and when applicable, to construct recombinant plasmids with *ppc*/*cs* genes under *lac* promoter, confirmation of the recombinant clones and expression of respective proteins and ultimately development of pseudomonads harboring the appropriate recombinant plasmids; for further investigations.

2.5 P-solubilization phenotype

P-solubilizing ability of the native as well as the transformant pseudomonads was tested on **(i)** Pikovskaya's (PVK) agar (Section 2.2.5; Pikovskaya, 1948) to monitor the ability to solubilize di-calcium phosphate and **(ii)** Tris buffered RP-Methyl red (TRP) agar plates which represents a much more stringent condition of screening for PSMs (Gyaneshwar et al, 1998). Liquid medium for RP solubilization is described in Section 2.2.4 with an addition of methyl Red as pH indicator dye and 1.5% agar for all the plate experiments. *Pseudomonas* cell suspension for these experiments was prepared as described in Section 2.9.1 and 3µl of it was aseptically spotted on the above mentioned agar plates and was allowed to dry completely followed by incubation at 30°C for 5-7 days. P solubilization was determined by monitoring the zone of clearance on PVK agar and red zone on the TRP agar plates. Media acidification from pH=8.0 to pH<5 on TRP broth was used as an indicator for P-solubilization and organic acid secretion.

2.6 Mutant Complementation Phenotype

E. coli ppc (JWK3928) and *cs* (W620) mutants were used to confirm the functionality of the cloned *ppc* and *cs* genes, respectively. The recombinant plasmids containing *ppc* and *cs* genes independently under *lac* promoter were transformed into respective mutants. The *ppc* transformants were selected on kanamycin and tetracycline while *cs* transformants were selected on streptomycin and kanamycin. These transformants were grown on M9 minimal medium with 0.2% (11.11mM) glucose as carbon source in presence and absence of 340µg/ml sodium glutamate, under shaking conditions at 30°C for *E. coli* JWK3928 and at 37°C for *E. coli* W620. Kanamycin, tetracycline and streptomycin were used at the final concentrations of 12.5µg/ml, 7.5µg/ml and 2.5µg/ml ($1/4^{th}$ of the concentration used for growth in LB broth). Both *ppc* and *cs* mutants exhibited glutamate auxotrophy (Izui et al., 1986; Underwood et al., 2002) as they could not grow on glucose as the sole carbon source in the absence of glutamate supplementation.

2.7 Physiological experiments

The physiological experiments were carried out using various WT and transformant pseudomonads which included growth, pH profile and enzyme assays.

2.7.1 Inoculum preparation

The inoculum for M9 and Tris minimal media containing free Pi was prepared by growing the *Pseudomonas* cultures overnight at 30°C in 3ml LB broth. Inoculum for the buffered RP broth (TRP) was prepared by growing the *Pseudomonas* cultures overnight at 30°C in 10ml of M9 minimal medium. Cells were harvested aseptically, washed twice by normal saline and finally re-suspended in 1ml normal saline under sterile conditions. Freshly prepared inoculum was used for all the experiments.

2.7.2 Growth characteristics and pH profile

Growth parameters and pH profile of the native as well as transformant pseudomonads were determined using three different media conditions including **(i)** TRP medium with RP as P source (Gyaneshwar et al, 1998). The media composition in this case was same as mentioned in Section 2.2.4; **(ii)** Tris buffered medium with KH_2PO_4 as P source: The media composition was same as mentioned in section 2.2.4 except for RP being substituted by free Pi in the form of KH_2PO_4 at the concentrations including 0.1mM, 1.0mM, 10.0mM and 20mM as and when required; and **(iii)** M9 minimal medium (Section 2.2.3). 100mM glucose was used as the carbon source for all the experiments unless and until stated categorically. In some experiments, Xylose (100mM) and fructose (100mM) were also used as carbon source.

In 150ml conical flasks, 30ml of relevant minimal broth containing free Pi was inoculated with cell suspensions to have 0.01-0.03 $O.D_{600nm}$ initially (0 hour O.D.). Similarly, for the TRP broth, the initial $O.D._{600nm}$ was about 0.09-0.15. The batch culture

studies were performed under aerobic conditions in Orbitek rotary shaker maintained at 30°C with agitation speed kept constant at 200rpm. 1ml samples were aseptically harvested at regular intervals (varying with every set of batch culture depending on media conditions) and were subjected to various analytical techniques.

2.7.3 Analytical techniques

The cell density determinations were done at 600nm as monitored spectrophotometrically. Change in absorbance was considered as the measure of growth and drop in pH of the media was taken as the measure of acid production. In all the cases, the observations were continued till the media pH reduced to less than 5. 1ml aliquots withdrawn aseptically at regular time intervals were immediately frozen at -20°C until further used for biochemical estimations. The stored samples were centrifuged at 9, 200x *g* for 1 min at 4°C and the culture supernatants derived were used to estimate residual glucose and organic acid analysis using HPLC. For HPLC analysis, the culture supernatant was passed through 0.2µm nylon membranes (MDI advanced microdevices, India) and the secreted metabolites were quantified using RP-18 column. The column was operated at room temperature using 0.02% orthophosphoric acid was used as mobile phase. at a flow rate of 0.8 ml min^{-1} and the column effluents were monitored using a UV detector at 210 nm. Standards of organic acids were prepared in double distilled water, filtered using 0.2µm membranes and were subjected to chromatography for determining the individual retention time. The organic acids were quantified by reference to the peak areas obtained for the authentic standards for Gluconic acid, 2 keto gluconic acid, Lactic acid, Oxalic acid, Maleic acid, Succinic acid, Formic acid, Citric acid, Malonic acid, Acetic acid, Propionic acid, Pyruvic acid and Tartaric acid (Merck, Germany and Hi-Media Laboratories and Sigma Pvt. Ltd.). The values were presented as the mean of three replicates. The glucose concentration in the medium was estimated using enzymatic kit (Reckon Diagnostics, India).

The physiological parameters like specific growth rate, specific total glucose utilization rate and biomass yield (Chao and Liao, 1993) and the organic acid yield were calculated as described below.

(i) Specific growth rate (h^{-1}):

$$k = \frac{(Log_{10}Nt_1 - Log_{10}Nt_2) \times 3.3}{(t_1 - t_2)\,(h)} \quad \text{where,}$$

N_1 and N_2 are the number of cells at time t_1 and t_2 respectively and (t_1-t_2) is the corresponding time interval in hours. 3.3 is the factor derived from the formula- number of generations (n)= $(Log_{10}N - Log_{10}N_0)/Log_{10}2$. The number of cells was calculated from $O.D._{600nm}$ using the correlation 1 $O.D._{600nm} = 1.5 \times 10^9$ cell/ml (Koch *et al*., 2001)

(ii) Specific total glucose utilization rate (Q_{Glc}):

$$Q_{Glc} = \frac{\Delta\text{Glucose}\ (t_1-t_2)\ (g/L)}{\Delta\text{dcw}\ (t_1-t_2)\ (g/L) \times \text{Time interval}\ (t_1-t_2)\ (h)} \quad \text{where,}$$

ΔGlucose (t_1-t_2) is the amount of glucose consumed over the time interval t_1-t_2; **Δ**dcw (t_1-t_2) is the difference in the dry cell weight (dcw) of the cells over the time interval t_1-t_2. Q_{Glc} is expressed as g glucose utilized/g dcw/h). Dry cell weight was calculated using the correlation 1 $O.D._{600nm}$ = 0.382mg/ml (Bugg *et al*., 2000).

(iii) Biomass yield

$$Y_{dcw/Glc} = \frac{\Delta\text{dcw}\ (t_1-t_2)\ (g/L)}{\Delta\text{Glucose}\ (t_1-t_2)\ (g/L) \times \text{Time interval}\ (t_1-t_2)\ (h)} \quad \text{where,}$$

All the parameters were as described for Specific glucose utilization rate. $Y_{dcw/Glc}$ is expressed as g of dry cell weight produced/ g glucose utilized/h.

(iv) Organic acid yield

$$\text{Organic acid yield} = \frac{\text{Amount of organic acid produced (g/L)}}{\text{Total glucose utilized (g/L) x dcw}}$$ where,

The amount of total glucose utilized was obtained by deducting the value of residual glucose concentration from the initial glucose concentration supplied in the medium. The difference between the total glucose utilized and gluconic acid produced was considered as glucose consumed. Hence, the total glucose utilized and not glucose consumed was taken into account for calculating specific glucose utilization rate. The statistical analysis of all the parameters was done using Graph Pad Prism (version 3.0) software.

2.8 Enzyme assays

2.8.1 Preparation of cells and cell free extracts

Glucose grown cells under above mentioned minimal media conditions were harvested in appropriate growth phase from 30ml of cell culture by centrifugation 9,200x *g* for 2 minutes at 4°C. Unlike citrate synthase (CS), isocitrate lyase (ICL) and isocitrate dehydrogenase (ICDH) which were assayed in the stationary phase, all the enzyme were assayed from mid-late log phase cell cultures. The preparation of cell free extracts for PPC, CS, PYC, G-6-PDH, ICDH and ICL assays was carried out according to Kodaki et al (1985) with an addition of 5mM $MgCl_2$ and 1mM EDTA for PYC assay. The cell pellet was washed once with 80mM phosphate buffer (pH=7.5) followed by re-suspension in same buffer containing 20% glycerol and 1mM DTT. The cells were then subjected to lysis by sonicating for maximum 1-1.5 minute in an ice bath, followed by centrifugation at 9,200x *g* at 4°C for 30 minutes to remove the cell debris. The supernatant was then used as cell-free extract for the enzyme assays. The whole cell preparation for GDH assay was done by washing the harvested cells (mid-late log phase cultures) thrice with normal saline to remove the residual glucose of the medium and re-suspending in 0.01M phosphate buffer (pH 6.0) with 5mM $MgCl_2$.

2.8.2 Enzyme Assay Protocols

2.8.2.1 PPC assay

PPC (EC 4.1.1.31) activity was estimated spectrophotometrically by monitoring the oxidation of NADH in a coupled assay with malate dehydrogenase (MDH) as described by Kodaki et al (1985) with modifications as follows. The coupled assay was divided in two steps. The assay mixture for first step of the reaction contained following ingredients in total volume of 0.9ml: Tris-H_2SO_4 (pH 8.0), 100mM; potassium PEP, 2mM; $MgSO_4$, 10mM; $KHCO_3$ 10mM and the enzyme solution (cell lysate).

After 20 minutes incubation at 30°C, the reaction was terminated using 25% TCA followed by 15 minutes incubation on ice bath. The supernatant recovered after centrifuging the resultant reaction mix at 9,200x *g* for 30 minutes at 4°C, was brought to pH 8.0 by using 7µl of 10N NaOH which was then used as the source of OAA in second step of the reaction for which the assay system contained 950µl of reaction mix from first step of reaction, 5units of MDH and 0.12mM NADH. The assay system volume was adjusted to 1ml using distilled water. The rate of oxidation of NADH recorded at 340nm was used to indicate concentration of OAA formed. Molar absorbance of NADH was taken as $6.22mM^{-1}cm^{-1}$ at pH 8.0. The absence of glycerol in the sonication buffer led to complete loss of PPC activity (Kodaki et al., 2005).

2.8.2.2 PYC assay

PYC (EC 6.4.1.1) activity was estimated by monitoring NADH oxidation in a coupled assay with MDH (Taylor et al., 1972) with modifications as follows. The assay mixture for first step of the reaction contained following ingredients in total volume of 0.9ml: Tris-HCl (pH 8.0), 100mM; Na-pyruvate, 5mM; ATP, 5mM; $MgCl_2$, 5mM; $NaHCO_3$, 50mM and the enzyme solution (cell lysate). Remaining steps and specific activity determination were same as in case of PPC activity.

2.8.2.3 G-6-PDH assay

G-6-PDH (EC 1.1.1.49) activity was determined spectrophotometrically at room temperature by following the reduction of NADP at 340nm as a function of time (Eisenberg and Dobrogosz, 1967). Molar absorbance of NADP was taken as $6.22 mM^{-1}cm^{-1}$ at pH 8.0. The reaction mixture of 1ml included: Tris-Cl (pH 8.2), 200mM; glucose-6-phosphate, 3.3mM; $MgCl_2$, 10mM; NADP, 0.1mM and cell extract.

2.8.2.4 GDH assay

GDH (D-glucose phenazine methosulphate oxidoreductase, (EC 1.1.5.2) was determined spectrophotometrically by following the coupled reduction of 2,6-dichlorophenolindophenol (DCIP) at 600nm (Quay et al., 1972). Molar absorbance of DCIP was taken as 15.1 mM^{-1} cm^{-1} at pH 8.75. The reaction mixture included: DCIP, sodium salt, 0.05mM; phenazine methosulfate, 0.66mM; sodium azide, 4mM; Tris-Cl buffer (pH 8.75), 16mM; D-glucose, 66mM; whole cells, and distilled water to 3.0ml.

2.8.2.5 ICL assay

ICL (4.1.3.1) activity was measured by a modified method of Dixon and Kornberg (1959). ICL catalyzes the hydrolysis of isocitrate into glyoxylate and succinate. The glyoxylate formed in the presence of phenylhydrazine was measured as glyoxylic acid phenylhydrazone at 324nm. The reaction mixture of 1ml consisted of following ingredients: potassium phosphate buffer (pH=7.0), 100mM; $MgCl_2$, 6mM; cysteine HCl, 12mM; phenylhydrazine HCl, 4mM; isoctrate; 8mM and cell extract. Molar absorbance coefficient of phenylhydrazine was taken as 17.4 $mM^{-1}cm^{-1}$. The rate of increase in absorbance in the linear range was used to calculate ICL activity.

2.8.2.6 ICDH assay

ICDH (1.1.1.42) activity was measured by following NADPH formation at 340nm (Garnak and Reeves, 1979). The reaction mixture contained the following in 1ml: Tris-HCl

(pH 7.5), 150mM; $MnCl_2$, 0.25mM; NADP, 0.65mM, isocitrate, 2.5mM and cell extract. Molar absorbance coefficient of NADP was taken as 6.22 $mM^{-1}cm^{-1}$.

2.8.2.7 CS assay

CS (4.1.3.7) activity was estimated by following the absorbance of 5,5-dithiobis(2-nitrobenzoic acid) (DTNB) at 412nm which would change due to its reaction with sulfhydryl group of CoA (Serre, 1969). The assay mixture per cuvette contained following ingredients in 1.0ml: Tris-HCl (pH=8.0), 93mM; acetyl CoA, 0.16mM; OAA, 0.2mM; DTNB, 0.1mM and cell lysate. The reaction was started by addition of OAA. Molar absorbance coefficient was taken as 13.6 $mM^{-1}cm^{-1}$ at 412nm. The rate of increase in absorbance was used to calculate CS activity.

All the enzyme activities were determined at 30°C and were expressed per mg total protein. Total protein concentration of the crude extract as well as whole cell suspensions was measured by modified Lowry's method (Peterson, 1979) using bovine serum albumin as standard. Corrections were made for Tris buffer. Enzyme activities were calculated using following formula

$$\text{Units/mg} = \frac{\Delta A_{y\ nm}/\text{min}}{€ \times \text{enzyme (sample) aliquot (ml)} \times \text{Total protein (mg/ml)}}$$

Where,

$\Delta A_{y\ nm}$ is the difference in the absorbance at any given wavelengths ($_{y\ nm}$) and € is the millimolar extinction coefficient at *y* nm.

One unit of enzyme activity was defined as the amount of protein required to convert 1 nmole of substrate per minute unless stated in the figure legend.

2.9 Enzymatic estimation of organic acids

Organic acids levels determined were confirmed by using enzymatic analysis. Culture supernatants were filtered through 0.2µm nitrocellulose membrane and different aliquots were used to assay for pyruvic and citric acids.

2.9.1 Pyruvic acid

Culture supernatant was used as source of pyruvate in reaction with lactate dehydrogenase (LDH) following the rate of NADH utilization (Cocaign-Bousquet et al., 1996) with several modifications. The rate of reduction in absorbance of NADH at 340nm was proportional to the amount of pyruvic acid present. The assay mixture per cuvette contained following ingredients in 1ml: Tris-HCl (pH=7.5), 200mM; NADH, 0.12mM; LDH, 5 U; pyruvate (variable). The assay volume was adjusted using distilled water. The standard curve was prepared using known concentrations of Na-pyruvate (4mM stock solution) while 5 and 10µl aliquots of the filtered culture supernatant were used to determine the extracellular pyruvic acid. Sample aliquots were selected so as to work within the linear range of standard curve.

2.9.2 Extracellular citric acid

Citric acid in the culture supernatants was analyzed using the method involving citrate lyase mediated cleavage of citrate to OAA which is subsequently utilized in MDH catalyzed reaction requiring NADH. Change in NADH absorbance would be proportional to citrate concentration (Petrarulo et al., 1995; Boehringer Mannheim/R-Biopharm Enzymatic BioAnalysis/Food Analysis Manual of Citric acid determination kit, Cat. # 10 139 076 035). The assay system per cuvette contained- 50mM phosphate buffer mix, 1.0ml; citrate lyase, 0.27 units (0.02ml of 13.3 units/ml stock); citric acid standard or test sample; 5U MDH; 0.1M NADH. Citric acid standards of 5µM, 10µM, 15µM and 20µM concentrations were used to generate standard curve. Difference in O.D. at 340nm after 4 minutes (time required for complete OAA utilization) of addition of citrate lyase was used for the calculations.

2.9.3 Intracellular citric acid

Pseudomonas transformant cultures grown on appropriate media were harvested in the late stationary phase and were pelleted by centrifuging at 9, 200x *g* for 2 minutes at 4°C. The pellet was washed with 1ml of 80mM phosphate buffer (pH=7.5) and the washed cells were suspended in the same buffer containing 20% glycerol. This homogenous cell

suspension was subjected to sonication for maximum 1-1.5 minute in an ice bath to have complete cell lysis, followed by centrifugation at 9, 200x *g* and 4°C for 30 minutes to remove cell debris. The recovered supernatant was filtered through 0.2µm nitrocellulose membrane and frozen immediately till further analysis (Petrarulo et al., 1995; Aoshima et al., 2003). This filtrate was used to estimate the amount of intracellular citric acid using the method described by Petrarulo et al (1995) with minor modifications.

According to this method citrate lyase converts citrate to OAA and acetate and the resultant OAA can rapidly react with phenylhydrazine at slightly acidic pH to form the corresponding phenylhydrazone which can absorb ultraviolet (UV) light. Increase in the absorbance at 330nm would be an expression of the citrate concentration. The assay system per cuvette contained- 50mM phosphate buffer mix, 1.0ml; 246mM phenylhydrazine, 0.02ml; citrate lyase, 0.27U (0.02ml of 13.3 units/ml stock); citric acid standard or test sample. Buffer mix contained 50mM phosphate buffer (pH=6.5), 0.1mM $ZnSO_4.7H_2O$ and 0.2g/L sodium azide. Citric acid standards of 5µM, 7.5µM, 10µM, 15µM and 20µM concentrations were used to generate standard curve. Difference in $O.D._{330nm}$ after 3 minutes of addition of citrate lyase was used for the calculations. To calculate the intracellular citrate concentration (in mM), cellular volume was assumed to be 1.63µl mg cdw^{-1} (Emmerling et al., 1999).

$$\text{Intracellular concentration (mM)} = \frac{\text{X nmoles/ml}}{\text{Dry cell mass (mg)} \times C_f \times 1.63}$$

where,

X nmoles/ml is calculated as follows-

$$\frac{\Delta O.D._{330nm}/3\text{min}_{(test)} \times \text{Std (nmoles)}}{\text{Test aliquot (ml)} \times \Delta O.D._{330nm}/3\text{min}_{(Std.)}}$$

C_f = concentration factor of the 25 ml cell culture

Dry cell mass (dcw) = $O.D_{600nm}$ x 0.382, where 0.382 is the factor correlating $O.D_{600}$ was with dry cell weight (Bugg *et al.*, 2000)

2.10 Inoculation of mung beans (*Vigna radiata*)

Mung bean seeds were surface sterilized by treating with 0.1% (w/v) mercuric chloride for ~3-5 minutes followed by 5 rounds of thorough washing with 100ml freshly sterilized distilled water (Ramakrishna et al., 1991). These seeds were placed in autoclaved petri-dishes containing moist filter paper and were allowed to germinate in dark for 24h at room temperature. *Pseudomonas* P4 was inoculated in 10ml sterile LB broth and was allowed to grow at 30°C with overnight shaking. Fresh culture was harvested by centrifuging at 9, 200x *g* for 2 minutes; the pellet was aseptically washed twice with sterile normal saline and finally was re-suspended in 4 ml of normal saline (Ramos et al., 2000). Healthy germinated seeds were incubated with this cell suspension in a sterile petri-dish under aseptic conditions for 10-15 minutes. Root tips of hence obtained *Pseudomonas* P4 coated mung bean seeds were implanted with the help of sterile forceps in autoclaved sugar tubes containing 50 ml of solidified Murashige-Skoog's (MS) Agar with the desired phosphate and carbon sources. Plants were allowed to grow at room temperature with sufficient light conditions for 5-7 days after which effect of *Pseudomonas* P4 inoculation was monitored in terms of overall plant growth.

MS medium was amended with 1% sucrose and 100mM glucose used as carbon sources while 1mg/ml RP was used as insoluble P source to replace KH_2PO_4 in the media, as and when required. RP containing media after autoclaving was cooled by continuous shaking (swirling) till the commencement of complete solidification so that the RP particles are homogenously distributed through the media. Effect of Al was checked in the presence of 400µM Al by supplemented in the form of $AlCl_3$.

2.11 Pot experiments- Interaction with mung beans (*Vigna radiata* GM4)

2.11.1 Preparation of inoculums:

A loopful of each of the seven bacterial strains was inoculated into a separate 50 ml aliquot of PB and incubated at 28±2ºC for 4 days in an incubator shaker.

2.11.2 Growth Analysis: Above ground parts

Plant height:

Measurements of plant height were taken at the crop maturity in three replicates of five plants each. Plant height was measured from the soil line to shoot tip. Plant height was measured by placing the plant on a centimeter scale. Plant population was uniform at the time of maturity of crop.

Leaf area:

The area of the leaf was taken by pressing the leaf on millimeter graph paper and tracing the exact outline. The area was measured by weighing the graph cuttings of the leaf (Shine et al., 2011). The calibration curve was prepared by weighing a 0–100 cm^2 area of graph paper.

Dry matter production

At maturity fifteen plants (five plants from each replicate) were randomly selected and the data on component part dry weights (leaf, root and shoot) were recorded. Leaf, stem and root were dried at 60 ºC for 72 hours. Pods were separated and the total numbers of branches were recorded. Dry weights of seed components were recorded after drying at 35–40 ºC for 10 days.

2.11.3 Growth Analysis: Below ground parts

Root length:

The measurements of root length were done in plants of all the eight varieties at 40 and 50 DAE. Roots were taken out carefully, washed and measured against a cm scale.

Root fresh and dry weight

Plant roots with nodules at each sampling were washed and dried on filter paper and weighed for the fresh weight. For dry weight roots were dried at 60^{o}C for 72 hours and weighed.

Number of root nodules/plant

Nodules on each root were counted carefully and recorded per plant.

Nodule fresh weight

Nodules were taken out at each sampling, washed and dried on filter paper. Weight was recorded in gm/plant for all treatments.

2.11.4 Antioxidant Enzymes / ROS scavenging enzyme activity:

(1) Superoxide Dismutase (SOD)

Two hundred mg of leaves were homogenized in a pre-chilled mortar and pestle under ice cold condition using 3.0 ml of extraction buffer, containing 50 mM sodium phosphate buffer (pH 7.4), 1 mM EDTA and 1% (W/V) polyvinylpyrolidone (PVP). The homogenates were centrifuged at 10,000 rpm for 20 minutes and the supernatants used for the assay (Costa *et al.*2002).

Total SOD (EC 1.15.1.1) activity was measured spectrophotometrically based on inhibition in the photochemical reduction of nitroblue tetrazoilum (NBT). The 3 ml reaction mixture contained 50 mM sodium phosphate buffer (pH 7.8),13 mM methionine, 75 µM NBT, 2 µM riboflavin, 0.1 mM EDTA and 0.1 ml enzyme extract, riboflavin was added last (Van Rossun *et al*.1997).After addition of all these components and mixing, test tubes were placed on stand 30 cm below a light source consisting of four 15-w fluorescent lamps. The photochemical inhibition was allowed to happen for 10 minutes and stopped by switching off the light source. The photoreduction in NBT was measured as increase in absorbance at 560 nm. Blanks and controls were run the same way but without illumination and enzyme,

respectively. One unit of SOD was defined as the quantity of enzyme required to inhibit the reduction of NBT by 50% in a reaction mixture. Enzyme unit of SOD was calculated according to formula given by Constantine and Stanley (1977).

$$\text{SOD unit} = \frac{\text{O.D. control (without enzyme)}}{\text{O.D. sample}} - 1 \text{ x } \frac{1}{\text{enzyme conc. (g)}}$$

$$\text{SOD U/g protein} = \frac{\text{SOD unit}}{\text{mg/g protein}}$$

(2) Catalase

Two hundred mg of acetone powder homogenized with a pre-chilled mortar and pestle under ice cold condition in 2.0 ml of extraction buffer, containing 0.1 M sodium phosphate buffer (pH 7.2) with the addition of 1 mM EDTA and 1% (w/v) polyvinylpyrolidone (PVP) and a pinch of activated charcoal. The homogenates were centrifuged at 10,000 rpm for 20 minutes and the supernatants were used for the assay (Mahatma *et al*. 2011).

Total catalase (EC 1.11.1.6) activity was determined in the supernatants by measuring the decrease in absorption at 240 nm as H_2O_2 (ε = 39.4 mM^{-1} cm^{-1}) got consumed according to the method of Aebi (1984) and enzyme activity expressed as mmol H_2O_2 oxidized min^{-1} g^{-1} protein. The 3 ml assay mixture contained 50 mM sodium phosphate buffer (pH 7.0), 30mM H_2O_2 and 50 µl enzyme extract. Enzyme unit of CAT was defined as:

$$\text{Mmol/min/g protein} = \frac{\Delta \text{ O.D.}}{\text{Enzyme conc.(g) x mg/g protein x } \varepsilon}$$

Where, ε = Extinction coefficient

Enzyme conc. (g) = Amount of enzyme in 3 ml reaction mixture

(3) Guaiacol Peroxidase (POX)

Two hundred mg of leaves were homogenized in a pre-chilled mortar and pestle under ice cold condition in 2.0 ml of extraction buffer, containing 0.1M sodium phosphate buffer (pH 7.2) with the addition of 1 mM β-mercaptoethanol and 1% (w/v) polyvinylpyrolidone (PVP). The homogenates were centrifuged at 10,000 rpm for 20 minutes and the supernatants used for the assay.

POX (EC 1.11.1.7) activity was determined in the supernatants of centrifuged homogenates by measuring the increase in absorption at 470 nm due to the formation of tetraguaiacol (ϵ=26.6$mM^{-1}cm^{-1}$) in a reaction mixture containing 50 mM sodium phosphate buffer pH 7.0, 0.1 mM EDTA, 0.05 ml enzyme extract, and 10 mM H_2O_2 (Costa *et al*.2002).

(4) Ascorbate peroxidase (APX)

Maize leaf samples were crushed with chilled acetone in pre-chilled mortar-pestle. To obtain fine acetone powder the homogenates were filtered and stored immediately at -20^o C. Hundred mg of acetone powder was then homogenized in a pre-chilled mortar and pestle under ice cold condition using 2.0 ml of extraction buffer, containing 0.1 M sodium phosphate buffer (pH 7.2), and 1% (w/v) polyvinylpyrolidone (PVP). The homogenates were centrifuged at 10,000 rpm for 20 minutes and the supernatants used for the assay (Mahatma et al., 2011).

APX (EC 1.11.1.11) activity was measured immediately in fresh crude extracts and assayed by procedure described by Nakano and Asada (1981). Three ml of the reaction mixture contained 50 mM sodium phosphate buffer pH 7.0, 0.1 mM H_2O_2, 0.5 mM ascorbic acid, 0.1 mM EDTA and 0.1 ml enzyme extract. The hydrogen peroxide dependent oxidation of ascorbate was followed by a decrease in the absorbance at 290 nm (ε = 2.8 mM^{-1} cm^{-1}). The enzyme unit of APX was defined similar to that of CAT activity as described.

2.11.5 Acid phosphatase

1 g of leaves were homogenized in 10ml ice cold 50mM citrate buffer (pH5.3) in a prechilled pestle and mortar.The homogenate is filtered through four layer of cheese clothe and the filtrate is centrifuged at 10,000g for 10 min. The supernatant is ready to use as enzyme source.

Acid phosphatase (3.1.3.2) hydrolyzes a number of phosphomonoesters and phosphoproteins.The enzyme phosphatase hydrolyzes p-nitrophenol phosphate. The released p-nitrophenol is yellow in colour in alkaline medium and is measured at 405nm. The optimum pH for acid and alkaline phosphatase are 5.3 and 10.5 respectively.3ml of substrate solution containing 1.49g EDTA,0.84 g citric acid and 0.03 g p-nitrophenyl phosphate in 10 ml water(pH 5.3)incubated at 37 for 5 min.0.5 ml of enzyme extract added and mixed well.0.05 ml sample immediately removed from the mixture and mixed with 9.5 ml of sodium hydroxide solution(0.085N).This correspond to zero time assay(blank). The remaining solution is incubated for 15 min at 37. 0.5 ml sample were drawn from the mixture and mix wit 9.5 ml of sodium hydroxide solution.Absorbance of the balk and incubated tubes were measured at 405 nm.Take 0.2-1.0 ml (4-20mM) of the standard ie. 100mM p-nitrophenol dilute to 10 ml with NaOH solution.Read the colour and draw the standard curve. Specific activity is expressed as m moles of p-nitrophenol released per min per mg protein.

2.11.6 Nitrate Assimilating Enzyme

Nitrate Reductase Activity. (Bhatnagar *et al*. 2007)

Two hundred mg leaf tissues were cut into small slices, and then suspended in reaction mixture (1 ml 5 % isopropanol, 1 ml 1 M potassium nitrate and 3 ml phosphate buffer, 0.1 M, pH 7.5). Incubation was carried out at 30^0C for two hrs in dark. After incubation 1.0 ml aliquots were withdrawn, to which 0.2 ml sulfanilamide, 0.2 ml of 0.2% NEDH solution was added. After 20 minutes, 4.0 ml of millipore water was added to each

test tube. The intensity of the colour developed was recorded at 570 nm in a spectrophotometer. A standard curve was prepared using sodium nitrite in the concentration range of 1-5 µg. Enzyme units are expressed in terms of µg nitrite released per minute per g tissue and calculated as:

$$\frac{\text{Conc. of µg nitrite derived from graph for unit O.D. value X O.D. value of sample}}{0.04 \times 120}$$

(1.0 ml reaction mixture is equivalent to 40 mg tissue)

2.11.7 Estimation of Water Soluble Protein Content

Protein concentration of each enzyme extract was estimated by method of Lowry *et al*. (1951).

(a) Reagents for Lowery's Method

(i) Solution A: 2% Na_2CO_3 in 0.1 N NaOH

(ii) Solution B: (a) 1% $CuSO_4.5H_2O$ solution

(b) 2% sodium potassium tartarate solution

Working solution of B : Prepared fresh before use by mixing equal volume of solution B (a) and B (b).

(iii) Solution C: Prepared fresh before use by mixing 50 ml of solution A and 1 ml of working solution of B.

(iv) Solution D: Folin & Ciocalteu reagent (1N).

Procedure (Folin Lowery's Method)

Enzyme extracts (25 µl) were taken in test tube and volume was made up to 1 ml with millipore water. A tube with 1 ml of water served as blank. Five ml of solution C was mixed by vortexing and kept for 10 min. Then 0.5 ml of solution D (Folin & Ciocalteu reagent) was added and vortexed. The tubes were allowed to stand at room temperature for 30 min. Absorbance was read at 660 nm. A standard curve was prepared using bovine serum albumin (BSA) in the concentration range of 10-80 µg.

Effect of constitutive helerologous overexpression of E. coli NADH insensitive cs gene on the physiology and glucose metabolism of P. fluorescens PfO-1

CHAPTER 3

3 Chapter 3

3.1 INTRODUCTION

Citrate synthase (CS) is a ubiquitous enzyme that catalyzes the first committed step of tricarboxylic acid (TCA) cycle involving condensation of oxaloacetate (OAA) and acetyl-CoA to form citrate. Hence it is the key enzyme governing the carbon flux into the TCA cycle which plays a dual function in the production of cellular energy and biosynthetic precursors under aerobic conditions and only latter under anaerobic conditions, respectively (Park et al., 1994).

3.1.1 Citrate synthase and NADH sensitivity

The CS of gram-negative bacteria are allosteric enzymes designated as type II. Type II CS is a homo-hexamer of identical subunits with monomer size of ~48kDa, and is strongly and specifically inhibited by NADH (Weitzman 1981; Nguyen et al., 2001). *Escherichia coli* and *Acinetobacter anitratum* CS are strongly homologous in amino acid sequence and more distantly resemble the nonallosteric Type I citrate synthase of eucaryotes (Bhayana et al., 1984; Donald et al., 1987; Julie et. al., 2006). *Pseudomonas* CS are also allosteric and their kinetic properties suggest as intermediate between *E. coli* and *A. anitratum* enzymes (Massarini et al., 1975; Higa et al., 1978). Two forms of CS (EC 4.1.3.7) have been found in several species of ***Pseudomonas,*** a 'large' form ***(Mr~ 1:*** **250000)** which **is** generally inhibited by NADH and a 'small' form ***(Mr~ 1:*** 100000) which is insensitive to these nucleotide effectors. Hence the NADH sensitivity of gram negative bacterial *CS* is attributed to subunit size (**Table 3.1**, **Fig. 3.1**). A mutant of ***Pseudomonas aeruginosa*** **PAC514** has been found to contain both a 'large' (CSI) and a 'small' (CSII) isozymes (Solomon & Weitzman, 1983; Mitchell et al., 1995).

Table 3.1: Distribution of large and small citrate synthases in *Pseudomonas* species (Coling et.al., 1986

Organism*	RNA homology group	Size of citrate synthase†	Percentage of 'small' citrate synthase‡	
			Gel filtration	FPLC
P. aeruginosa NCIB 8295	I	L + S	14	21
P. aeruginosa 8602	I	L + S	6	18
P. aeruginosa PAC 514	I	L + S	90	98
P. aeruginosa PAO 1	I	L + S	16	NT
P. fluorescens	I	L + S	25	25
P. putida	I	L + S	21	22
P. stutzeri	I	L + S	31	23
P. alcaligenes	I	S		
P. chlororaphis	I	S		
P. acidovorans	III	L		
P. saccharophila	III	S		
P. testosteroni	III	L		
P. diminuta	IV	L		
P. maltophilia	V	S		

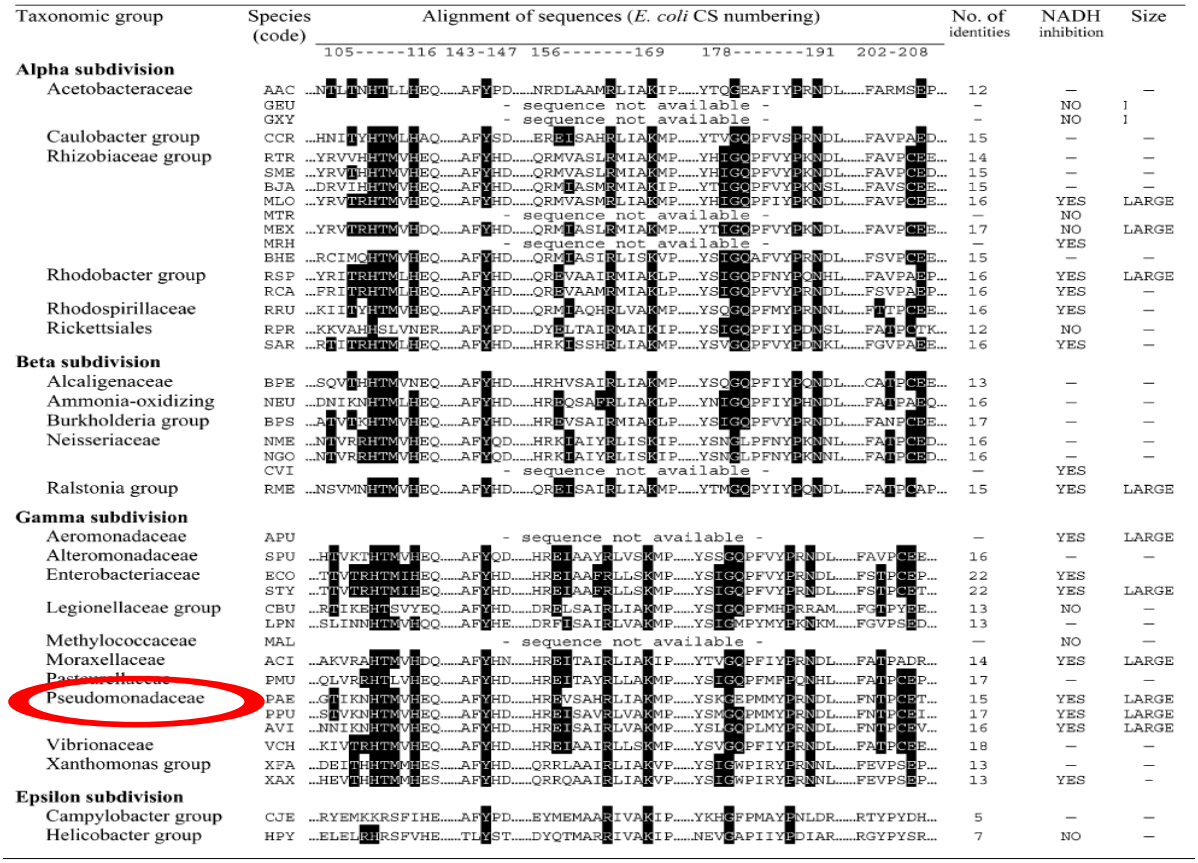

Figure 3.1: Correlation of Gram-Negative Bacterial Citrate Synthase Subunit Size and NADH Sensitivity with the Presence of NADH-Interacting Residues As Identified in the *E. coli CS*-NADH Complex (Robert et al., 2003)

3.1.2 Homology between *E. coli* and *P. fluorescens* citrate synthase

Clustal W multiple alignments show 71% homology between *E. coli* and *P. fluorescens cs* and posses similar regulatory properties.Individual *P. fluorescens* strains also exhibit variations in the coding region of cs (**Fig. 3.2-3.3**)

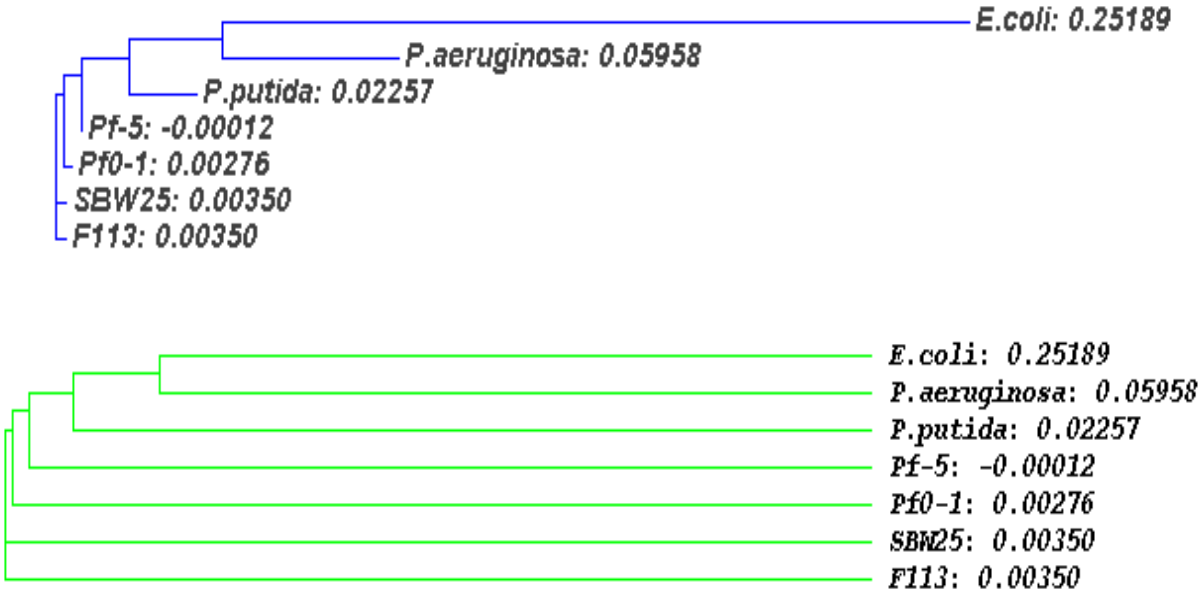

Figure 3.2: Phylogram and cladogram tree

3.1.3 Citrate overproduction through citrate synthase overexpression:

The study of the effect of *cs* gene manipulation on citric acid secretion and overall cellular metabolism can have tremendous applications in agriculture. *E. coli* lacking functional *cs* gene failed to utilize glucose unless supplemented with glutamate (or other TCA cycle intermediates) and had reduced growth as compared to the wild type (Vandedrinck et al., 2001; De Maeseneire et al., 2006). On the other hand, *cs* gene overexpression or underexpression in *E. coli* had no effect on growth on glucose while on acetate as sole carbon source; CS levels strongly affected the growth rate (Vandedrinck et al., 2001). Transgenic tobacco plants overexpressing *Pseudomonas aeruginosa cs* gene under the control of CaMV promoter increased excretion of citrate (Bucio et al., 2000). These citrate secreting plants enhanced the P solubilization efficiency and yielded more leaf and fruit biomass when grown under P-limiting conditions.

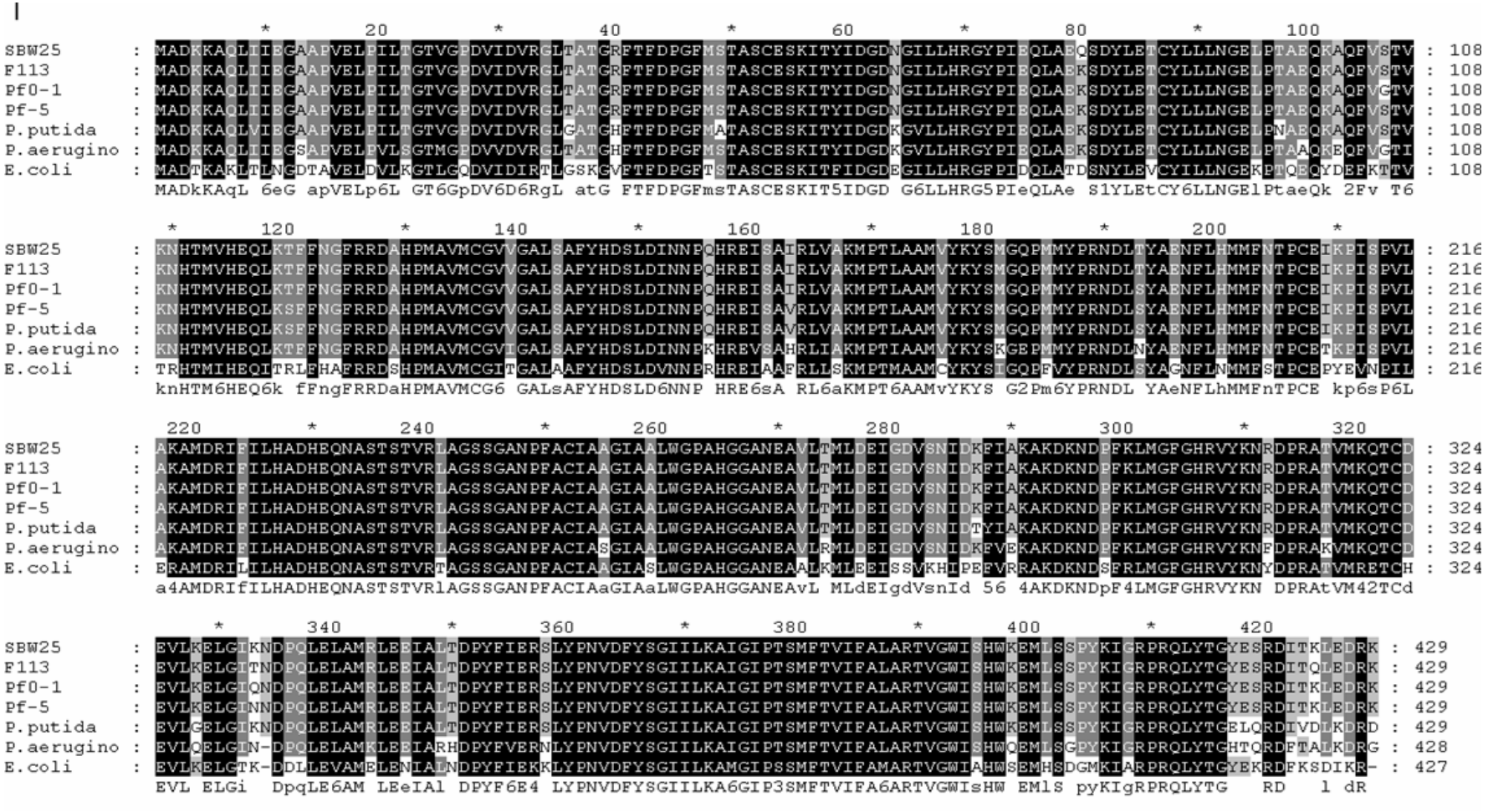

Figure 3.3: CS homology by ClustalW analysis between *E. coli* and fluorescent pseudomonads. Enclosed black areas indicate identical amino acid residues.

Overexpression of mitochondrial citrate synthase in *Arabidopsis thaliana* improved growth on a phosphorus-limited soil and improved the growth of carrot cells on Al-phosphate medium; the effect suspected to be due to enhanced secretion of citric acid (Koyama et al., 1999; 2000). Similar studies in *Nicotiana benthamiana* elicited Al induced citrate excretion (Deng et al., 2009) and conferred Al-tolerance in *S. cerevisiae* and canola (*Brassica napus cv Westar*) (Anoop et al, 2003). However, up to 11-fold overproduction of CS did not increase the rate of citric acid production by *Aspergillus niger*, suggesting that citrate synthase contributes little to flux control in the pathway involved in citric acid biosynthesis by the strain (Ruijter et al., 2000). On the other hand, *E. coli* K and B isocitrate dehydrogenase (*icd*) mutants accumulated high levels of citrate when grown on glucose with a concomitant increase in *CS* activity upto more than 2 fold (Lakshmi and Helling, 1976; Aoshima et al., 2003). Similarly, *B. subtilis icd* mutant in early stationary phase accumulated ~15 fold higher intracellular citrate levels as compared to the wild type (Matsuno et al., 1999). *glt*A gene overexpression in *E. coli* increased the maximum cell dry weight by 23% and reduced acetate secretion (De Maeseneire et al., 2006).

Metabolic studies in *E. coli* demonstrated that high citric acid yields could be attained on glucose and depending on the host metabolism; glucose transport, flux though catabolic pathways and the regulatory mechanisms influenced by intracellular metabolite pools appear to facilitate the citrate accumulation (Elias, 2009). It was also postulated that increasing CS activity in *P. fluorescens* for citric acid overproduction from glucose is a better strategy than *icd* mutation in *E. coli*, which reduces biomass and growth (Aoshima et al., 2003). The amount of citric acid produced by *P. fluorescens* overexpressing *E. coli cs* gene was similar to that secreted by the phosphate solubilizing *Bacillus coagulans* and *Citrobacter koseri* on glucose (Gyaneshwar et al., 1998). But the amount of citric acid secreted by this approach is insufficient for effective P solubilization in field condition. Hence further strategies are required to increase the citrate level.

3.1.4 Rational of the present study

Functional properties of nine sequence variants of *E. coli* CS at NADH binding site had had varied inhibition in kinetic parameters for catalysis (Fig. 3.5) (Stockell et al., 2003). In three cases, Y145A, R163L, and K167A, NADH inhibition has become extremely weak (**Table 3.2, Fig. 3.4**).

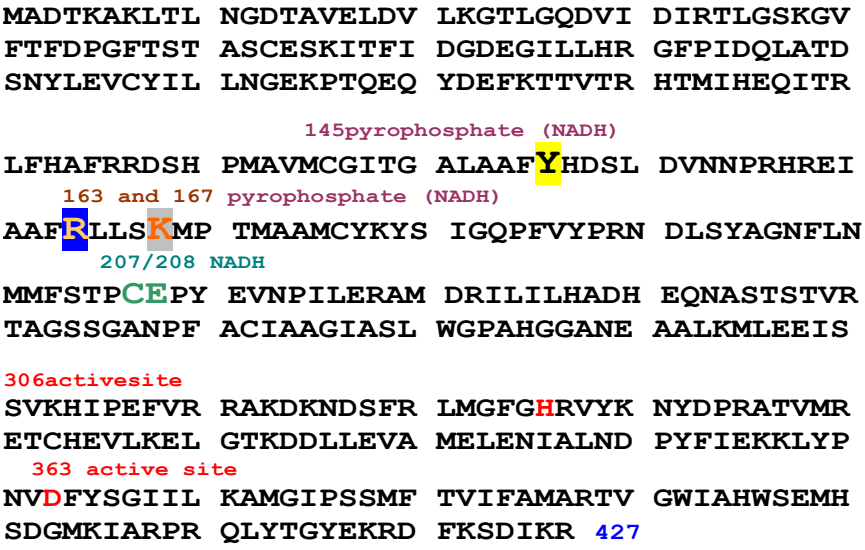

Figure 3.4: *E. coli cs* protein sequence showing the regulatory variants

Table 3.2: NADH binding and inhibition by variant citrate synthases (Stokell et al., 2003)

Variant	Kd (µM)	Ki (µM)	Maximum inhibition(%)
Wild type	1.6±0.1	2.8±0.4	100±10
R109L	1.16±.04	1.7±0.2	96±6
H110A	5.2±0.2	121±11	97±3
T111A	6.6±0.2	80±15	87±6
Y145F	**>100**	**790±210**	**100±3**
R163L	**5.81±.04**	**400±80**	**77±8**
K167A	**4.1±0.2**	**630±130**	**100±10**
Q128A	6.1±0.5	18±3	100±7
N189A	6.9±0.8	242±26	96±5
T204A	10.2±0.4	165±36	100±7

The present study demonstrates the effect of overexpression of NADH insensitive *cs* variants e.g., Y145F, R163L, and K167A on citric acid accumulation and secretion by *P. fluorescens* PfO-1.

3.2 WORK PLAN

The experimental plan of work includes the following-

3.2.1 Bacterial strains used in this study

Table 3.3: List of bacterial strains used.

Bacterial strains	Characteristics	Source/Reference
E. coli DH5α	F-φ80Δ*lac*ZΔM15Δ(*lac*ZYA-*arg*F) U169 *rec*A1 *end*A1 *hsd*R17 (rk-, mk+) *pho*A *sup*E44 λ-*thi*-1 *gyr*A96 *rel*A1	Sambrook and Russell,2001
E. coli W620	*cs* mutant strain exhibiting glutamate auxotrophy, CGSC 4278 - *glnV44 gltA6 galK30 LAM-pyrD36 relA1 rpsL129 thi-1*; Str^r	*E. coli* Genetic Stock Center
P. fluorescens PfO-1	Wild type strain	
Pf (pAB8)	*P. fluorescens* PfO-1 with pAB8; Km^r	This sudy
Pf(pAB7)	*P. fluorescens* PfO-1 with pAB7; Km^r	This sudy
Pf (pR163L)	*P. fluorescens* PfO-1 with pR163L; Km^r	This sudy
Pf(pK167A)	*P. fluorescens* PfO-1 with pK167A; Km^r	This sudy
Pf(pY145F)	*P. fluorescens* PfO-1 with pY145F; Km^r	This sudy

Detailed characteristics of these strains and plasmids are given in **Section 2.1** Parent strains and the transformants of *E. coli* and *Pseudomonas fluorescens* were respectively grown at 37ºC and 30ºC with streptomycin and kanamycin as and when required, at final concentrations varying for rich and minimal media as described in **Section 2.2, Table 2.4**

3.2.2 Cloning and expression of NADH insensitive *E. coli cs* gene in *P. fluorescens* PfO-1

The strategy for construction of recombinant *P fluorescens* strain harbouring NADH insensitive *cs* gene are depicted in **Fig. 3.5.**

3.2.2.1 Construction of *Pseudomonas* stable plasmid containing *E. coli NADH* insensitive *cs* gene under *lac* promoter

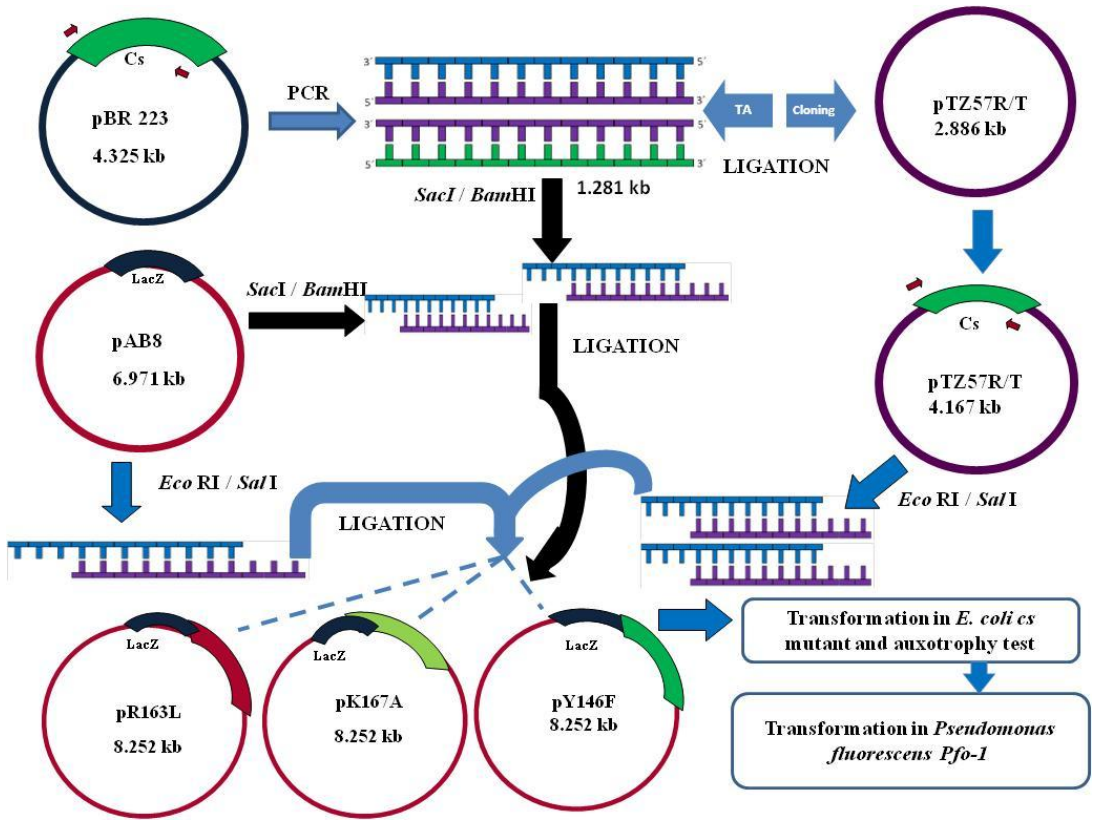

Figure 3.5: Schematic representation of construction of pseudomonad stable vectors containing NADH insensitive *E. coli cs* gene under *lac* promoter. Blue arrows indicate strategy1 and black arrow indicate strategy 2

3.2.2.1.1 Incorporation of NADH insensitive *E. coli cs* in pUCPM18:

PCR amplification of pBR322 plasmid containing NADH insensitive *E. coli cs* (*gltA*) gene are carried out using gene specific primer (Table 3.4) to get an amplification of 1281 bp each of *R163L, K167A, Y145F*

Table 3.4: NADH insensitive *cs* primers

Primer	Oligonucleotide Sequence(5'-3'end)	Tm/GC%
Ec*CS*ApaI SacIF	5'**CGAGCTC***GGGCCC*TTTTTCACGGAGGAAACC ACAATG GCT GAT ACA AAA GC	59.6˚C, 52.2%
Ec*CS*KpnIBamHI R	**CGGGATTC***CGGATCCG* TTA ACG CTT GAT ATC GC	59.6˚C, 46.2%

SacI ApaI: CGAGCTC*GGGCCC* ***KpnI*** **BamHI:** GG**GGTACC**CGGATCCG

RBS: 5'CACG**GAGGA**ATCAACTT **3'**

Cloning of the isolated *cs* gene was carried out in broad host range cloning vector pUCPM18 having kanamycin resistance gene using two strategies. In one strategy the amplified 1281 bp gene was directly cloned into pUCPM18 km^r vector in SacI/BamHI site under *lac* promoter. In another strategy the amplified product was cloned into pTZ57R using InsT/Aclone™ PCR product cloning kit, MBI Fermentas and transformed into *E. coli* DH5α. The presence of the appropriate plasmid was checked by PCR and restriction enzyme digestion and subcloned into pUCPM18 kan^r vector in *EcoRI*/*SalI* restriction site (**Fig.3.6**)

3.2.2.1.2 Functional confirmation of *CS* expressed from pR163L, pK167A and pY145F

E. coli W620, which exhibited glutamate auxotrophy due to mutation in *cs* gene, was used to determine the functionality of the *cs* gene. pAB7, pR163L, pK167A and pY145F along with the respective controls pAB8 plasmids were transformed into *E. coli* W620 (**Table 2.1, Section 2.2**). The transformants were selected on agar plates with streptomycin and kanamycin (doses as recommended in **Section 2.2**) and confirmed the presence of

respective plasmids. Subsequently these were subjected to auxotrophy complementation studies (**Section 2.6**).

3.2.2.1.3 Development of *P. fluorescens* PfO-1 harboring NADH insensitive *E. coli cs* gene

The recombinant plasmids pR163L, pK167A and pY145F along with control pAB8 and plasmid containg wild type *cs* gene pAB7 were transformed by elecroporation in *P. fluorescens* PfO-1 (**Section 5.2.2**). The transformants were selected on pseudomonas agar plate containing kanamycin and were confirmed by fluorescence and restriction enzyme digestion of the isolated plasmids from the respective strains (**Section 2.4.5**).

3.2.3 Effect of NADH insensitive *E. coli cs* gene expression on the physiology and glucose metabolismof of *P. fluorescens* PfO-1.

P. fluorescens PfO-1 transformants were subjected to physiological experiments involving growth and organic acid production profiles on M9 minimal medium with 100mM glucose as carbon source. The samples withdrawn at regular interval were analyzed for O.D.600nm, pH, and extracellular glucose (**Section 2.7.2**). Stationary phase cultures harvested at the time of pH drop were subjected to organic acid estimation using HPLC (**Section 2.7.3**). The physiological parameters were calculated as in section 2.7.3. The enzyme assays were performed as described in 2.8, with *CS*, G-6-PDH,ICDH PYC being assayed in both mid-log to late-log and stationary phase cultures while ICL and GDH are being assayed in the mid log and stationary phase cultures respectively.

3.3 RESULTS

3.3.1 Construction of *Pseudomonas* stable plasmid containing NADH insensitive *E. coli cs* gene under *lac* promoter

The plasmids pR163L. pK167A and pY145F containing *E. coli NADH insensitive cs* gene *r163l, k16a* and *y146f* respectively under *lac* promoter of pUCPM18 plasmid with km^r gene were constructed in a two step cloning procedure schematically represented and discussed in section (**Fig. 3.6).** All plasmids were confirmed based on restriction digestion pattern (**Fig. 3.7-3.14)**) and PCR (**Fig. 3.15**).The plasmids pAB8 and pAB7 were taken as a control for all the experiments.

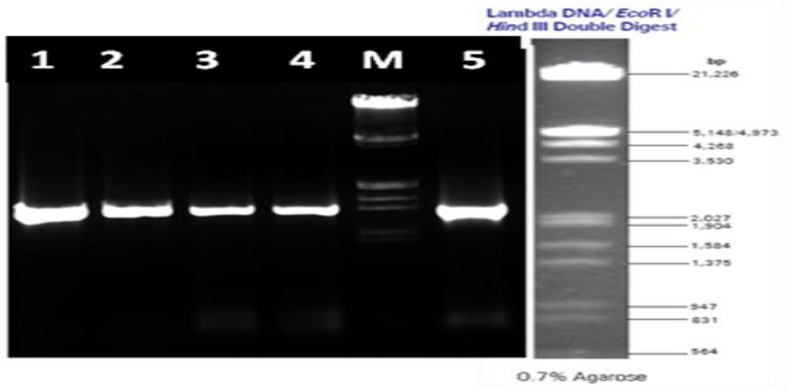

Figure 3.6: PCR amplification of NADH insensitive *cs* gene. *R163L* (Lane1), *K167A (Lane2), Y145F* (Lane3); pCC*gltA* (Lane4), pES*gltA* (Lane5) each of 1281 bp

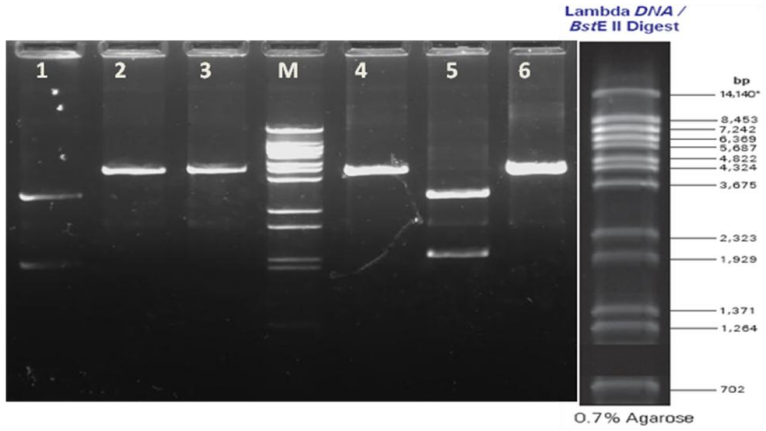

Figure 3.7: Restriction digestion pattern of pTZ57R/T *Y146F* clone with *Sac*I. Lane1, 5: plasmid with Y145F gene in right orientation (2886 bp and 1281 bp).Lane 2, 3, 4, 6: plasmid with *Y145F* in opposite orientation (4167 bp). Lane M: Molecular weight marker (MWM)-Lamda DNA cut with *BstE*II

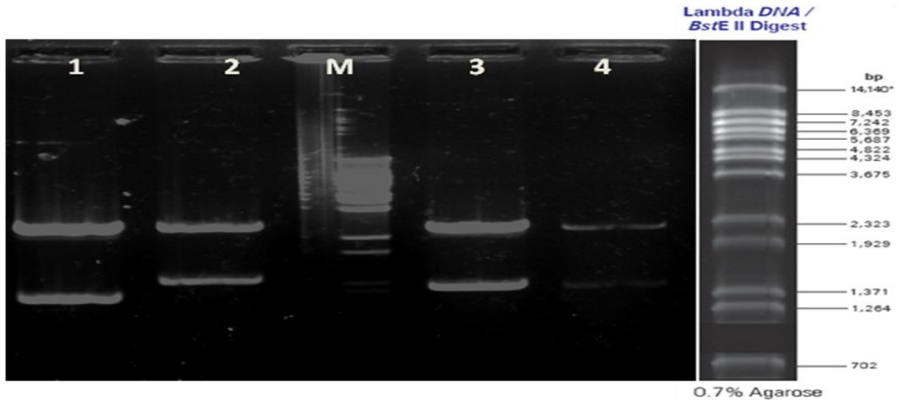

Figure 3.8: Restriction digestion pattern of pTZ57R/T *K167A* clone . Lane1-Lane4: pTZ57R/T *K167A* plasmid digested with *KpnI*(2886 bp and 1281 bp) . Lane M: Molecular weight marker(MWM)-Lamda DNA cut with *BstE*II

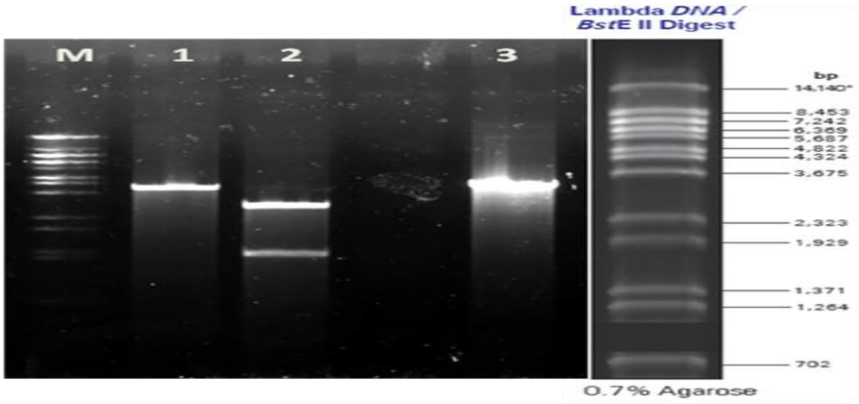

Figure 3.9: Restriction digestion pattern of pTZ57R/T *R146L*clone with *KpnI*. Lane1, 3: plasmid containing gene in opposite orientation (4167 bp). Lane 2: plasmid containing gene in right orientation (2886 bp and 1281 bp). Lane M: Molecular weight marker(MWM)-Lamda DNA cut with *BstE*II

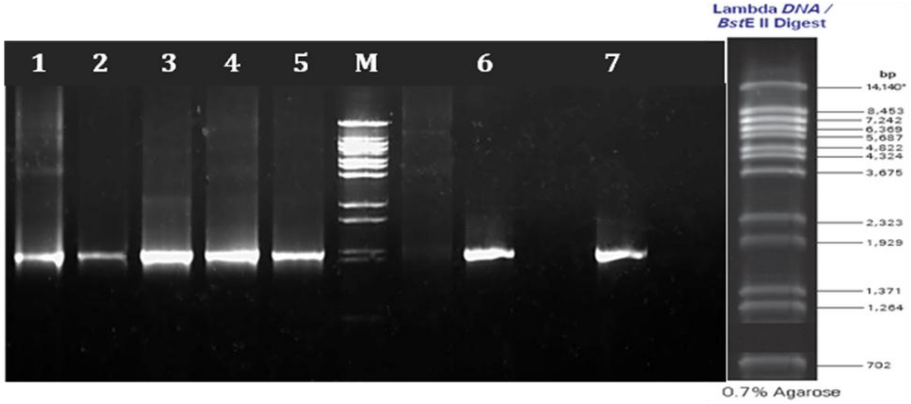

Figure 3.10: PCR amplification of TA clones. Lane1, 2: *R163L*; Lane3, 4:*Y145F*; Lane5, 6: *K167A* Lane7: wild type *cs* gene each gene of 1281 bp; Lane M: Molecular weight marker (MWM)-Lamda DNA cut with *BstE*II.

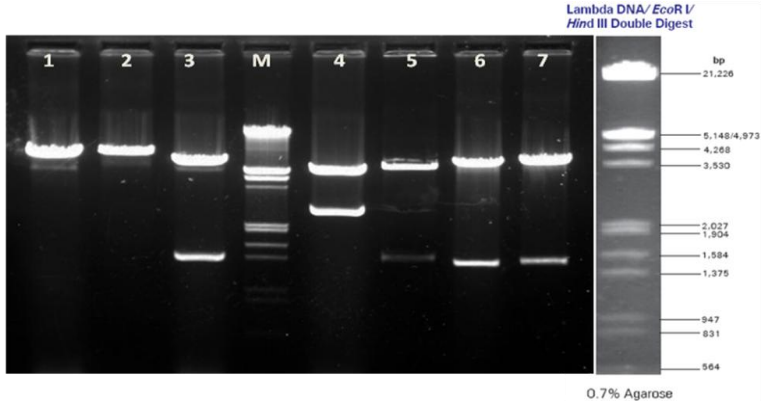

Figure 3.11: Restriction digestion pattern for pY145F. Lane1: pY145F linearizes with SacI (8252bp); Lane2: pY145F linearizes with BamHI (8252 bp); Lane3: pY145F digested with *EcoRI-SalI* (6971bp,1281bp); Lane4: pY145F digested with *EcoRI-BglII*(6971bp,2918 bp);Lane5: pAB8 digested with *EcoRI-BglII*

(5334bp,1637 bp); Lane6:pY145F digested with ApaI (6971 bp,1281 bp); Lane6: pY145F digested with *KpnI* (6971 bp,1281 bp); LaneM:MWM with Lamda DNA *EcoRI*/HindIII double digest.

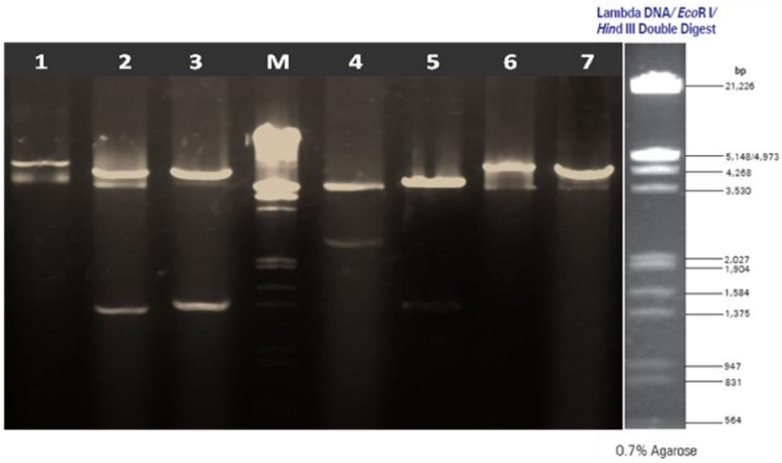

Figure 3.12: Restriction digestion pattern for pK167A. Lane1: pK167A plasmid linearized with BamHI (8252bp); Lane2; pK167A digested with ApaI (6971bp, 1281bp); Lane3: pK167A digested with *EcoRI-SalI*(6971bp,1281bp);Lane4: pK167A digested with *EcoRI-BglII* (5334bp,2918 bp); lane5:pAB8 digested with *EcoRI-BglII* (5550bp,1421bp); lane6: pK167A plasmid linearized with SacI (8252bp); Lane7: pK167A plasmid linearized with *EcoRI* (8252bp); laneM: MWM lamda DNA *EcoRI*/HindIII double digest

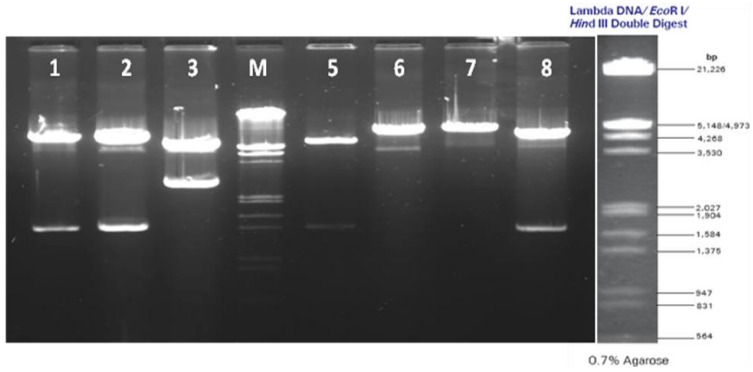

Figure 3.13: Restriction digestion pattern for pR163L. Lane1: pR163L digested with *KpnI* (6971bp,1281bp); Lane2: pR163L digested with *EcoRI-SalI* (6971bp,1281bp); Lane3: pR163L digested with *EcoRI-BglII*(5334bp,2918 bp); Lane5: pAB8 digested with *EcoRI-BglII* (5550bp,1421bp); lane6: pR163L linearized withApaI(8252bp); lane7: pR163L linearized with SacI(8252bp) ; Lane8: pR163L digested with *EcoRI* (6971bp,1281bp); laneM: MWM lamda DNA *EcoRI*/HindIII double digest

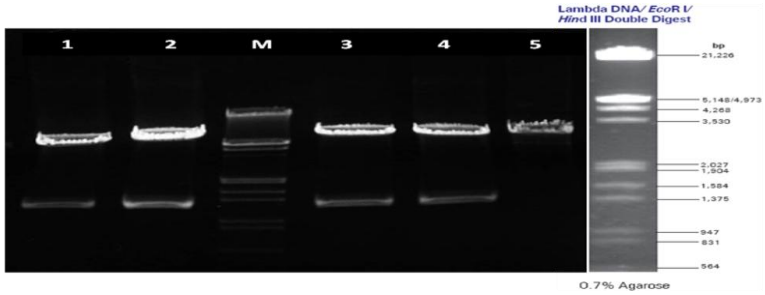

Figure 3.14: Restriction digestion pattern for pUCPM18 Km^r containing NADH insensitive *cs* gene digested with EcoRI-BamHI (StrategyII). Lane1,Lane2: pY145F (6971bp,1281bp); Lane3: pR163L ((6971bp,1281bp); Lane4: pK167A (6971bp,1281bp); Lane5: pAB8 (6971bp,1281bp);LaneM: MWM containing LamdaDNA EcoRI-HindIII double digest.

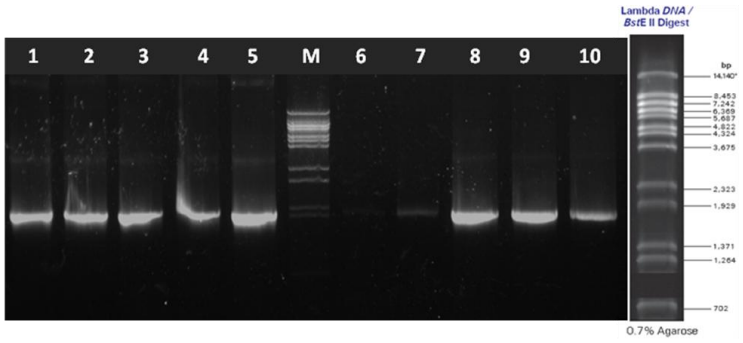

Figure 3.15: **PCR amplification of NADH insensitive gene cloned in pUCPM18 km^r vector**. Lane1-Lane3: pUCPM18 Km^r containing Y145F gene; Lane4,5: pUCPM18 Km^r containing R163L gene; Lane6-Lane10:pUCPM18 Km^r containing K167 gene;each gene of 1281bp;LaneM: MWM containing lamda DNA cut with BstEII.

3.3.2 *E. coli cs* mutant complementation

E. coli cs mutant strain harboring pAB7, pR163L, K167A and pY145F could grow on M9 minimal medium containing glucose as carbon source o when induced with 0.1mM IPTG without glutamate supplementation unlike the controls pAB8 (**Fig.3.16**).

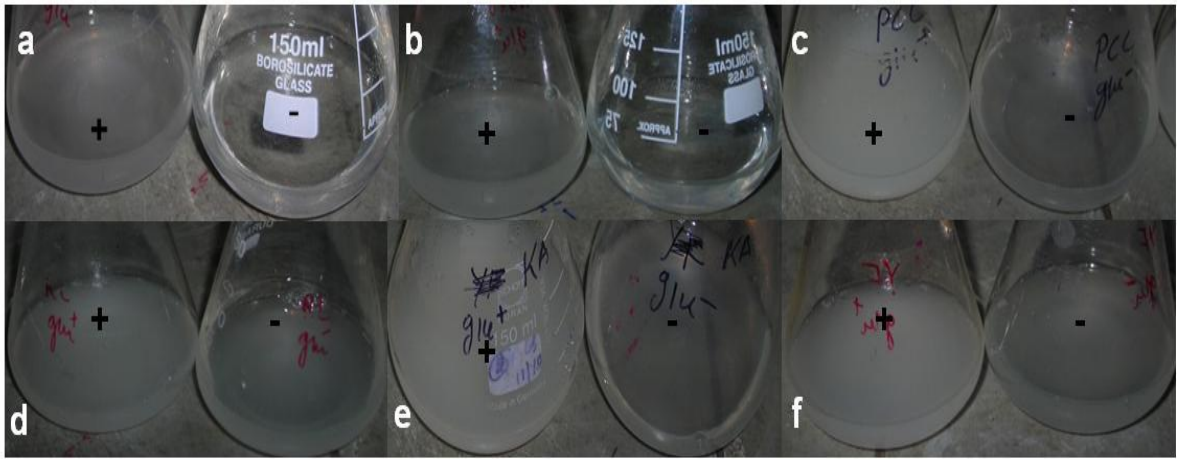

Figure 3.16: Complementation of *E. coli* W620 mutant phenotype by wild type and NADH insensitive *cs* plasmids. a: *E. coli* W620-deletion mutant of *cs* gene b: *E. coli* W620 with pAB8 plasmid c: *E. coli* W620 with pAB7 plasmid d: *E. coli* W620 with pR163L plasmid e: *E. coli* W620 with pK167 plasmid f: *E. coli* W620 with pY145F plasmid. All plasmid bearing strains are induced with 0.1mM IPTG. Growth is monitored on M9 medium with 0.2% glucose (Section) +/– at the corners of each image indicates absence and presence of 340µg/ml glutamate in the medium, respectively.

3.3.3 Partial sequencing of pY145F plasmid

Partial sequencing of the PCR product amplified from pY146F plasmid when analysed using NCBI BLAST (Basic Local Alignment Seaech Tool) and Ribososmal Database Project (RDP) II, online homology search programs, revealed maximum identity (99%) to *E. coli* citrate synthase (GenBank Accession number AAA23892) (**Fig. 3.17-3.18**).

>YFPCRPRODUCT_YFFOR_S702

CNCNNANCGGCACCCTGAACGGGGATACAGCTGTTGAACTGGATGTGCTGAAAGGCACGC
TGGGTCAAGATGTTATTGATATCCGTACTCTCGGTTCAAAAGGTGTGTTCACCTTTGACC
CAGGCTTCACTTCAACCGCATCCTGCGAATCTAAAATTACTTTTATTGATGGTGATGAAG
GTATTTTGCTGCACCGCGGTTTCCCGATCGATCAGCTGGCGACCGATTCTAACTACCTGG
AAGTTTGTTACATCCTGCTGAATGGTGAAAAACCGACTCAGGAACAGTATGACGAATTTA
AAACTACGGTGACCCGTCATACCATGATCCACGAGCAGATTACCCGTCTGTTCCATGCTT
TCCGTCGCGACTCGCATCCAATGGCAGTCATGTGTGGTATTACCGGCGCGCTGGCGGCGT
TCTTTCACGACTCGCTGGATGTTAACAATCCTCGTCACCGTGAAATTGCCGCGTTCCGCC
TGCTGTCGAAAATGCCGACCATGGCCGCGATGTGTTACAAGTATTCCATTGGTCAGCCAT
TTGTTTACCAGCGCAACGATCTCTCCTACGCCGGTAACTTCCTGAATATGATGTTCTCCA
CGCCGTGCGAACCGTATGAAGTTAATCCGATTCTGGAACGTGCTATGGACCGTATTCTGA
TCCTGCACGCTGACCATGAACAGAACGCCTCTACCTCCACCGTGCGTACCGCTGGCTCTT

CGGGTGCGAACCCGTTTGCCTGTATCGCAGCAGGTATTGCTTCACTGTGGGGACCTGCGC
ACGGCGGTGCTAACGAAGCGGCGCTGAAAATGCTGGAAGAAATCAGCTCCGTTAAACACA
TTCCGGAATTTGTTCGTCGTGCGAAAGACAAAAATGATTCTTTCCGCCTGATGGGCTTCG
GTCACCGCGTGTACAAAATTACGACCCGCGCGCCACCGTAATGCGTGAAACCTGCCATGA
AGTGCTGAAAGAGCTGGGCACGAANNTGACCTGCTGNAGT

Figure 3.17: Partial sequence of *E. coli* NADH insensitive *cs* gene

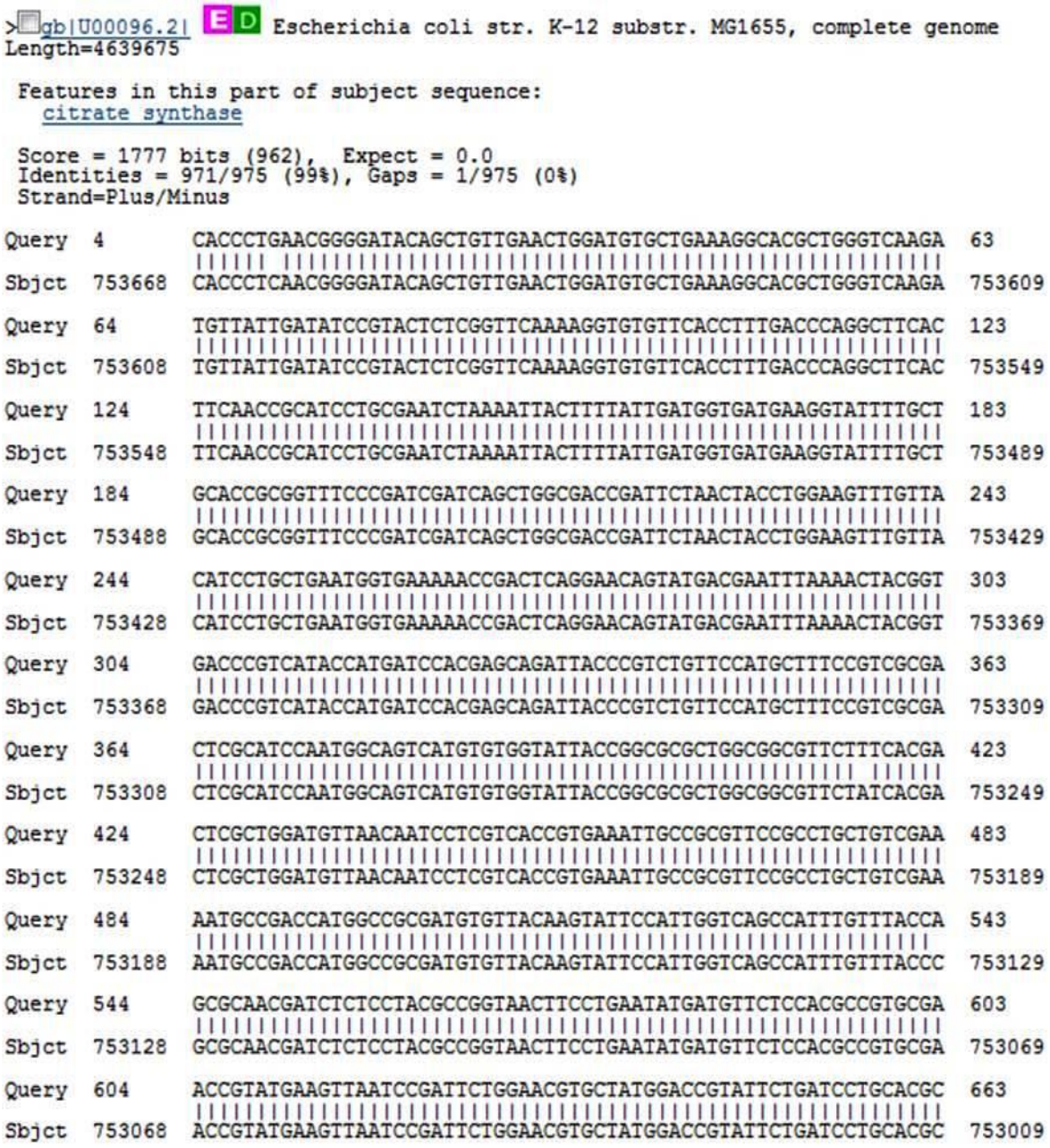

>gb|U00096.2| Escherichia coli str. K-12 substr. MG1655, complete genome
Length=4639675

Features in this part of subject sequence:
citrate synthase

Score = 1777 bits (962), Expect = 0.0
Identities = 971/975 (99%), Gaps = 1/975 (0%)
Strand=Plus/Minus

```
Query  4       CACCCTGAACGGGGATACAGCTGTTGAACTGGATGTGCTGAAAGGCACGCTGGGTCAAGA  63
              ||||||  ||||||||||||||||||||||||||||||||||||||||||||||||||||
Sbjct  753668  CACCCTCAACGGGGATACAGCTGTTGAACTGGATGTGCTGAAAGGCACGCTGGGTCAAGA  753609

Query  64      TGTTATTGATATCCGTACTCTCGGTTCAAAAGGTGTGTTCACCTTTGACCCAGGCTTCAC  123
              ||||||||||||||||||||||||||||||||||||||||||||||||||||||||||||
Sbjct  753608  TGTTATTGATATCCGTACTCTCGGTTCAAAAGGTGTGTTCACCTTTGACCCAGGCTTCAC  753549

Query  124     TTCAACCGCATCCTGCGAATCTAAAATTACTTTTATTGATGGTGATGAAGGTATTTTGCT  183
              ||||||||||||||||||||||||||||||||||||||||||||||||||||||||||||
Sbjct  753548  TTCAACCGCATCCTGCGAATCTAAAATTACTTTTATTGATGGTGATGAAGGTATTTTGCT  753489

Query  184     GCACCGCGGTTTCCCGATCGATCAGCTGGCGACCGATTCTAACTACCTGGAAGTTTGTTA  243
              ||||||||||||||||||||||||||||||||||||||||||||||||||||||||||||
Sbjct  753488  GCACCGCGGTTTCCCGATCGATCAGCTGGCGACCGATTCTAACTACCTGGAAGTTTGTTA  753429

Query  244     CATCCTGCTGAATGGTGAAAAACCGACTCAGGAACAGTATGACGAATTTAAAACTACGGT  303
              ||||||||||||||||||||||||||||||||||||||||||||||||||||||||||||
Sbjct  753428  CATCCTGCTGAATGGTGAAAAACCGACTCAGGAACAGTATGACGAATTTAAAACTACGGT  753369

Query  304     GACCCGTCATACCATGATCCACGAGCAGATTACCCGTCTGTTCCATGCTTTCCGTCGCGA  363
              ||||||||||||||||||||||||||||||||||||||||||||||||||||||||||||
Sbjct  753368  GACCCGTCATACCATGATCCACGAGCAGATTACCCGTCTGTTCCATGCTTTCCGTCGCGA  753309

Query  364     CTCGCATCCAATGGCAGTCATGTGTGGTATTACCGGCGCGCTGGCGGCGTTCTTTCACGA  423
              |||||||||||||||||||||||||||||||||||||||||||||||||||| |||||||
Sbjct  753308  CTCGCATCCAATGGCAGTCATGTGTGGTATTACCGGCGCGCTGGCGGCGTTCTATCACGA  753249

Query  424     CTCGCTGGATGTTAACAATCCTCGTCACCGTGAAATTGCCGCGTTCCGCCTGCTGTCGAA  483
              ||||||||||||||||||||||||||||||||||||||||||||||||||||||||||||
Sbjct  753248  CTCGCTGGATGTTAACAATCCTCGTCACCGTGAAATTGCCGCGTTCCGCCTGCTGTCGAA  753189

Query  484     AATGCCGACCATGGCCGCGATGTGTTACAAGTATTCCATTGGTCAGCCATTTGTTTACCA  543
              ||||||||||||||||||||||||||||||||||||||||||||||||||||||||||||
Sbjct  753188  AATGCCGACCATGGCCGCGATGTGTTACAAGTATTCCATTGGTCAGCCATTTGTTTACCC  753129

Query  544     GCGCAACGATCTCTCCTACGCCGGTAACTTCCTGAATATGATGTTCTCCACGCCGTGCGA  603
              ||||||||||||||||||||||||||||||||||||||||||||||||||||||||||||
Sbjct  753128  GCGCAACGATCTCTCCTACGCCGGTAACTTCCTGAATATGATGTTCTCCACGCCGTGCGA  753069

Query  604     ACCGTATGAAGTTAATCCGATTCTGGAACGTGCTATGGACCGTATTCTGATCCTGCACGC  663
              ||||||||||||||||||||||||||||||||||||||||||||||||||||||||||||
Sbjct  753068  ACCGTATGAAGTTAATCCGATTCTGGAACGTGCTATGGACCGTATTCTGATCCTGCACGC  753009
```

Figure 3.18 : NCBI BLAST analysis of partial cs sequence

Pairwise alignment of the sequence with original *E. coli* K12 NADH sensitive *cs* sequence from database using EBI parwise alignment tool, revealed a mutation of tyrosine residues in 146 amino acid position to phenylalanine (**Fig. 3.19**).

```
PCR              1 --------------CNCNNANCGGCACCCTGAACGGGGATACAGCTGTTG     36
                                 ..|..|.| .|||||||.||||||||||||||||||
ORIGINAL         1 atggctgatacaaaagcaaaac-tcaccctcaacggggatacagctgttg     49

PCR             37 AACTGGATGTGCTGAAAGGCACGCTGGGTCAAGATGTTATTGATATCCGT     86
                   ||||||||||||||||||||||||||||||||||||||||||||||||||
ORIGINAL        50 aactggatgtgctgaaaggcacgctgggtcaagatgttattgatatccgt     99

PCR             87 ACTCTCGGTTCAAAAGGTGTGTTCACCTTTGACCCAGGCTTCACTTCAAC    136
                   ||||||||||||||||||||||||||||||||||||||||||||||||||
ORIGINAL       100 actctcggttcaaaaggtgtgttcacctttgacccaggcttcacttcaac    149

PCR            137 CGCATCCTGCGAATCTAAAATTACTTTTATTGATGGTGATGAAGGTATTT    186
                   ||||||||||||||||||||||||||||||||||||||||||||||||||
ORIGINAL       150 cgcatcctgcgaatctaaaattacttttattgatggtgatgaaggtattt    199

PCR            187 TGCTGCACCGCGGTTTCCCGATCGATCAGCTGGCGACCGATTCTAACTAC    236
                   ||||||||||||||||||||||||||||||||||||||||||||||||||
ORIGINAL       200 tgctgcaccgcggtttcccgatcgatcagctggcgaccgattctaactac    249

PCR            237 CTGGAAGTTTGTTACATCCTGCTGAATGGTGAAAAACCGACTCAGGAACA    286
                   ||||||||||||||||||||||||||||||||||||||||||||||||||
ORIGINAL       250 ctggaagtttgttacatcctgctgaatggtgaaaaaccgactcaggaaca    299

PCR            287 GTATGACGAATTTAAAACTACGGTGACCCGTCATACCATGATCCACGAGC    336
                   ||||||||||||||||||||||||||||||||||||||||||||||||||
ORIGINAL       300 gtatgacgaatttaaaactacggtgacccgtcataccatgatccacgagc    349

PCR            337 AGATTACCCGTCTGTTCCATGCTTTCCGTCGCGACTCGCATCCAATGGCA    386
                   ||||||||||||||||||||||||||||||||||||||||||||||||||
ORIGINAL       350 agattacccgtctgttccatgctttccgtcgcgactcgcatccaatggca    399

PCR            387 GTCATGTGTGGTATTACCGGCGCGCTGGCGGCGTTCTTTCACGACTCGCT    436
                   ||||||||||||||||||||||||||||||||||||.|||||||||||||
ORIGINAL       400 gtcatgtgtggtattaccggcgcgctggcggcgttctatcacgactcgct    449
```

Figure 3.19: EBI pairwise alignment of NADH insensitive and wild type *cs* gene showing the position of mutation

3.3.4 Heterologous overexpression of *E. coli NADH insensitive cs* gene in *P. fluorescens* PfO-1

pY146F plasmid transformed in *P. fluorescens* PfO-1 by electrporation. The transformants showed resistance against gentamycin. Restriction enzyme digestion of the isolated plasmid revealed the authenticity of the plasmid (**Fig.3.20**).

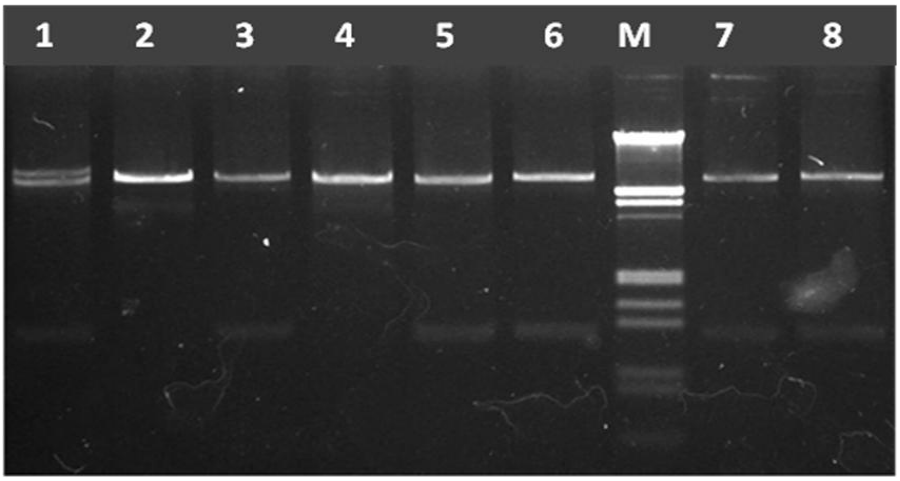

Figure 3.20: EcoRI-BamHI restriction digestion pattern for pUCPM18 Km^r containing *E. coli* NADH insensitive *cs* gene from *P. fluorescens* PfO-1 and *P. fluorescens* ATCC13525 transformants. Lane1: *P. fluorescens* PfO-1 with pR163L plasmid (6971,1281bp);Lane2: *P. fluorescens* PfO-1 with pAB8 plasmid (6971 bp); Lane3: *P. fluorescens* ATCC13525 pR163L (6971 ,1281 bp);Lane4: *P. fluorescens* ATCC13525 with pAB (6971 bp);Lane5: *P. fluorescens* PfO-1 with pAB7 (6971,1281 bp);Lane6: *P. fluorescens* ATCC13525 with pAB7(6971, 1281 bp);Lane7: *P. fluorescens* ATCC13525 with Y146F(6971, 1281 bp); Lane8: *P. fluorescens* PfO-1 with Y146F (6971,1281 bp); LaneM: MWM with Lamda DNA *EcoRI*/HindIII double digest

3.3.5 Biochemical effects of *E. coli cs* gene overexpression in *P. fluorescens* PfO-1

3.3.5.1 Alterations in citrate synthase activity

P. fluorescens PfO-1 harbouring pY145F showed maximum *CS* activity of 424.6±16.1U and 333.4±8.5U in the mid log and stationary phase, respectively, on M9 minimal medium in the presence of 100 mM glucose which is about 4.7 and 5.6 fold higher than that in the control Pf(pAB8), that showed 90.3±6.7U and 60±14.7 CS activity respectively. Also Pf(pY145F) showed the highest *cs* activity amongst all the other variants which is 2 fold,1.7 fold and 1.96 fold higher as compared to the wild type *cs* bearing strain *Pf*(pAB7) and other two NADH insensitive *cs* bearing strain *Pf* (pR163L) and *Pf* (K167A) respectively in the mid log phase (**Fig.3.21**).

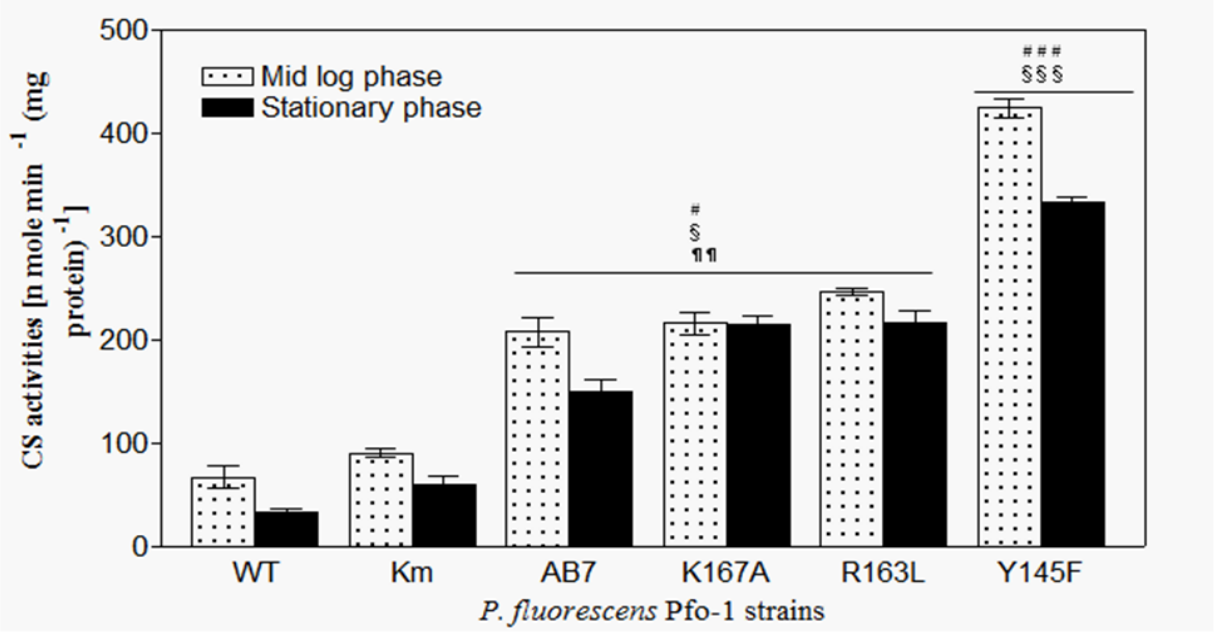

Figure 3.21: Citrate synthase activity of *P. fluorescens* PfO-1 transformants. The activity have been estimated using wild type, *Pf* (pAB7), *Pf* (pAB8) , *Pf* (pK16A), *Pf* (pR163L) and *Pf* (pY146F) cultures grown on M9 minimal medium with 100mM glucose from mid log phase and stationary phase cultures. Values are represented in the units of nmoles/min/mg total protein. The values are depicted as Mean ± S.E.M of 4 independent observations. # Comparison of parameters with respective Wild type, § with respect to Vector control pAB8, ¶ comparision between parameter of pY146F with pAB7,pR163L and pK167A.###, §§§,¶¶¶P<0.001; .##, §§,¶¶P<0.01; .#, §,¶P<0.05

3.3.5.2 Alterations in G-6-PDH, ICDH, ICL, PYC, and GDH activities

The effect of overexpression is also being monitored at the level of key enzymes of glucose catabolism in both mid log and stationary phase of growth. In *Pf* (pY146F) the periplasmic GDH activity increased by 2.1,1.4 and 1.26 fold as compared to the wild type, *Pf* (pAB8) and *Pf* (pAB7), respectively, in the stationary phase. There is a significant alteration in GDH activity found in vector control *Pf* (pAB8) as compared to the wild type strain. Similarly a significant increase in PYC activity (2.4, 2.1 and 0.15 fold in the mid log and 6.5, 4.1, 1.7 old in the stationary phase) was observed as compared to the respective controls. ICL and ICDH activities in both mid log and stationary phase and G6PDH activities in the stationary phase cultures remained unaltered. However in the mid log phase an altered G6PDH activities had increase in activity in *Pf* (pAB8) and *Pf* (pAB7) and significant decrease in *Pf*(pY146F) were monitored as compared to the wild type strain (**Fig. 3.22**).

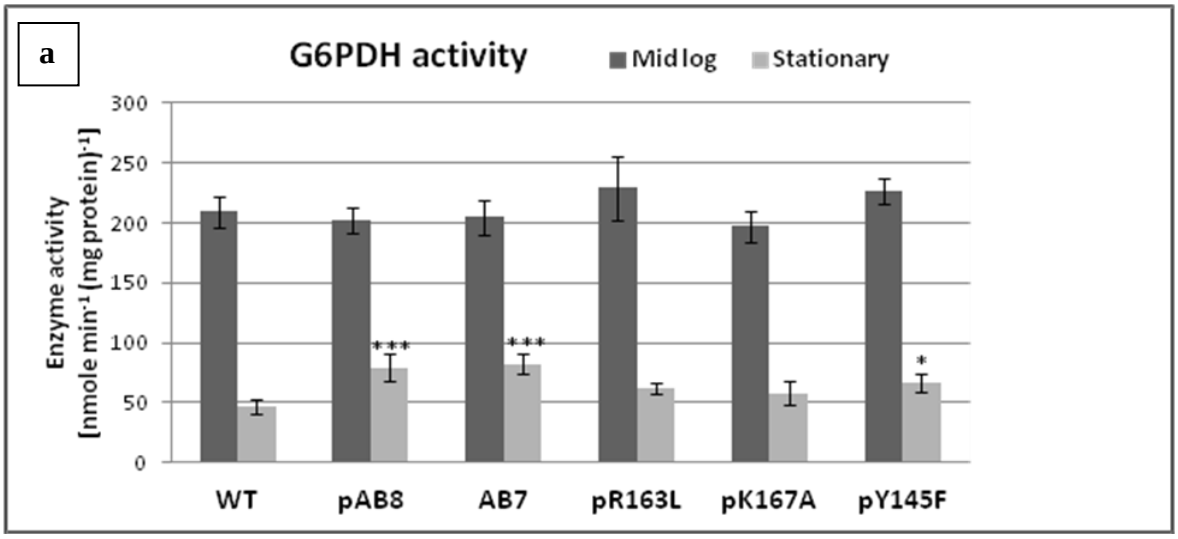
a
G6PDH activity
Mid log
Stationary
Enzyme activity
[nmole min-1 (mg protein)-1]
300
250
200
150
100
50
0
***
***
*
WT
pAB8
AB7
pR163L
pK167A
pY145F

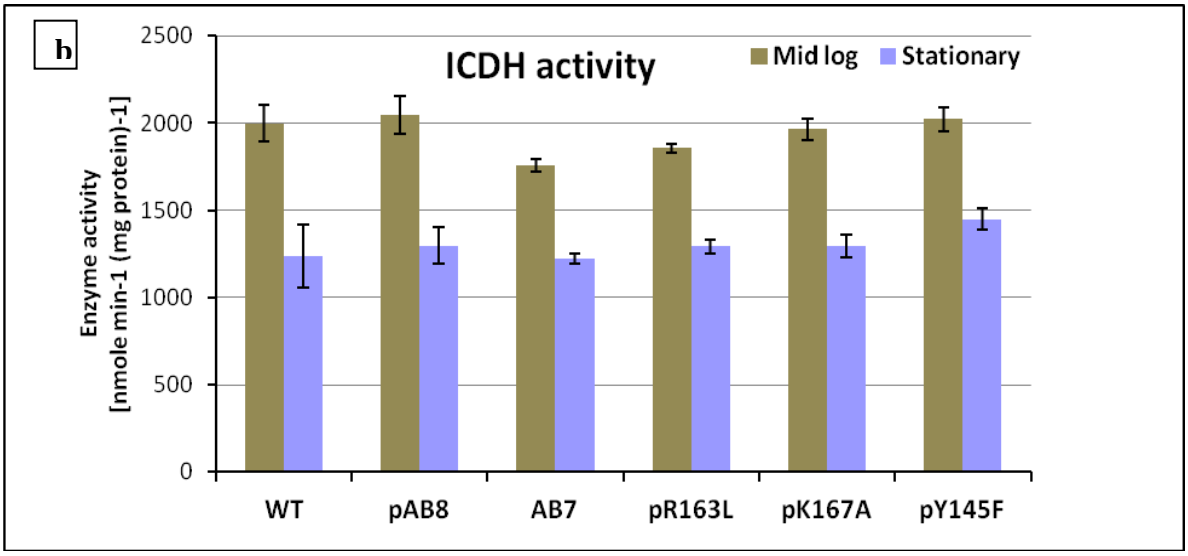
b
ICDH activity
Mid log
Stationary
Enzyme activity
[nmole min-1 (mg protein)-1]
2500
2000
1500
1000
500
0
WT
pAB8
AB7
pR163L
pK167A
pY145F

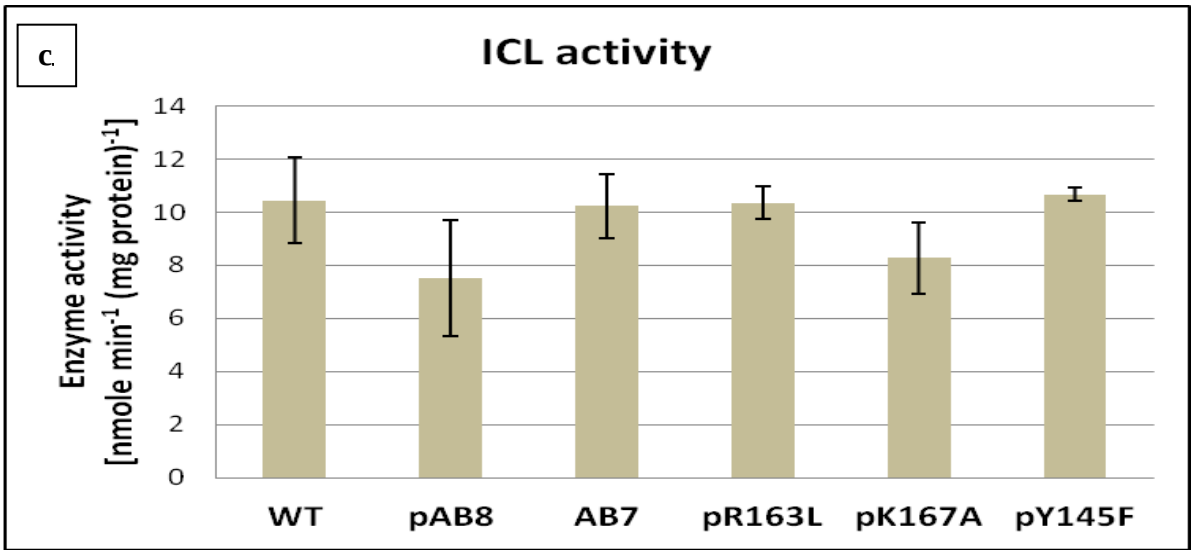
c
ICL activity
Enzyme activity
[nmole min-1 (mg protein)-1]
14
12
10
8
6
4
2
0
WT
pAB8
AB7
pR163L
pK167A
pY145F

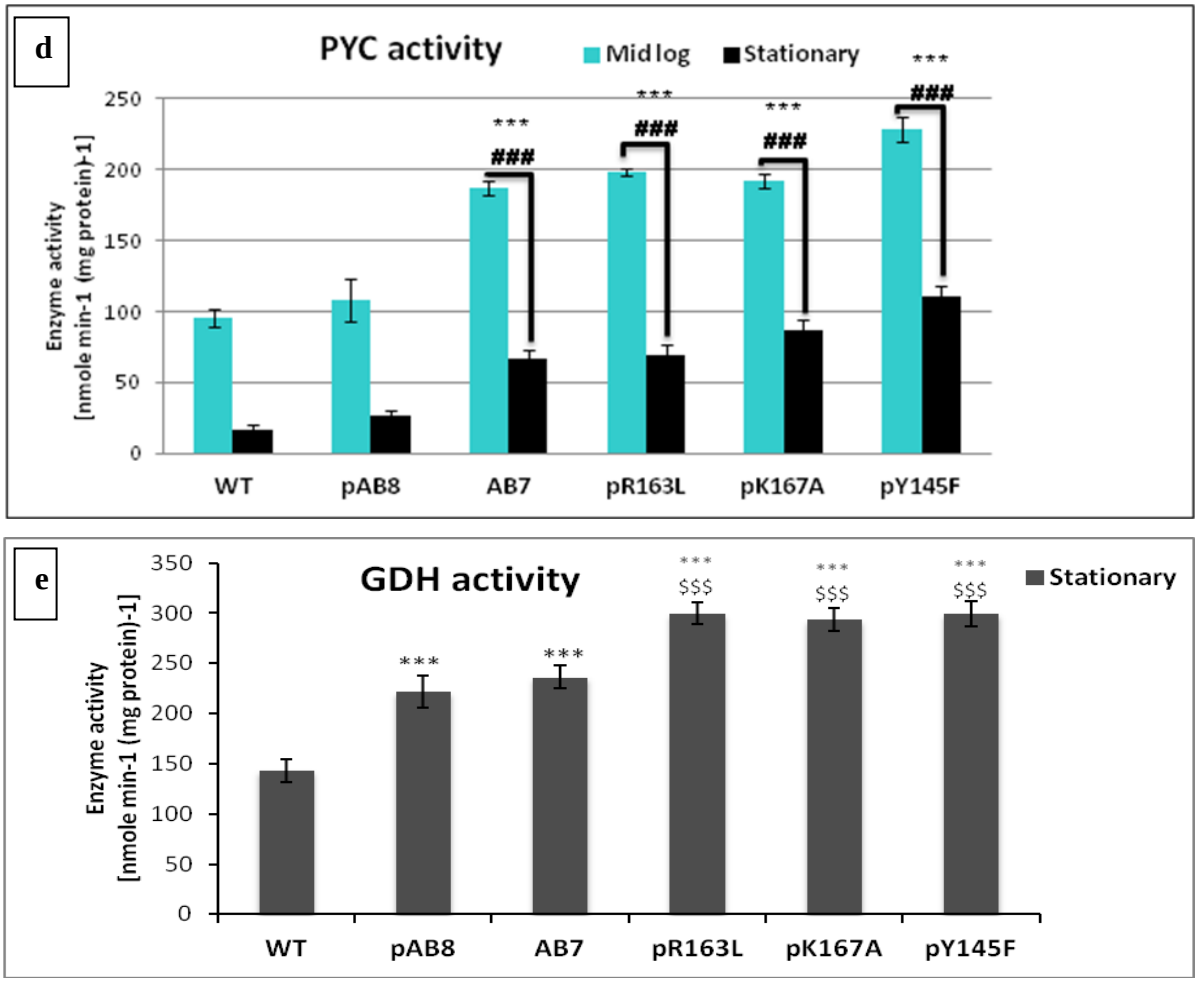

Figure 3.22: Activities of enzymes G-6-PDH (a) , ICDH (b), ICL (c), PYC (d), and GDH e) in *P. fluorescens* PfO-1 *cs* transformants. The activities have been estimated using wild type, *Pf*(pAB7), *Pf* (pAB8), *Pf* (pK16A), *Pf* (pR163L) and *Pf* (pY146F) cultures grown on M9 minimal medium with 100mM glucose. All the enzyme activities were estimated from mid log phase and stationary phase cultures except ICL and GDH which were estimated only in mid log and stationary phase respectively. All the enzyme activities are represented in the units of nmoles/min/mg total protein, . The values are depicted as Mean ± S.E.M of 4 (N=4) independent observations. *Comparison of parameters with respective Wild type; $ Comparison with respect to pAB8 and ,# comparision between parameters of pY146F with pAB7, pR163L and pK167A.***,$$$,###P<0.001; **,$$,##P<0.01; *,$,#P<0.05

3.3.5.3 Organic acid secretion

The NADH insensitve *cs* overexpression caused a significant alterations in both intracellular and extracellular citric acid lvels and yields. Intracellular citric acid levels in *Pf*(pY146F) increased by 5.7, 6.9 and 2.6 fold while there is a 5, 7.9 and 2.9 fold increase in

intracellular citrate yield as compared to wild type strain , *Pf*(pAB8)and *Pf*(pAB7) respectively.Corresponding extracellular citrate levels incresed by 57, 51.6 and 1.9 fold with an increse of extracellular citrate yield by 39.8, 29.9 and 2.39 fold compared to respective controls (**Fig.3.23**).

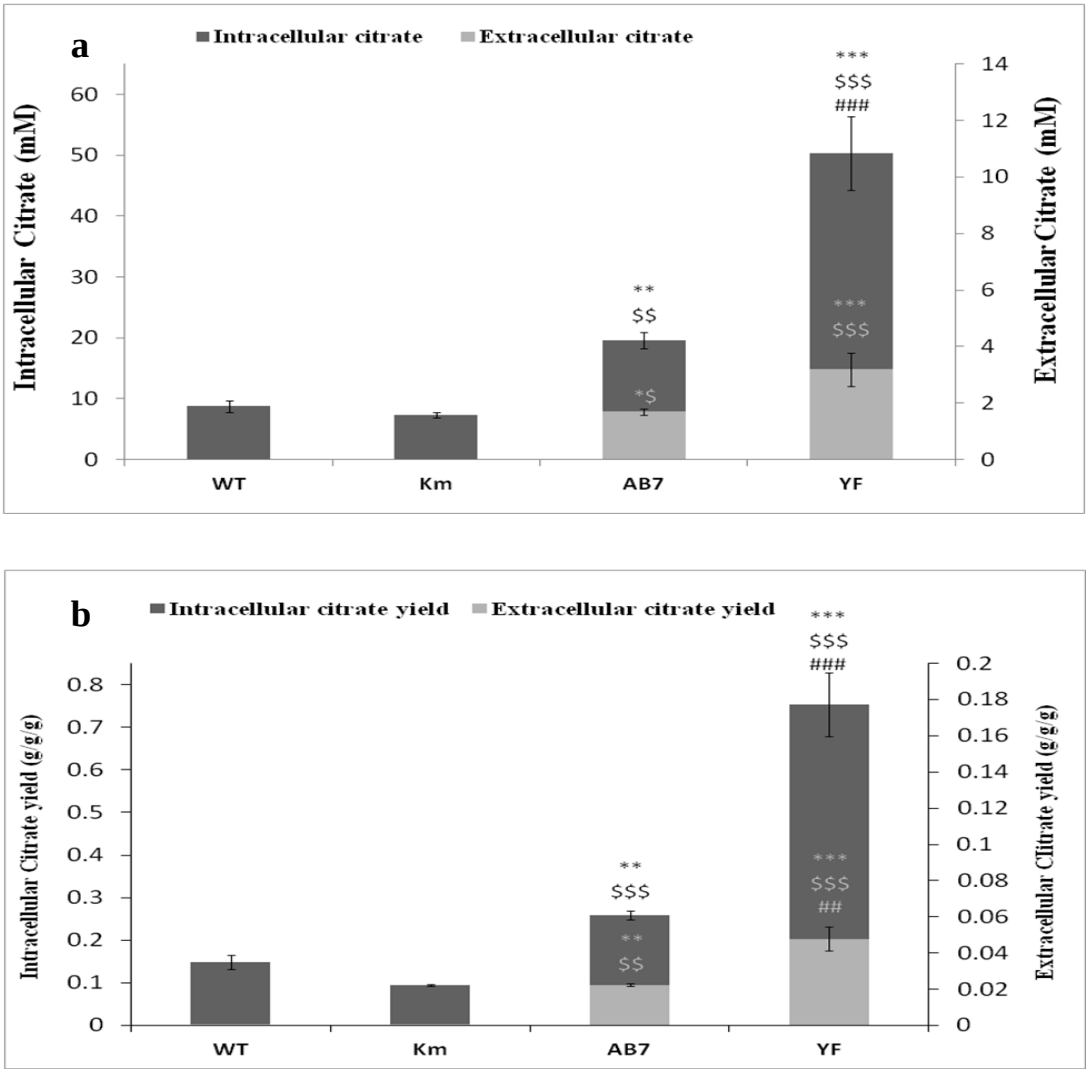

Figure 3.23 : Citric acid levels and yields in *P. fluorescens* PfO-1 wild type and plasmid bearing strains Km, AB7and YF.Intracellular citrate levels(a) and yields(b) are represented in black bars and extracellular citrate levels(a) and yields(b) are represented in grey bars. Organic acid yields were estimated from stationary phase cultures grown on M9 medium with 100mM glucose and are expressed as g/g of glucose utilized/g dry cell mass. Results are expressed as Mean ±S.E.M of 4 independent observations. . * comparision of parameters with wild type control; $ comparision of parameters with vector control pAB8,# comparision between parameters of AB7 and YF.***,$$$,###P<0.001; **,$$,##P<0.01; *,$,#P<0.05

The NADH insensitve *cs* overexpression also caused quantitative changes in secretion of gluconic, pyruvic and acetic acid levels. Stationary phase culture supernatents of *Pf* (pY145F) showed 4.4, 3.8 and 1.6 fold increased level of gluconic acid compared to wild type strain, *Pf*(pAB8) and *Pf*(pAB7), respectively (**Fig. 3.24**). On the other hand, pyruvic acid levels in the extracellular medium decreased significantly by 2.54 , 2 and 1.4 fold while acetic acid level increased by 2.9, 2.5 and 1.46 fold, respectively, compared to the controls.

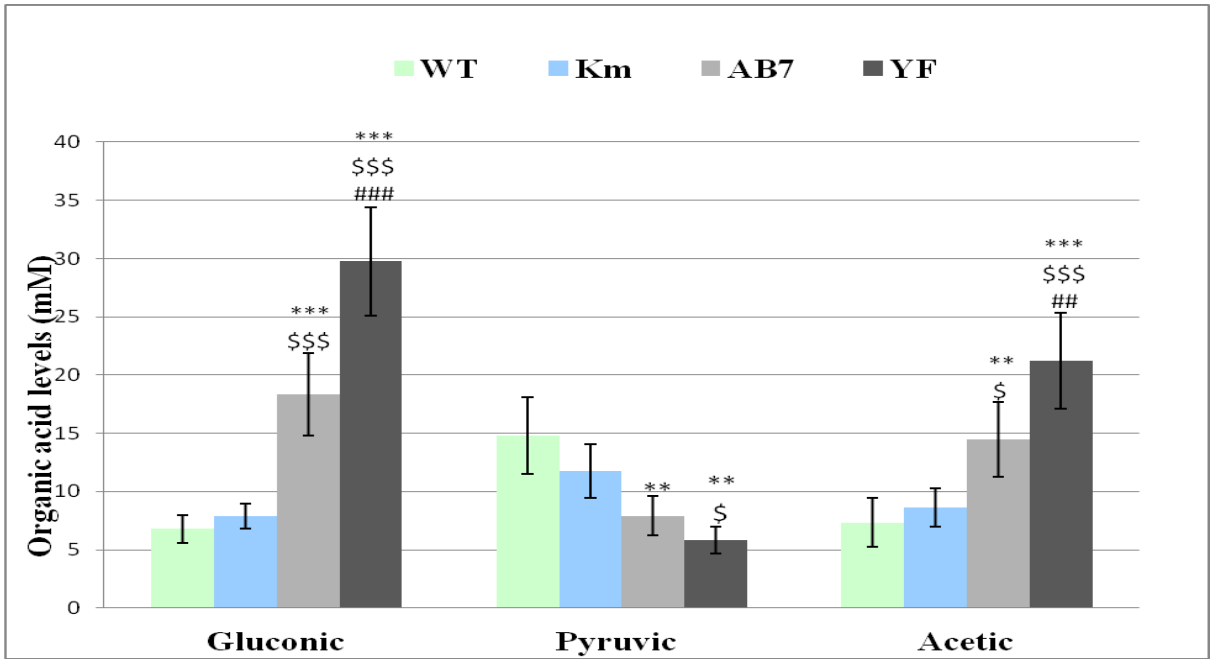

Figure 3.24:Organic acid secretion from *P. fluorescens* Pf0-1 NADH insensitive *cs* transformants. Gluconic, pyruvic and acetic acid levels in mM of Wild type, pAB8,pAB7,pYF designated as respective colours in the graph. Parameters estimated from stationary phase cultures grown on M9 medium with 100mM glucose.Results are expressed as Mean ±S.E.M of 4 independent observations. * comparision of parameters with wilt type control; $ comparision of parameters with vector control pAB8,# comparision between parameters of AB7 and YF.***,$$$,###P<0.001; **,$$,##P<0.01; *,$,#P<0.05

3.3.6 Effect of NADH insensitive *E. coli* cs overexpression on growth, biomass and glucose utilization of *P. fluorescens* PfO-1

In the presence of excess glucose, increase in *CS* activity did not significantly affect the growth profile and acidification of the medium within 30 h. However, there is a significant enhancement of pH drop in case of Y146F compared to wild type *cs* bearing strain and other control strain. Specific growth rate, specific total glucose utilization rate and total amount of glucose utilized after 30h remained unaffected. The amount of glucose consumed intracellularly is reduced by 1.49 fold in *Pf* (pY146F) as compared to *Pf* (pAB8). The increase in *CS* activity in *Pf*(pY146F) strain improved the biomass yield by 3.2, 2.38 and 2 fold compared to WT, *Pf* (pAB8) and *Pf* (pAB7), respectively (**Table 3.5, Fig. 3.25**).

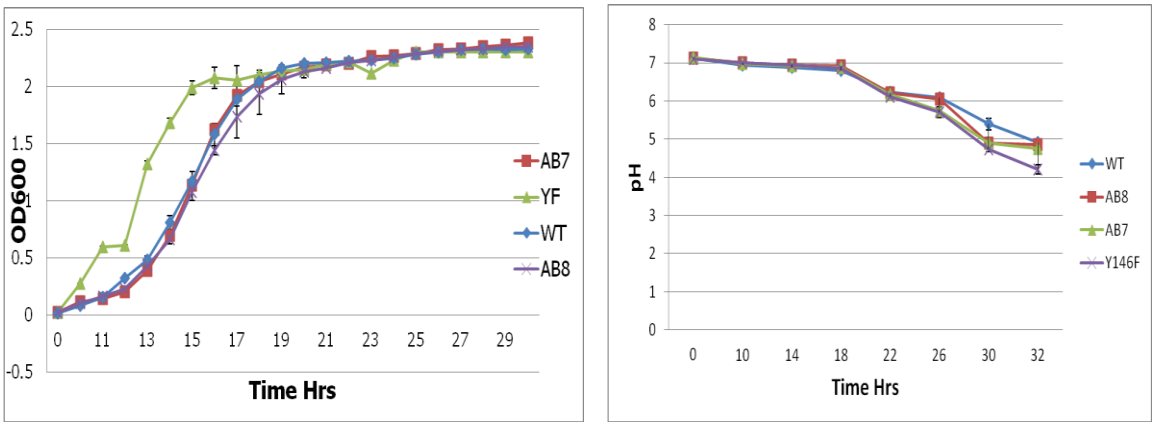

Figure 3.25: Growth and pH profiles of *P. fluorescens* PfO-1 *cs* transformants on M9 minimal medium with 100mM glucose. The values plotted represent the Mean±S.D of 4-6 independent observations.

Table 3.5: Physiological variables and metabolic data from *P. fluorescens* Pf0-1 *cs* transformants grown on M9 medium with 100mM glucose

Bacterial strain	**Sp. Growth rate** $\mu(h^{-1})^{\dagger}$	**Total glucose utilized(mM)**‡	**Glucose consumed (mM)** ‡	**Biomass yield** Ydcw/Glc† (g g^{-1})	**Sp. Glucose utilization rate** QGlc† [g (g dcw)$^{-1}$ h^{-1}]
WT	0.42±.03	50.45±7.08	45.94±6.62	0.12±0.02	4.5±0.55
Pf (pAB8)	0.59 ± 0.04	69.88 ± 9.4	62.22 ± 8.5	0.16 ± 0.03	7.20 ± 1.3

Pf (pAB7)	0.65 ± 0.04	65.86 ± 4.86	48.6 ± 3.57	0.19± 0.04	6.35 ± 1.56
Pf(pY145F)	0.61±0.06	71.46±6.7	41.71±5.75$$$	0.38±0.01$$$	6.8±1.03

. The results are expressed as Mean ± S.E.M of readings from 4-6 independent observations. † Biomass yield (Ydcw/Glc), specific growth rate (μ) and specific glucose consumption rate (QGlc) were determined from the mid-log phase of each experiment. ‡ Total glucose consumed and glucose utilized were determined at the time of pH drop (30h) for *Pf* (Y146F), *Pf* (pAB7) and *Pf* (pAB8) *Comparison of parameters with respective wild type; $ Comparison of parameters with *Pf* (pAB8) and # comparision between parameters of pY146F and pAB7. .***,$$$,###P<0.001; **,$$,##P<0.01; *,$,#P<0.05

3.4 DISCUSSION

Present study demonstrates the effect of overexpression of NADH insensitive *E. coli cs* in metabolically distinct *P. fluorescens* PfO-1. Three *E. coli* NADH insensitive *cs* R163L, K167A and Y145F when constitutively overexpressed under *lac* promoter in *P. fluorescens* PfO-1, a maximum of 5.6 fold and 2 fold overexpression was obtained in *Pf* (Y145F) as compared to the control and strain bearing the wild type *cs* gene. Our data is supported by a study of Duckworth et al., (2003) which showed maximum weakening of NADH binding in case of Y145F. The study carried out in *E. coli* K12 strain showed Ki value of 790 ±210 μM for Y145F as against wild type *cs* with a Ki value of 2.8 ±0.4 μM for 100 percent inhibition by NADH (**Table.3.2**) which clearly indicates weakening of NADH binding to the active site and enhancement of *CS* activity.

In our earlier work when *E. coli* wild type *cs* gene was constitutively overexpressed under *lac* promoter in *P. fluorescens* ATCC 13525 a 2 fold enhanced activity was observed compared to the control strain (Buch et al., 2009). In the present study, as a consequence of 5.6 fold increase in CS activity in *Pf* (pY145F) there is a 6.9 fold elevated intracellular citrate level which is accompanied by 51.6 and 29.6 fold enhancement of extracellular citrate levels and yields. Remarkably the high citrate accumulation in *Pf* (pY145F) had no effect on growth. This pattern of accumulation of intracellular citric acid was similar to *P. fluorescens* ATCC13525 overexpressing *E. coli* wild type *cs* gene in which 2 fold increase in CS activity lead to 2 fold elevated intracellular citrate level and 26 fold enhancement of

extracellular citrate yield (Buch et al., 2009). In another study *icd* mutant of *E. coli* K and B strains resulted in an increase of ~3.8 and 2.5 fold CS activity and enhanced citrate accumulation but unlike our study, in this case citrate accumulation had a negative effect on growth of the *E. coli* strains (Aoshima et al., 2003). Overexpression of mitochondrial CS genes also resulted in increased citrate efflux in cultured carrot cells (Koyamaet al. 1999), Arabidopsis (Koyama et al. 2000), and canola (Anoop et al. 2003) plants

Increase in intracellular citrate level and yield by 1.9 and 2.39 fold, respectively, in *Pf* (pY145F) compared to *Pf* (pAB7) does not lead to similar increase in extracellular citrate levels. Citric acid being the substrate of central carbon metabolism must be transported into and out of the cell for efficient bioactivity. Therefore low level of extracellular citrate can be attributed to weak efflux transport mechanism in *P. fluorescens*. The transport of citric acid in gram negative bacteria is mediated by hydroxycarboxylate transporters which are a family of secondary transporter. These transporters are either H^+ or Na^+ symporters or they catalyze exchange between two substrates. (Lolkema and Sobczak, 2005). From database it is clear that the citrate transport in fluorescent pseudomonads is H^+ dependent. The low efficiency of the native citrate transport can be attributed to the low intracellular proton concentration compared to the outer membrane proton concentration. The active transport system for citrate excretion also appears to be the main rate-determining factor in citrate overproduction by yeasts (Anastassiadis and Rehm**,** 2005) while in addition to citrate export, transport of sugar and ammonia into the cell are also crucial for citric acid production by *A. niger* (Papagianni, 2007).

Increased gluconic acid levels with simultaneous reduction in pyruvic acid levels could be explained by increased PYC activity in *Pf* (pY145F), which could probably divert pyruvate flux towards increased OAA biosynthesis to meet the increased CS activity. Even in *A. niger* the enhancement of anaplerotic reactions replenishing TCA cycle intermediates predisposes the cells to form high amounts of citric acid (Legisa and Mattey, 2007). However, *cs* overexpression in *A. niger* did not affect PYC activity (Ruijter et al., 2000). Enhancement of biosynthetic reactions due to shortage of TCA cycle intermediates was also observed in citric acid accumulating *E. coli* K and B strains in the form of increased glyoxylate pathway (Aoshima et al., 2003; Kabir and Shimizu, 2004). However, similar

increase in flux through glyoxylate shunt was not apparent in *Pf* (pY145F) as evident from very low and unaltered ICL activity detected in *Pf* (pAB8) and *Pf* (pY145F). Low ICL activity was consistent with earlier reports in *P. fluorescens* ATCC13525 and *P. indigofera* in which ICL contributed negligibly to glucose metabolism (Buch et al., 2009; Diaz-Perez et al., 2007).

The phosphoenolpyruvate carboxylase reaction and the glyoxylate shunt are utilized for the supply of oxaloacetate to the TCA cycle. The glyoxylate shunt contributes to supplying oxaloacetate via glyoxylate, succinate, fumarate and malate by using isocitrate in the TCA cycle and acetyl-CoA which is produced by acetate catabolism. Our experimental results using the *cs* overexpression strain suggest that *P. fluorescens* PfO-1 might use the phosphoenolpyruvate carboxylase rather than the glyoxylate shunt reaction for maintaining intracellular oxaloacetate levels to adapt to the higher OAA demand which is supported by the increase in acetate production in *Pf* (pY145F) compared to the control. Enhanced CS activity in *Pf* (PY145F) also increased the periplasmic glucose oxidation which is reflected by increase in GDH activity and gluconic acid production. Moreover, significant decrease in glucose consumption without affecting the glucose utilization suggested the involvement of direct oxidation pathway for carbon flux distribution in *P. fluorescens.* The increased carbon flow through glycolysis led to increased protein synthesis that is reflected to increased biomass.The citrate induced oligosaccharide synthesis was reported in *Agrobacterium* sp. ATCC 31749 (Ruffing et al., 2011)

The central carbon metabolism network gets to the heterologous overexpression of NADH insensitive *E. coli cs* in *P. fluorescens* PfO-1 (**Fig. 3.26**). The conditions created in the present work include: improvement of glucose uptake, improvement of CS activity and citrate production compared to the earlier report by Buch et al. (2003), suppression of pyruvate secretion and enhanced acetate production, increased direct oxidation of glucose leading to more gluconate production.

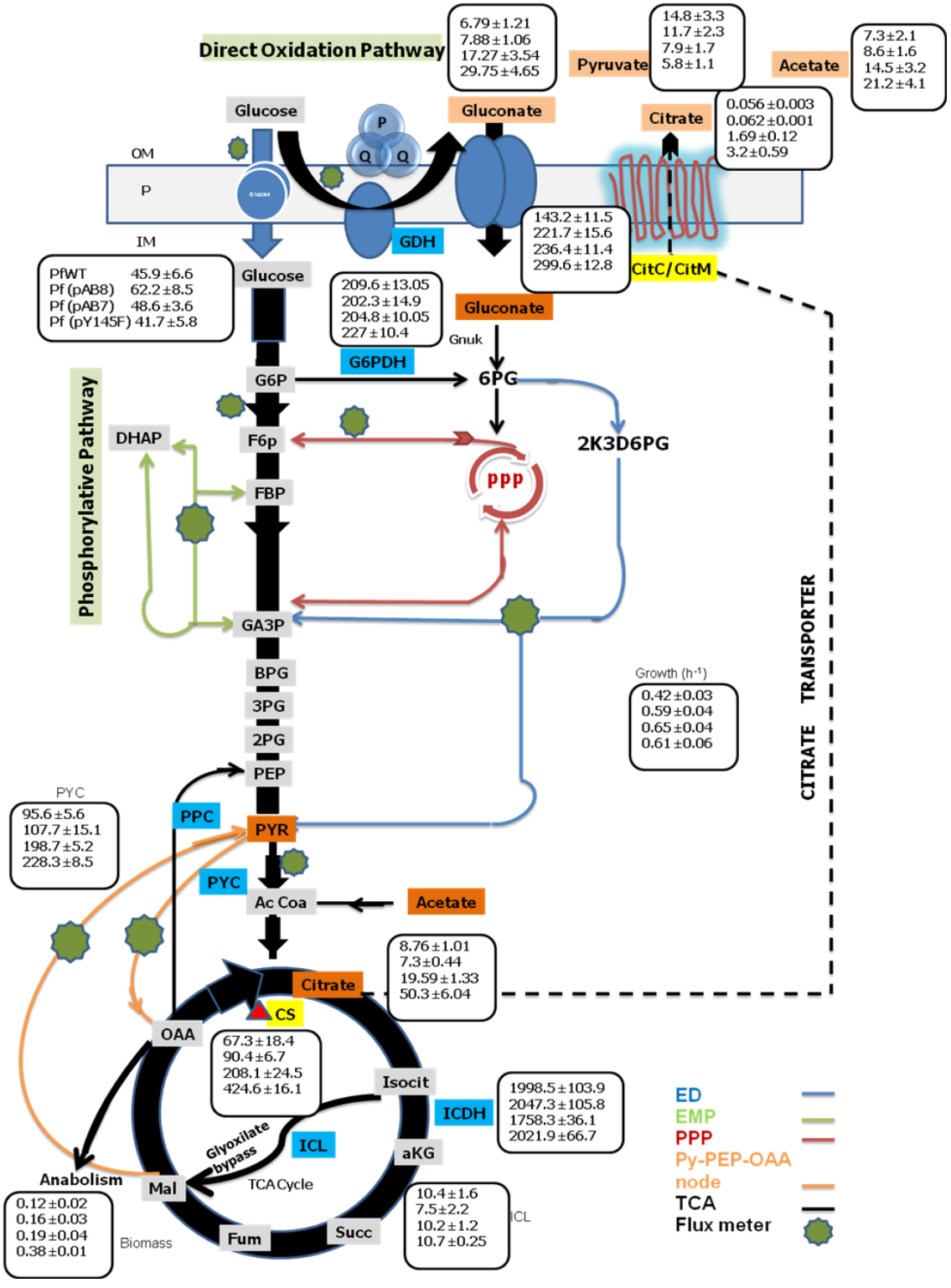

Figure 3.26: Key metabolic fluctuations in *P. fluorescens* PfO-1 overexpressing NADH insensitive *E. coli* CS

Metabolic characterization of engineered P. fluorescens PfO-1coexpressing E. coli NADH insensitive cs and S. tphimurium sodium citrate transporter or B. subtilis magnesium citrate transporter operon

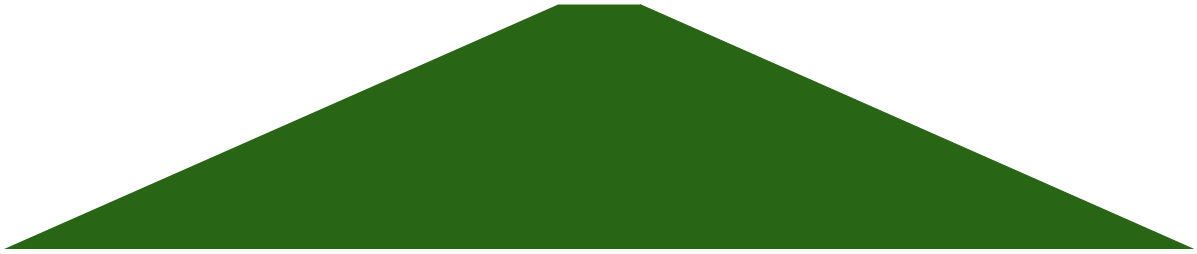

CHAPTER 4

4 INTRODUCTION

4.1 Citrate transport in plants, fungi, and bacteria

Secretion of metabolites across plasma membrane requires the presence of transport mechanisms. Organic acids cannot pass the membrane barrier by simple diffusion and hence transport proteins are required for secretion of citrate, oxalate and succinate. The efflux of organic anions e.g., malate, citrate, or oxalate is an important mechanism for Al resistance in cereal and noncereal species. Overexpression of gene, encoding a transporter reported to enhance citrate efflux and Al tolerance in several plant species (**Table 4.1**). Members of the multidrug and toxin compound extrusion (MATE) family of proteins control Al-activated citrate efflux from barley (*Hordeum vulgare*) and sorghum (*Sorghum bicolor*). MATE proteins are widely present in bacteria, fungi, plants, and mammals (Omote et al. 2006), but there is no apparent consensus sequence conserved in all MATE proteins. MATE proteins are proposed to transport small, organic compounds (Omote et al., 2006). In contrast to MATE genes in the bacterial and animal kingdom, plants contain more MATE-type transporters (Furukawa et al., 2007). These proteins are characterized by having 400 to 700 amino acids with 12 transmembrane helices.

Table 4.1: Enhanced organic acid efflux by transporter gene expression (Ryan et al., 2011)

Transporter gene	**Transgenic strategy**	**Proposed mechanism**
Al^{3+} activated malate transporter (TaLMT1)	Arabidopsis gene expressed in Arabidopsis, wheat gene expressed in wheat and Arabidopsis	Enhanced malate efflux
Multidrug and toxic compound efflux gene (MATE) called Frd3	Arabidopsis gene expressed in Arabidopsis	Enhanced citrate efflux

Multidrug and toxic compound efflux gene (MATE) (HvAACT1)	Barley gene expressed in tobacco plants	Enhanced citrate efflux
H+ pyrophosphatase AVP1	Over-expression of endogenous gene in Arabidopsis, tomato and rice	Enhanced organic acid efflux
Multidrug and toxic compound efflux gene (SbMATE)	Sorghum gene expressed in Arabidopsis Atalmt1 mutant	Enhanced citrate efflux
Al3+ activated malate transporter (HvALMT1)	Barley gene expressed in barley	Enhanced malate efflux
Multidrug and toxic compound efflux gene (ZmMATE1)	Maize gene expressed in arabidopsis	Enhanced citrate efflux

Citrate secretion is a common characteristic feature of many anamorphic fungal species like *Aspergillus* and *Penicillium* (Burgstaller, W., 1993; 2005). Total intracellular citrate level in *A. niger* is between 2 - 30 mM. In *P. simplicissimum,* citrate levels are between 10 - 50 mM during the growth in batch cultures and between 20 mM and 60 mM in chemostat cultures (Gallmetzer and Burgstaller, 2001). More than 1 M citrate secretion is achieved in *A. niger* in improved biotechnological production processes (Netik et al., 1997; Ruijter et al., 2002). Citrate overflow mechanism in *A. niger* is very different from bacteria and is pH dependent (must be < 3). In addition to pH, other factors *viz* carbon source type and concentration, N source and P concentration, excessive aeration and Mn^{2+} limiting condition are contribute towards citrate secretion in fungus (Mlakar and Legisa, 2006). An efflux of protons was postulated as the main charge-balancing ion flow in *Penicillium cyclopium* (Roos and Slavik, 1987).

Very few bacterial species like *Corynebacterium*, *Arthrobacter*, *Brevibacterium*, *Bacillus sp.*, *Bradyrhizobium japonicum*, and *Citrobacter koseri* are known to secrete or accumulate citrate at levels much lower than fungi (Gyaneshwar et al., 1998; Khan et al., 2006). A proton efflux could either be coupled directly to citrate secretion via a

citrate/proton symport similar to the secretion of lactate together with protons in *Escherichia coli* and *Lactobacillus lactis* (Konings et al., 1992). The membrane potential generating secondary transporters involved in malolactic (MelP) and citrolactic (citP) fermentation process are well reported in several lactic acid bacteria. The nature of transporters differ from "usual" secondary transporters in two aspects: (i) they translocate net negative charge across the membrane, and (ii) they catalyze efficient heterologous exchange of two structurally related substrates (Bandell et al., 1997). The electrochemical gradient of protons across the cytoplasmic membrane is a major store of free energy in the bacterial cell. Usually, the proton motive force (pmf) is generated by translocation of protons against the gradient across the cell membrane which results in the two components of the pmf, a membrane potential and a pH gradient. Proton pumping is catalyzed by primary transport systems at the expense of some source of chemical energy or light.

E. coli cannot utilize citrate as a sole source of carbon and energy (Dimroth, 1987; Kastner 2000). On the other hand, the facultative anaerobic bacteria *Klebsiella pneumoniae* and *Salmonella typhimurium* and many other species of the *Enterobacteriacaea* can grow aerobically or anaerobically, utilizing citrate as the sole carbon source. Most of the bacteria have transport proteins in the cytoplasmic membrane that mediate the transport of citrate. The carriers belong to the class of secondary transporters that use the free energy stored in transmembrane electrochemical gradients of ions to drive the transport of the substrates. The citrate transporter CitH of *K. pneumoniae* is driven by the proton motive force (van de Rest et al., 1991)) while the transporters CitS and CitC of *K. pneumoniae* and *Salmonella* serovars are driven by both pmf and sodium, respectively. CitM of *Bacillus subtilis* is driven by magnesium ion motive force (Ishiguro et al., 1992; Lolkema, 1994; Boorsma et al., 1996). *Klebsiella pneumoniae citS* gene is expressed during anaerobic growth on citrate (Bott et al., 1995; Dimroth and Thomer, 1986).

Mechanistically these transporters catalyze coupled translocation of citrate and H^+ and/or Na^+ and Mg^{2+} (symport). A special case are the citrate carriers of lactic acid bacteria that take up citrate by an electrogenic uniport mechanism or by exchange with lactate, a

product of citrate metabolism (citrolactic fermentation) (Marty-Teysset et al., 1996, Ramos et al., 1994). These citrate transporters are involved in secondary metabolic energy generation (Konings et al., 1995). In contrast with most citrate transporters, a member of the CitMHS family characterized from the soil bacterium *Bacillus subtilis*, transport citrate in complex with a bivalent metal ion. This facilitates the utilization of citrate which is available in the metal-ion-complexed state. The best-characterized members of the family are BsCitM and BsCitH. The former transports citrate in complex with Mg^{2+} and is the major citrate-uptake system during growth on citrate under aerobic conditions (Korm et al., 2000; Yamamoto et al., 2000; Li et al., 2002: Warner et al., 2002).

These Secondary transporters of the bacterial CitMHS family fall under the group of 2-hydroxycarboxylate transporter (2HCT) family. The 2HCT family of secondary transporters contains 54 unique members that are all found in the bacterial kingdom. The well characterized members of the family are transporters for citrate, malate and lactate, substrates that contain the 2-hydroxycarboxylate motif, hence the name of the family. The transporters are either H^+ or Na^+ symporters or they catalyze exchange between two substrates. Na^+ coupled citrate transporters like CitS of *Klebsiella pneumoniae* and CitC of *Salmonella enterica* found in the γ subdivision of the phylum Proteobacteria are involved in the fermentative degradation of citrate to acetate and carbon dioxide yielding ATP. Citrate is cleaved by citrate lyase yielding acetate and oxaloactetate, which is decarboxylated yielding pyruvate. The latter step results in the transmembrane pH gradient. Secondary transporters are widely distributed in nature and they come in a great genetic and structural diversity, probably reflecting many different translocation mechanisms. (**Table 4.2**, Lolkema, 2006).

Table 4.2: Characterized members of the 2HCT family (Lolkema, 2006).

Trans-porter	Bacterium	Substrates	Transport mode	Function
CitS	*Klebsiella pneumoniae*	citrate	Na^+ symport	citrate fermentation
CitC	*Salmonella typhimurium*	citrate	Na^+ symport	citrate fermentation
CitW	*Klebsiella pneumoniae*	citrate, acetate	exchange	citrate fermentation
MleP	*Lactococcus lactis*	malate, lactate	exchange	malolactic fermentation
CitP	*Leuconostoc mesenteroides*	citrate, lactate	exchange	citrolactic fermentation
CimH	*Bacillus subtilis*	citrate, malate	H^+ symport	unknown
MalP	*Streptococcus bovis*	malate	H^+ symport	malate fermentation
MaeN	*Bacillus subtilis*	malate	Na^+ symport	growth on malate

4.1.1 Structural Model of 2-HCT transporters

The transporters in the 2HCT family are integral membrane proteins consisting of about 440 amino acid residues (Lolkema, 2006). The core of the structure is formed by two homologous domains that are connected by a large hydrophilic loop that resides in the cytoplasm. The domains contain 5 transmembrane segments (TMSs) each and they have opposite orientations in the membrane. They are likely to originate from a duplication of an internal gene fragment coding for an odd number of TMSs. In the structural model of the transporters in the 2HCT family, the loops between the 4th and 5th TMSs in each domain fold back in between the TMSs and form so called re-entrant or pore loops (**Fig. 4.1**). The pore loop in the N-terminal domain (region VB) enters the membrane-embedded part from the periplasmic side of the membrane, the one in the C-terminal domain (region XA) from the cytoplasmic side (trans pore loops). The two re-entrant loops are believed to be in close vicinity in the 3D structure and to form the translocation pathway for co-ions and substrates. The binding site is believed to be positioned at the membrane-cytoplasm interface where an arginine residue interacts directly with the bound substrate. Different families may have additional TMSs at the N- or C-termini or in between the two domains. The transporters of the 2HCT family have one additional TMS at the N-terminus locating the latter in the cytoplasm. The odd number of TMSs in each domain forces the orientation of the two domains in the membrane to be opposite; the N-terminus of the N-terminal and C-terminal domains resides in the periplasm and cytoplasm, respectively. The pore loops contain an

extraordinarily high fraction of residues with small side chains (glycine, serine, and alanine) which may reflect a compact packing of the loops in between the TMSs. The regions containing the pore loops are among the best conserved regions in the transporter families. The two pore loops would be in close contact in the 3D structure in a single pore that alternately would be opened to either side of the membrane during the catalytic cycle.

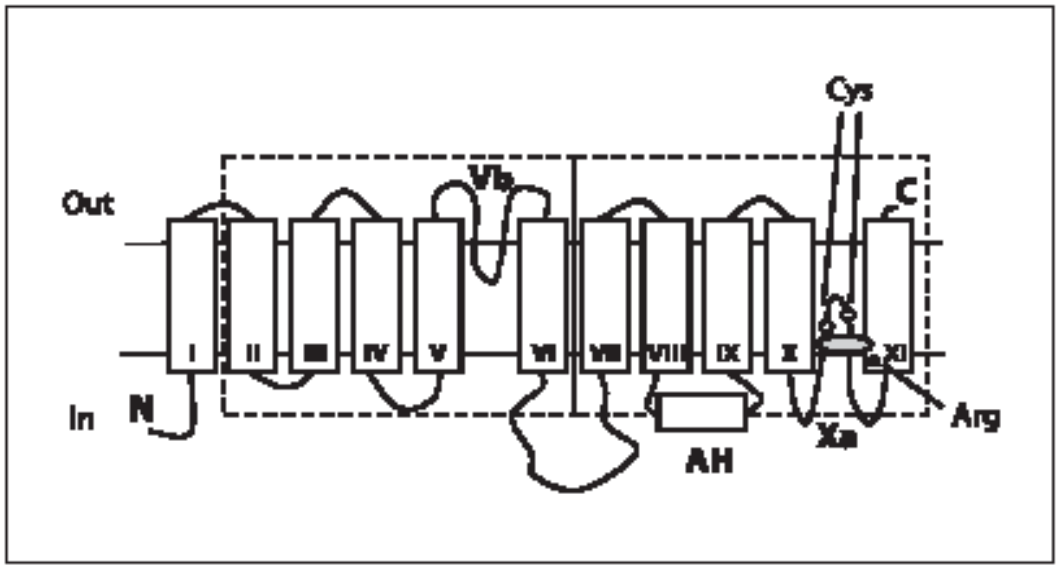

Figure 4.1: Structural model for 2HCT family transporters (Lolkema, 2006).

The substrate-binding site is located at the membrane-cytoplasmic interface, which positions it deep down in the pore when opened to the external face of the membrane. The cytoplasmic pore loop (XA) extends into the pore beyond the binding site, making cysteine residues in the loop accessible from the periplasmic side even when substrate is bound. Opening and closing of the pore to either site of the membrane would be controlled by binding of the substrate and co-ions. The accessibility of cysteine residues in the cytoplasmic pore loop was shown to be different in different catalytic states of the transporter by experiment.

4.1.2 Factors contributing to the low efficiency of the native transporter in fluorescent pseudomonads

Citrate transporter of fluorescent pseudomonads falls under the Major Facilitator Superfamily (MFS) which is a large and diverse group of secondary transporters that includes uniporters, symporters, and antiporters. MFS proteins facilitate the transport of citric acid across cytoplasmic or internal membranes solely by proton driven citrate symport mechanism. Transcriptome analysis of MFS protein have been reported in several pseudomonads *viz.*, *Pseudomonas syringae* Cit7 (359 amino acid, accession AEAJ01000831.1), *Pseudomonas putida* KT2440 (434amino acids, accession AE015451.1, *Pseudomonas aeruginosa* PAO1 (429 amino acids, accession NC_002516.2), *Pseudomonas aeruginosa* PA7 (429amino acids, accession NaC_009656.1).

Enhanced accumulation of intracellular citric acid in *P. fluorescens* leads to secretion of citrate by the organism whereas the wild type does not secrete any citric acid to the extracellular medium. But the secretion is not at par with the intracellular accumulation revealing the low efficiency of the citrate transporter (Buch et al., 2009). The low efficiency of the native citrate transporter in *Pseudomonas* sp. can be attributed to lower intracellular proton levels limiting the citrate efflux. *Pseudomonas* sp. being neutrophiles always try to maintain a lower extracellular pH compared to intracellular pH indicating that proton concentration is higher outside (**Table 4.3**). pH homeostasis in these bacteria resist the change in pH across the cell membrane and does not allow overflow of proton across the membrane.

Citric acid secretion could be stabilized if there were a mechanism whereby the cells could secrete elevated levels (Delhaize et al. 2004). Na^+ dependent citrate transporters are highly specific for citrate. The major species transported across the cell is $HCit^{2-}$. It accumulates citrate at the expense of Na^+ concentration gradient generated by various sodium ion pumps.

Table 4.3: pH homeostasis in bacteria (White, 2010)

BACTERIA	pH_{out}	pH_{in}	pH_{in}-pH_{out}
Neutrophile	6-8	7.5-8	+
Acidophile	1-4	6.5-7	+
Alkaliphile	**9-12**	**8.4-9**	-

Reaction :

$$Hcit^{2-} + 2Na^{+} + H^{+}\ (out) \rightleftharpoons Hcit^{2-} + 2Na^{+} + H^{+}\ (in)$$

Mainly these transporters function in citrate uptake inside the cells. **Fig. 4.2** represents the schematic representations of the pathways-

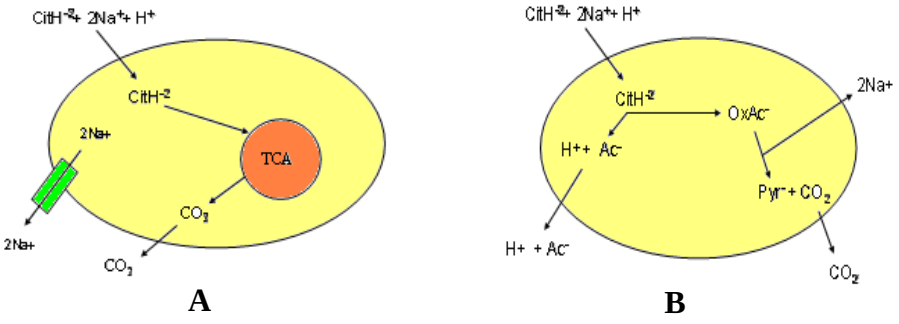

Figure 4.2: Na^{+} efflux mechanisms in bacteria. (A). Aerobic and (B). Anaerobic conditions (Lolkema, 1994).

All bacterial cells although maintain an intracellular Na^{+} concentration lower than the extracellular, intracellular concentration above 20mM is harmful to *E. coli* and in halophiles is above 3M (Lolkema, 1994). Bacterial cells protect from the adverse effects of Na^{+} by primary and secondary Na^{+} extrusion system. NhaA, the Na^{+}/H^{+} antiporter is the system responsible for adaptation to Na^{+} and alkaline pH (**Fig. 4.3)**. All bacterial cells maintain the optimum intracellular Na^{+} levels by (i) Symport with metabolites and antiport against H^{+} are widely used mechanisms in almost all bacteria for Na^{+} influx and efflux; (ii)

Decarboxylases and ATPases function in anaerobic bacteria. Decarboxylases act as Na^+ pumps for efflux and ATPases use the energy obtained by influx of Na^+ down its concentration gradient for ATP synthesis; (iii) Marine organisms have respiratory chain mechanism for efflux of Na^+ to maintain sodium motive force (smf) and flagella motors which use energy derived from influx of Na^+ down the concentration gradient.

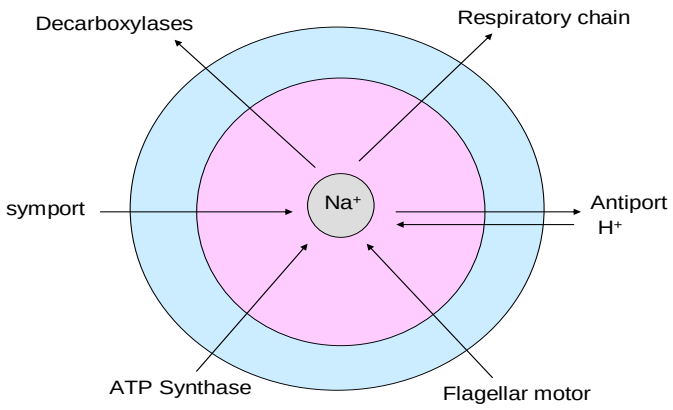

Figure 4.3: Bacterial stress responses and Na^+ homeostasis (Storz et al.,1996)

4.2 Rationale of the present work

Reversibility is recognized as a fundamental feature of coupled vectorial transport systems. Therefore, the decarboxylase systems could also function in reversible manner wherein the direction of operation depends on the cation gradient and free energy change under the conditions of the physiological steady state. Heterologous overexpression of citrate symporter coupled to Na^+ and Mg^{2+} may play an important function as an alternative pump for efflux of Na^+ and/or Mg^{2+} (**Fig.4.2**) along with citrate. The present study demonstrates the effect of heterologous overexpression of *S. tphimurium* Na^+ dependent and *B. subtilis* Mg^{2+} dependent citrate transporter on citric acid secretion by *P. fluorescens* PfO-1.

4.3 WORK PLAN

The experimental plan of work includes the following-

4.3.1 Bacterial strains used in the study

Table 4.4: List of bacterial strains used.

Bacterial strains	**Characteristics**	**Source/Reference**
E. coli DH5α	F-φ80Δ*lac*ZΔM15Δ(*lac*ZYA-*arg*F) U169 *rec*A1 *end*A1 *hsd*R17 (rk-, mk+) *pho*A *sup*E44 λ-*thi*-1 *gyr*A96 *rel*A1	Sambrook and Russell, 2001
E. coli W620	CGSC 4278 - *glnV44 gltA6 galK30 LAM-pyrD36 relA1 rpsL129 thi-1*; Str_r	*E. coli* Genetic Stock Center
Salmonella typhimurium	Sewage isolate	Kumar, 2012
Bacillus subtilis 168	Wild type strain	ATCC
P. fluorescens Pfo-1	Wild type strain	
Pf (pGm)	*P. fluorescens* Pfo-1 with pUCPM18; Gm^r	This Chapter
Pf(pCitC)	*P. fluorescens* Pfo-1 with pCitC; Gm^r	This Chapter
Pf (pCitM)	*P. fluorescens* Pfo-1 with pCitM; Gm^r	This Chapter
Pf(pYFpCitC)	*P. fluorescens* Pfo-1 with pY146F and pCitC double transformant ; Km^r, Gm^r	This Chapter
Pf(pYC)	*P. fluorescens* Pfo-1 with pYC; Gm^r	This Chapter

Detailed characteristi*cs* of these strains and plasmids are given in Sectio 2.1. Parent strains and the transformants of *E. coli* and *Pseudomonas* were respectively grown at 37ºC and 30ºC with streptomycin, kanamycin and gentamycin as and when required, at final concentrations varying for rich and minimal media as described in Section 2.2, Table 2.4.

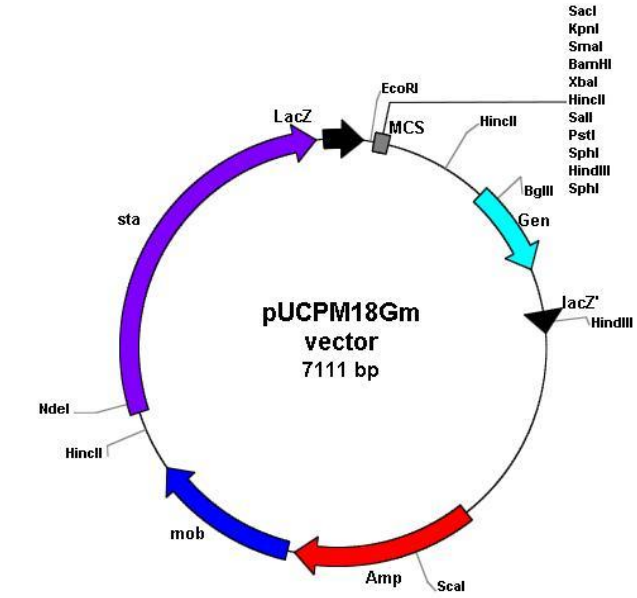
SacI
KpnI
SmaI
BamHI
XbaI
HincII
SalI
PstI
SphI
HindIII
SphI
EcoRI
MCS
HincII
BglII
Gen
LacZ
LacZ'
HindIII
sta
pUCPM18Gm
vector
7111 bp
NdeI
HincII
mob
Amp
ScaI

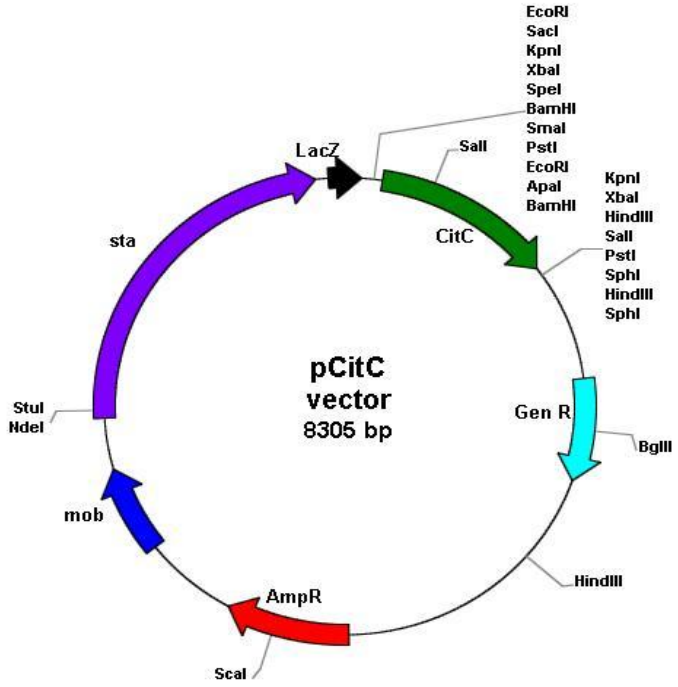
EcoRI
SacI
KpnI
XbaI
SpeI
BamHI
SmaI
PstI
EcoRI
ApaI
BamHI
SalI
LacZ
KpnI
XbaI
HindIII
SalI
PstI
SphI
HindIII
SphI
CitC
sta
pCitC
vector
8305 bp
StuI
NdeI
Gen R
BglII
mob
HindIII
AmpR
ScaI

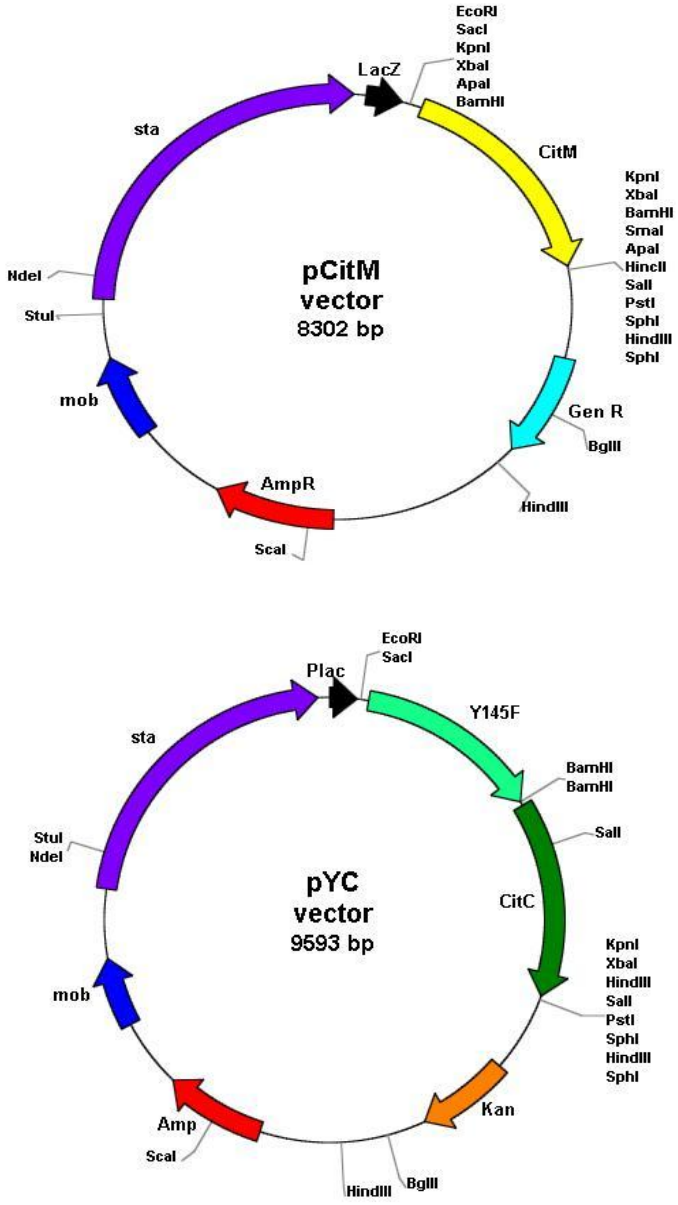

Figure 4.4: Restriction enzyme map of broad host range pUCPM18 vector having gentamycin resistance. (a) pUCPM18Gm vector, (b) pUCPM18 vector containing *citC* gene in XbaI site,(c) pUCPM18 vector containing *citM* gene in EcoRI-SalI site, (d) pUCPM18Gm vector containing NADH insensitive *cs* Y145F gene and *citC* gene under the same *lac* promoter.

4.3.2 Construction of *Pseudomonas* stable plasmid containing *S. tphimurium* Na^+ citrate transporter (*citC*) and *B. subtilis* Mg^{2+} citrate transporter (*citM*) genes under *lac* promoter

The strategy for construction of pCitC and pCitM plasmid and their transformation in *P. fluorescens* PfO-1 strain harbouring NADH insensitive *cs* gene are depicted in **Fig.4.5-4.6.**

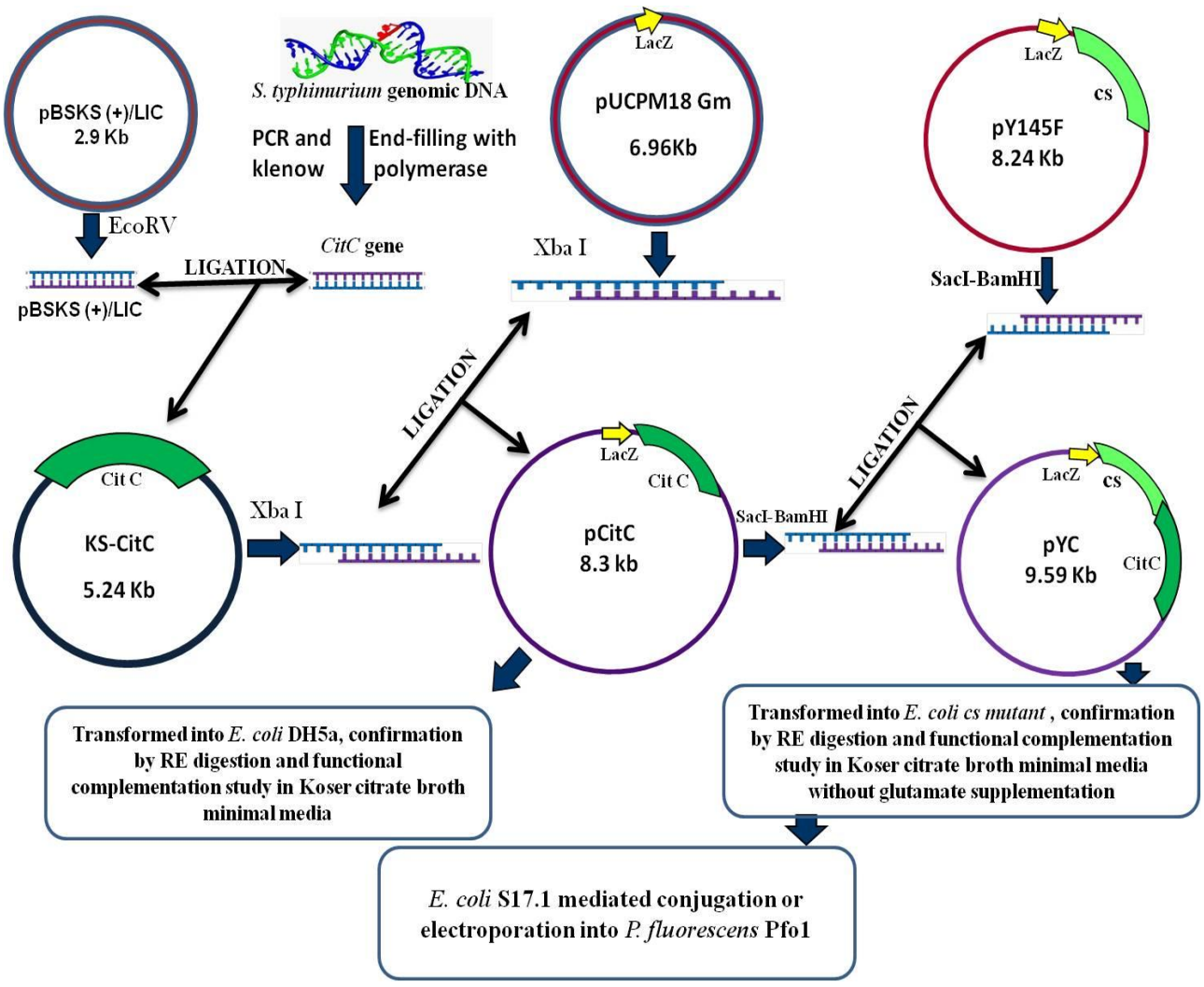

Figure 4.5: Strategy for cloning of *Salmonella typhimurium* citrate transporter (*citC*) gene and YC operon in broad host range vector pUCPM18 having gentamycin resistance.

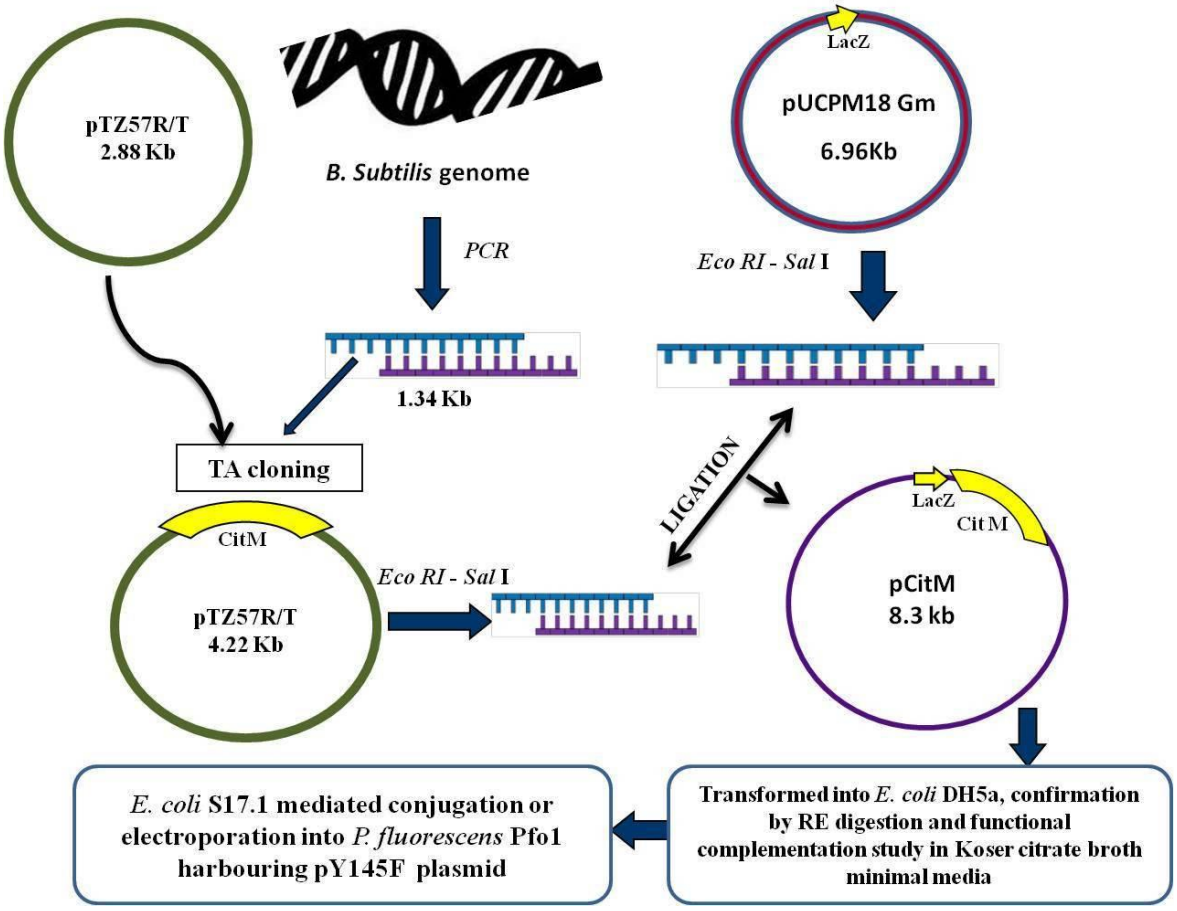

Figure 4.6: Strategy for cloning of *Bacillus subtilis* citrate transporter (*CitM*) gene in broad host range vector pUCPM18 having gentamycin resistance.

Gene specific primers are designed using *citC* gene sequence from *Salmonella typhimurium* LT2 strain (ATCC 700720, Gene Bank accession number: EMBL P0A2F8) and *citM* gene sequence from *B. subtilis* 168 strain (Gene Bank accession number: U62003) (**Table 4.5**). Cloning of isolated *citC* gene was carried out in pBluescript vector using *Sma*I site and confirmed by double digestion with *EcoR*I-*Sal*I and *EcoR*I-*BamH*I restriction site (**Fig. 4.5).** Subcloning of *citC* gene was carried out in pUCPM18 Gm vector having gentamycin resistance and the recombinant plasmid was confirmed by restriction mapping.In the other strategy the isolated *citM* gene was first cloned into pTRZ57/R

followed by cloning into broad host range vector pUCPM18Gm using EcoRI-SalI restriction site. All constructs were confirmed by restriction enzyme digestion and PCR.

Table 4.5: List of primers. *Pseudomonas* sp. specific RBS highlighted in yellow is added in each primer before the start side

Primer	Sequence (5'-3')	Tm/GC%
Na^+ dependent citrate transporter		
FNa^+ApaI BamHI:	GGGGGCCCCGGGATCCCG CACGGAGGAATCAACTTATG ACC AAC ATG ACC CAG GCT TC	59.6˚C, 52.2%
RNa^+KpnI XbaI	GGGGTACCCCGCTCTAGAGC TTA CAC CAT CAT GCT GAA CAC GAT GC	59.6˚C, 46.2%
Mg^{2+} dependent citrate transporter		
F ApaI BamHI	GGGGGCCCCGGGATCCCGCACGGAGGAATCAACTT ATG TTA GCA ATC TTA GGC TTT CTC ATG ATG	57.7˚C, 40%
R KpnI XbaI	GGGGTACCCCGCTCTAGAGC TTA TAC GGA AAT AGA GAT CGC ACC G	58.2˚C 48%

ApaI BamHI: GGGGGCCCCGGGATCCCG KpnI XbaI: GGGGTACCCCGCTCTAGAGC

RBS: 5'CACG**GAGGA**ATCAACTT **3'**

4.3.3 Functional confirmation of *CitC and CitM* gene expressed from pCitC and pCitM plasmids.

E. coli DH5 α being a mutant of citrate transporter was used to determine the functionality of the transporter gene. *E. coli* DH5α containing pCitC and pCitM along with the respective controls pGm plasmid subjected to growth on Koser citrate broth containing citric acid as a sole carbon source supplemented with 100mg/ml thymine and 0.1mM IPTG.

4.3.4 Development of *P. fluorescens* PfO-1 harboring pYF-pCitC and pYF-pCitM plasmid.

The recombinant plasmids pCitC and pCitM were transformed by elecroporation in *P. fluorescens* PfO-1 harbouring NADH insensitive cs plasmid pY145F. The double transformants were selected on pseudomonas agar plate containing both kanamycin and gentamycin. *P. fluorescens* PfO-1 containing pAB8 and pGm dual plasmids were used as

control in the experiments. All transformants were confirmed by fluorescence and restriction enzyme digestion of the isolated plasmids from the respective strains

4.3.5 Effect of transporter gene expression on the citric acid secretion and overall physiology and glucose metabolism of *P. fluorescens* PfO-1.

P. fluorescens PfO-1 transformants were subjected to physiological experiments involving growth and organic acid production profiles on M9 minimal medium with 100mM glucose as carbon source. The samples withdrawn at regular interval were analyzed for O.D.600nm, pH, and extracellular glucose. Stationary phase cultures harvested at the time of pH drop were subjected to organic acid estimation using HPLC (**Section 2.7.3**). The physiological parameters were calculated as in section. The effectiveness of the transporters were compared based on the improvement of citric acid secretion ability. The enzyme assays were performed as described in Section, with *CS*, G-6-PDH, ICDH PYC being assayed in both mid-log to late-log and stationary phase cultures while ICL and GDH are being assayed in the mid log and stationary phase cultures, respectively.

4.3.6 Construction of *Pseudomonas* stable plasmid containing *cs* Y145F and *citC/citM* genes under *lac* promoter as operon.

The recombinant construction,functional and biochemical characterization of pYC is constructed in similar way as depicted in section..

4.4 RESULTS

4.4.1 Cloning of *S. tphimurium* Na^+ citrate transporter (*citC*) and *B. subtilis* Mg^{2+} citrate transporter (*citM*) gene:

Gradient PCR amplification of genomic DNA isolated from *Salmonella typhimurium* sewage isolate and *B. subtilis* 168 strains was carried out using gene specific primer to get an amplicon of 1341 bp *citC* gene (**Fig. 4.7-4.8)**. The PCR product was also confirmed by restriction enzyme mapping (**Fig. 4.9**). The plasmids pCitC and pCitM containing *S. tphimurium* sodium citrate transporter (*citC*) and *B. subtilis* magnesium citrate transporter

(*CitM*) gene, respectively, under *lac* promoter of pUCPM18 plasmid with Gm^r gene were constructed as schematically represented and discussed in section 4.3.2**.** All plasmids were confirmed based on restriction digestion pattern (**Fig. 4.10-4.13)**) and PCR (**Fig. 4.14**).

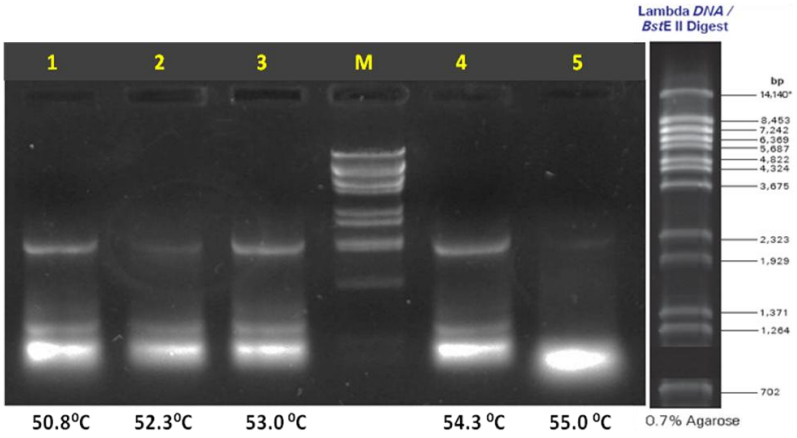

Figure 4.7: PCR amplification of CitC gene from *S. tphimurium* genome. Lane1-5: *citC* gene at different annealing temperature mentioned in the subsequent lane (1342bp). LaneM: MWM lambda DNA BstEII digest.

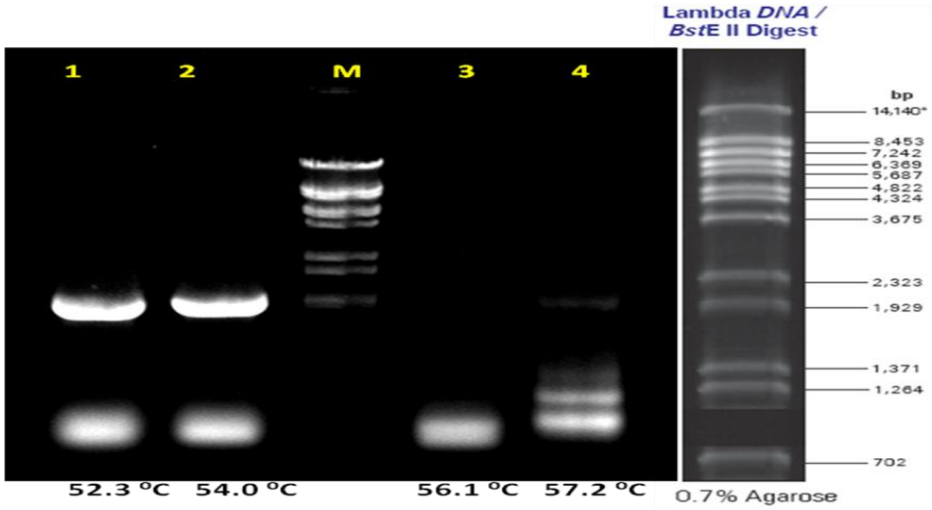

Figure 4.8: PCR amplification of *CitM* gene from *B. subtilis* genome. Lane1-4: *citM* gene at different annealing temperature mentioned in the subsequent lane (1341bp); laneM: MWM lambda DNA BstEII digest.

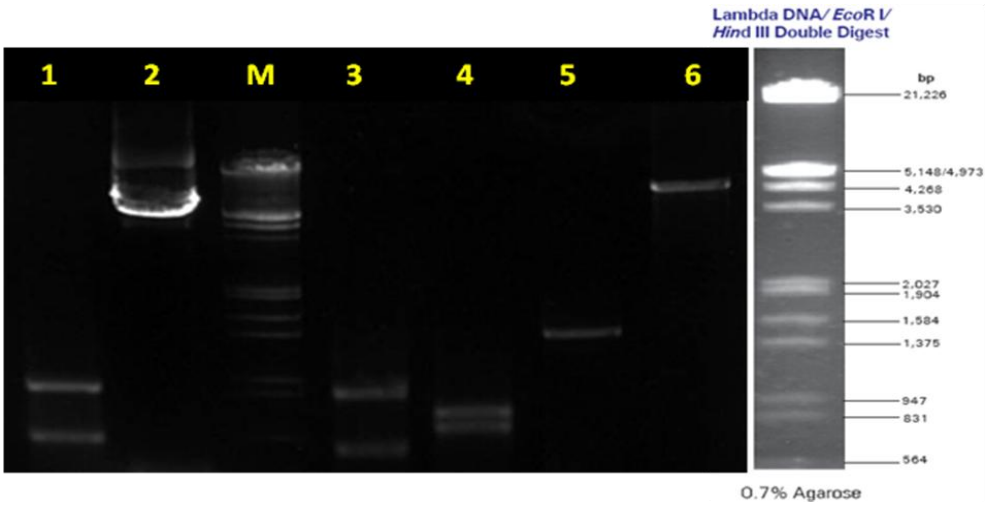

Figure 4.9: Restriction enzyme mapping of *citC* and *citM* gene. Lane1: CitC PCR product digested with SalI (0.733Kb, 0.51Kb), Lane2: undigested pUCPM18Gm plasmid; Lane3: CitM PCR product digested with XhoI (0.814Kb, 0.488Kb), Lane4: CitM PCR product digested with HindIII (0.688Kb, 0.614Kb); Lane5: CitC PCR product (1.34Kb); Lane6: pUCPM18Gm plasmid digested with BamHI (6.97Kb)

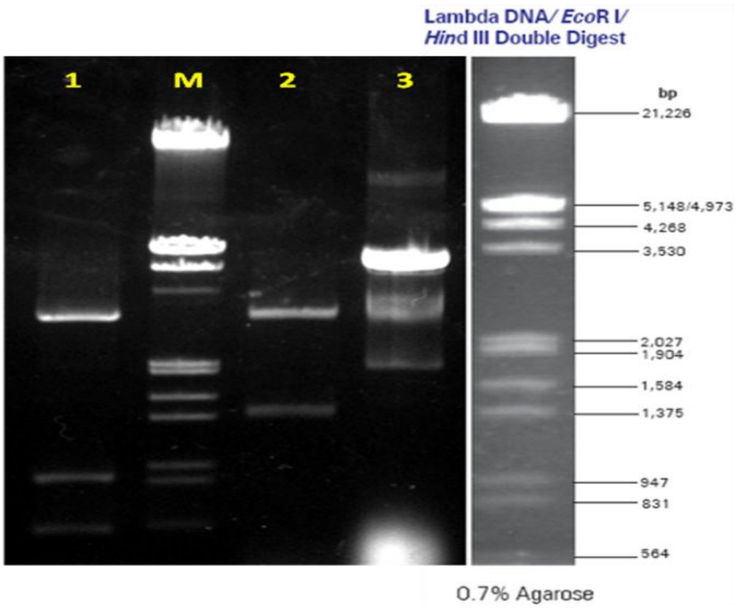

Figure 4.10: Restriction enzyme digestion pattern for pBluescript KS CitC clone. Lane1: pBluescript CitC plasmid digested with EcoRI-SalI (2.9 Kb, 0.8 Kb, and 0.5 Kb); Lane 2: pBluescript CitC plasmid digested with EcoRI-BamHI (2.9Kb,1.341Kb), Lane3: undigested pBluscriptKS plasmid; LaneM:MWM lambda DNA cut with EcoRI-HindIII

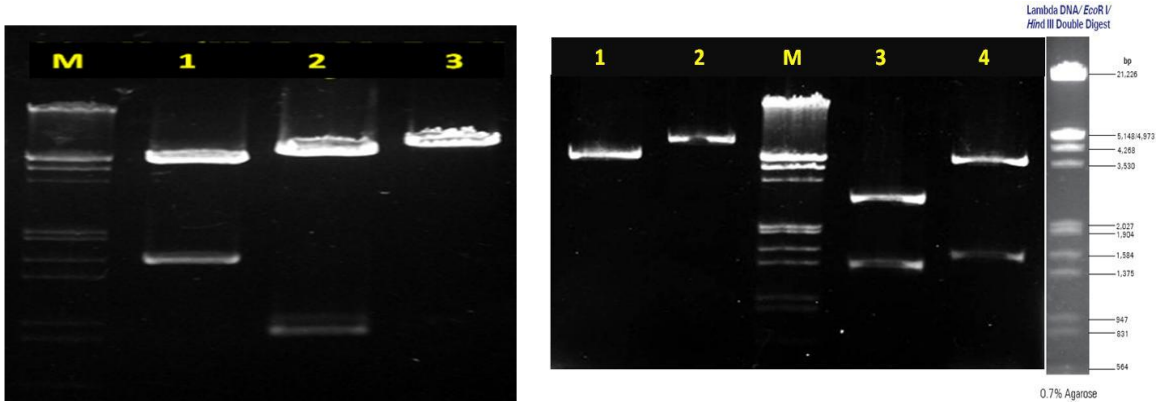

Figure 4.11: Restriction enzyme digestion pattern of pUCPM18Gm vector. Lane1:pUCPM18Gm digested with HindIII(5.3Kb,1.6Kb); lane2: pUCPM18Gm digested with EcoRI-BglII (6Kb,0.9Kb); pUCPM18Gm digested with EcoRI (6.9Kb).

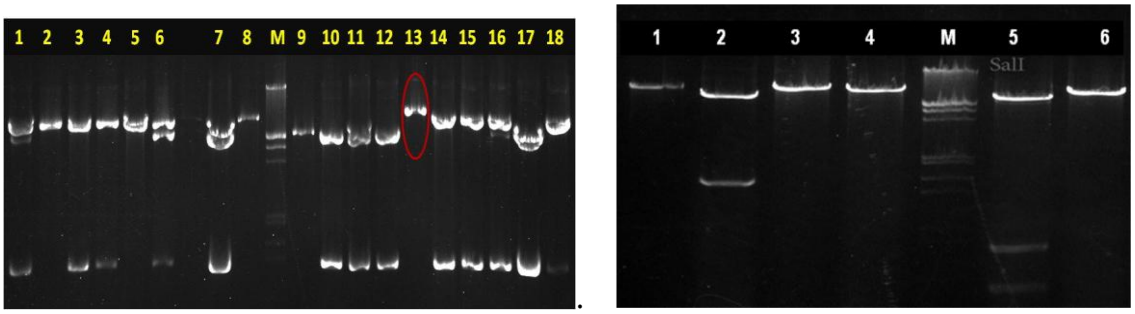

Figure 4.12: Restriction enzyme digestion pattern of pUCPM18Gm CitC vector. (a) Lane1-18: pCitC plasmid digested with BamHI, Lane 13 showing the right orientation clone (8.3Kb). (b) Lane1: pCitC plasmid digested with EcoRI ; Lane2: pCitC plasmid digested with HindIII; Lane3: pCitC plasmid digested with BamHI; Lane4: pCitC plasmid digested with KpnI; Lane5: pCitC plasmid digested with EcoRI-SalI (6.9Kb, 0.81Kb, 0.488 Kb) ; Lane6: pCitC plasmid digested with ScaI (8.3Kb)

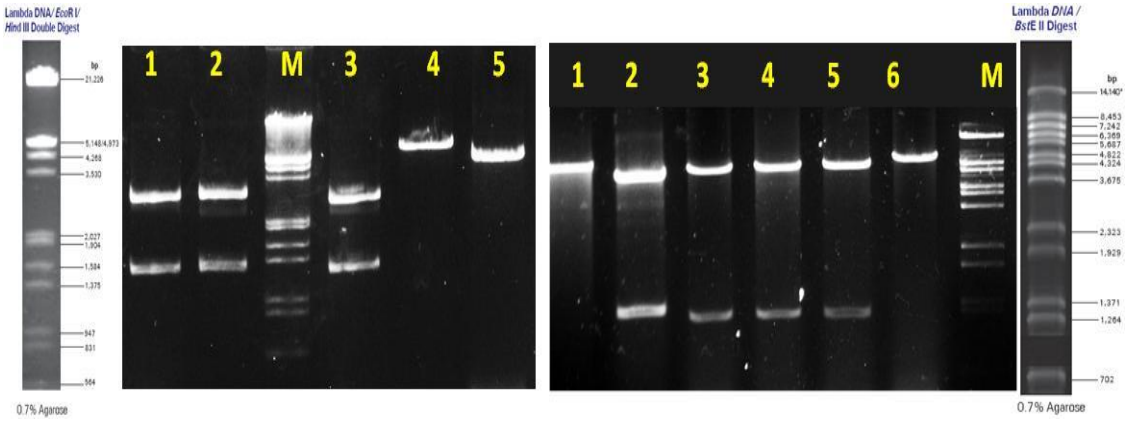

Figure 4.13: Restriction enzyme digestion pattern of pCitM clone. (a) Lane1: pTRZ57/R CitM digested with BamHI (2.88Kb,1.34Kb); Lane2: pTRZ57/R CitM digested with EcoRI-SalI (2.88Kb,1.34Kb); Lane3: : pTRZ57/R CitM digested with KpnI; Lane4:pUCPM18Gm vector digested with EcoRI-SalI (6.9Kb); Lane5: pUCPM18Amp vctor digested with EcoRI-SalI; LaneM: MWM lambda DNA EcoRI-HindIII double digest. (b) Lane1:pCitC plasmid digested with bamHI (8.3Kb); lane2:pCitC plasmid digested with XbaI (6.9Kb,1.34 Kb); Lane3:pCitM plasmid digested with BamHI (6.9Kb,1.34Kb); Lane4:pCitM plasmid digested with XbaI (6.9Kb,1.34Kb); Lane5:pCitM plasmid digested with KpnI (6.9Kb,1.34Kb); lane6::pCitM plasmid digested with ApaI (8.3 Kb); LaneM: MWM lambda DNA BstEII digest.

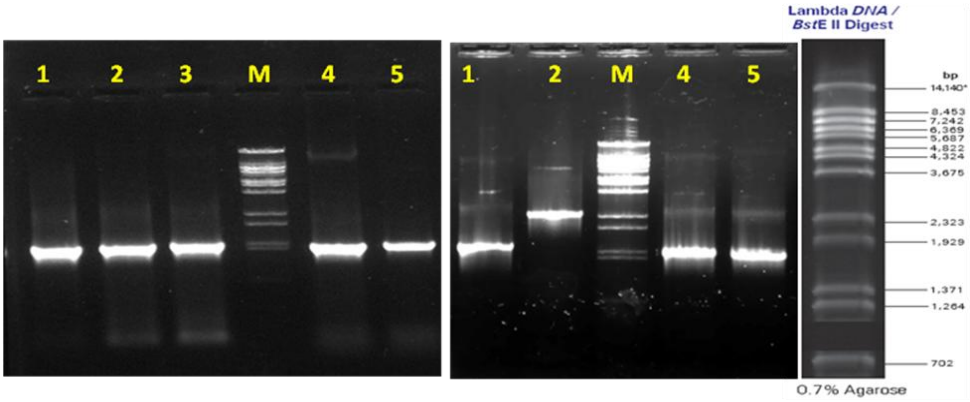

Figure 4.14: PCR amplification of *citC* and *citM* transporter gene cloned in pUCPM18 Gm^r vector.(a) Lane1-2: pUCPM18Gm vector containing *citC* gene ; Lane3-5: pUCPM18Gm vector containing *CitM* gene amplified using gene specific primer.. (b) Lane1: pUCPM18Gm vector containing *citC* gene amplified using p*lac* forward and *CitC* reverse primer; Lane2: pUCPM18Gm vector containing c*itM* gene amplified using plac forward and CitM reverse primer; Lane 3-4: pUCPM18Gm containing *citC* and *citM* gene, respectively amplified by using gene specific primer.

4.4.2 Construction of *Pseudomonas* stable vector containing NADH insensitive *cs* gene Y145F and *S. tphimurium citC* gene under *lac* promoter of pUCPM18 Gm^r plasmid:

The plasmid pYC containing NADH insensitive *cs* gene Y145F and *S. tphimurium citC* gene under *lac* promoter of pUCPM18 Gm^r plasmid were constructed as schematically represented (**Fig. 4.5**).The plasmids were confirmed by restriction enzyme digestion and PCR (**Fig. 4.15**)

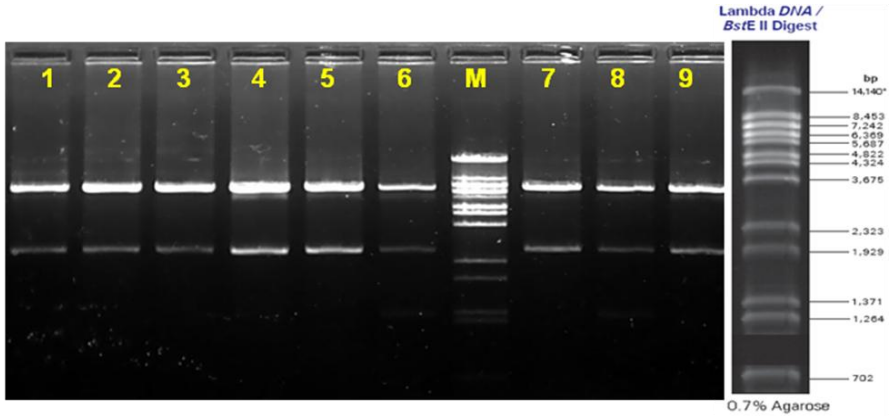

Figure 4.15: Restriction enzyme digestion pattern of pYC plasmid containing NADH insensitive Y145F gene and *S. tphimurium* sodium citrate transporter gene under same lac promoter in pUCPM18 Gm. Lane1-9: pYC plasmid digested with EcoRI-XbaI (6.97 Kb,2.62Kb), LaneM: MWM lambda DNA BstEII digest.

4.4.3 Confirmation by sequencing

4.4.3.1 16s rRNA gene partial sequence of *Salmonella* sp. WT

Analysis of the 16s sequence data of *Salmonella* sp. sewage isolate using NCBI blast online homology programme revealed maximum identity (99%) to *Salmonella*..The GenBank accession number obtained for this partial 16S rDNA sequence is JN555586 and the accession profile is given in **Fig.4.16.**

```
LOCUS       JN555586                887 bp    DNA     linear   BCT 06-SEP-2011
DEFINITION  Salmonella sp. WT 16S ribosomal RNA gene, partial sequence.
ACCESSION   JN555586
VERSION     JN555586.1  GI:345286192
KEYWORDS    .
SOURCE      Salmonella sp. WT
  ORGANISM  Salmonella sp. WT
            Bacteria; Proteobacteria; Gammaproteobacteria; Enterobacteriales;
            Enterobacteriaceae; Salmonella.
REFERENCE   1  (bases 1 to 887)
  AUTHORS   Kumar,P., Adhikary,H., Kumar G,N. and G,A.
  TITLE     A metabolic study of engineered fluorescence Pseudomonads strains
            for high citric acid secretion
  JOURNAL   Unpublished
REFERENCE   2  (bases 1 to 887)
  AUTHORS   Kumar,P., Adhikary,H., Kumar G,N. and G,A.
  TITLE     Direct Submission
  JOURNAL   Submitted (30-JUL-2011) Biochemistry, M S University of Baroda,
            Faculty of Science, Vadodara, Gujarat 390002, India
COMMENT     Sequences were screened for chimeras by the submitter using
            Ribosomal Database Project (RDP) II.
FEATURES             Location/Qualifiers
     source          1..887
                     /organism="Salmonella sp. WT"
                     /mol_type="genomic DNA"
                     /strain="WT"
                     /isolation_source="unprocessed sewage"
                     /db_xref="taxon:1077200"
                     /country="India: Vadodara, Gujarat"
                     /lat_lon="22.30 N 73.20 E"
     rRNA            <1..>887
                     /product="16S ribosomal RNA"
```

Salmonella sp. WT 16S ribosomal RNA gene, partial sequence

GenBank: JN555586.1

GenBank Graphics

```
>gi|345286192|gb|JN555586.1| Salmonella sp. WT 16S ribosomal RNA gene, partial
sequence
CGTCGCACGACAAAAGAGGGCGACTTTCCGCGCTCTCTCCATCAGATGCGCCGAGATGTGATCAGCTAGT
TGCTGAGGTAACGGCTCACCAGGGCGACGNTCCCTAGCTGGTCTGAGAGGATGACCAGCCACACGGGAAT
TGAGACACGGTCCAGACTCATACGGGAGGCAGCAGTGGGGAATATTGCACAATGGGCGCACGCTTGATGC
AGCCATGCCGCGTGTATGAAGAAGGCTTTCGGGTTGTAAAGTACTTTTAGCGGGGAGGAAGGTGTTGTGG
TTNATAACCGCAGCAATTGACGTTACCCGCAGAAGAAGCACCGGCTAACTCCGTGCCAGCAGCCGCGGTA
ATACGGAGGGTGCAAGCGTTAATTGGAATTACTGGGCGTAAAGCGCACGCAGGCGGTCTGTCAAGTAGGA
TGTGAAATCCCCGGGCTCAACCTGGGAACTGCATTCGAAACTGGCAGGCCTGAGTCTCTAGAGGGGGGTA
GAATTCCAGGTGTAGCGGTGAAATGCGTAGAGATCTGGAGGAATACCGGTGGCGAAGGCGGCCCCCTGGA
CAAAGACTGACGCTCAGGTGCGAAAGCGTGGGGAGCAAACAGGATTAGATACCCTGGTAGTCCACGCCGT
AAACGATGTCTACTTGGAGGTTGTGCCCTGAGGCGTGGCTTCCGGAGCTAACGCGTTAAGTAGACCGCCT
GGGGAGTACGGCCGCAAGGTTAAAACTCAAATGAATTGACGGGGGCCCGCACAAGCGGTGGAGCATGTGG
TTTAATTCGATGCAACGCGAAGAACCTTACCTGGTCTTGACATCCACAGAACTTTCCAGAGATGGAAAGG
TGCCTTCGGGAACCGTGAGACAGGTGCTGCATGGCTGTCGTCCAGCC
```

Figure 4.16: GenBank accession result of partial 16S rDNA sequence of *Salmonella* sp. WT

4.4.3.2 Partial SPA sequencing of *citC* and *citM* gene

NCBI-BLAST analysis of the SPA sequencing results done by using both forward and reverse primer revealed maximum homology of the c*itC* gene to *S. enteric sp. enteric serover* Heidelberg Na^+ citrate (OH^-) antiporter and *S. enteric sp. enteric* serover Gallinarum citrate sodium symporter (98%) and of the *citM* gene to *B. subtilis* subsp. *subtilis* str. 168 transporter of divalent metal ion /citrate complexes and *B. subtilis* c*itM* gene (96%).

```
>YFCitc_CitcFor_S665
NNGNGGGCGGACGGAGAAAAAGGGGGCTAGCGATTTACTCAGATTCAAAATCTTTGGTAT
GCCGCTACCGCTTTATGCCTTTGCATTAATTACTTTATTACTTTCTCATTTTTATAATGC
TATACCGACTGACTTAGTCGGTGGTTTTGCCCTTATGTTTGTGATGGGGGCCATTTTTGG
TGAAATCGGCAAACGTTTACCGATCTTCAATAAATATATTGGCGGCGCACCGGTTATGAT
ATTTCTGGTTGCAGCTTATTTTGTCTATGCTGGCATATTTACGCAAAAAGAAATTGATGC
GATCAGCAACGTAATGGATAAAAGCAACTTCCTTAACCTGTTTATCGCAGTGTTGATCAC
AGGCGCGATCCTGTCGGTAAACCGTAAGCTGCTATTAAAATCACTGCTGGGCTATATCCC
AACCATCCTCGCCGGGATTGTCGGCGCGTCCCTTTTCGGTATCGTCATTGGTCTGTGCTT
CGGTATCCCGGTCGACCGTATCATGATGCTGTACGTTCTGCCGATTATGGGCGGTGGTAA
CGGCGCGGGCGCCGTGCCTCTGTCTGAAATTTATCACTCGGTTACCGGACGTTCTCGCGA
AAAGTATTACTCAACGGCTATTGCTATTCTGACCATTGCGAATATCTTCGCCATTATTTT
CGCCGCCCTCCTCGATATGATAGGCAAAAAATACACCTGGCTTAGCGGTGAAGGTGAGTT
GGTTCGTAAGGCTTCCTTCAAAACCGAAGATGATGAAAAGGCCGGTCAGATTACCCATCG
TGAAACGGCGGTTGGCATGGTGCTATCCACCACCTGCTTCCTGCTGGCCTATGTTGTTGC
AAGAAAATTCTGCCCAGCATCGGCGGCGTCTCTATTCACTACTTCGCCTGGATGGTTCTG
ATTGTTGCTGCGCTGAACGCATCAGGCTTTTGCTCACGGAGATTAAGCCGGGGCGAANCT
CTTTCTGACTTCTTCCTCAAACAGCTGCTGGGGGNATGGA
>YFCitc_CitcRev_S665
NNCNTTTGTAGGCCGGATAACCAGCACAATACCGCCGCCCAGACGAGAGGAAATTTGTGC
ATATGAANTGAGGTTCATACGGTTACAGGCGGAGAGCACTTCCAGATCGCCGGAGCCGCC
GCGGTTGGCCATACAAAGACCCGCAGTAATGGATGATTCAATCGGGTAGAAGCCAATCAA
CCAGCCCCCGATAGCTGCGCCGACGACTGCGCCGACCACGATGATCGCGGCGATAACGAC
GTTCGCGAACGTCAGGGCATCGATGATCTCTTGCAGATCGGTGTAGCAAACACCCACACC
TACCATCAATACCCACAGCAGCTGTTTGGAGAAGAAGTCAGAAAGACGTTTCGCCCCGGC
TTTAATCTCCGGTGAGCAAAGGCCTGATGCGTTCAGCGCAGCAACAATCAGAACCATCCA
GGCGAAGTAGTGAATAGAGACGCCGCCGATGCTTGGCAGAATTTTCTTGGCAACAACATA
GGCCAGCAGGAAGCAGTGGTGGATAGCACCATGCCAACCGCCGTTTCACGATGGGTAATC
TGACCGGCCTTTCATCATCTCGGTTTGAAGGAAGCCTTACGAACCAACTCACTTCACTGC
TAGTCAGTGTATTTTTGCCTATCANATCGAGGAGGCGCNAANNATGNGAANNTATCGCAT
GTCAGAATAGCATNCCGTTNAGTAATACTNTCGCGAGAACGTCNGTAACCGAGTGGATAA
AGTTGCNNACGNGGCCGGNCCCNNNCNTNCACGCCNNATCGNNAACGTACGNCTCTTGAT
ACGTCGACCGNNCNAGCCAANCATGACCATCGNNNNACNCGAATCNGNGGATGNTGAATN
NNNNANGATTTATACCGCTACGGTTACCGCACGATCCGCCNNNNNANNGGGANACGGTAA
GNNNNCTTACNNNCGTGTCGTGNNCGCCANGNCCGNNATNCGCANAGACAANATN
```

Figure 4.17: **Partial SPA sequence of *Salmonella* sp. *citC* gene**

```
>gb|CP003416.1|  Salmonella enterica subsp. enterica serovar Heidelberg str. B1
complete genome
Length=4750465

 Features in this part of subject sequence:
   Na(+)Citrate OH(-) antiporter

 Score = 1742 bits (943),  Expect = 0.0
 Identities = 977/993 (98%), Gaps = 5/993 (1%)
 Strand=Plus/Minus

Query  2       GGCGGACGGAGAAAAAGGGGGCTAGCGATTTACTCAGATTCAAAATCTTTGGTATGCCGC  61
               ||| ||||||||||||||||||||||||||||||||||||||||||||||||||||||||
Sbjct  798493  GGC-GACGGAGAAAAAGGGGGCTAGCGATTTACTCAGATTCAAAATCTTTGGTATGCCGC  798435

Query  62      TACCGCTTTATGCCTTTGCATTAATTACTTTATTACTTTCTCATTTTTATAATGCTATAC  121
               ||||||||||||||||||||||||||||||||||||||||||||||||||||||||||||
Sbjct  798434  TACCGCTTTATGCCTTTGCATTAATTACTTTATTACTTTCTCATTTTTATAATGCTATAC  798375

Query  122     CGACTGACTTAGTCGGTGGTTTTGCCCTTATGTTTGTGATGGGGGCCATTTTTGGTGAAA  181
               ||||||||||||||||||||||||||||||||||||||||||||||||||||||||||||
Sbjct  798374  CGACTGACTTAGTCGGTGGTTTTGCCCTTATGTTTGTGATGGGGGCCATTTTTGGTGAAA  798315

Query  182     TCGGCAAACGTTTACCGATCTTCAATAAATATATTGGCGGCGCACCGGTTATGATATTTC  241
               ||||||||||||||||||||||||||||||||||||||||||||||||||||||||||||
Sbjct  798314  TCGGCAAACGTTTACCGATCTTCAATAAATATATTGGCGGCGCACCGGTTATGATATTTC  798255

Query  242     TGGTTGCAGCTTATTTTGTCTATGCTGGCATATTTACGCAAAAAGAAATTGATGCGATCA  301
               |||||||||||||||||||||||||||||||||||| ||||||||||||||||||||
Sbjct  798254  TGGTTGCAGCTTATTTTGTCTATGCTGGCATATTTACGCAGAAAGAAATTGATGCGATCA  798195

>gb|CP003047.1|  Salmonella enterica subsp. enterica serovar Gallinarum/pullor
str. RKS5078, complete genome
Length=4637962

 Features in this part of subject sequence:
   citrate-sodium symporter

 Score = 1742 bits (943),  Expect = 0.0
 Identities = 977/993 (98%), Gaps = 5/993 (1%)
 Strand=Plus/Minus

Query  2       GGCGGACGGAGAAAAAGGGGGCTAGCGATTTACTCAGATTCAAAATCTTTGGTATGCCGC  61
               ||| ||||||||||||||||||||||||||||||||||||||||||||||||||||||||
Sbjct  68359   GGC-GACGGAGAAAAAGGGGGCTAGCGATTTACTCAGATTCAAAATCTTTGGTATGCCGC  68301

Query  62      TACCGCTTTATGCCTTTGCATTAATTACTTTATTACTTTCTCATTTTTATAATGCTATAC  121
               ||||||||||||||||||||||||||||||||||||||||||||||||||||||||||||
Sbjct  68300   TACCGCTTTATGCCTTTGCATTAATTACTTTATTACTTTCTCATTTTTATAATGCTATAC  68241

Query  122     CGACTGACTTAGTCGGTGGTTTTGCCCTTATGTTTGTGATGGGGGCCATTTTTGGTGAAA  181
               ||||||||||||||||||||||||||||||||||||||||||||||||||||||||||||
Sbjct  68240   CGACTGACTTAGTCGGTGGTTTTGCCCTTATGTTTGTGATGGGGGCCATTTTTGGTGAAA  68181

Query  182     TCGGCAAACGTTTACCGATCTTCAATAAATATATTGGCGGCGCACCGGTTATGATATTTC  241
               ||||||||||||||||||||||||||||||||||||||||||||||||||||||||||||
Sbjct  68180   TCGGCAAACGTTTACCGATCTTCAATAAATATATTGGCGGCGCACCGGTTATGATATTTC  68121

Query  242     TGGTTGCAGCTTATTTTGTCTATGCTGGCATATTTACGCAAAAAGAAATTGATGCGATCA  301
               |||||||||||||||||||||||||||||||||||| ||||||||||||||||||||
Sbjct  68120   TGGTTGCAGCTTATTTTGTCTATGCTGGCATATTTACGCAGAAAGAAATTGATGCGATCA  68061
```

Figure 4.18: NCBI-BLAST analysis of the partial *citC* sequence

>PCITM_CitMFor_S701
CCGGGGNGGGNGNTGTNNCNGAGGCCNNNNTTTTTTTGTTTCNTTTNNCTATNNNNNNNN
NNNNNAATGGCAATTGAATCATGAACAAAACGGGCTTTCAGTATTAAACCAGCCATTAGT
TTTTGACGCCCGAAATTGGTGTTCGGCTCCTTAATCCGCCCCGGGAATTTTGGGAATTTT
ACCTGGAAAGTTGGGGGGGGAACAATGGAATGGAATTTTTCGGGGGGGAATTTCCAGCCA
ANGTTCGCGCCCGAAANGGGGGGGGTCAATTGAATTTAATTGTTTTTGCCCAAATTCTTT
AATATTTTTTTGGGGAAATTTTATTGAAATTGGAAAAACCCGGGGCCCCGGGTTTTTGAA
ATCCCCAAAGGGGGTTGGGGGAAAAAAATTTTTTTAAAACCAGGGGGNCNAAAAAGGGGA
AAAACCCCCCTTTTAAAAAAAAATTTTTTTTTTTTCCGGGGGAAACAACCCGGGTTTTTT
TTTAAAAAAAAGGCCCCCCCCCCCCCCCTTTGAAAAAAAGAAAAAAAAGGGGNCCCCCC
CCCCCACCCCTTTAAATGGGGTTTTTCCCAAAAAAAGGGGCCCCCCCAGGGGTTTTTTCC
CCCCCCCTTTTTTTTTTTGNNCCNGNAAGAGGGGNACCCCCCCGGGCCCAAAATTTTTTT
TTTTTTTGGGGNGAAAGGAAAAACCCCCCCGGGGAGAAACCCCCCCCCCGGGGGGGAAAA
AATTTCTNGAAAAAAAACTTTTTTTTTTTTTTTTGGGGGGGGAANTGGNGCCCCCCCCCC
CCCCCAAAAGGGGGGGGGGGAAAAAAAAAACCCCCCCCCGGGGGGGGGGGGGTGTTTTTTT
TTTCCCCCCCCCCCGGGGGGAATTTTTTTAAAGGCGCCCCACAACAAAAAAAAAATACCT
CCCCCCCCCCCCTCNTTCTTAAAAAAAAAGGGGGGGGGGAGGAGGGCGCT
>PCITM_CitMRev_S701
NTTNAATCAGAGCGATAGCCGTCATGACGATCACTGCGAGAACCGCCCATTTCAATGCNA
NTTTTTGATGGTCATCAATAGAAACTCCGACGAGTCCGACAAGCAAATGAGTGGATGGCA
CAAGCGGACTCAGCATATGAATCGGCTGGCCGATAATAGAGGCTCTGGCAATTTCCACTT
TATCCACACCGTATGCGACAGCTGTTTCTGATAAAATCGGCAGCACCCCGTAGAAATACG
CGTCATTCGGCATCAAAAATGTGAAAATGCCGCTTGTTAAGGCAACAATCGCCGGGATCA
ATCCGCCCATTTGTTCCGGTATCATGGACACGAGCGAGATCGCCATTTCATCAACCATTT
TCGTGCCTGTCAAAATCCCCGTGAAACACCCCCGCAGCAAAAATCATTGAACCGATGCCA
GCACGTTGTGGAAATGCGCCGCGATGCCTGTCTCTGAGCTCAAAANNGGGAAAATTNACN
ATTCAGCGCAATANAAAACGNNNNACNANCAGTCCGGTNAACCTAATTTTCCCNNAACAA
ACTCNNNTTAAANAANNCGTNANAATANTTNANCNNNANGNTNNNCGTTCANTATTTNAA
NNNGGNCNNNNTTGCTTGNTGGTGTTCATTANCNCCAANGGTTTTCNTNNTNNNNANCAA
ANAATGCACNTAAGNNCCGTNNAAGAAGAACTCGGCTNGANCGNNGATANCNAGGGATNN
CNCTGGGNGNNNCTNNGANNTNNCGGGTNCCANNANCNNNGATCGGAAAANN

Figure 4.19: Partial SPA sequence of *B. subtilis* 168 strain *citM* gene

```
>emb|AL009126.3|  Bacillus subtilis subsp. subtilis str. 168 complete genome
Length=4215606

 Features in this part of subject sequence:
   transporter of divalent metal ions/citrate complexes

 Score =  830 bits (449),  Expect = 0.0
 Identities = 482/500 (96%), Gaps = 8/500 (2%)
 Strand=Plus/Minus

Query  4       AATCAGAGCGATAGCCGTCATGACGATCACTGCGAGAACCGCCCATTTCAATGCNANTTT  63
               ||| |||||||||||||||||||||||||||||||||||||||||||||||||| | |||
Sbjct  835656  AAT-AGAGCGATAGCCGTCATGACGATCACTGCGAGAACCGCCCATTTCAATGCGAATTT  835598

Query  64      TTGATGGTCATCAATAGAAACTCCGACGAGTCCGACAAGCAAATGAGTGGATGGCACAAG  123
               ||||||||||||||||||||||||||||||||||||||||||||||||||||||||||||
Sbjct  835597  TTGATGGTCATCAATAGAAACTCCGACGAGTCCGACAAGCAAATGAGTGGATGGCACAAG  835538

Query  124     CGGACTCAGCATATGAATCGGCTGGCCGATAATAGAGGCTCTGGCAATTTCCACTTTATC  183
               ||||||||||||||||||||||||||||||||||||||||||||||||||||||||||||
Sbjct  835537  CGGACTCAGCATATGAATCGGCTGGCCGATAATAGAGGCTCTGGCAATTTCCACTTTATC  835478

Query  184     CACACCGTATGCGACAGCTGTTTCTGATAAAATCGGCAGCACCCCGTAGAAATACGCGTC  243
               ||||||||||||||||||||||||||||||||||||||||||||||||||||||||||||
Sbjct  835477  CACACCGTATGCGACAGCTGTTTCTGATAAAATCGGCAGCACCCCGTAGAAATACGCGTC  835418

Query  244     ATTCGGCATCAAAAATGTGAAAATGCCGCTTGTTAAGGCAACAATCGCCGGGATCAATCC  303
               ||||||||||||||||||||||||||||||||||||||||||||||||||||||||||||
Sbjct  835417  ATTCGGCATCAAAAATGTGAAAATGCCGCTTGTTAAGGCAACAATCGCCGGGATCAATCC  835358

Query  304     GCCCATTTGTTCCGGTATCATGGACACGAGCGAGATCGCCATTTCATCAACCATTTTCGT  363
               ||||||||||||||||||||||||||||||||||||||||||||||||||||||||||||
Sbjct  835357  GCCCATTTGTTCCGGTATCATGGACACGAGCGAGATCGCCATTTCATCAACCATTTTCGT  835298

Query  364     GCCTGTCAAAATCCCCGTGAAACACCCCCGCAGCAAAAATCATTGAACCGAT-GCCAGCA  422
               |||||||||||||||||||| ||||||||||||||||||||||||||||| ||||||| |
Sbjct  835297  GCCTGTCAAAATCCCCGTGAA-CACCCCCGCAGCAAAAATCATTGAACCGATAGCCAGCA  835239

Query  423     CGTTG-TGGAAATGCGCCGCGATGC-CTGTCTCTGA-GCTcaaaannggggaaaattnacn  479
               ||||| ||||| |||||||||||||| |||||||||| |||| | |  |||| |||| ||
Sbjct  835238  CGTTGCTGGAA-TGCGCCGCGATGCGCTGTCTCTGATGCTCGAGATTGGGATAATTCACA  835180

Query  480     attcagcgcaatanaaaacg  499
               || |||||||||| ||||||
Sbjct  835179  AT-CAGCGCAATACAAAACG  835161

>gb|U62003.1|BSU62003  Bacillus subtilis CitM gene, complete cds
Length=1750

 Score =  830 bits (449),  Expect = 0.0
 Identities = 482/500 (96%), Gaps = 8/500 (2%)
 Strand=Plus/Minus

Query  4     AATCAGAGCGATAGCCGTCATGACGATCACTGCGAGAACCGCCCATTTCAATGCNANTTT  63
              ||| |||||||||||||||||||||||||||||||||||||||||||||||||| | |||
Sbjct  1554  AAT-AGAGCGATAGCCGTCATGACGATCACTGCGAGAACCGCCCATTTCAATGCGAATTT  1496

Query  64    TTGATGGTCATCAATAGAAACTCCGACGAGTCCGACAAGCAAATGAGTGGATGGCACAAG  123
              ||||||||||||||||||||||||||||||||||||||||||||||||||||||||||||
Sbjct  1495  TTGATGGTCATCAATAGAAACTCCGACGAGTCCGACAAGCAAATGAGTGGATGGCACAAG  1436

Query  124   CGGACTCAGCATATGAATCGGCTGGCCGATAATAGAGGCTCTGGCAATTTCCACTTTATC  183
              ||||||||||||||||||||||||||||||||||||||||||||||||||||||||||||
Sbjct  1435  CGGACTCAGCATATGAATCGGCTGGCCGATAATAGAGGCTCTGGCAATTTCCACTTTATC  1376

Query  184   CACACCGTATGCGACAGCTGTTTCTGATAAAATCGGCAGCACCCCGTAGAAATACGCGTC  243
              ||||||||||||||||||||||||||||||||||||||||||||||||||||||||||||
Sbjct  1375  CACACCGTATGCGACAGCTGTTTCTGATAAAATCGGCAGCACCCCGTAGAAATACGCGTC  1316

Query  244   ATTCGGCATCAAAAATGTGAAAATGCCGCTTGTTAAGGCAACAATCGCCGGGATCAATCC  303
              ||||||||||||||||||||||||||||||||||||||||||||||||||||||||||||
Sbjct  1315  ATTCGGCATCAAAAATGTGAAAATGCCGCTTGTTAAGGCAACAATCGCCGGGATCAATCC  1256

Query  304   GCCCATTTGTTCCGGTATCATGGACACGAGCGAGATCGCCATTTCATCAACCATTTTCGT  363
              ||||||||||||||||||||||||||||||||||||||||||||||||||||||||||||
Sbjct  1255  GCCCATTTGTTCCGGTATCATGGACACGAGCGAGATCGCCATTTCATCAACCATTTTCGT  1196

Query  364   GCCTGTCAAAATCCCCGTGAAACACCCCCGCAGCAAAAATCATTGAACCGAT-GCCAGCA  422
              |||||||||||||||||||| ||||||||||||||||||||||||||||| ||||||| |
Sbjct  1195  GCCTGTCAAAATCCCCGTGAA-CACCCCCGCAGCAAAAATCATTGAACCGATAGCCAGCA  1137

Query  423   CGTTG-TGGAAATGCGCCGCGATGC-CTGTCTCTGA-GCTcaaaannggggaaaattnacn  479
              ||||| ||||| |||||||||||||| |||||||||| |||| | |  |||| |||| ||
Sbjct  1136  CGTTGCTGGAA-TGCGCCGCGATGCGCTGTCTCTGATGCTCGAGATTGGGATAATTCACA  1078

Query  480   attcagcgcaatanaaaacg  499
              || |||||||||| ||||||
Sbjct  1077  AT-CAGCGCAATACAAAACG  1059
```

Figure 4.20: NCBI-BLAST analysis of the partial *citM* sequence

4.4.4 Functional complementation of pCitC, pCitM and pYC plasmids in *E. coli.*

E. coli DH5α containing pCitC, pCitM and pYC plasmid grow on Koser citrate broth medium induced with 0.1mM and 0.2 mM IPTG and supplemented with 100 mg/ml thiamine whereas *E. coli* DH5α containing pGm plasmid failed to grow (**Fig. 4.21).**

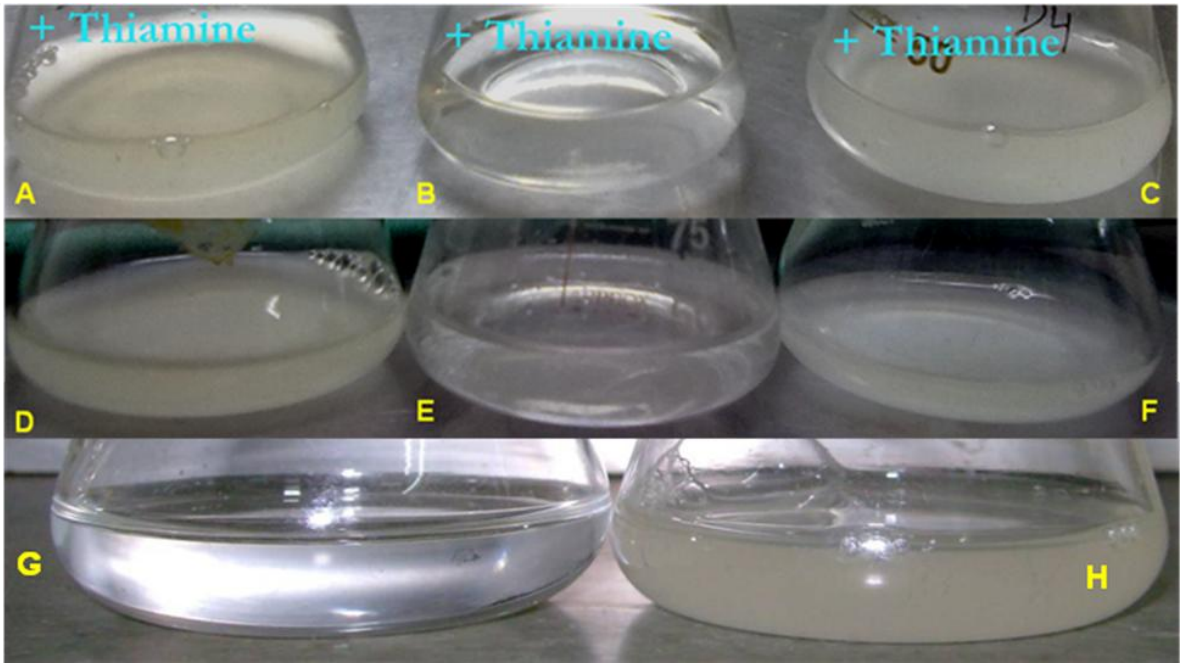

Figure 4.21: Growth of *E. coli* DH5α on Koser citrate broth. *E. coli* DH5α containing: pCitC plasmid induced with 0.1mM IPTG (A), pGm plasmid induced with 0.1mM IPTG (B), pCitC plasmid induced with 0.2mm IPTG (C), pCitM plasmid induced with 0.1mM IPTG (D), pGm plasmid induced with 0.1mM IPTG (E), pCitM plasmid induced with 0.2mM IPTG (F), pGm plasmid induced with 0.1mM IPTG (G), pYC plasmid induced with 0.1mM IPTG (H). All plasmid bearing strains are supplemented with 100mg/ml thiamine and antibiotic 1/4th of the recommended dose.

4.4.5 Effect of *citC* and *citM* overexpression on citric acid secretion in *P. fluorescens* PfO-1 harbouring NADH insensitive *cs*

Overexpression of *citC* in *Pf* (pY145F) strain caused both qualititative and quantitative changes in citric acid levels and yields. *citM* does not cause any significant difference in citric acid levels and yields when compared to *Pf* (pY145F) without any external citrate transporter.

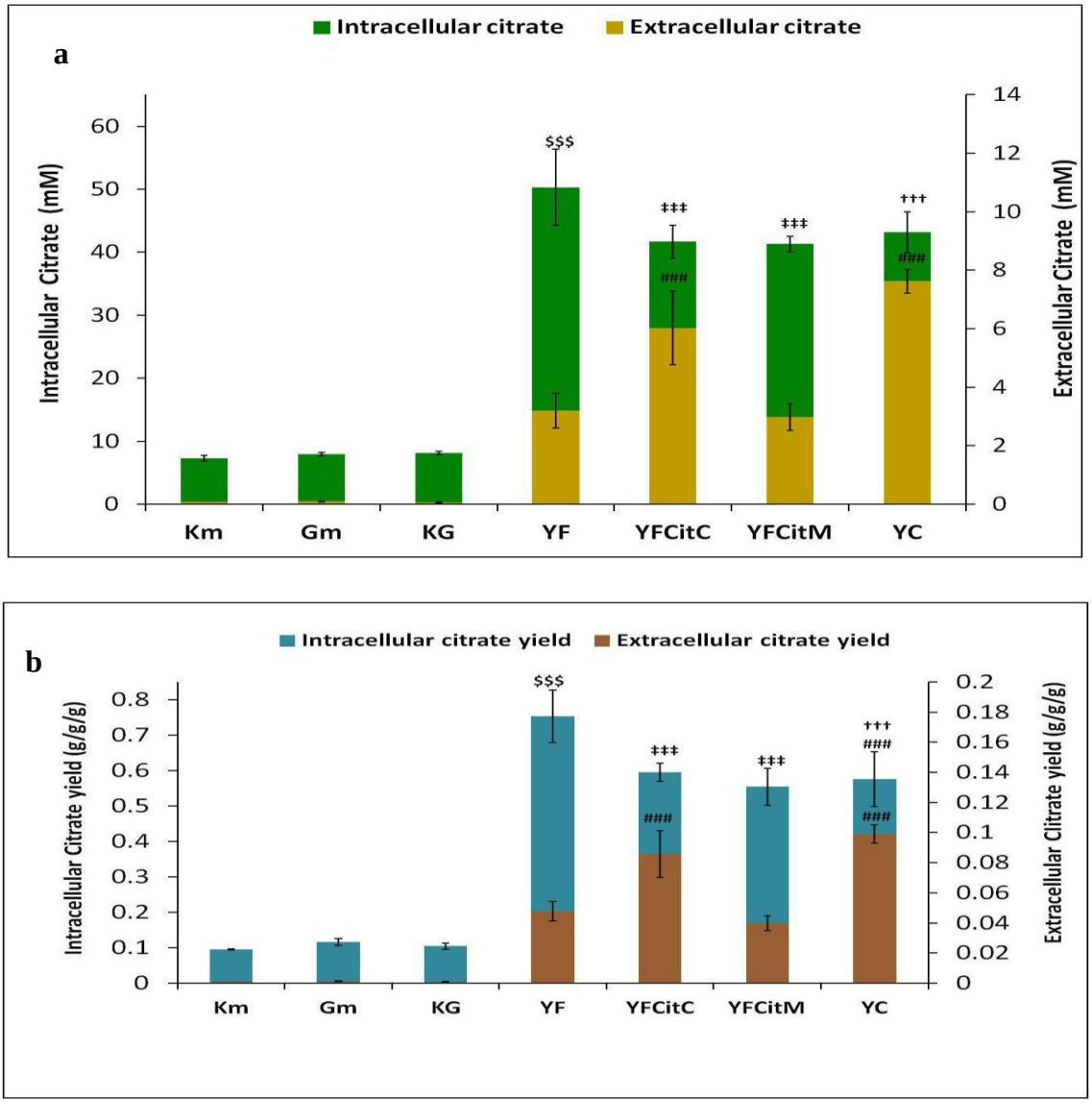

Figure 4.22 : Citric acid levels and yields in *P. fluorescens* PfO-1 overexpressing citrate transporter.Intracellular and extracellular citrate levels(a) are represented in **green** and **orange** bars

respectively. Intracellular and extracellular citrate yields are represented in **blue** and **magenta** bars respectively. Organic acid yields were estimated from stationary phase cultures grown on M9 medium with 100mM glucose and are expressed as g/g of glucose utilized/g dry cell mass. Results are expressed as Mean ±S.E.M of 4 independent observations. $ comparision of parameters with vector control Km, †comparision of parameters with vector control Gm, ‡ comparision of parameters with vector control KG, # comparision of parameters YF and YFCitC, YF CitM and YC. $$$, †††,‡‡‡,###,P<0.001; $$,††,‡‡##P<0.01; $,†,‡,#P<0.05

Extracellular citric acid levels in *Pf*(pYFCitC) and *Pf*(pYC) increase by 1.88 and 2.3 fold as compared to *Pf* (pY146F) which is 92.6 and 84.6 fold higher as compared to vector control strain respectively. Corresponding extracellular citrate yield increased by 1.79 and 2.07 fold with an increase of 103.4 and 76 fold compared to respective vector controls (**Fig. 4.22**). Although there is an approximately 1.26 fold decrease intracellular citrate yield amongst the citrate transorter bearing strain this is not statistically significant. All experiments were further continued with *Pf*(pYC) and *pf* (pGm) as control.

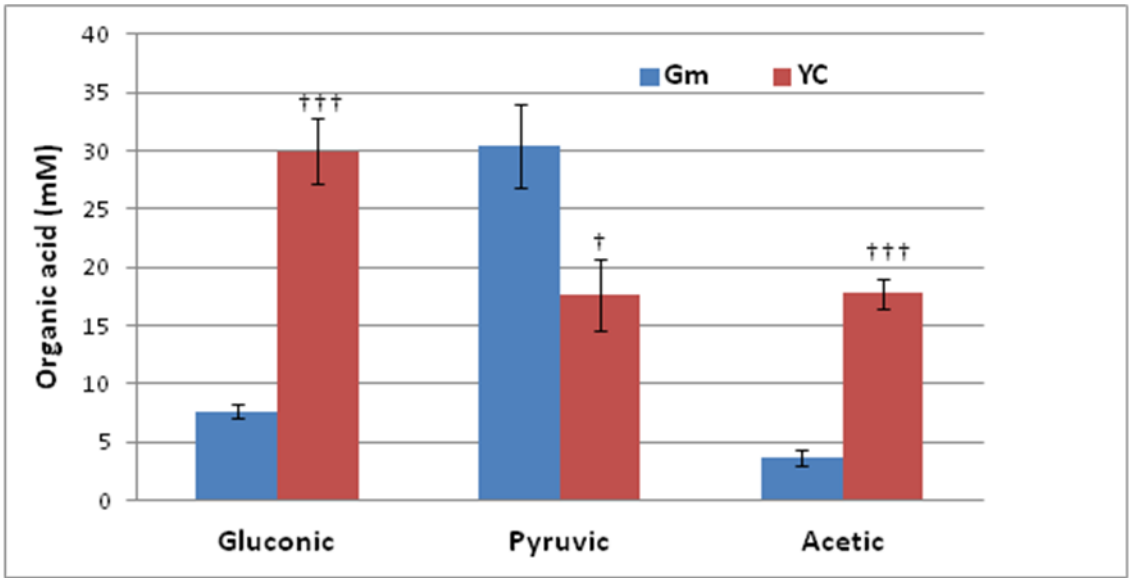

Figure 4.23: Organic acid secretion from *P. fluorescens* Pf0-1 overexpressing citrate transporter. Gluconic, pyruvic and acetic acid levels (mM) were estimated from Pf(pYC) with respect to control strain Pf(pGm) designated as respective colours in the graph. Parameters estimated from stationary phase cultures grown on M9 medium with 100mM glucose. Results are expressed as Mean ±S.E.M of 4 independent observations. †Comparison with respect to pGm †††P<0.001; ††P<0.01; †P<0.05.

The YF-CitC overexpression caused quantitative changes in secretion of gluconic, pyruvic and acetic acid levels. Stationary phase culture supernatents of *Pf* (pYC) showed 3.91 and 4.81 fold elevated gluconic and acetic acid levels, respectively, and 1.73 fold decreased pyruvic acid level as compared to *Pf*(pGm) (**Fig. 4.23**).

4.4.6 Alterations in G-6-PDH, CS, ICDH, ICL, PYC, and GDH activities

In *Pf* (pYC) the periplasmic GDH activity increased by 1.46 fold as compared to the *Pf* (pGm) in late log to stationary phase of growth. Similarly a significant increase in G6PDH, PYC and CS activities by 1.46, 4.74 and 4.5 fold, respectively, were observed as compared to the controls. However, ICL and ICDH activities in the stationary phase cultures remained unaltered (**Fig. 4.24**).

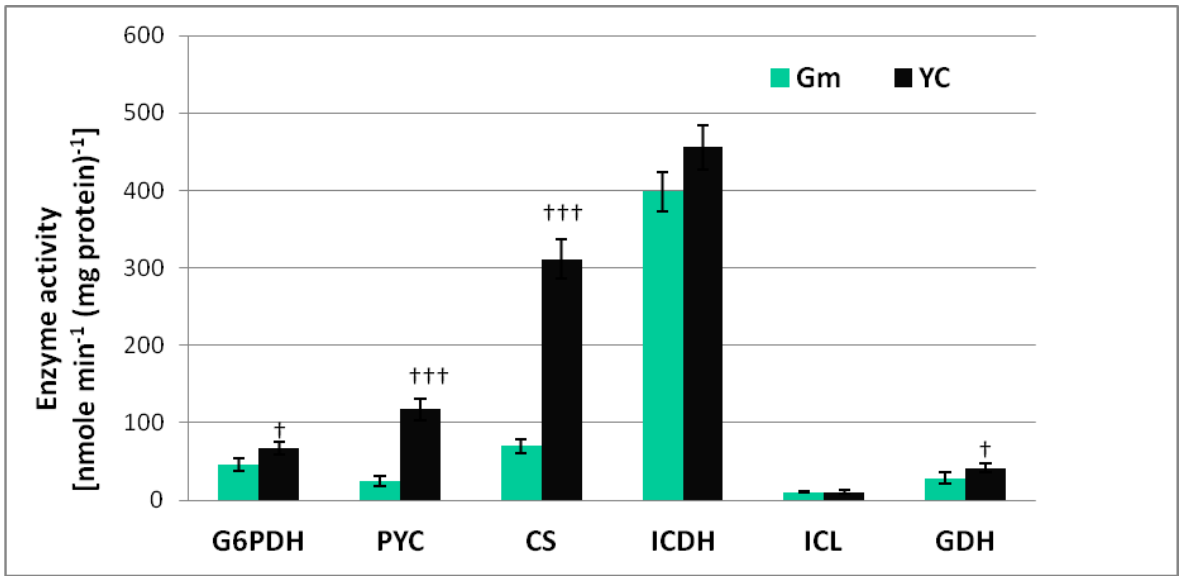

Figure 4.24: Activities of enzymes G-6-PDH, ICDH, ICL, PYC, and GDH in *P. fluorescens* PfO-1 overexpressing citrate transporter. The activities have been estimated using *Pf* (pYC) and vector control *Pf* (pGm) cultures grown on M9 minimal medium with 100mM glucose. All the enzyme activities were estimated from mid log phase and stationary phase cultures except ICL and GDH which were estimated only in mid log and stationary phase respectively. All the enzyme activities are represented in the units of nmoles/min/mg total protein. The values are depicted as Mean ± S.E.M of 4 (N=4) independent observations. †Comparison with respect to pGm †††P<0.001; ††P<0.01; †P<0.05.

4.4.7 Effect of *citC* overexpression on growth, biomass and glucose utilization of *P. fluorescens* PfO-1

In the presence of excess glucose, increase in CS activity did not significantly affect growth profile and acidification of the medium within 30 h. However, there is a significant pH drop was found in case of *Pf* (pYC) compared to wild type and control strain. Specific growth rate, specific total glucose utilization rate after 30h remained unaffected. Total amount of glucose utilized increased by 1.44 fold and glucose consumed intracellularly is reduced by 1.27 fold in *Pf* (pYC) as compared to *Pf* (pGm). The increase in CS activity in *Pf* (pYC) strain improved the biomass yield by 2.58 fold compared to *Pf* (pGm) (**Table 4.6, Fig. 4.25**).

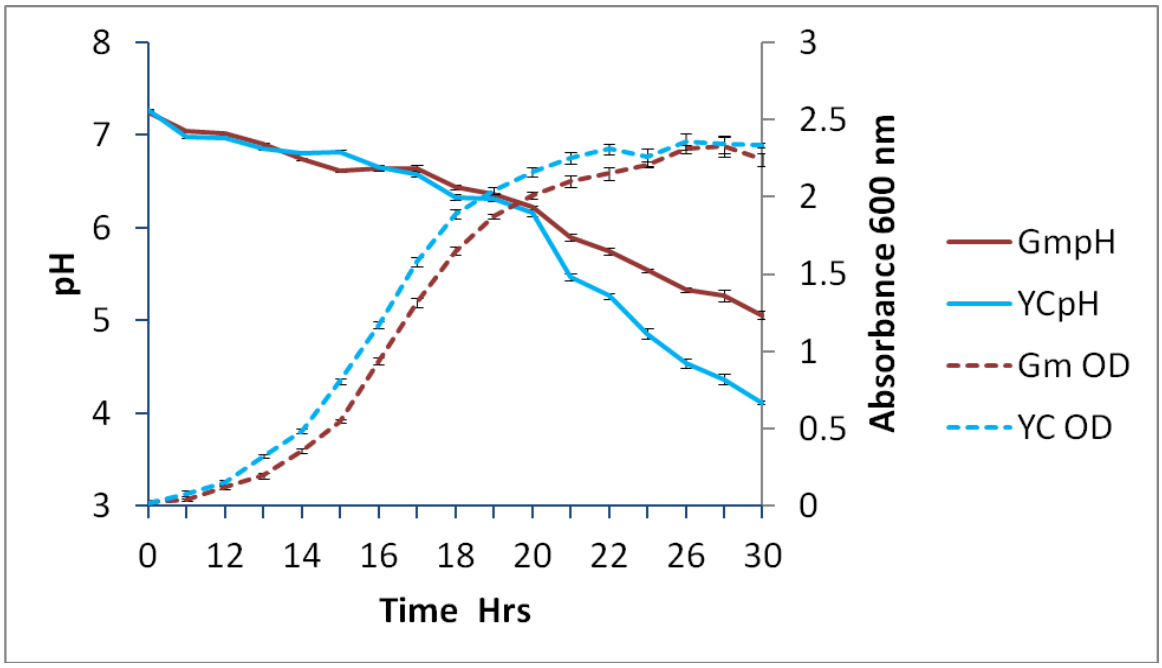

Figure 4.25: Growth and pH profiles of *P. fluorescens* PfO-1 pYC and pGm transformants on M9 minimal medium with 100mM glucose. The values plotted represent the Mean±S.D of 4-6 independent observations.

Table 4.6: Physiological variables and metabolic data from *P. fluorescens* Pf0-1 pYC and pGm transformants grown on M9 medium with 100mM glucose

Bacterial strain	Sp. Growth rate $\mu(h^{-1})^{\beta}$	Total glucose utilized(mM)$^{\epsilon}$	Glucose consumed (mM) $^{\epsilon}$	Biomass yield Ydcw/Glc $^{\beta}$ (g g^{-1})	Sp. Glucose utilization rate QGlc $^{\beta}$ [g (g dcw)$^{-1}$ h^{-1}]
***Pf* (pGm)**	0.52±.006	54.23±4.76	46.54±4.49	0.12± 0.031	6.6±0.85
***Pf* (pYC)**	0.53±0.02	67.47±6.97 †	37.52±7.59 †	0.31± 0.053††	7.01±0.45

. The results are expressed as Mean ± S.E.M of readings from 4-6 independent observations. $^{\beta}$ Biomass yield (Ydcw/Glc), specific growth rate (μ) and specific glucose consumption rate (QGlc) were determined from the mid-log phase of each experiment. $^{\epsilon}$Total glucose consumed and glucose utilized were determined at the time of pH drop (30h) for *Pf* (YC) and control strain *Pf* (Gm). †Comparison with respect to pGm †††P<0.001; ††P<0.01; †P<0.05

4.4.8 Phosphate solubilization phenotype by *P. fluorescens* PfO-1 transformants harboring pYC plasmid expressing NADH insensitive *cs* and *S. tphimurium citC* gene under p*lac.*

PfO-1 (pYC) showed an improved MPS phenotype over PfO-1(pGm) in both PVK agar and TRP agar medium (**Fig. 4.26**).

PfO-1 (pGm) **PfO-1 (pYC)**

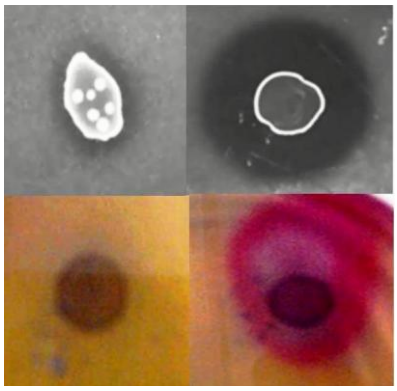

Strain	Zone diameter(cm)
Pf (pGm)	0.69±0.05
Pf (pYC)	1.62±0.23††

Figure 4.26: Diameter of zone of clearance and colouration formed by fluorescent pseudomonad transformants on Pikovskaya's agar and tris rock phosphate agar containing 75mM glucose and 75 mM Tris HCl pH 8.0. The results were noted after an incubation of 120 h at 30 ºC and are given as mean ± S.D. of three independent observations. † as compared to control Pf(pGm), †††<.001, ††<0.01 and †<0.05.

4.5 Discussion:

The present study demonstrates heterologous overexpression of *S. tphimurium* Na^+ citrate and *B. subtilis* Mg^{2+}·citrate transporter in citric acid secretion by metabolically distinct *P. fluorescens* PfO-1. Approximately 85 fold increases in extracellular citrate level compared to vector control *Pf* (pGm) and 2.5 fold as compared to *Pf* (pY145F with endogenous transporter were achieved in the present study due to *CitC* overexpression. Considering the high amount of intracellular citrate accumulation after overexpression of NADH insensitive *cs* Y145F, the extracellular levels were relatively low suggesting that the endogenous citrate transporter (H^+citrate) was inefficient. An efficient transport system for citrate secretion was considered to rate limiting in case of yeast (Anastassiadis and Rehm, 2005) while in addition to citrate transport, transport of sugar and ammonia into the cell was important for citrate production in *A. niger* (Papagianni, 2007).

The CitM transporter from *B. subtilis* transports citrate as a complex with Mg^{2+}. Functional expression and characterization of *B. subtilis* CitM in *E. coli* DH5α is reported in many studies (Boorsma et al., 1996; Li et al., 2002). In the present study, c*itM* gene overexpression in *P. fluorescens* PfO-1 harbouring NADH insensitive *cs* gene does not lead to enhanced extracellular citrate level. c*itM* gene expression is induced when citrate is present in the growth medium (Warner 2000: Blancato 2006). The expression of *citM* gene is under the strict control of the medium composition and carbon catabolite repression. In a similar manner, *citM* gene is also inducible by citrate and repressed by glucose in *B. subtilis* (Bergsma et al., 1983; Boorsma et al., 1996).

Increased gluconic acid levels with simultaneous reduction in pyruvic acid levels could be explained by increased PYC activity in *Pf* (pYC), which could probably diverts

pyruvate flux towards increased OAA biosynthesis to meet the increased CS activity. Even in *A. niger* the enhancement of anaplerotic reactions replenishing TCA cycle intermediates predisposes the cells to form high amounts of citric acid (Legisa and Mattey, 2007). However, similar increase in flux through glyoxylate shunt was not apparent in *Pf* (pYC) as evident from very low and unaltered ICL activity detected in *Pf* (pGm) and *Pf* (pYC). Low ICL activity was consistent with earlier reports in *P. fluorescens* ATCC13525 and *P. indigofera* in which ICL contributed negligibly to glucose metabolism (Buch et al., 2009; Diaz-Perez et al., 2007).

Enhanced CS activity in *Pf* (pYC) also increased the periplasmic glucose oxidation which is reflected by increase in GDH activity and gluconic acid production**.** Significant increase in G6PDH activity is monitored in *Pf* (pYC). Significant decrease in glucose consumption and increase in total glucose utilization accounts for the carbon flux distribution in *P. fluorescens* PfO-1. The increased carbon flow through glycolysis led to increased protein synthesis that is reflected to increased biomass. The citrate induced oligosaccharide synthesis was reported in *Agrobacterium* sp. ATCC 31749 (Ruffing et al., 2011).

The summary of the result is depicted in the **Fig. 4.27.**

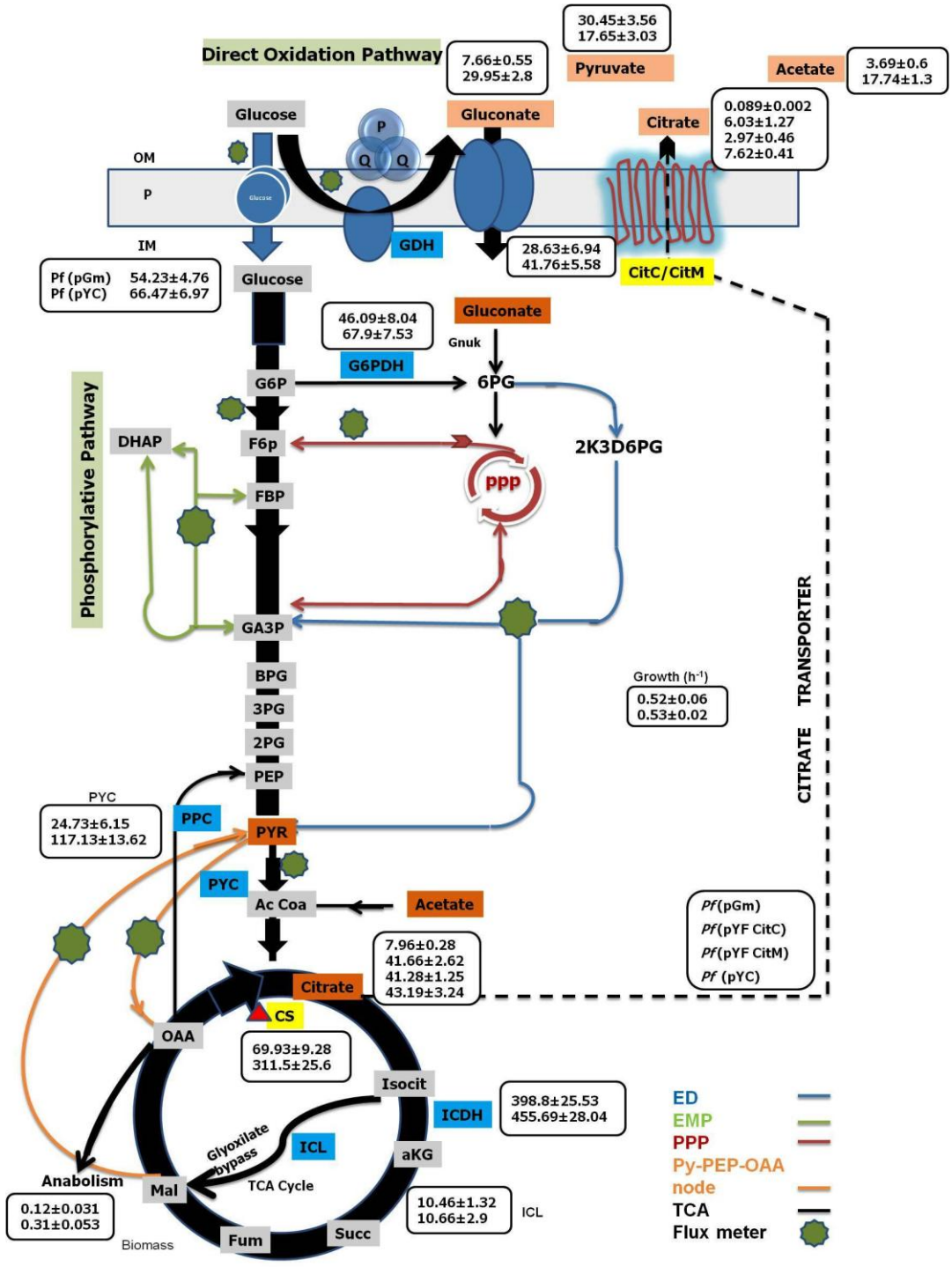

Figure 4.27: Key metabolic fluctuations in *P. fluorescens* PfO-1 overexpressing NADH insensitive *E. coli* CS and *S. tphimurium* Na^+ citrate transporter

Genomic integration of E. coli NADH insensitive cs and S.typhimurium Na^+ dependent citrate transporter operon in fluorescent pseudomonads using Mini-Tn7 transposon site specific integration system and study their effects on glucose metabolism.

CHAPTER 5

5 CHAPTER

5.1 INTRODUCTION

5.1.1 Low copy number plasmid Vs high copy number plasmid based expression

Multicopy plasmids are used as a tool for recombinant gene expression, particularly the over-expression of genes. The advantages of these vectors over low copy plasmid vectors are - they are typically small (~5 kb) and high copy number results in good expression of the recombinant genes in the host organism. However, high copy number vectors are also have disadvantages as the recombinant vector may be structurally or segregationally unstable (1984; O'Connor et al., 1989; Balbas and Bolivar, 1990). Most plasmids are known to cause metabolic burden on the cell and significant shift in the normal metabolism depending on the host organism, plasmid nature, and environmental conditions (Glick 1995; Mcloughlin, 1994; Buch et al., 2010b; Sharma et al., 2011). This metabolic burden has been attributed to the increased demand for nucleotides for replication of plasmid DNA and translation of plasmid-encoded genes (Birnbaum and Bailey, 1991; Vind et al., 1993; Jones et al., 2000).

The maintenance of plasmid DNA in *E. coli* has been demonstrated to have diverse effects on the physiology and cellular metabolism including alteration in ATP biosynthesis as well as perturbations in host DNA replication, transcription, and translation (Rozkov et al. 2004; Ow et al. 2006; Wang et al. 2006; Chou 2007; Ow et al. 2009;). Presence of *colE*1 based plasmid has been demonstrated to significantly alter several metabolic pathways in *E. coli* depending on the growth conditions. Presence of plasmids adversely affected the growth and gluconic acid secretion of phosphate solubilizing *Enterobacter asburiae* PSI3 under phosphorus limitated condition (Sharma et al. 2011). Similarly, other hosts like *E. asburiae* PSI3, *Azotobacter vinelandii*, *Azospirillum brasilense*, and *Pseudomonas putida* GR12-2 also showed impaired growth, phosphate solubilization, nitrogen fixation, siderophore production, and indole acetic acid biosynthesis, under various experimental conditions (Glick 1995; Sharma et al. 2011), while in *P. chlororaphis* and *P. fluorescens* WCS365

showed reduced competitiveness and variable stability, respectively, under rhizospheric conditions (Eisenlohr and Baron 2003). PGPR traits that have been shown to be adversely affected by metabolic load include environmental fitness in soils, indole acetic acid (IAA) production (De Leij et al., 1998; Holguin and Glick, 2001), competitiveness in rhizosphere colonization and nitrogen fixation (Eisenlohr and Baron, 2003). These disadvantages suggests that multi- copy plasmids may not be the best option for metabolic engineering applications, even when the objective is to increase the intracellular concentration of an enzyme in order to improve the product concentration and flux through an existing pathway.

Low-copy plasmids may reduce the specific activity of the gene product but can compensate on the productivity by reducing the burden effects associated with high plasmid copy number while allowing the use of strong promoters to maximize gene expression. Chromosomal insertion of genes into bacterial genome is an alternative to introduction of foreign genes on plasmid and this may cause less metabolic burden.

5.1.2 Genomic integration: single copy gene insertion using mini Tn7 transposon

The mini-Tn7 transposon is a great tool for single copy tagging of bacteria in a site-specific manner at a unique and neutral site without any deleterious effects. The Tn7 transposon was originally discovered by Barth et al., (1976) on the plasmid R483 (IncIα) as an element carrying the resistance genes trimethoprim (Tm^R) and streptomycin/ spectinomycin (Sm^R / Sp^R), which could be transposed to other replicons. The Tn7 transposon is of 14 kb encodes for five genes involved in the transposition process (**Fig.5.1**). These genes are flanked by the ends of the transposon, named the left (Tn7L) and the right (Tn7R) end (Lichtenstein and Brenner, 1982; Rogers et al., 1986). The Tn7 transposition process has been studied intensively in *Escherichia coli* in which Tn7 inserts with high efficiency and unique orientation into one specific location named the attTn7 site. This site of insertion is located just downstream of the coding region, in the transcriptional terminator, of the *glm*S gene and thereby does not disrupt the gene (Gringauz, et al., 1988). The *glm*S gene encodes a glucosamine synthetase, which is required for cell wall synthesis

(Volger et al., 1989). It is conserved among many bacteria and therefore Tn7 is likely to have the same specific insertion site in many different bacteria, some have already been tested (**Fig. 5.1, Table 5.1**). The transposon genes required for specific insertion into the attTn7 site, are tnsABCD, and they function in *trans.* Thus, sequences located in the 3'end of the coding region of *glm*S are recognised by transposase proteins directing the actual insertion into the attTn7 site, down-stream of the *glmS* gene**.** However, if this site is unavailable the transposon can insert into other sites with low frequency (Peters, J. E. et al., 2001**).**

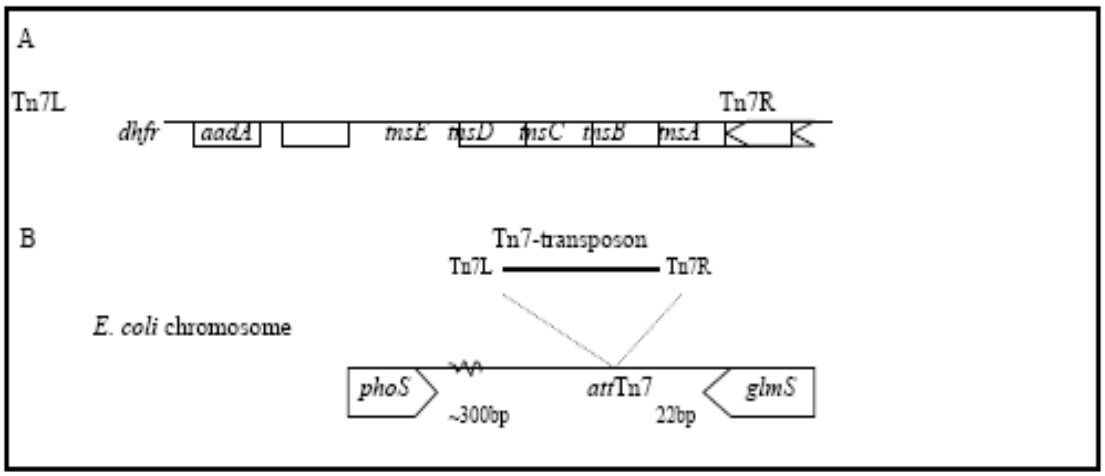

Figure 5.1: Map of transposon Tn7 (A) and its insertion site attTn7 in *Escherichia coli* (B). The gene *dhfr* encodes dihydrofolate reductase providing trimethoprim resistance and *aad*A encodes adenylyltransferase, which provides resistance to streptomycin and spectinomycin (the figure is redrawn from Craig et al., 1989).

The mini-Tn7-based gene integration system has been used for gene complementation, gene expression analysis, strain construction, and reporter gene-tagging of *Pseudomonas aeruginosa* and *Yersinia pestis*, particularly in biofilm and animal models. Heterologous genes including *lacZ* (β-galactosidase), *est* (esterase), and *gfp* (green fluorescent protein) under the control of the methanol dehydrogenase promoter have been integrated into the intergenic region between *glmS* and *dha*T via the delivery of mini-Tn7 in *Methylobacterium extorquens.* A gene encoding for different fluorescent protein and luciferase protein along with promoter was integrated into the chromosomes of *Erwinia chrysanthemi , Pseudomonas fluorescens , Pseudomonas syringae , and Pseudomonas*

putida and many gram negative bacteria by the Tn7-based delivery system (**Fig. 5.2**) (Koch et al., 2001, Lambersten et al., 2004,Hee et al.,2008). This gene delivery system developed was applied to other organisms, such as *Burkholderia* spp. and *Proteus mirabilis*, which were determined to have multiple glmS-linked attTn7 sites and secondary, non-*glmS*-linked attTn7 site, respectively. Thus mini Tn7 transposition is a powerful technique for the integration or excision of a gene of interest at a single-copy on the chromosomal level, which makes it possible to conduct a variety of experiments, including insertional random mutagenesis, gene expression analysis, protein functional studies, or the gene-tagging of bacteria in living organisms.

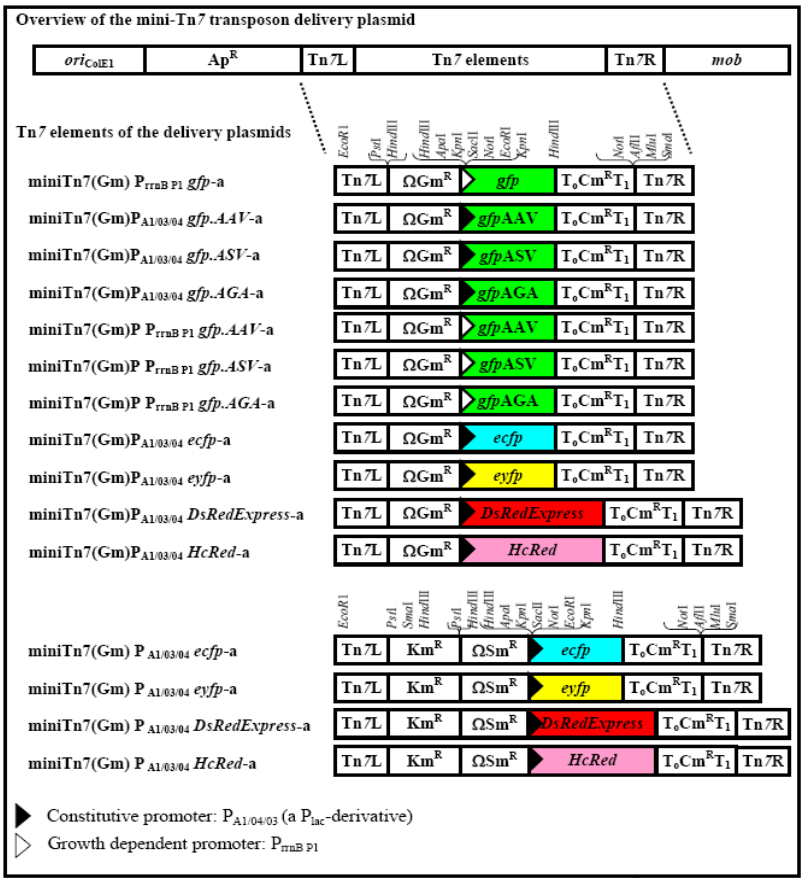

Figure 5.2: **The Tn7 delivery plasmids.** The resistance genes are: gentamicin resistance (Gm^R) provided by aacC1 encoding acetyltransferase-3-1(Cm^R) provided by cat encoding chloramphenicol-acetyl-transferase, kanamycin resistance (Km^R) provided by neomycin phosphotransferase (nptII), all plasmids are based on pUC19 and carry resistance to ampicillin. Ω shows that the resistance gene is flanked by transcription and

translation terminators (Fellay et al., 1987). All constructs contain the ribosomal binding site, RBSII, in front of the fluorescent gene and terminator T_0 and T_1 flanking *cat*. (Koch et al., 2001)

Table 5.1: Literature overview of bacteria tested for insertion of Tn7 (Lambertsen, 2004 supplementary data)

Bacterium	Specific insertion	Test
Caulobacter crescentus	Yes	Southern
Desulfovibrio desulfuricans G20	Yes	Southern
Escherichia coli	Yes	Southern
Escherichia coli BE6	-	-
Erwinia chrysanthemi EC16	Yes	Southern
Klebsiella pneumonia	-	-
Methylophilus methylotrophus	-	-
P. fluorescens CHA0	Yes	Southern
Pseudomonas DS-S73	Yes	-
Pseudomonas S108	Yes	-
Pseudomonas aeruginosa PAC and PAO1161	Yes	Southern
Pseudomonas aeruginosa PAO1	Yes	Southern
Pseudomonas aeruginosa PAOE1A	-	-
Pseudomonas corrugate strain 2140	-	Southern
Pseudomonas fluorescens 701E1	Yes	Southern
Pseudomonas fluorescens DR54	Yes	PCR
Pseudomonas putida KT2440	Yes	PCR, Southern
Pseudomonas putida GR12-*2*	Yes	Southern
Pseudomonas putida R20	No	Southern
Pseudomonas putida PH6	No	Southern
Pseudomonas solanacearum	Yes	Southern
Pseudomonas syringae pv. glycinea PsgR4	Yes	Southern
Rhodospirillum rubum	-	Southern
Salmonella thyphimurium	-	-
Serratia marcescens	-	-
Sphingomonas yanoikuyae B1	Yes	Southern
Xanthomonas campestris pv. *campestris* NC PPB 1145	Yes	Southern

The present study describes the genomic integration of *E. coli* NADH insensitive *cs* Y145F and *S. tphimurium* sodium citrate transporter *citC* gene into fluorescent

pseudomonads genome and compares its effect to plasmid based expression on glucose catabolism and citric acid secretion. All the experiments were carried out in buffered Tris HCl (pH8.2) minimal medium in phosphate deficient condition mimicking the soil environment.

5.2 WORK PLAN

The experimental plan of work includes the following-

5.2.1 Bacterial strains used in the study

Table 5.2: Wild type and recombinant strains used in the study.

Bacterial strains/Plasmids	Characteristics	Source/Reference
***E. coli* DH5α**	F-φ80Δ*lac*ZΔM15Δ(*lac*ZYA-*arg*F) U169 *rec*A1 *end*A1 *hsd*R17 (rk-, mk+) *pho*A *sup*E44 λ-*thi*-1 *gyr*A96 *rel*A1	Sambrook and Russell, 2001
SM101 AKN68	*E. coli* SM101::λpir helper plasmid pUXBF13 providing the Tn7 transposes proteins Amp^r	A generous gift of Prof. Soren Molin,DTU, Denmark
JM101 AKN69	*E. coli* JM101 containing miniTn7(Gm) $P_{A1/04/03}$-eyfp plasmid Gm^r, Cm^r	A generous gift of Prof. Soren Molin, DTU, Denmark
***E. coli* DH5α pYCInt**	*E. coli* DH5α containg *yc* operon in mini Tn7 delivery plasmid AKN69 under p*lac*	This Chapter
***P. fluorescens* PfO-1**	Wild type strain	A generous gift of Prof. Mark Sylvi, USA
***P. fluorescens* Pf-5**	Wild type strain	A generous gift of Prof. L. Thomashow USA

***P. fluorescens* CHAO-1**	Wild type strain	
***P. fluorescens* ATCC13525**	Wild type strain	ATCC
***P. fluorescens* P109**	Wild type strain	A generous gift of Prof. B. N. Johri
***P. fluorescens* Fp315**	Wild type strain	A generous gift of Prof. B. N. Johri
***Pf* (pGm)**	*P. fluorescens* strain with pUCPM18; Gm^r	Ch3
Pf(pYC)	*P. fluorescens* strains with pYC; Gm^r	Ch4
***Pf* (Int)**	*P. fluorescens* strains genomic integrant, Gm^r	This Chapter

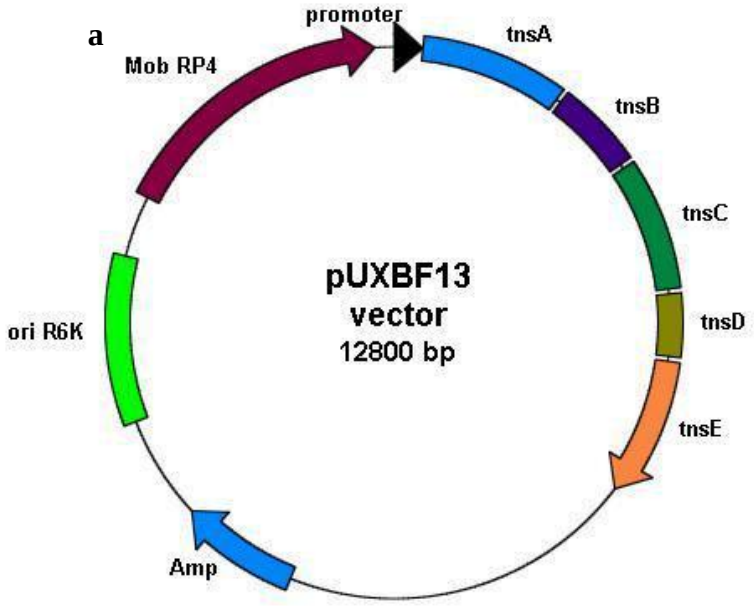

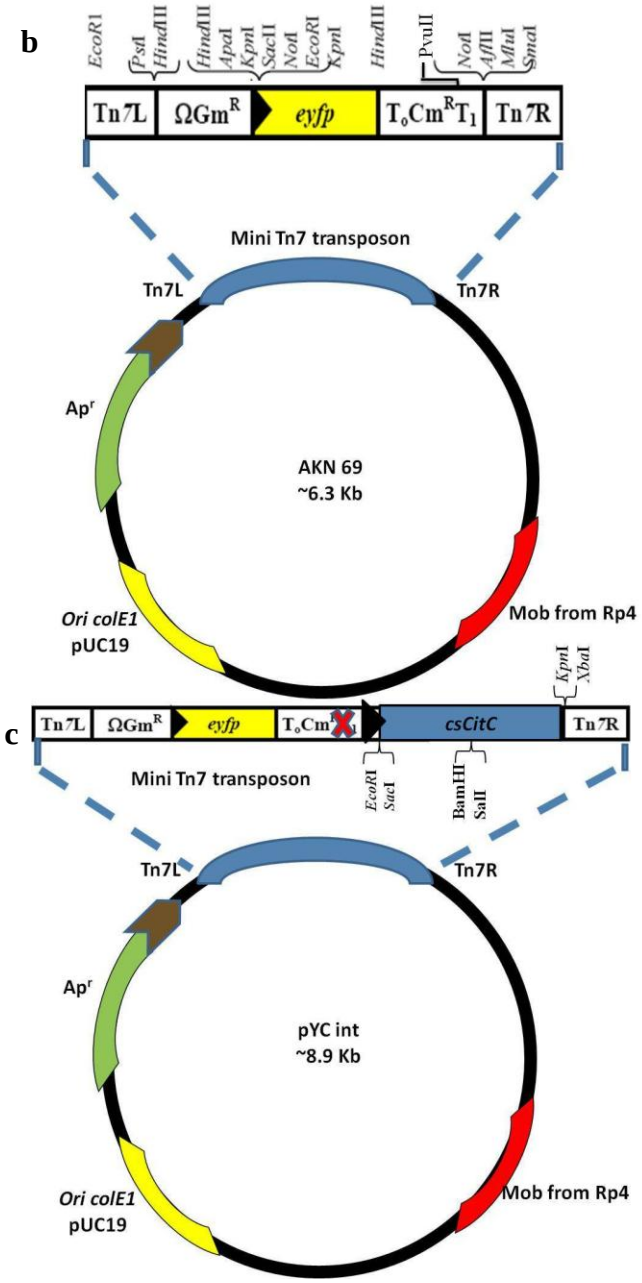

Figure 5.3: Vector map of mini tn7 helper plasmid (a), mini tn7 delivery plasmid (b), and mini tn7 delivery plamsid with yc gene cloned along with p*lac* (c).

5.2.2 Recombinant plasmid construction and genomic integration

The strategy for construction of mini Tn7 delivery plasmid containing *yc* gene under p*lac* and insertion into *P. fluorescens* genome is depicted in **Fig. 5.4.**

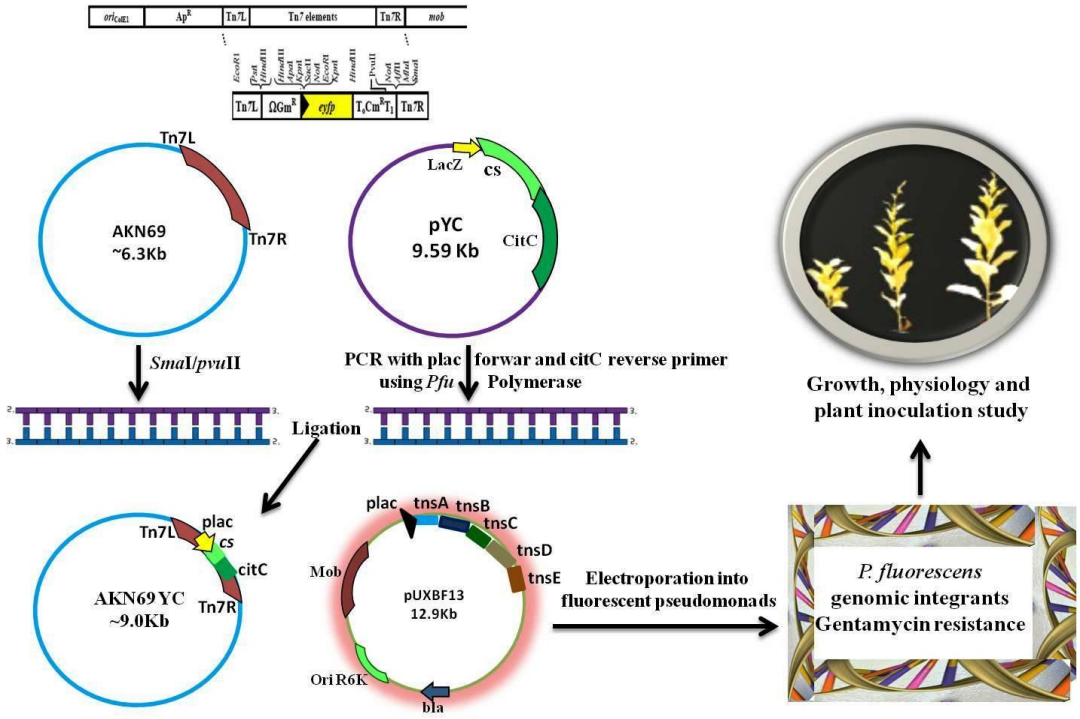

Figure 5.4: Strategy for cloning and genomic integration.

yc operon along with p*lac* is amplified using p*lac* forward primer and *citC* gene reverse primer from pYC plasmid using high fidelity *taq* polymerase to obtain blunt end product. Cloning of isolated *citC* gene was carried out in AKN 69 t vector using SmaI site after disruption of chloramphenicol resistance gene using PvuII enzyme. The clone was confirmed by double digestion with *EcoR*I-*Xba*I restriction site. Functional confirmation of the recombinant plasmid was done by growing *E. coli* DH5 containing pYCint on Koser citrate broth containing citric acid as a sole carbon source supplemented with 100mg/ml thymine and 0.1mM IPTG.

The mini Tn7 recombinant plasmid along with pUXBF13 containing the transposase genes is delivered into *P. fluorescens* strains by the electroporation method as described by Choi et al. (2006). For preparation of electrocompetent cell, 6 ml culture of *P. fluorescens* strains were grown overnight in LB medium at 30ºC with shaking (225rpm) in a sterile 25 ml conical flask. The whole culture is then evenly distributed into four sterile micro centrifuge tubes and centrifuged at 16,000g and room temperature for 2 min, using a sterile 1-ml disposable pipette tip, the supernatant were dispensed and discarded into a biological waste container. Each cell pellet is suspended in 1 ml of 300 mM sucrose (kept at room temperature) and centrifuged as mentioned earlier. Cultures were pipetted carefully to avoid aerosolization of pathogenic bacteria and/or contamination of the pipette. Plugged pipette tips were used to avoid contamination of the pipette. The sucrose solution was stored at room temperature because cold sucrose resulted in greatly reduced transformation competency. The supernatant was discarded and each cell pellet was suspended in 1 ml of 300 mM sucrose and centrifuged. Finally, the four cell pellets were resuspended in a combined volume of 200 µl of 300 mM sucrose. This was sufficient for two electroporations. 100 µl of electrocompetent cells were transferred asceptically to a 2-mm gap-width electroporation cuvette. Using a 1–100 µl gel-loading tip, 50 ng each of mini-Tn7 element DNA (pYCInt and pUXBF13) were added and mixed by gentle stirring with the gel-loading pipette tip to avoid air bubbles. The volume of DNA ensured not to exceed 10 µl per 100 µl of electrocompetent cells to avoid arching during the electroshock. Electroporation was carried out using BioRad electroporator with the following settings: 25 µF, 200 Ω, 2.5 kV (the time constant should be < 5 ms). Immediately 1 ml of LB medium is added and incubated with shaking (225 r.p.m.) for 1 h at 37 ºC. 100 µl of the mixture plated on an LB+Gm30 plate) and the remaining cultures were transferred to a sterile microcentrifuge tube and centrifuged at 16,000g at room temperature for 2 min. The supernatant was discarded and pellet was resuspended in 200 µl of LB medium and plated on another LB+Gm30 plate. Plates were incubated at 37 ºC overnight or until colonies have grown. 4-6 colonies from each plate were regrown on LB medium containing gentamycin and the respective cultures were streaked on pseudomonas agar plate containing gentamycin.

Preliminary confirmations of the genomic integrants were done by monitoring the growth on gentamycin plate and fluorescens and finally confirmed by PCR with gene specific primer (**Table 5.3**)

Table 5.3: Primer pair used for the PCR test of genomic integrants.

Name of the primer	Sequence	Annealing site	Tm
Tn7-Gm	5'ATATCGACCCAAGTACCGCC	Nt 509 from the strat site of aaC1 gene	57.4
csR	**CG*GGATTC*C*GGATCC*G**TTAACGCTTGATATCGC	Cs gene reverse primer	59.6˚C, 46.2%

5.2.3 Effect of genomic integration on physiology, biochemical properties and overall glucose catabolism of fluorescent pseudomonads

P. fluorescens genomic integrants were subjected to physiological experiments involving growth and organic acid production profiles on Tris HCl (pH 8.0) rock phosphate minimal medium with 75 mM glucose as carbon source. The samples withdrawn at regular interval were analyzed for O.D.600nm, pH, and extracellular glucose. Stationary phase cultures harvested at the time of pH drop were subjected to organic acid estimation using HPLC (Section 2.7.3). The physiological parameters were calculated as in section. The effectiveness of the genomic integrants were compared with the wild type and plasmid bearing strains of fluorescent pseudomonads. The enzyme assays (CS, G-6-PDH, ICDH, PYC, ICL and GDH) were performed with cell free extracts of late log to stationary phase cultures as described in Section.

5.3 RESULTS

5.3.1 Construction of integration delivery plasmid containing NADH insensitive *cs* Y145F and *S. tphimurium citC* operon under *lac* promoter:

The plasmid pYCint containing NADH insensitive *cs* Y145F and *S. tphimurium citC* operon under *lac* promoter was constructed in the SmaI site of AKN69 vector as schematically represented (**Fig. 5.4**). The recombinant plasmid was confirmed by restriction enzyme digestion (**Fig. 5.5**) and PCR (**Fig. 5.6**).

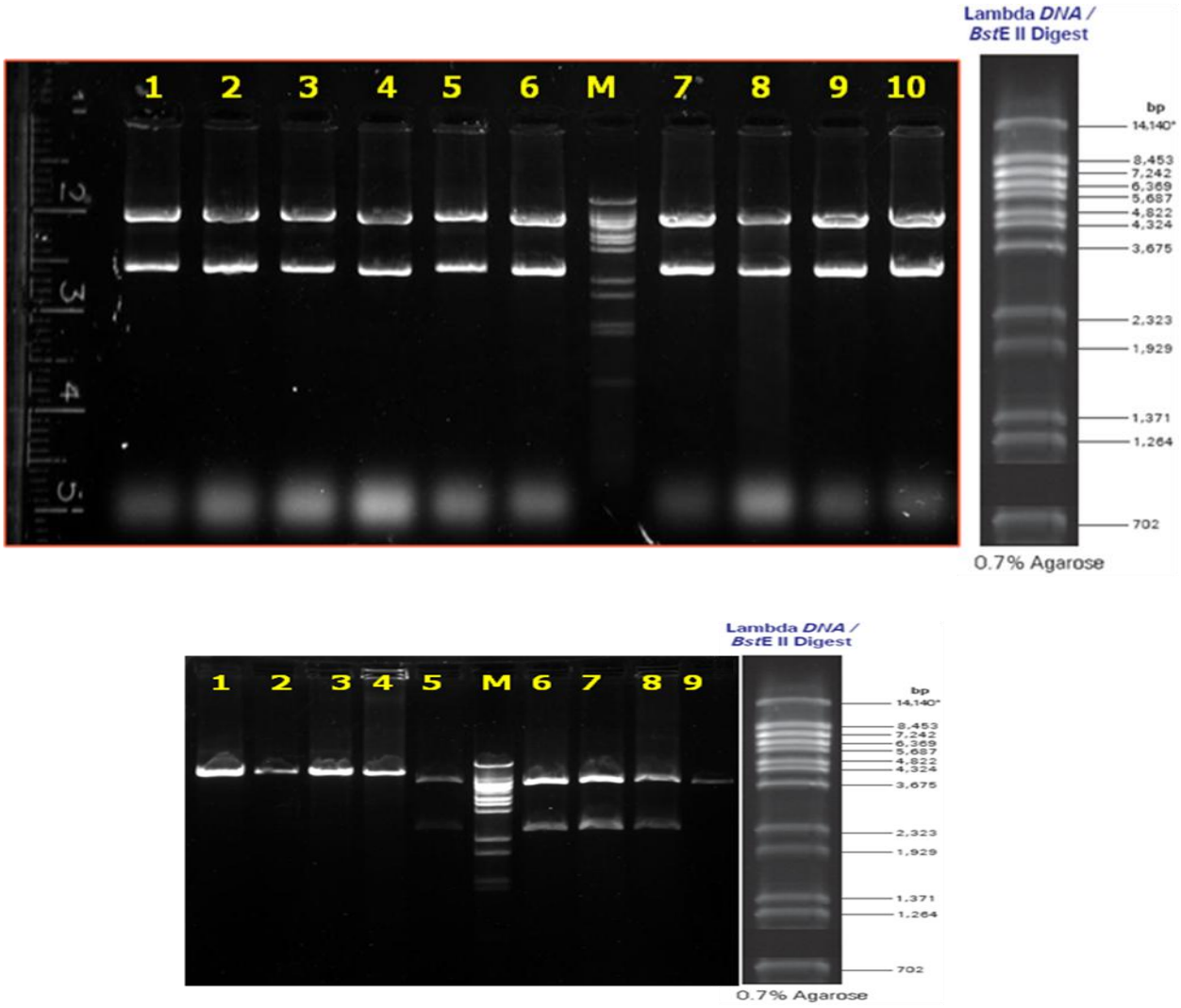

Figure 5.5: Restriction enzyme digestion pattern of pYCInt plasmid containing NADH insensitive Y145F and *S. tphimurium* sodium citrate transporter operon under *lac* promoter. (A) Lane 1-10: pYCInt plasmid

digested with EcoRI-XbaI (6.3Kb, 2.6kb); (B)Lane1-4: NotI digestion pattern of pYCInt plasmid (~8.9 Kb); Lane 6-9: pYCInt plasmid digested with EcoRI-XbaI (6.3Kb, 2.6kb).LaneM: MWM lambda DNA BstEII digest.

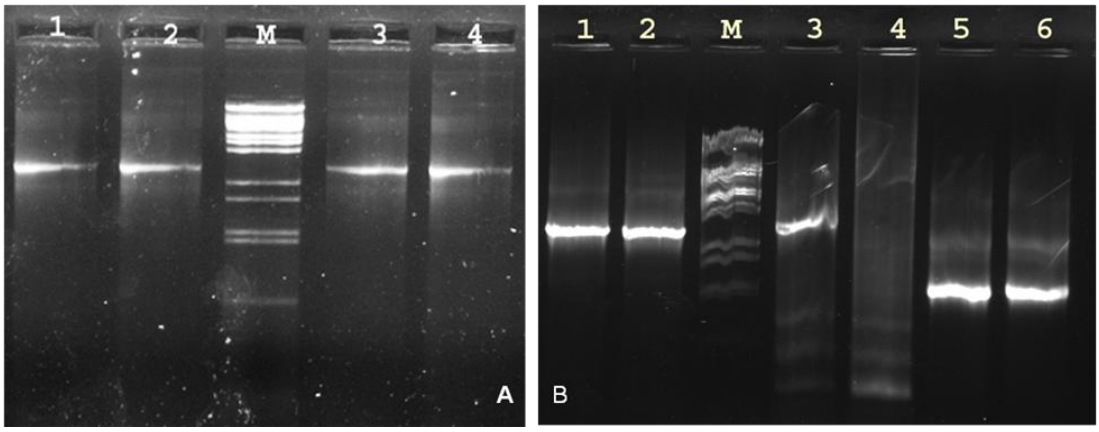

Figure 5.6: PCR amplification of p*lac yc* gene cloned in integration delivery plasmid AKN69. (A) lane 1-4:p*lac yc* amplicon (2.6Kb); (B) lane 1-5: p*lac yc* amplicon (2.6Kb).; lane5: cs gene amplicon (1.28Kb); Lane 6: citC gene amplicon (1.34Kb). LaneM: MWM lambda DNA BstEII digests.

5.3.2 Characterization of *lacYC* operon genomic integrants of *P. fluorescens* strains.

The integration delivery plasmid inserts p*lac yc* operon along with gentamycin resistance gene. Hence, when the *P. fluorescens* transformants were selected on pseudomonas agar plate containing gentamycin at 50 µg/ml, the integrants were able to grow and show fluorescence while the wild type pseudomonads failed to grow on gentamycin (**Fig. 5.7**). PCR of the genomic DNA using specific primer (**Table 5.3**) resulted in an amplicon of 2.8 kb confirming the genomic integration (**Fig. 5.8**).

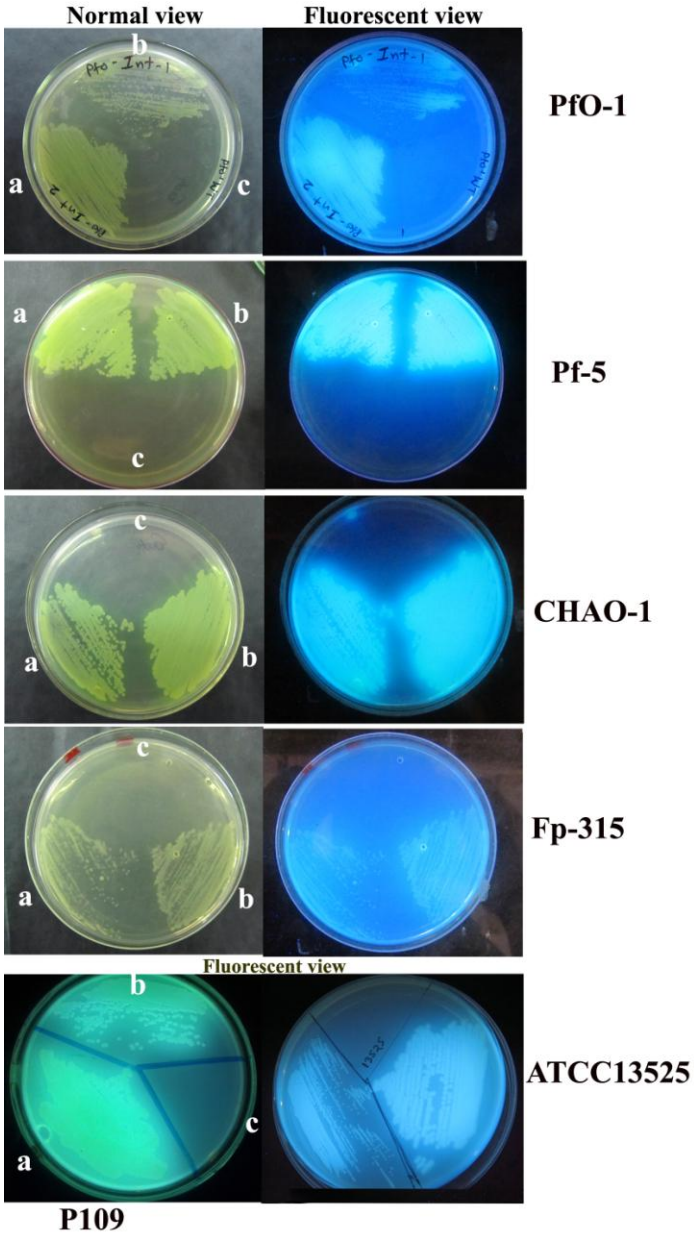

Figure 5.7: Natural fluorescence and antibiotic resistance of genomic Integrants of *P. fluorescens* PfO-1, *P. fluorescens* Pf-5, *P. fluorescens* CHAO-1, *P fluorescens* Fp315, *P. fluorescens* P109 and *P. fluorescens* ATCC13525. Pseudomonas agar plates containing ampicillin and gentamycin each at 50 µg/ml. (a) *P. fluorescens* pYC plasmid transformants (b) *P. fluorescens* genomic integrants; (c) *P. fluorescens* wild type.

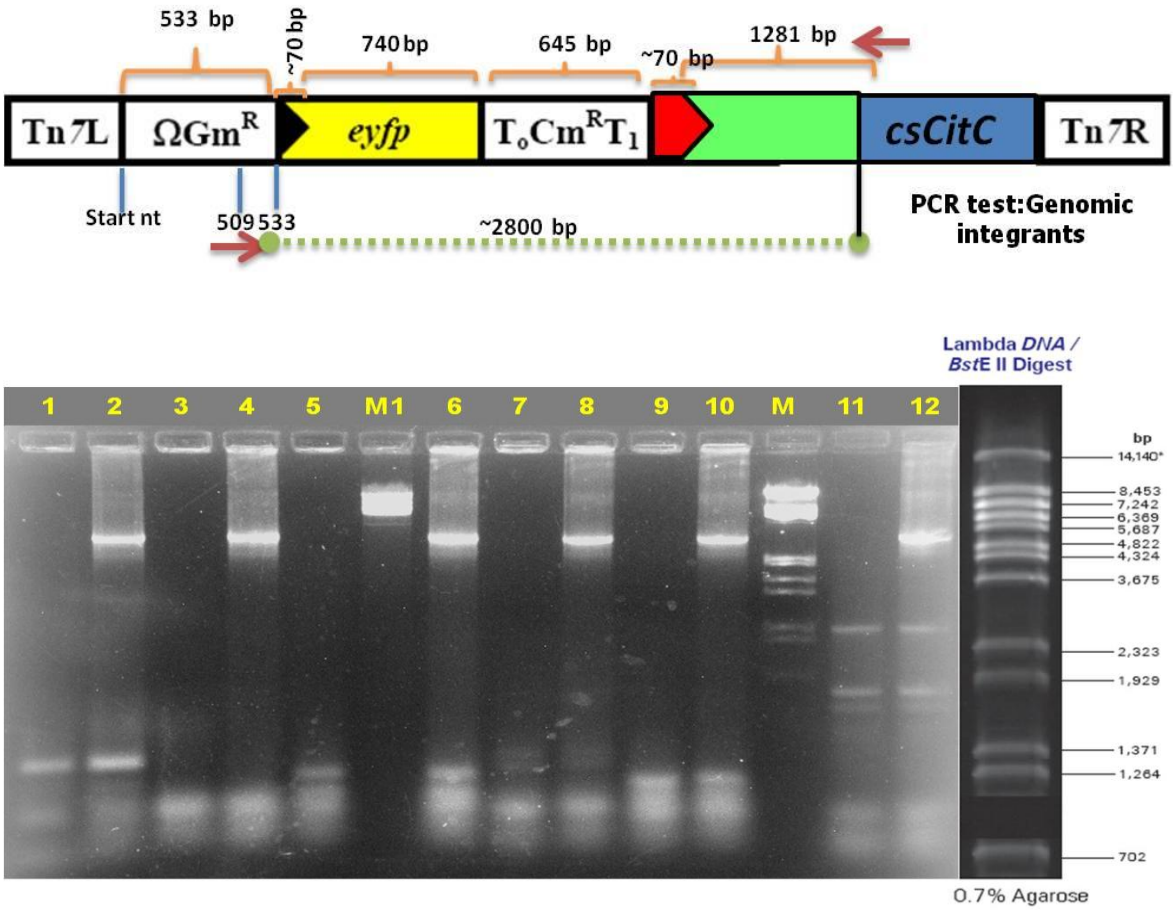

Figure 5.8: PCR test of genomic DNA isolated from *P. fluorescens* wild type and genomic integrants using Tn7-Gm (510 nt from the start site of Gm^r gene)and *cs* reverse primer (~2800 bp). Lane1: *P. fluorescens* PfO-1 WT, Lane2: *P. fluorescens* PfO-1 genomic integrant (..); Lane3: *P. fluorescens* Pf-5 WT; lane4; *P. fluorescens* Pf-5 genomic integrant; Lane 5: *P. fluorescens* CHAO-1 WT; Lane6: *P. fluorescens* CHAO-1 genomic integrant; lane 7: *P. fluorescens* ATCC13525 WT; lane8: *P. fluorescens* ATCC13525 genomic integrant; Lane 9: *P. fluorescens* P109 WT; lane10: *P. fluorescens* P109 genomic integrant; Lane11: *P. fluorescens* Fp315 WT; Lane12: *P. fluorescens* Fp315 genomic integrant. LaneM: MWM with Lambda DNA BstEII digests.

5.3.3 Physiological characterization of *P. fluorescens yc* operon genomic integrants.

The growth characteristics of *P. fluorescens yc* operon genomic integrants were determined upon grown under buffered-RP (TRP, 75mM Tris HCl pH 8.0) broth minimal medium containign75mM glucose (**Fig 5.9**). *P. fluorescens* Fp315 genomic integrants

showed an enhanced growth rate by 1.6 fold as compared to the plasmid transformants. Growth rate of *P. fluorescens* Pf-5 plasmid transformants drastically reduced (1.7 fold) as compared to the wild type culture and genomic integrants. But no growth difference was found with other strains. All strains acidified the medium within 72-96 hr of growth but genomic integrants of PfO-1 and Fp315 acidified the medium pH below 5 much faster within 48 hr.

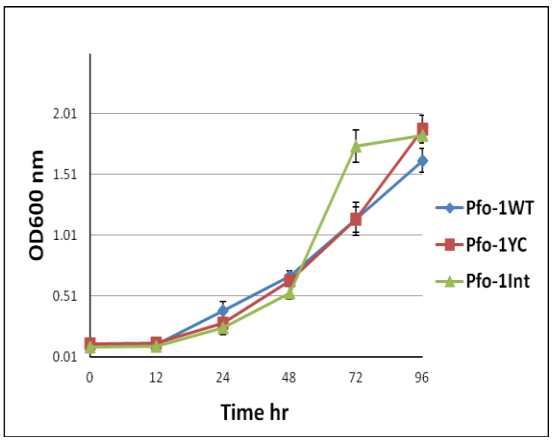

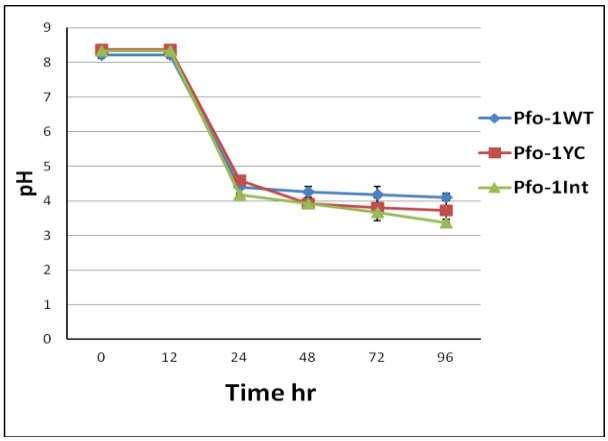

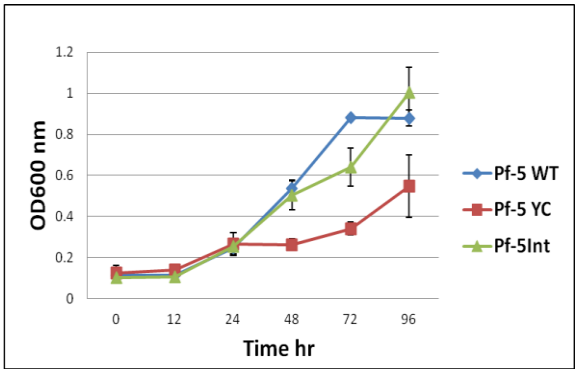

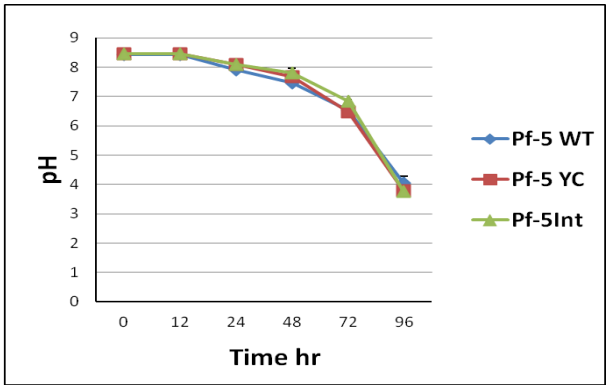

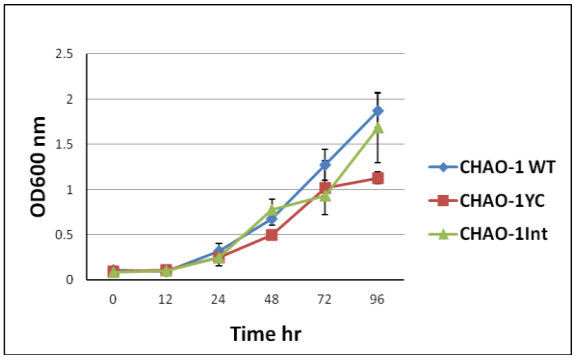

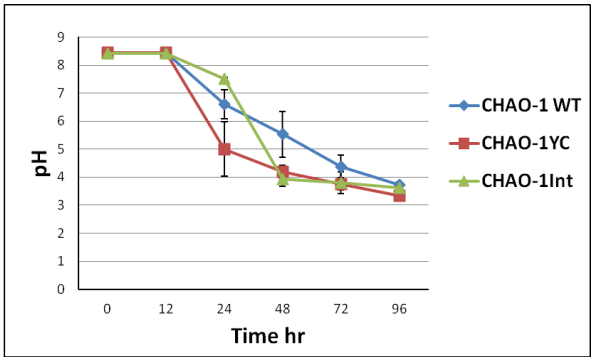

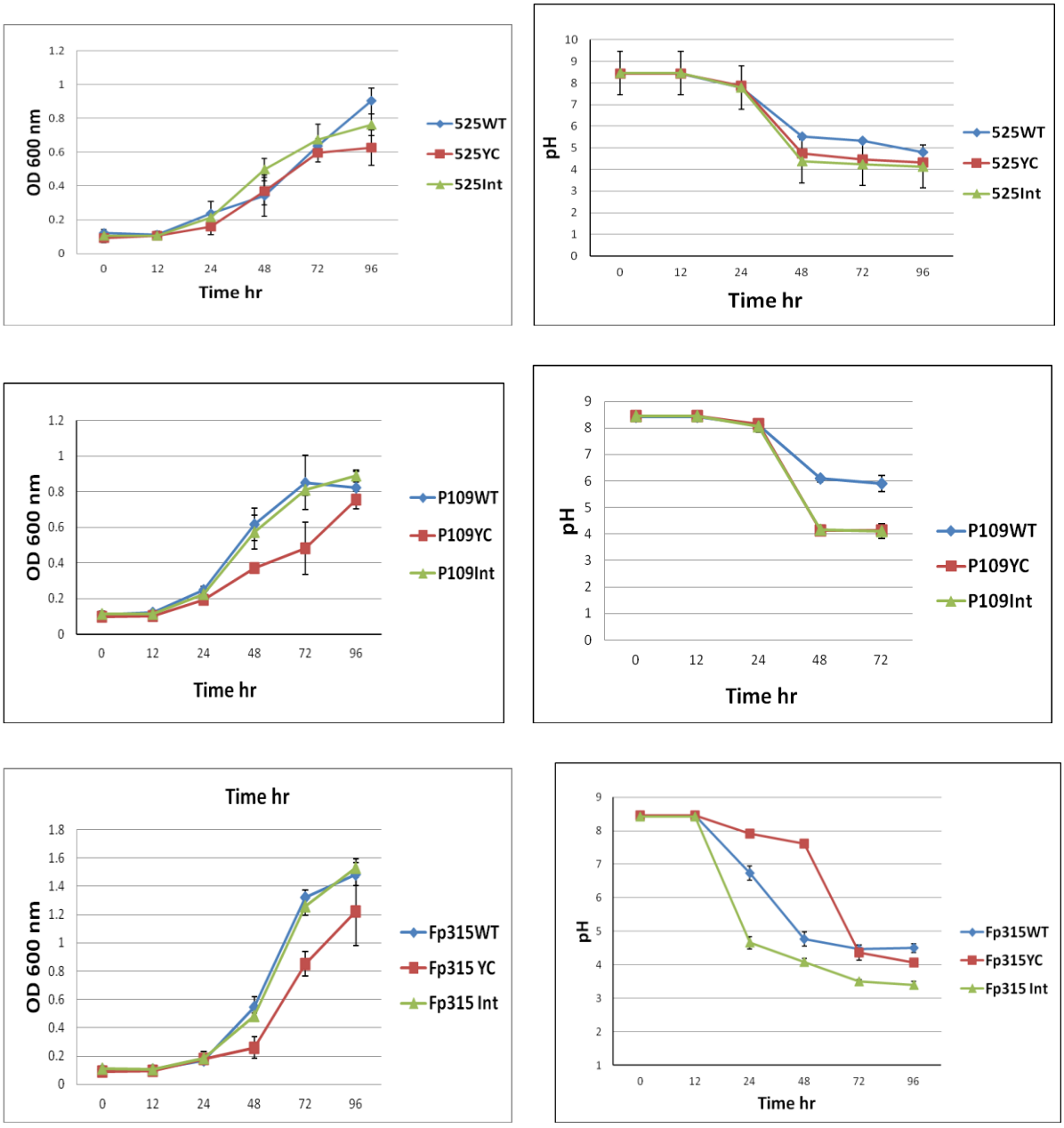

Figure 5.9: Growth profile and media acidification of genomic integrants and plasmid transformants of *fluorescent pseudomonads including* selected native isolates on TRP medium. The growth and media acidification were monitored on TRP medium with 75 mM tris HCl (pH 8.0), 75mM glucose and 1mg/ml RP. The values are plotted as Mean ± S.D. of 3 independent observations.

Both qualitative and quantitative changes in total glucose utilization ,glucose consumption and specific glucose utilization rate were monitored amongst the strains (**Table 5.4**) *P. fluorescens* CHAO-1genomic integrants showed an increase in total amount of glucose utilized by 1.36 fold and 1.25 fold as compared to the wild type and plasmid transformant respectively , whereas . *P. fluorescens* P109 genomic integrants showed a 1.3 fold decrease in the total glucose utilization.

Total glucose utilization remain unaltered in *P. fluorescens* PfO-1, Pf-5 and ATCC 13525.The amount of glucose consumed decreased by 1.57 fold and 1.3 fold as compared to wild type and Pf(pYC) in *P. fluorescens* PfO-1 genomic integrant, respectively. Similar decrease was observed in *P. fluorescens* Pf-5, ATCC13525 and Fp315 strains by 2.5, 1.26 and 2.26 respectively as compared to wild type strain. On the other hand, an increased glucose consumption by 1.26 fold and 3 fold were observed in ATCC13525 and P109 genomic integrant, respectively, as compared to wild type strain. Glucose consumption remain unaltered in *P. fluorescens* CHAO-1 genomic integrant. The biomass yield and specific glucose utilization rate were remained unaltered in *P. fluorescens* CHAO-1 and ATCC13525 genomic integrants. Biomass yield was increased by 3.5, 2.2, 2.1 and 1.7 fold in *P. fluorescens* PfO-1, Pf-5, P109 and Fp315, respectively as compared to wild type control. *P. fluorescens* Fp315 genomic integrant showed a decrease in specific glucose utilization rate by 1.44 fold whereas 1.96 fold increase in specific glucose utilization rate were monitored in Pf-5 as compared to the wild type control (**Table 5.4**).

Parameter	PfO-1			Pf-5			CHAO-1			ATCC 13525			P109			Fp315		
	WT	YC	Int	WT	YC	Int	WT	YC	Int	WT	YC	Int	WT	YC	Int	WT	YC	Int
μ(h-1)	0.24±0.035	0.29± 0.05	0.31± 0.02	0.27± 0.04	0.16± 0.02 †	0.22± 0.04	0.28± .03	0.23± 0.02	0.3± 0.03	0.21± 0.05	0.19± 0.03	0.17± 0.02	0.26± 0.04	0.21± 0.02	0.22± 0.02	0.34± 0.04	0.3± 0.03	0.47±0.05 ‡
TGD (mM)	54.68±6.59	56.89± 3.3	56.06± 6.68	70.9± 3.42	67.15± 4.3	61.6± 5.05	47.2± 3.65	51.06± 3.79	64.0± 5.55† ‡	49.3± 4.23	44.2± 4.34	39.13± 5.2	70.2± 4.4	45.75± 3.78†† †	52.56± 4.03††	62.14 ±4.35	50.66± 3.76†	70.27±3.7 ‡‡
GC (mM)	30.6±2.91	25.16± 2.35	19.2± 2.21‡‡	55.8± 4.2	26.32± 3.6†††	22.38± 3.16 †††	11.5± 2.17	14.52± 2.53	13.5± 3.05	43.9± 3.9	34.7± 3.27†	34.33± 2.89†	6.68± 1.45	32.21± 3.61†† †	20.21± 3.31†† ‡‡	34.01 ±3.87	15.16± 3.13††	17.83±3.3 ††
BMY(g/g)	0.075±0.00 6	0.17± 0.025 ††	0.26± 0.016 †††‡‡	0.06± 0.01	0.1± 0.02	0.13± 0.02†	0.16± 0.01	0.19± 0.01	0.21± 0.02†	0.07± 0.02	0.11± 0.01	0.079± 0.01	0.11± 0.01	0.19± 0.02 †††	0.23± 0.005† ††	0.21± 0.01	0.31± 0.01 †††	0.36±0.01 †††‡‡
QGlc (g/g/hr)	1.79±0.12	2.51± 0.41	1.98± 0.45	4.11± 0.23	7.23± 0.37 †††	8.08± 0.27†† †	3.19± 0.23	4.52± 0.39†	3.88± 0.49	2.67± 0.37	1.23± 0.21† †	1.83± 0.24†	1.25± 0.06	2.75± 0.26 †††	1.62± 0.23 ‡‡	3.17± 0.35	6.53± 0.43 †††	4.58±0.34 †‡‡

Table 5.4: Physiological variables from *P. fluorescens* transformant strains grown on75 mM glucose in TRP minimal medium. Growth rate (μ), Biomass yield (BMY) and specific glucose utilization rate (QGlc) were estimated from mid log phase cultures and total glucose depleted (TGD) and glucose consumption (GC) were determined at the time of pH drop (96 hrs). The values are depicted as Mean ± S.E.M of 4 (N=4) independent observations. †comparison of parameters with vector control Gm, ‡ comparison of parameters between pYC plasmid transformants and genomic integrants of fluorescent pseudomonads. †††,‡‡‡,P<0.001; ††,‡‡##P<0.01; †,‡,#P<0.05.

5.3.4 Effect of *yc* operon genomic integration on citric acid biosynthesis and secretion in fluorescent pseudomonads.

On TRP medium, in presence of 75 mM glucose the organic acid identified were citric acid and gluconic acid. In all *P. fluorescens* strains CHAO-1, ATCC13525 and Fp315 strains, intracellular citrate level by 4.6, 3.16 and 4.45 fold, respectively, as compared to the control strain (**Fig. 5.10**). However, the intracellular citrate levels were found to be similar in both genomic integrant and plasmid bearing strains. The citrate synthase activity correlated with the intracellular citrate levels. *P. fluorescens* Pf-5(Int) and P109(Int) showed a similar increase in intracellular citrate level by 3.5 and 3.27 fold respectively as compared to the control. Exception of this effect was Pfo-1(Int), in which the intracellular citrate level is 1.3 fold less as compared to Pfo-1(pYC). This data when compared with the respective plasmid bearing strain showed a significant reduction in citrate level by 1.27 and 1.5 fold, respectively. An enhancement of extracellular citrate levels in were achieved in both plasmid bearing and genomic integrants of *P. fluorescens* strains when compared to their respective control *Pf* (pGm) strain (**Fig. 5.11**; **Table 5.5**)

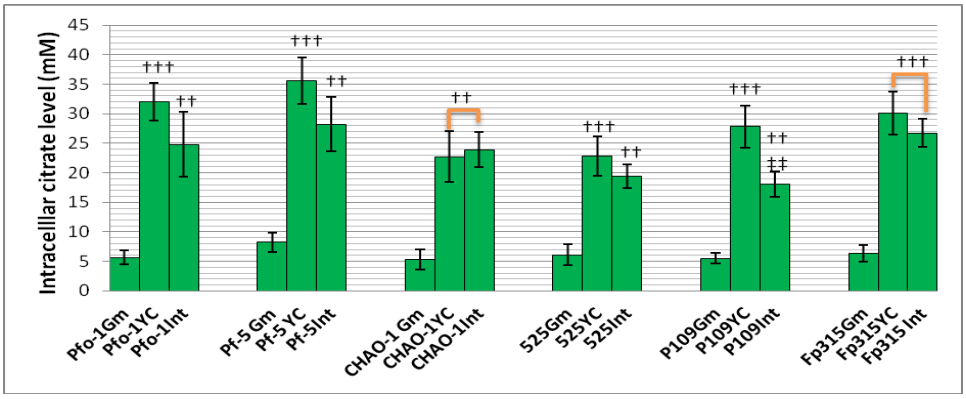

Figure 5.10 : Intracellular citric acid levels in *P. fluorescens* strains p*lac yc* genomic integrants. Citric acid levels were estimated from stationary phase cultures grown on 75 mM Tris HCl (pH8.0) rock phosphate (TRP) medium with 75 mM glucose . Results are expressed as Mean ±S.E.M of 3 independent observations. †comparison of parameters with vector control Gm, ‡ comparison of parameters between pYC plasmid transformants and genomic integrants of fluorescent pseudomonads. †††, ‡‡‡, P<0.001; ††, ‡‡P<0.01; †, ‡,P<0.05.

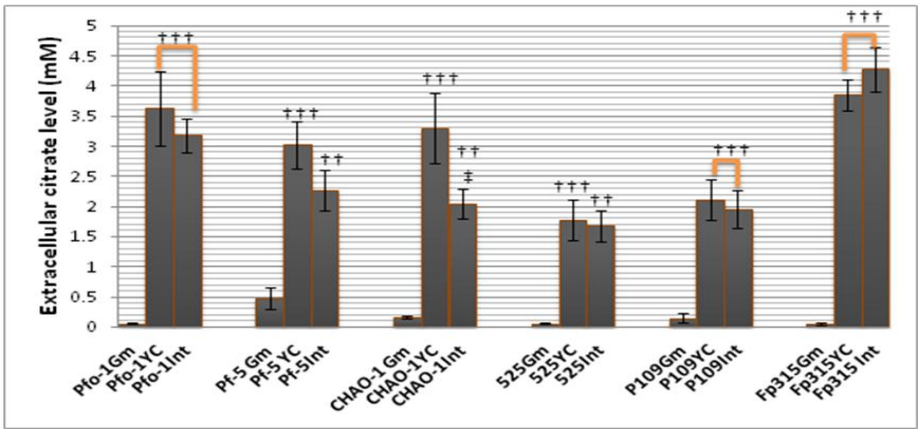

Figure 5.11 : Extracellular citric acid levels in *P. fluorescens* strains p*lac yc* genomic integrants. Citric acid levels were estimated from stationary phase cultures grown on 75 mM Tris HCl (pH8.0) rock phosphate (TRP) medium with 75 mM glucose . Results are expressed as Mean ±S.E.M of 3 independent observations. †comparison of parameters with vector control Gm, ‡ comparison of parameters between pYC plasmid transformants and genomic integrants of fluorescent pseudomonads. †††, ‡‡‡, P<0.001; ††, ‡‡P<0.01; †, ‡, P<0.05

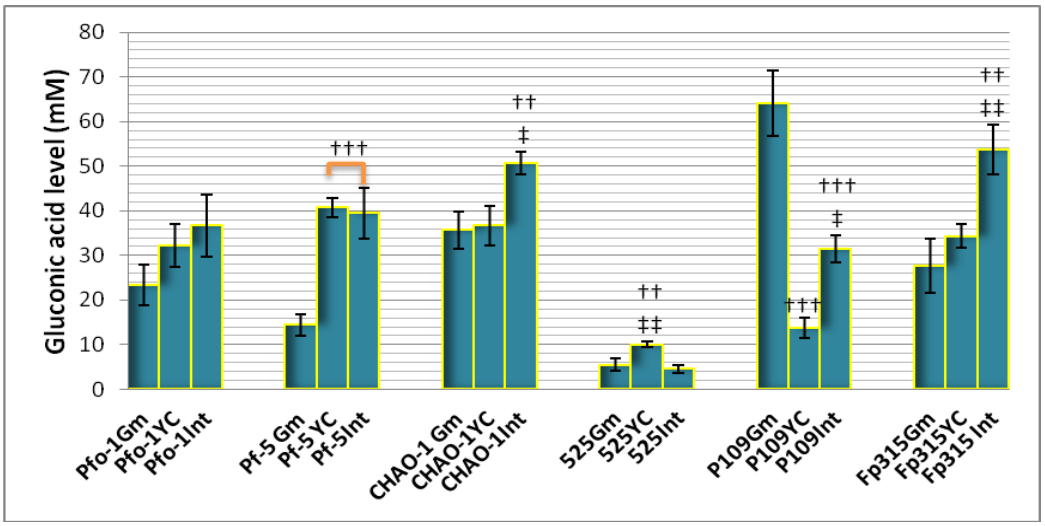

Figure 5.12 : Gluconic acid levels in *P. fluorescens* strains *yc* operon genomic integrants. Gluconic acid levels were estimated from stationary phase cultures grown on 75 mM Tris HCl (pH8.0) rock phosphate (TRP) medium with 75 mM glucose . Results are expressed as Mean ±S.E.M of 3 independent observations. †comparison of parameters with vector control Gm, ‡ comparison of parameters between pYC plasmid transformants and genomic integrants of fluorescent pseudomonads. †††,‡‡‡,P<0.001; ††,‡‡P<0.01; †,‡,P<0.05

Table 5.5: Extracellular citrate levels in *P. fluorescens* plasmid bearing strains and genomic integrants of *yc* operon.

P. fluorescens strains	Extracellular citrate level (mM)	Fold increase
PfO-1 (pYC)	3.63±0.62	60
PfO-1(Int)	**3.18±0.27**	**53**
Pf-5(pYC)	3.02±0.39	6.4
Pf-5 (Int)	2.26±0.33	4.8
CHAO-1 (pYC)	3.3±0.57	20.6
CHAO-1 (Int)	2.05±0.24	12.8
ATCC13525 (pYC)	1.77±0.34	29.5
ATCC13525 (Int)	1.67±0.26	27.8
P109 (pYC)	2.12±0.35	14.1
P109 (Int)	1.95±0.32	13.0
Fp315 (pYC)	3.86±0.26	77.2
Fp315 (Int)	**4.27±0.27**	**80.5**

The values are represented as Mean ±S.E.M of 3 independent observations. The fold increase is calculated in comparison to the extracellular citrate level of *Pf* (pGm) as a control.

The gluconic acid level and GDH activity showed positive correlation amongst the strains (**Table 5.6, Fig. 5.12).**

Table 5.6: Comparison of GDH activity and gluconic acid levels of *P. fluorescens* plasmid bearing strains and genomic integrants of *yc* operon.

***P. fluorescens* strains**	**GDH activity nmole/min/mg protein**	**Gluconic acid level (mM)**	**GDH activity fold increase/decrease**	**Gluconic acid level-fold increase/decrease**
PfO-1 (pYC)	54.4±5.4ns	32.2±4.79 ns	1.6	1.38
PfO-1(Int)	76.3±8.5 ††	36.7±6.95 ns	2.25	1.57
Pf-5(pYC)	91.3±4.4 ††	40.7±2.2 †††	1.69	2.83
Pf-5 (Int)	103.2±9.1††	39.5±5.65 †††	1.91	2.74
CHAO-1 (pYC)	23.5±3.7 ns	36.7±4.45 ns	UD	UD
CHAO-1 (Int)	73.07±10.6 †††	50.6±2.56 ††	2.7	1.42
ATCC13525 (pYC)	63.1±9.3 ns	10.04±0.67 ††	UD	1.8
ATCC13525 (Int)	43.5±6.6 ns	4.54±0.97 ns	1.4 decrease	1.2 decrease
P109 (pYC)	26.2±8.2 †††	13.8±2.33 †††	3.3 decrease	4.6 decrease
P109 (Int)	37.5±5.6 †††	31.4±3.01 †††	2.32 decrease	2.04 decrease
Fp315 (pYC)	73.8±9.1 †††	34.3±2.6 ns	2.11	1.27
Fp315 (Int)	79.2±8.3 †††	53.8±5.5 ††	2.26	1.99

The values are represented as Mean ±S.E.M of 3 independent observations. The fold increase is calculated in comparison to the extracellular citrate level of *Pf* (pGm) as a control. UD signifies undetectable, †comparison with *Pf* (pGm). †††p<0.001, †† p<0.01, † p<0.05, ns p>0.05.

5.3.5 Alterations in G-6-PDH, CS, ICDH, ICL, PYC, and GDH activities

The effect of genomic integration of p*lac yc* gene was also monitored at the level changes of key enzymes involved in periplasmic direct oxidation and intracellular phosphorylative pathways of glucose catabolism along with PYC, participating in anaplerotic reactions of *P. fluorescens* in order to correlate the alterations in physiological variables and organic acid profile. Significant variations were observed amongst the different strains (**Fig. 5.13**). All genomic integrants showed no alteration in ICDH and ICL activities with an exception of Pf-5 (pYC) and Pf-5 (Int) which showed an increase in ICDH activity by 1.7 fold and ICL activity by 2.7 fold, respectively, as compared to wild type strain. Interestingly, majority of genomic integrants of *yc* operon showed CS activity at par with the plasmid transformants. The CS activity is increased by 3.17 and 2.64 fold in *P. fluorescens* PfO-1 *yc* operon genomic integrant and plasmid bearing strains, respectively. Similarly, the increase was 4.73 and 4.6 fold in Pf-5, 4.1 and 2.7 fold in CHAO-1, 6 fold each in ATCC13525, 1.9 and 2.2 fold in P109 and 3.4 and 2.65 fold in Fp 315 as compared to the respective wild type controls. Remarkably, the CHAO-1 genomic integrant showed 1.5 fold higher CS activity than that of CHAO-1(pYC) strain. Both plasmid bearing strain and genomic integrants showed a decrease in G6PDH activity which indicates the diversion of glucose flux more towards the direct oxidation pathway.

50% reduction in G6PDH activity was observed in both PfO-1 (Int) and PfO-1(pYC) as compared to control. Similarly, the fold decrease in other strains are 11.7 and 8.9 fold in Pf-5, 1.94 and 5.6 fold in ATCC 13525, 1.8 and 1.6 fold in Fp315 were observed in this enzyme activity. Unlike the other strains, CHAO-1 showed a significant enhancement of G6PDH activity by 3 fold as compared to the vector control.

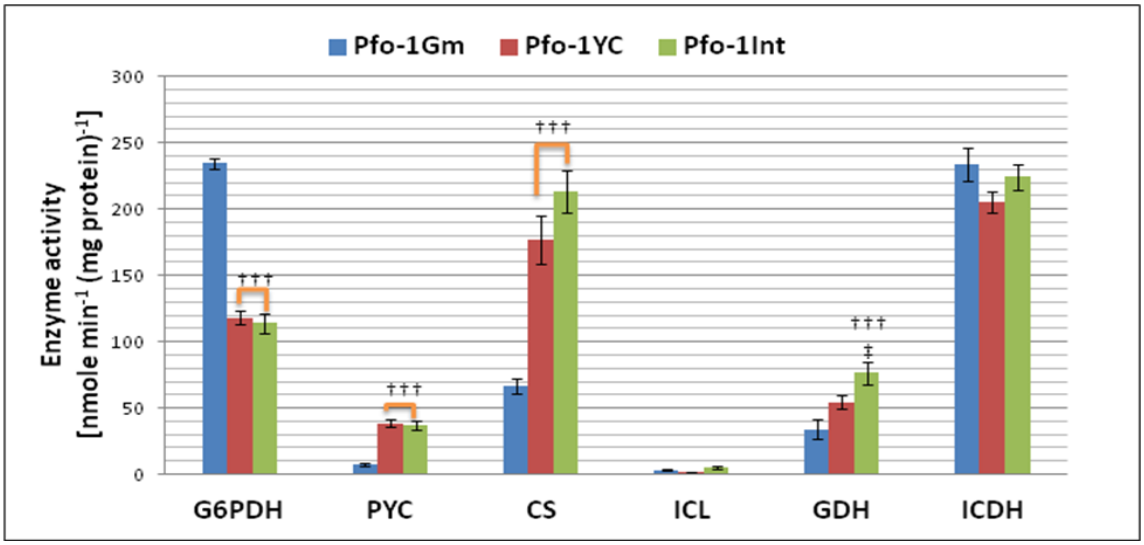

Figure 5.13: Activities of enzymes G-6-PDH, ICDH, ICL, PYC, and GDH in *P. fluorescens* PfO-1 *yc* operon genomic integrants. The activities have been estimated using vector control *Pf* (pGm), plasmid transformants of *Pf* (pYC) and *yc* operon genomic integrants. Cultures were grown on TRP minimal medium with 75 mM glucose. All the enzyme activities were estimated from mid log phase to stationary phase cultures and are represented in the units of nmoles/min/mg total protein. The values are depicted as Mean ± S.E.M of 3 (N=3) independent observations. †comparison of parameters with vector control Gm, ‡ comparison of parameters between pYC plasmid transformants and genomic integrants of fluorescent pseudomonads. †††,‡‡‡,P<0.001; ††,‡‡P<0.01; †,‡,P<0.05.

The percentage change in G6PDH activity were correlaed with Change in GDH activity. GDH activity increased by 2.6 fold in PfO-1(Int),1.9 fold Pf-5(Int),2.74 fold in CHAO-1(Int), 2.6 fold in Fp315(Int) as compared to the resoective control strain.A significicant decrease in GDH activity observed in ATCC13525(Int) (1.4 fold) and P109(Int) (2.76 fold) as compared to the control. PYC activity remain unaltered in *P. fluorescens* PF-5,CHAO-1, P109 and Fp315 genomic integrants whereas an increase by 5 fold and 2.8 fold in *P. fluorescens* PfO-1(Int) and ATCC13525(Int) respectively were observed compared to control (**Fig 5.14-5.18**).

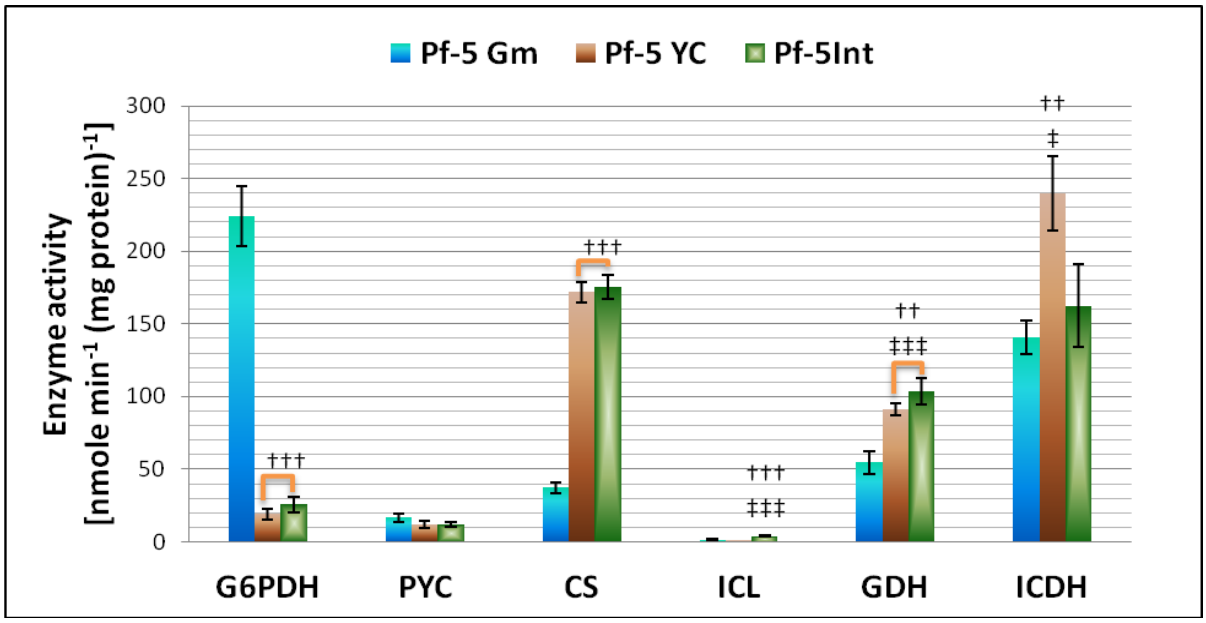

Figure 5.14: Activities of enzymes G-6-PDH, ICDH, ICL, PYC and GDH in *P. fluorescens* Pf-5 *yc* operon genomic integrants. The activities have been estimated using vector control *Pf* (pGm), plasmid transformants of *Pf* (pYC) and *yc* operon genomic integrants. Cultures were grown on TRP minimal medium with 75 mM glucose. All the enzyme activities were estimated from mid log phase to stationary phase cultures and are represented in the units of nmoles/min/mg total protein. The values are depicted as Mean ± S.E.M of 3 (N=3) independent observations. †comparison of parameters with vector control Gm, ‡ comparison of parameters between pYC plasmid transformants and genomic integrants of fluorescent pseudomonads. †††, ‡‡‡, P<0.001; ††, ‡‡P<0.01; †, ‡, P<0.05.

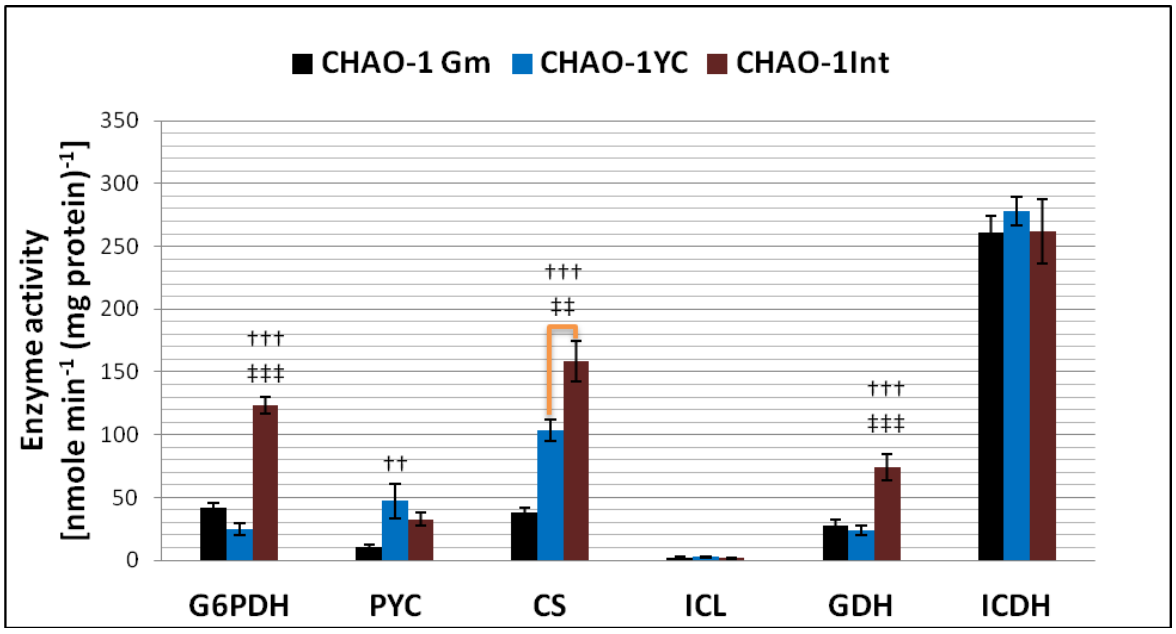

Figure 5.15: Activities of enzymes G-6-PDH, ICDH, ICL, PYC, and GDH in *P. fluorescens* CHAO-1 *yc* operon genomic integrants. The activities have been estimated using vector control *Pf* (pGm), plasmid transformants of *Pf* (pYC) and *yc* operon genomic integrants. Cultures were grown on TRP minimal medium with 75 mM glucose. All the enzyme activities were estimated from mid log phase to stationary phase cultures and are represented in the units of nmoles/min/mg total protein. The values are depicted as Mean ± S.E.M of 3 (N=3) independent observations. †comparison of parameters with vector control Gm, ‡ comparison of parameters between pYC plasmid transformants and genomic integrants of fluorescent pseudomonads. †††, ‡‡‡, P<0.001; ††, ‡‡P<0.01; †, ‡, P<0.05.

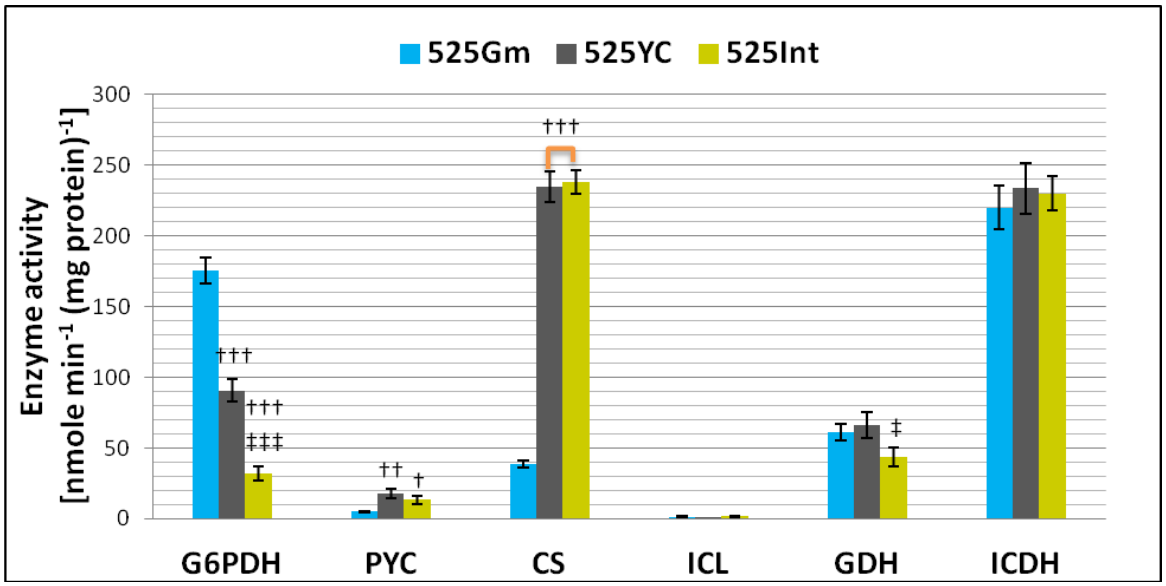

Figure 5.16: Activities of enzymes G-6-PDH, ICDH, ICL, PYC, and GDH in *P. fluorescens* ATCC 13525 *yc* operon genomic integrants. The activities have been estimated using vector control *Pf* (pGm), plasmid transformants of *Pf* (pYC) and *yc* operon genomic integrants. Cultures were grown on TRP minimal medium with 75 mM glucose. All the enzyme activities were estimated from mid log phase to stationary phase cultures and are represented in the units of nmoles/min/mg total protein. The values are depicted as Mean ± S.E.M of 3 (N=3) independent observations. †comparison of parameters with vector control Gm, ‡ comparison of parameters between pYC plasmid transformants and genomic integrants of fluorescent pseudomonads. †††, ‡‡‡, P<0.001; ††, ‡‡P<0.01; †,‡,P<0.05

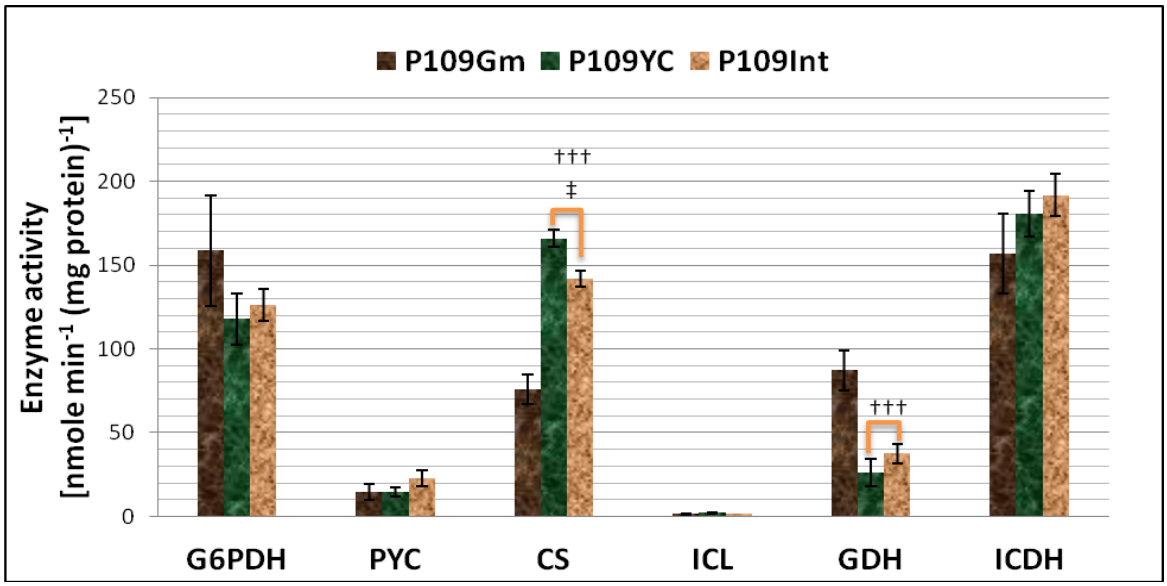

Figure 5.17: Activities of enzymes G-6-PDH, ICDH, ICL, PYC, and GDH in *P. fluorescens* P109 *yc* operon genomic integrants. The activities have been estimated using vector control *Pf* (pGm), plasmid transformants of *Pf* (pYC) and *yc* operon genomic integrants. Cultures were grown on TRP minimal medium with 75 mM glucose. All the enzyme activities were estimated from mid log phase to stationary phase cultures and are represented in the units of nmoles/min/mg total protein. The values are depicted as Mean ± S.E.M of 3 (N=3) independent observations. †comparison of parameters with vector control Gm, ‡ comparison of parameters between pYC plasmid transformants and genomic integrants of fluorescent pseudomonads. †††, ‡‡‡, P<0.001; ††, ‡‡P<0.01; †, ‡, P<0.05

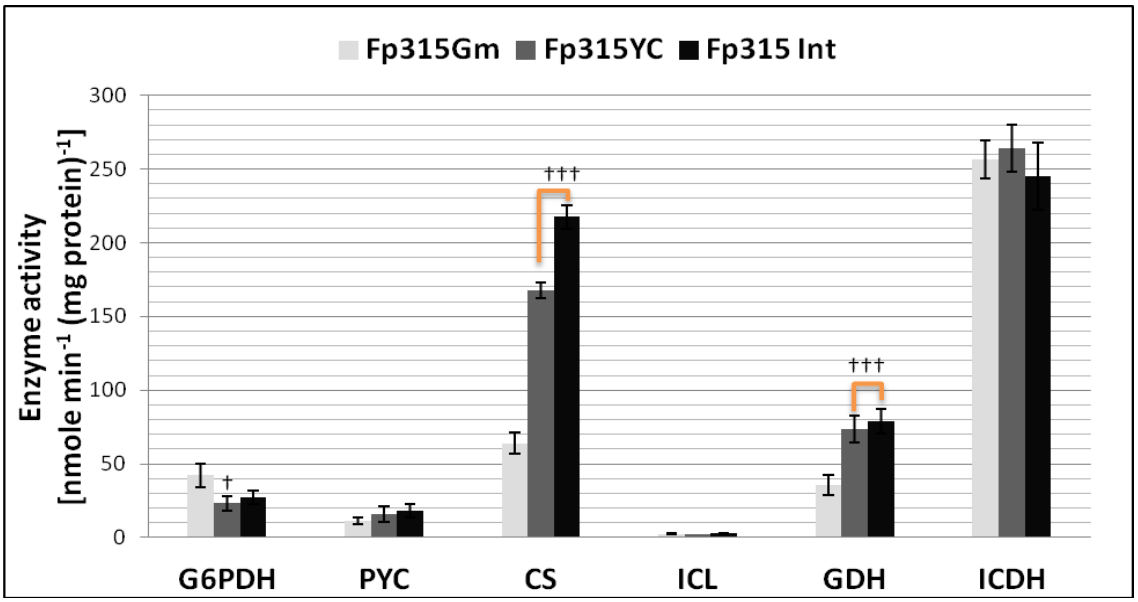

Figure 5.18: Activities of enzymes G-6-PDH, ICDH, ICL, PYC, and GDH in *P. fluorescens* Fp 315 *yc* operon genomic integrants. The activities have been estimated using vector control *Pf* (pGm), plasmid transformants of *Pf* (pYC) and *yc* operon genomic integrants. Cultures grown on TRP minimal medium with 75 mM glucose. All the enzyme activities were estimated from mid log phase to stationary phase cultures and are represented in the units of nmoles/min/mg total protein. The values are depicted as Mean ± S.E.M of 3 (N=3) independent observations. †comparison of parameters with vector control Gm, ‡ comparison of parameters between pYC plasmid transformants and genomic integrants of fluorescent pseudomonads. †††, ‡‡‡, P<0.001; ††, ‡‡P<0.01; †, ‡, P<0.05

5.4 Discusion

Genetic engineering of microorganisms involves the use of extra-chromosomal plasmid for heterologous expression of desired genes. Plasmid DNA is known to cause metabolic burden on the cell and alter its metabolism depending on the host organism, plasmid nature, and environmental conditions (Buch et al., 2010b; Sharma et al., 2011). Hence the genetic manipulations need be directed to the chromosomal integration as it would lead not only to increased stability but also decrease the metabolic load caused by the presence of the plasmids to nullify the pleotropic effects on the host metabolism. The present study demonstrates the effect of genomic integration of *E. coli* NADH insensitive *cs* Y145F gene and *S. tphimurium citC* gene on fluorescent pseudomonads. Previous chapters

describe the effect of heterologous overexpression on M9 minimal media. The study is an attempt to describe the following aspects on phosphate deficient buffered media: 1) Effect of genomic integration of heterologous gene on *P. fluorescens* physiology and glucose metabolism, (2) comparison of the effects of similar genetic modification between the plasmid transformants and genomic integrants of the same strain. (3) Comparison of the effect of similar genetic modification on different strains of PGPR fluorescent pseudomonads including natural isolates.

Remarkably, CS activity in genomic integrants remain unaltered as compared to the plasmid based expression with mid copy number plasmid pUCPM18 Gm. In addition, *P. fluorescens* CHAO1 genomic integrants showed 35% improvement on CS activity. Similar study carried out wherein gene encoding polyphosphate kinase (PPK) were overexpressed usind low copy mini F plasmid as well as multicopy pMB1 based plasmid (Carrier et al., 1998) in *E. coli* DH10B strain. PPK activity with low copy plasmid caused a 20 fold increase in polyphosphate (poly P) content in the early stage of growth whereas the enhancement was 80% in the stationary phase. The profile using multicopy plasmid depicted a different behavior of product content per cell versus culture time. PolyP increased dramatically within the first 3 h; however, the high product levels were not maintained in stationary phase. At 24 h, the polyP levels were the same as those obtained using a low-copy plasmid, dropping to one- fourth of that observed at 3 h (Jones et al., 2000)

Our result was in consistent with the above study. The whole study indicate that overexpression of gene using plasmid could alter the enegy status of the cell such that overall productivity may compromised. The extra resources of the cell is diverted toward recombinant protein synthesis from a multicopy plasmid can severely burden the host cell, as indicated by the slow growth rate of the multicopy plasmid-bearing strain. Genomic integrants thus play a role in overcoming these obstacles

Evaluating the effect of engineered genetic modifications on P-solubilization and plant growth promotion ability of fluorescent pseudomonads

CHAPTER 6

6 Chapter

6.1 INTRODUCTION

Phosphorus (P) is one of the major essential macronutrients limiting the plant growth and is applied to the soil as chemical phosphate fertilizer. Of the total soil P, only 1 to 5% is in a soluble and plant-available form. The overall P use efficiency following phosphate fertilizer application is low because of the rapid formation of insoluble complexes (Goldstein and Krishnaraj, 2007; Vassilev and Vassileva, 2003). Hence, during agricultural crop production frequent application of soluble forms of inorganic P cause leaching to the ground water and results in eutrophication of aquatic systems (Del Campillo et al., 1999; Kloepper 2009). To maintain the sustainability and soil fertility research efforts are concentrated to make use of less expensive, eco friendly sources of P nutrients such as rock phosphate (Whitelaw, 2000; Arcand 2006). Rock phosphate originates from igneous, sedimentary, metamorphic, and biogenic sources, with sedimentary being the most widespread (van Straaten, 2002). Microorganisms are an integral part of the soil P cycle and in particular, are effective in releasing P from rock phosphate (Richardson 2011). Therefore, phosphate solubilizing microorganisms with other plant growth promoting abilities have attracted the attention of agriculturists as soil inoculums to improve the plant growth and yield (Goldstein et al., 1999; Armarger, 2002; Fasim et al., 2002; Khan et al., 2007).

Plant growth promoting rhizobacteria (PGPR) are soil bacteria that can benefit plant growth by different mechanisms (Glick, 1995; Archana et al., 2012), and P-solubilization ability of the microorganisms is considered to be one of the most important traits. The use of PGPR as phosphate biofertilizer is advantageous in the sustainable agricultural practices. The mechanism of mineral phosphate solubilization by PGPR strains is associated with the release of low molecular weight organic acids mainly gluconic citric and oxalic acid which through their hydroxyl and carboxyl groups chelate the cations bound to phosphate, thereby converting it into soluble forms (Goldstein, 1995; Chen et al., 2006). However, P-solubilization is a complex phenomenon, which depends on many factors such as nutritional, physiological and growth conditions of the culture (Reyes et al., 1999).

PGPR benefit the plant growth directly by solubilization of insoluble phosphorous, nitrogen fixation, sequestering of iron by production of siderophores, producing metabolites such as auxins, cytokinins, gibberellins, lowering of ethylene concentration. The indirect growth promotion occurs via antibiotic production, synthesis of antifungal metabolites and cell wall lysing enzymes, competing for sites of root colonization, induced systemic resistance (Ahemad and Khan, 2011). The premier example of PGPR agents occur in many genera including *Actinoplanes, Agrobacterium, Alcaligens, Amorphosporangium, Arthrobacter, Azospirillum, Azotobacter, Bacillus, Burkholderia, Cellulomonas, Enterobacter, Erwinia, Flavobacterium, Gluconacetobacter, Microbacterium, Micromonospora, Pseudomonas, Rhizobia, Serratia, Streptomyces, Xanthomonas*, etc. One of the dominant genera among PGPR is *Pseudomonas* spp. *Pseudomonas sp*. is widespread bacteria in agricultural soils and has many traits that make them well-matched as PGPR; the most effective strains have been fluorescent *Pseudomonas* spp. The selective advantages of fluorescent pseudomonads as PGPR includes: (i) grow rapidly and utilize seed and root exudates; (ii) colonize and multiply in the rhizosphere and spermosphere environments and in the interior of the plant; (iii) produce a wide spectrum of bioactive metabolites (i.e., HCN, antimicrobials, siderophores, volatiles, proteases, phosphate solubilizing enzymes and growth promoting substances) and are responsible for the natural suppressiveness of some soils to soil borne pathogens; (iv) compete aggressively with other microorganisms; and (v) adapt to environmental stresses (Lugtenberg 2009; Aeron et al., 2011, Saharan et al., 2011; Akhtar et al., 2012).

The beneficial effects of PGPR seen under greenhouse conditions are often not repeatable under field conditions and the results in terms of crop growth and yields are highly variable (Gyaneshwar et al. 2002; Viveros –Martinez et al., 2010). Understanding the influence of environmental factors is widely recognized as a key to improve the level and reliability of PGPR (Dutta et al., 2010). Over-expression of genes involved in soil inorganic phosphate solubilization in natural PGPR can improve the capacity of microorganisms when used as inoculants (Bashan et al., 2000). Studies carried out so far have shown that following appropriate regulations, genetically modified microorganisms can be applied

safely in agriculture (Armarger, 2002; Morrissey et al., 2002). Chromosomal insertion of the genes is one of the tools to minimize the risks of using genetically modified microbes in agricultural filed.

The dissemination of bacteria in the field has remained marginal, with the exception of rhizobia and agrobacteria. Inoculation of plants with P-solubilizing microorganisms in controlled experiments improved the growth and P nutrition, especially under glasshouse conditions and in fewer cases in the field (Whitelaw, 2000; Gyaneshwar *et al*., 2002; Jakobsen *et al*., 2005; Khan *et al*., 2007; Rodríguez and Fraga, 2006; Harvey *et al*., 2009; Khan *et al*., 2010). But, the effectiveness of PSMs in the laboratory or controlled conditions may not be operable in soils (Richardson 2011). Plant growth promotion abilities of biofertilizers are strongly influenced by climate changes and are restrictive to certain cultivars, climate, and soil conditions (Figueiredo et al., 2010; Kern et al.2011). The phosphate solubilization can be accompanied by a number of activities such as production of plant stimulants, enzyme production, biocontrol activity and organic acid production (Vassilev et al. 2006; 2007a; 2007b; 2008; 2009b).

Efficacy of PGPR in field conditions is determined mainly by their survival in harsh environmental conditions including high concentrations of environmental contaminants, salts, extremes of pH and temperature, and competition with other organisms. Isolation of stress tolerant PSM is gaining importance to enhance the efficacy of PSM (Thakuria et al. 2004; Chaiharn et al., 2008; Vassilev 2012). A large number of PGPR representing diverse genera have been isolated over past 50 years. Despite of their natural means of plant growth promotion ability, strains are genetically modified because of their inconsistent performance and requirement of uneconomically high dose application (Carmen, 2011). Additionally, several plant growth promoting traits can be combined in a single organism for long-term cell survival under a variety of environmental conditions (Defez, 2006). Inoculation of *Medicago tranculata* plant with indole-3-acetic acid-overproducing strain of *Sinorhizobium meliloti* improved both the shoot and root fresh weigh, nitrogen fixation ability, P mobilization, oxidative damage and salt tolerance (Imperlini et al., 2009; Bianco and Defez,

2009; 2010a,b). Hence, genetic modification of native strains may help to survive, adapt and function better in the rhizosphere and improve plant nutrition.

Catabolic versatility of the fluorescent pseudomonads appears to be orchestrated by specific regulatory network of central metabolism which is exemplified by the diversity in the nature and number of enzymes of the *anaplerotic node*, their allosteric regulation and gene expression (Sauer and Eikmanns, 2005). Genetic engineering strategies developed for a particular organism may not necessarily work for other organism or even organism of the same species. Therefore, it is necessary to investigate the effects of genetic modification in multiple host organisms. In this study, six diverse *P. fluorescens* strains were subjected to similar genetic modification for citric acid secretion leading to P solubilization and plant growth promotion.

6.2 WORK PLAN

6.2.1 Bacterial strains

Fluorescent pseudomonad strains used in the study are lised in the table 6.1

P. fluorescens **strains/Plasmids**	**Characteristics**	**Source/Reference**
PfO-1	6.4Mb, 60.5%GC, 5736genes, (Accession CP000094)Wild type strain	A generous gift of Prof. Mark Sylvi, USA (Silby, 2009)
Pf-5	Cotton rhizopsheric isolate produces DAPG, Plt, and Prn, ACC(+), L-Methionine (+) 7Mb, 63.3%GC, 6137 genes, (Accession CP000076)	A generous gift of Prof. L. Thomashow USA
CHAO-1	Tobacco rhizopsheric isolate, naturally suppressive to black root rot caused by *Thielaviopsis basicola* , produces DAPG, Plt, Prn, HCN, IAA,ITS, Phz, salicylic acid, pyochelin, a pyoverdine siderophore	Weller, 2007

	(pseudobactin), and other bioactive metabolites. ACC(-), L-Methionine (+).	
ATCC13525	Wild type strain	ATCC
P109	Wild type strain, ACC(-), P^+	A generous gift of Prof. B. N. Johri
Fp315	Wild type strain, ACC(-), P^+	A generous gift of Prof. B. N. Johri
Pf(pYC)	*P. fluorescens* strains with pYC; Gm^r	Ch4
Pf (Int)	*P. fluorescens* strains genomic integrant, Gm^r	Ch5

Table 6.1 : List of plasmids and bacterial strains used in the study. DAPG: 2, 4–Diacetyl pholorglucinol, HCN: Hydrogen Cyanide, IAA: Indole-3-acetic acid, ITS: internal transcribed spacer, Phz: Phenazine, Pit: Pyoluteorin, Prn: Pyrrolnitrin,

All the strains were grown in shake flask using TRP (pH 8.2) medium containing 75mm Tris HCl and 75 mM glucose. For inoculums preparation during plant experiment the cultivation was carried out at 30 ºC in an orbital shaker at 200 rpm until all the culture reached to an OD of 0.8-1.0.

6.2.2 In vitro characterization of genomic integrants for P- solubilization ability

The di-calcium phosphate solubilizing ability of the wild type and the transformant strains of fluorescent pseudomonads was tested on Pikovskaya's agar (Pikovskaya, 1948). Bacterial inoculums were prepared by aseptically harvesting the Luria-Bertanni broth grown cultures after washing the cell-pellet twice with 0.85% saline and re-suspending in 1 ml of the same under sterile conditions. Resultant cell suspension was aseptically spotted on the agar plates and was allowed to dry completely followed by incubation at 30 ºC for 5–7 days. Rock phosphate solubilizing ability was monitored using 75 mM Tris buffered TRP minimal agar medium (Buch et al., 2008) following the same procedure mentioned above. P-Solubilization on Pikovskaya's agar was determined by monitoring the phosphate solubilization index (PSI) whereas the growth and formation of a red zone on buffered

Senegal rock phosphate Methyl Red agar plates were used to demonstrate P-solubilization and acid production in TRP agar medium using rock phosphates as the mineral P.

Batch culture studies were performed by shaking 30 ml of the TRP minimal broth medium (in 150 ml conical flasks), inoculated to an initial cell density at 600 nm (OD600) of about 0.1 (approximately 10^8cfu/ml), on a rotary shaker maintained at 30 ºC with agitation speed of 200 rpm. Drop in the media pH from pH 8.0 to < 5 on TRP broth was used to indicate rock-phosphate solubilization. Quantitative estimation of phosphate solubilization in broth was carried out in culture supernatant by Aemes method (..). In each case, three replicates were used.

6.2.3 Soil preparation

The soil used for the experiment was collected from the uncultivated land at Amri Village, 3 Km away from Navsari Agricultural University, Navsari Gujarat and analysis of the sample prior to experiments showed 1001.0 Kg/ha, 2.32 Kg/ha, 96.48 Kg/ha NPK respectively with a pH 8.4 (1:2.5) and EC (1:2.5) 0.27. The soil pH was determined in 1:2.5 soil:water suspensions using an automatic glass electrode pH meter (Systronic model-361). Phosphorus was evaluated by phosphomolybdic acid methods (Trivedy et al., 1998).

6.2.4 Seed surface sterilization and seed bacterization

Seeds of *Vigna radiata* GM4 obtained from Navsari Agriculture University, Navsari, Gujarat and were washed repeatedly with autoclaved distilled water and soaked in distilled water for 10 minutes. Later seed directly soaked into respective cultures. For uniform treatment of the seed with culture, flasks were kept in an orbital shaker at 500 rpm for 2 h. The average bacterial counts were 10^8 cfu/seed. Seed were treated with *P. fluorescens* strains each containing wild type strain (WT), plasmid transformants of *yc* operon (pYC) and *yc* operon genomic integrant (Int). In all experiments, two controls were used. One is absolute control where no fertilizer and no inoculum was added designated as untreated (UT) and the other control was single super phosphate (SSP) control where recommended dose of SSP was added as soil application with no added inoculum.

6.2.5 Greenhouse experiment

Bacteria coated Mung bean seeds were shown in polybags containing unsterile field soil and reared in a green house (25-30 °C). The pots were irrigated time to time to maintain the moisture level in green house. The growth parameters were recorded and biochemical characterization was carried out at 45 days after emergence. Each treatment had 5 replications (6 seeds per replicate).

6.2.6 Growth parameter assessment

All the plant growth parameters were estimated at 45 days after sowing (DAS).

6.2.7 Biochemical characterization

All antioxidant enzymes (SOD, Catalase, Gpox, and APX) and acid phosphatase and NR specific activities were monitored

6.2.8 Statistical analysis

The experiments were carried out in a completely randomized design (CRD) for *Vigna radiata*. The experimental data was analyzed statistically at 5% level of significance using two factorial CRD analysis.

6.3 RESULTS

6.3.1 P solubilization phenotype characterization of *P. fluorescens yc* operon genomic integrant strains in buffered and unbuffered media.

Genomic integrants *P. fluorescens* PfO-1 and Fp315 *yc* operon showed maximum di calcium phosphate solubization ability on Pikovskaya's agar as compared to the plasmid transformants of *yc* operon (pYC) and plasmid transformants of only citrate synthase without any external transporter (pYF) and wild type. Phosphate solubilization index when calculated varied in the order of PfO-1WT< PfO-1(pGm) < PfO-1(pYF) < PfO-1(pYC) < PfO-1(Intyc). Fp315 showed similar pattern of P solubilization when tested on both di calcium and buffered rock phosphate medium (**Fig. 6.1**). Based on this phenotype, the *P. fluorescens* strains were characterized based on their solubilization ability both on

Pikovskaya's agar and TRP agar medium (**Fig. 6.2-6.3**). All strains showed significant improvement on solubilization index as compared to their respective wild type control (**Fig. 6.4**).

On TRP medium, all cultures showed an improvement in the zone of colouration as compared to the wild type. Moreover, the genomic integrants of PfO-1, Pf-5 and Fp315 showed faster rock phosphate solubilization as evident from the appearance of zone of coloration within 48-72 h of growth as compared to 96-120 h of plasmid transformants and wild type. Except Fp315 wild type, none of the wild type cultures could show zone of coloration on TRP medium containing 75mM Tris HCl (pH 8.2) and 75 mM glucose.

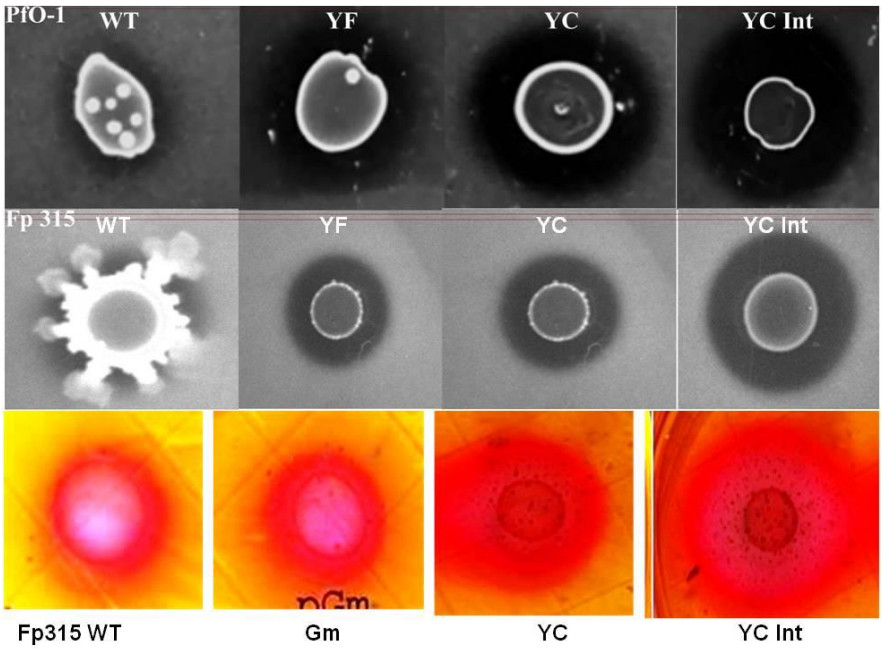

Figure 6.1: P solubilization phenotype of transgenic *P. fluorescens*PfO-1 and Fp315 strains during 96-120 h of growth. WT: wild type strain; Gm: *P. fluorescens with* pUCPM18Gm vector; YF: *P. fluorescens* with pYF plasmid; YC: *P. fluorescens* with pYC plasmid; YCInt: *P. fluorescens* yc operon genomic integrant.

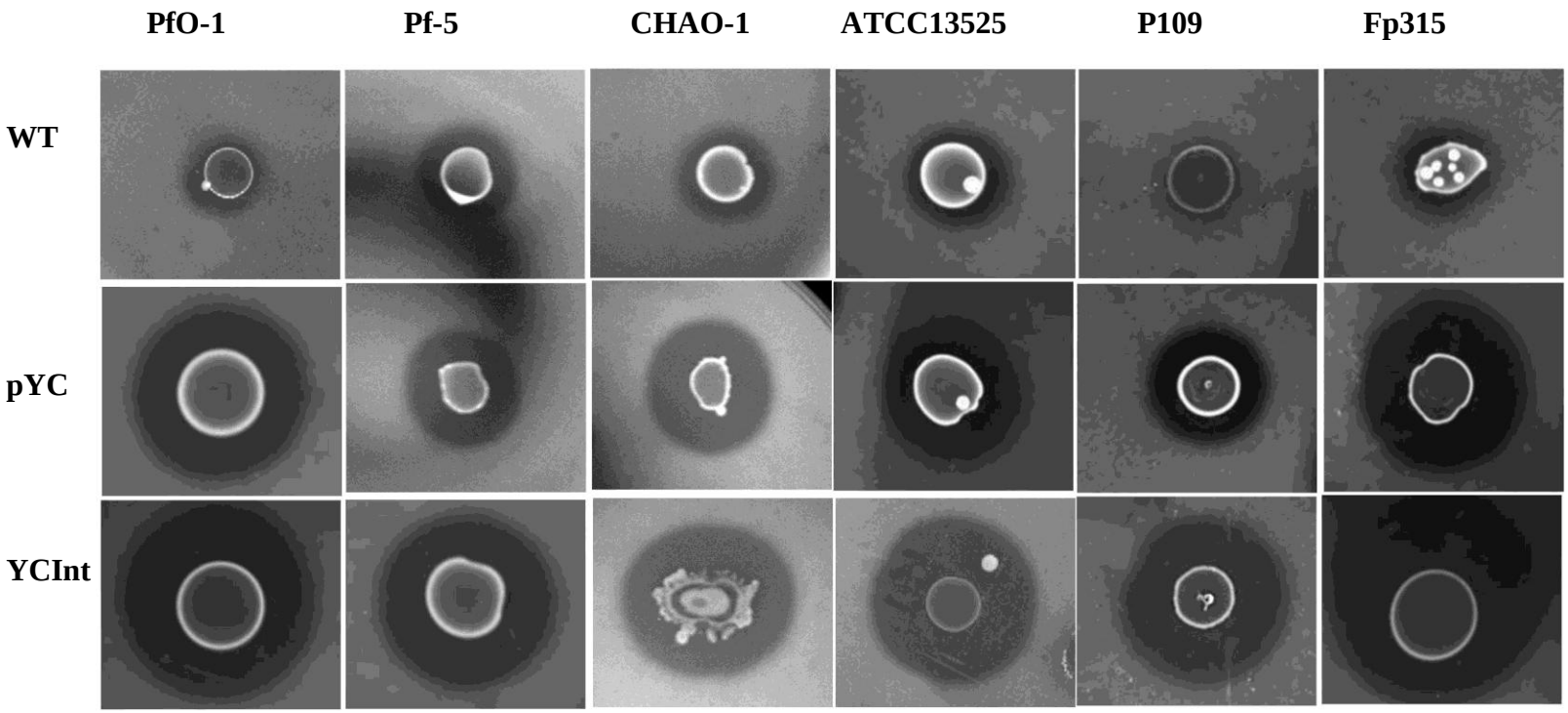

Figure 6.2: Zone of clearance of transgenic *P. fluorescens* strains in Pikovskyas agar medium during 96-120 h of growth. WT: wild type strain; Gm: *P. fluorescens with* pUCPM18Gm vector; YC: *P. fluorescens* with pYC plasmid; YCInt: *P. fluorescens* yc operon genomic integrant.

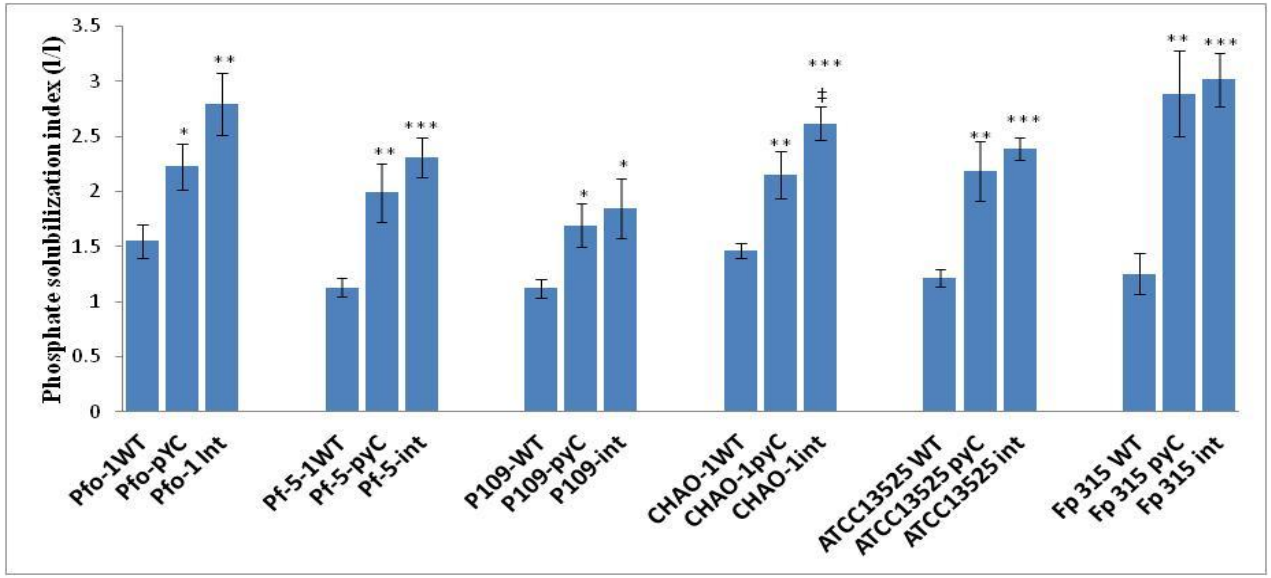

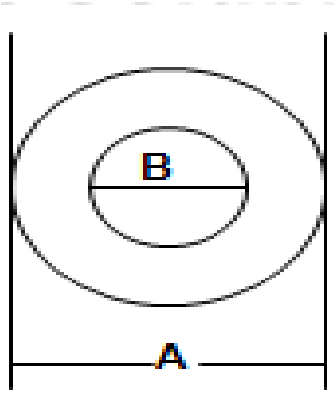

PSI= A/B

Srains	PfO-1	Pf-5	CHAO-1	ATCC13525	P109	Fp315
WT	1.55±0.15	1.13±0.09	1.46±0.07	1.22±0.08	1.12±.08	1.25±0.18
pYC	2.22±0.21	1.99±0.27	2.15±0.22	2.18±0.27	1.69±0.19	2.89±0.39
INT	2.79±0.28	2.31±0.18	2.62±0.16	2.39±0.1	1.85±0.27	3.02±0.24

Figure 6.3: P solubilization index on Pikovskyas agar of *P. fluorescens yc* operon genomic integrants during 96-120 h of growth. WT: wild type strain; YC: *P. fluorescens* with pYC plasmid; YCInt: *P. fluorescens* yc operon genomic integrant.

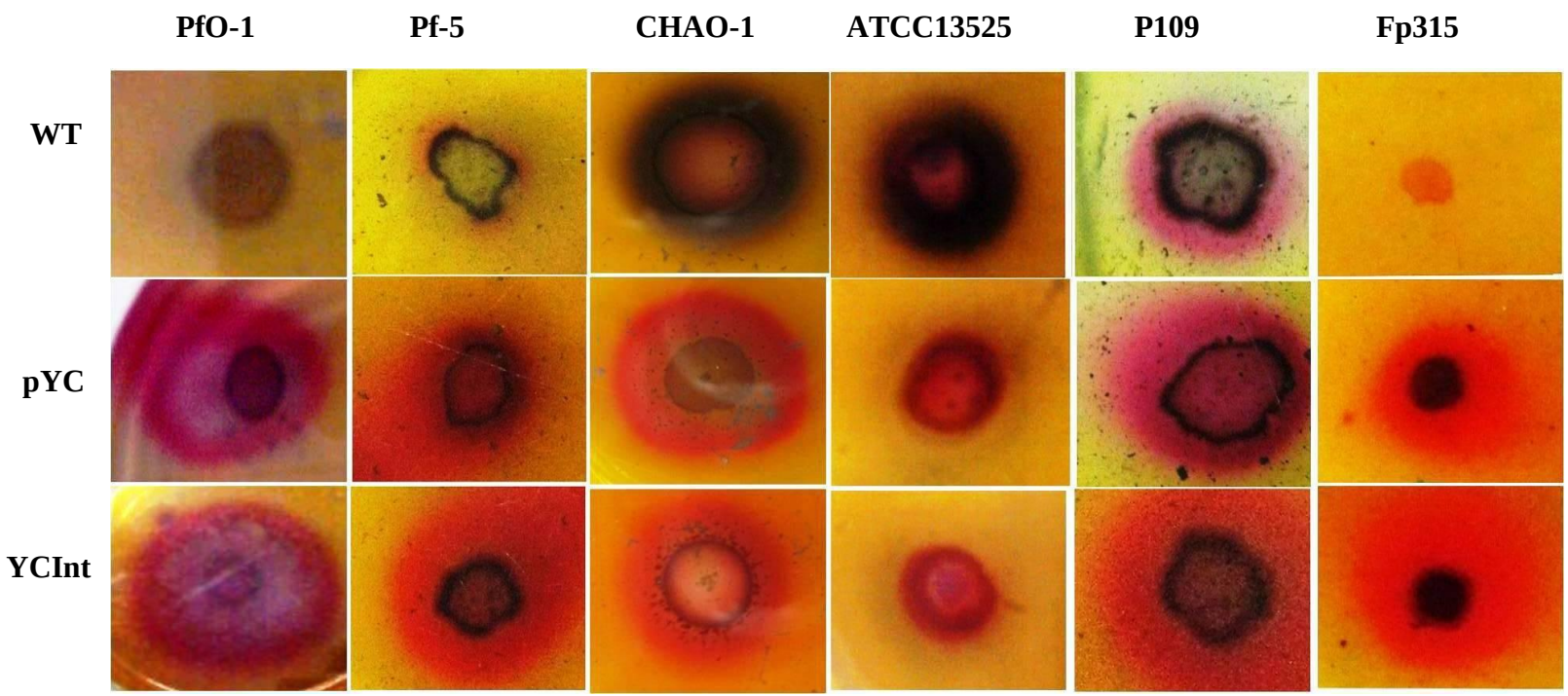

Figure 6.4: **Zone of colouration of transgenic *P. fluorescens* strains in TRP agar medium during 96-120 h of growth.** WT: wild type strain; Gm: *P. fluorescens with* pUCPM18Gm vector; pYC: *P. fluorescens* with pYC plasmid; YCInt: *P. fluorescens* yc operon genomic integrant.

6.3.1.1 P solubilization activity on buffered broth medium

All *P. fluorescens yc* operon plasmid transformants and genomic integrants showed significant enhancement of Pi release as compared to the wild type strains with an exception of P109 wherein compared to the wild type no improvement of Pi release was observed. *P. fluorescens* Fp315 genomic integrant showed a maximum Pi release of 983.4±58.78 µM which was even 1.37 fold higher as compared to plasmid transformants. In contrast, ATCC13525 genomic integrant showed a decrease in Pi level by 1.5 fold as compared to the plasmid transformants. The Pi release among the *P fluorescens* genomic integrants was in the increasing order of ATCC13525< P109 < Pf-5 < CHAO-1 < PfO-1 < Fp315 (**Fig. 6.5**).

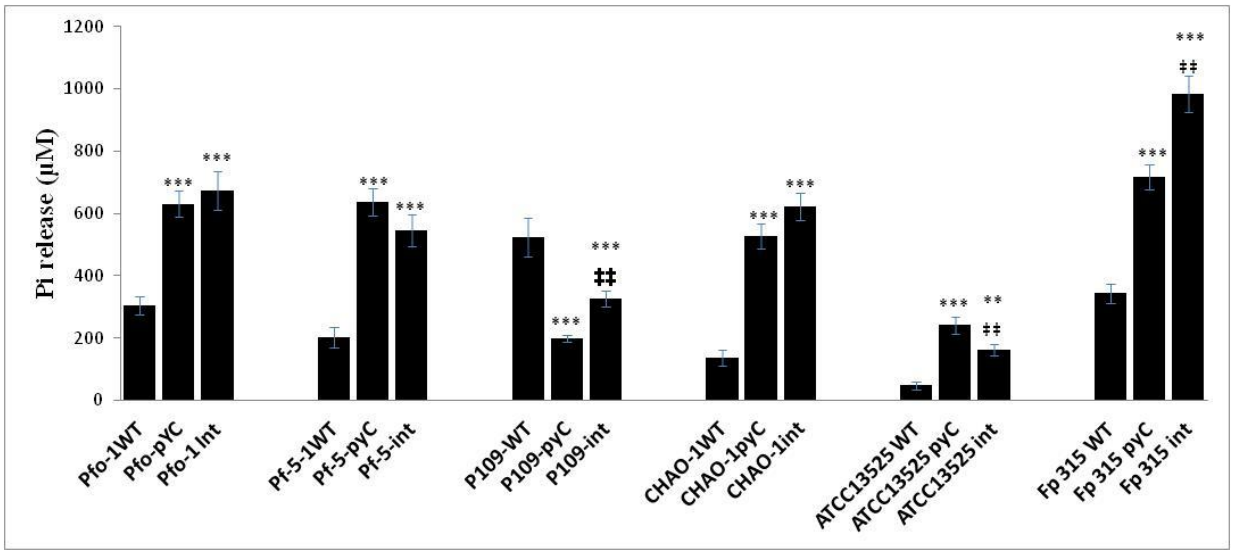

Figure 6.5: Pi release of transgenic *P. fluorescens* strains in TRP broth medium during 96-120 h of growth.

6.3.2 Greenhouse experiments

Mung bean inoculation studies in greenhouse were carried till 45 days after emergence. All growth and biochemical parameters were statistically analyzed using two factorial CRD. The results indicate that all treatments worked significantly well as compared to the UT control and many treatments were at par or significantly better as compared to the SSP control. Analysis of variance results revealed significant influence of genomic integration on growth promotion of mung bean plants (**Appendix I**).

6.3.2.1 Growth parameters

6.3.2.1.1 Leaf number

Treatments involving inoculum of PfO-1(Int), Pf-5 (pYC), Pf-5 (Int), P109 (pYC), p109 (Int), CHAO-1 (Int), ATCC13525 (pYC), ATCC13525 (Int), Fp315 (Int) showed significant increase in leaf number and were similar to the SSP control as compared to the untreated control (**Fig. 6.6**). All treatments showed better growth as compared to the uninoculated control (**Fig. 6.7**).

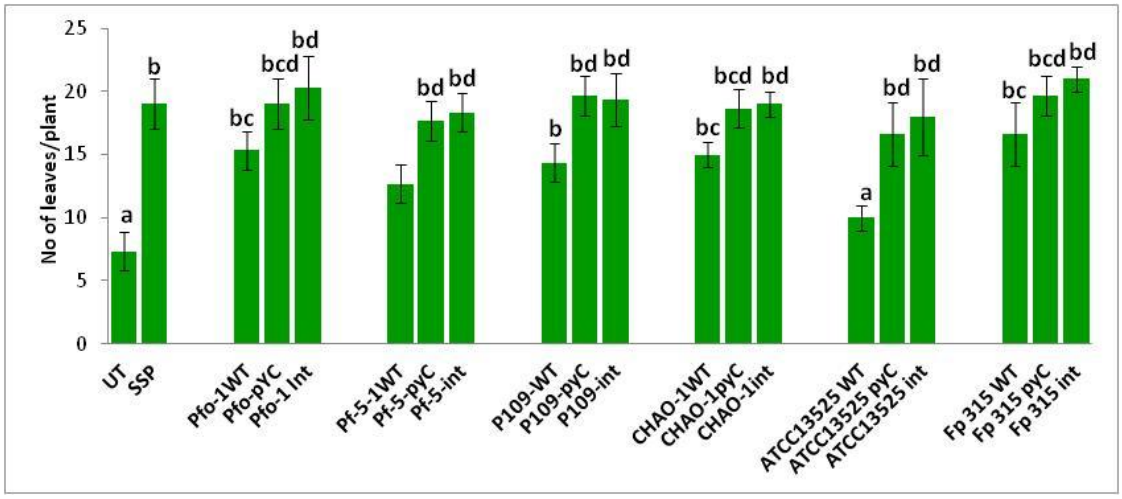

Figure 6.6: Effect of *P. fluorescens* genomic integrants on leaf number of mung bean (*Vigna radiata*) at 45 Days after sowing. Columns labeled with the same letter represents non significantly different means ($p<0.05$) after ANOVA

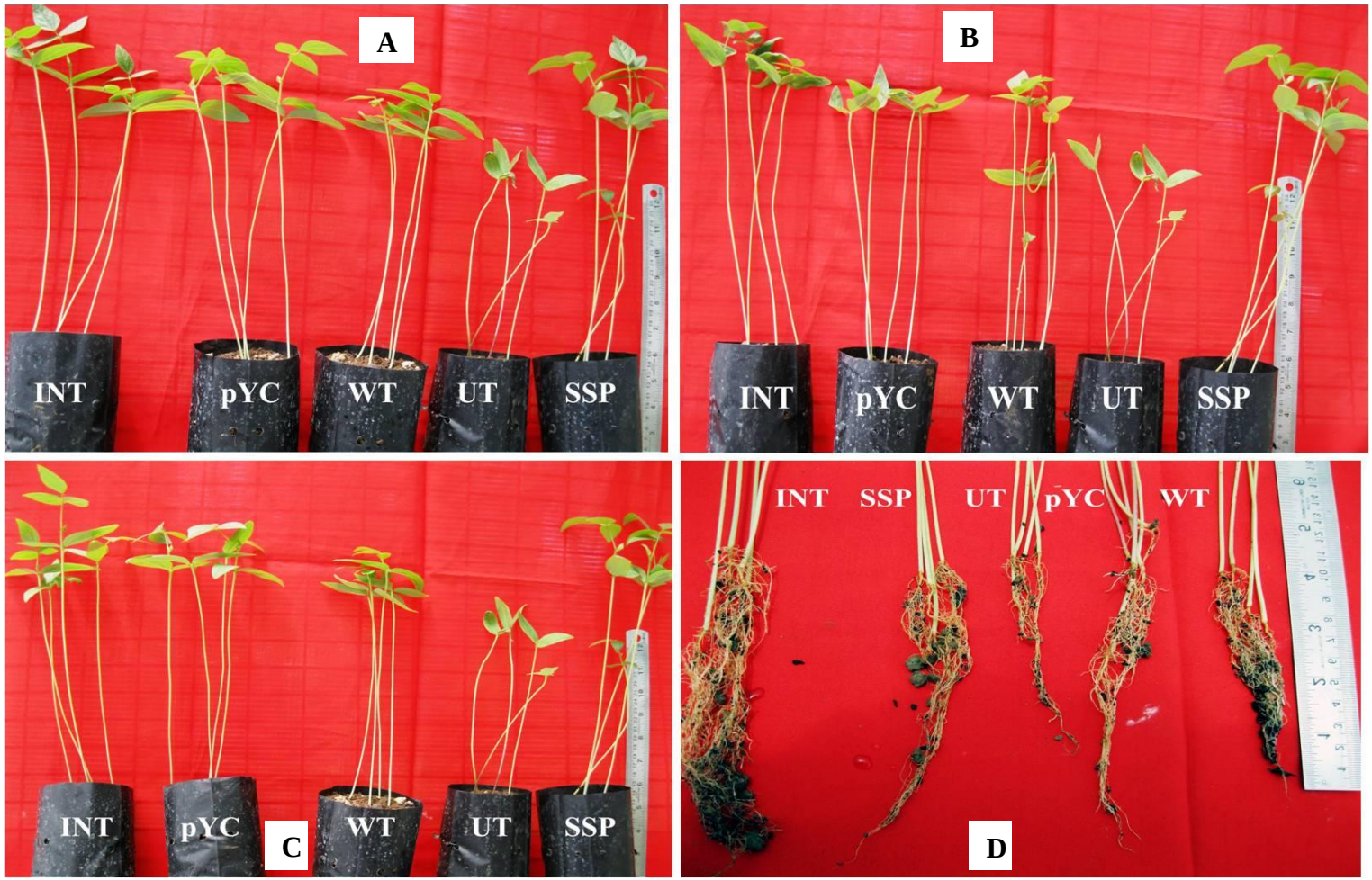

Figure 6.7: The pot results of *Vigna radiata* GM4 at 20 days after showing (DAS). The treatments are Single super phosphate (SSP) and untreated (UT) as control, Wild type (WT), yc operon plasmid transformants (pYC) and yc operon genomic integrant (INT). A: *P. fluorescens* PfO-1; B-D: *P. fluorescens* Fp315

6.3.2.1.2 Shoot and root length and dry matter accumulation

The mung bean plant inoculated with plasmid transformants and genomic integrants of all the *P. fluorescens* strains showed similar shoot length, root length, shoot dry weight and root dry weight as compared to the SSP control. All treatments showed significant improvement in shoot length and root length as compared to the untreated control except P109WT and ATCC13525WT (**Fig. 6.8**).

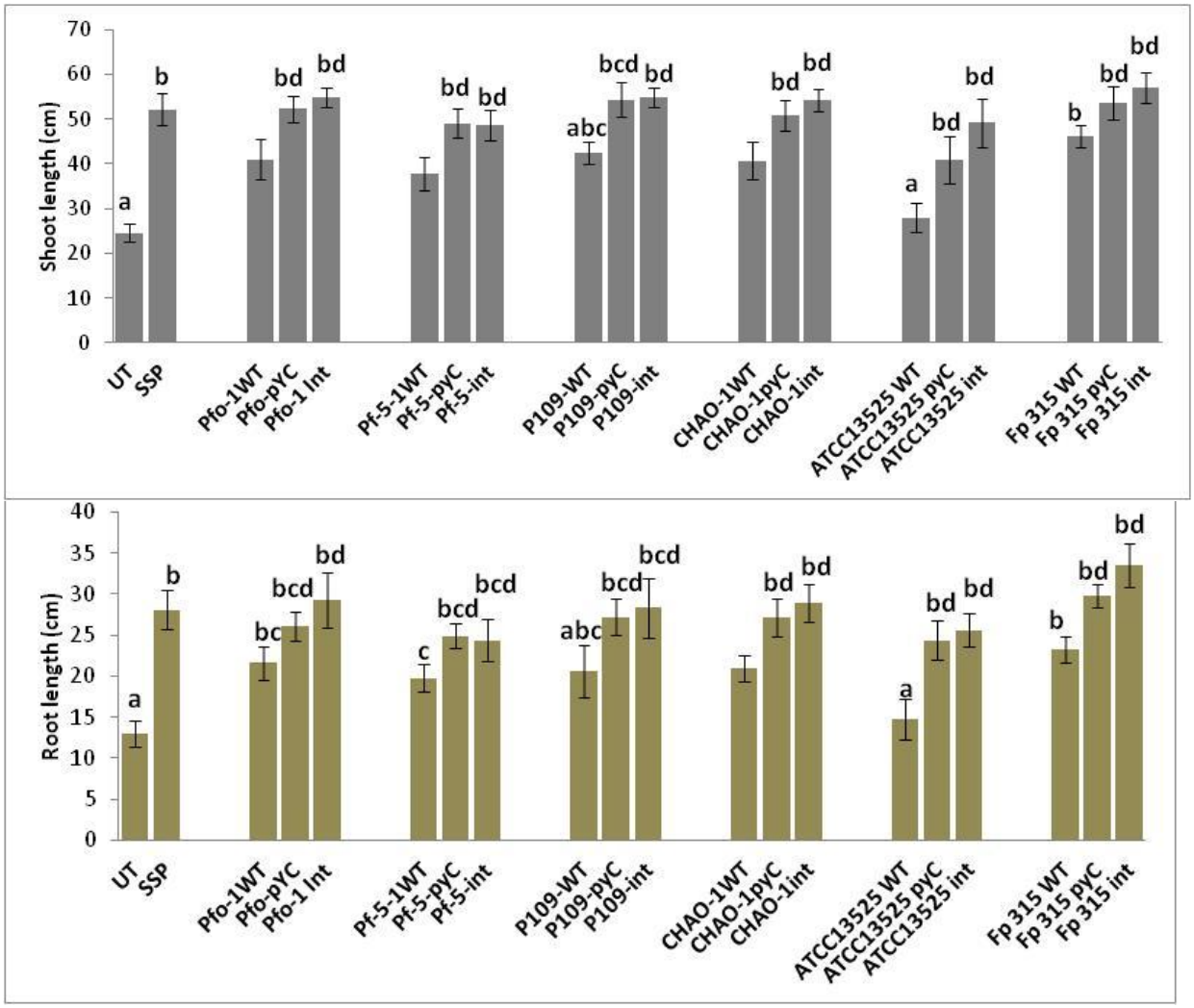

Figure 6.8: Effect of *P. fluorescens* genomic integrants on shoot length and root length of mung bean (*Vigna radiata* GM4) at 45 Days after sowing. Columns labeled with the same letter represents non significantly different means ($p<0.05$) after ANOVA

6.3.2.1.3 Dry matter accumulation

Similarly, PfO-1 WT showed no significant improvement in shoot dry weight and ATCC13525WT in both shoot and root dry weight as compared to the untreated plant (**Fig. 6.9**).

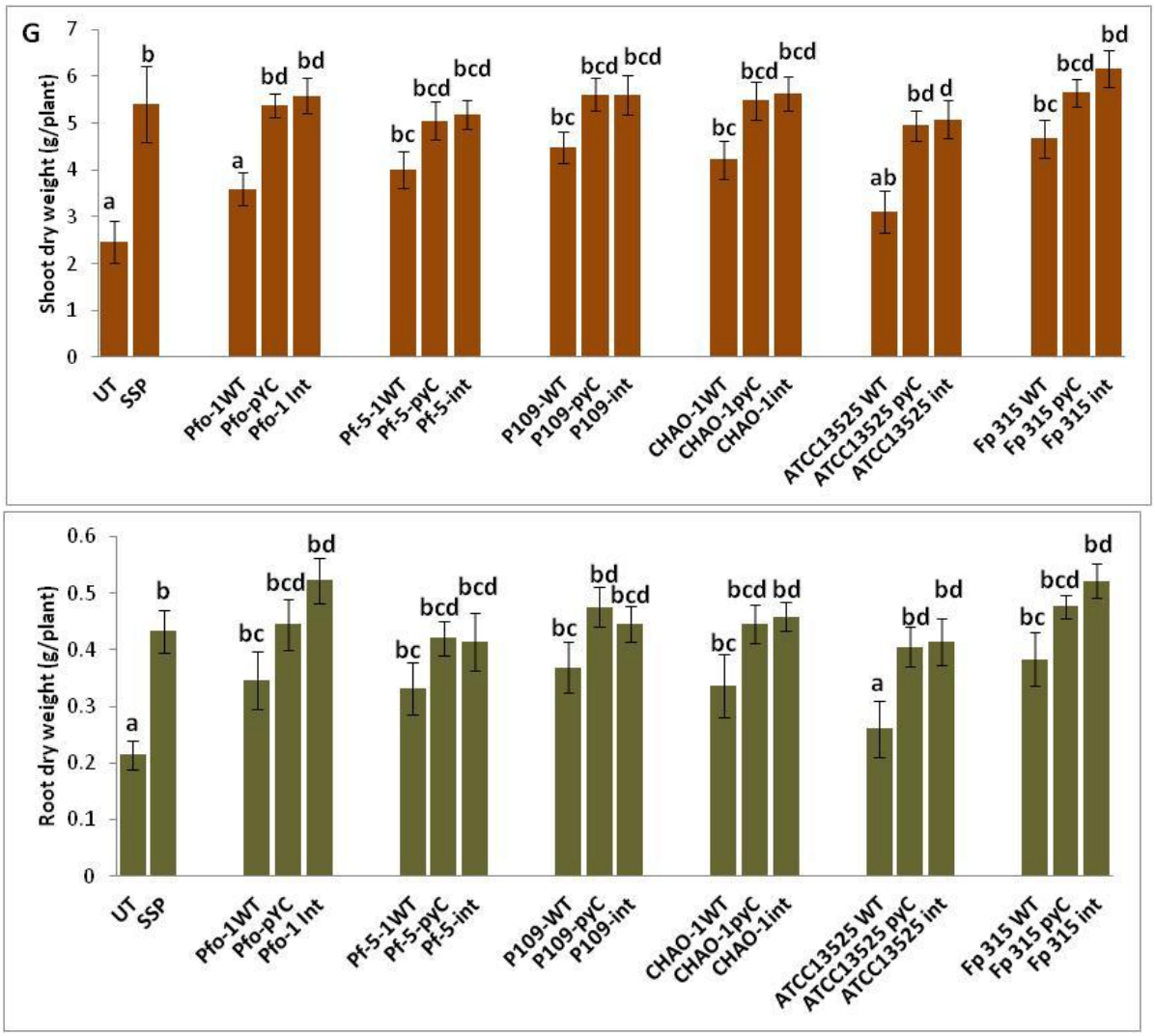

Figure 6.9: Effect of *P. fluorescens* genomic integrants on Shoot and root dry weight of mung bean (*Vigna radiata*) at 45 Days after sowing. Columns labeled with the same letter represents non significantly different means ($p<0.05$) after ANOVA

6.3.2.2 Nodulation

All the *P. fluorescens* strain *yc* operon plasmid transformants and genomic integrants showed significant increase in nodule number as compared to the untreated control and similar nodule number as compared to the SSP control. The best nodulation was observed in PfO-1(Int), Fp315 (pYC) and Fp315 (Int), nodule number of which were significantly superior to the SSP control. Similarly, nodule dry weight recorded from treatment of PfO-1 (pYC), PfO-1 (Int), P109 (pYC), P109 (Int), CHAO-1(pYC), ATCC13525 (Int), Fp315 (pYC) and Fp315 (Int) were significantly better than the SSP control (**Fig. 6.10**).

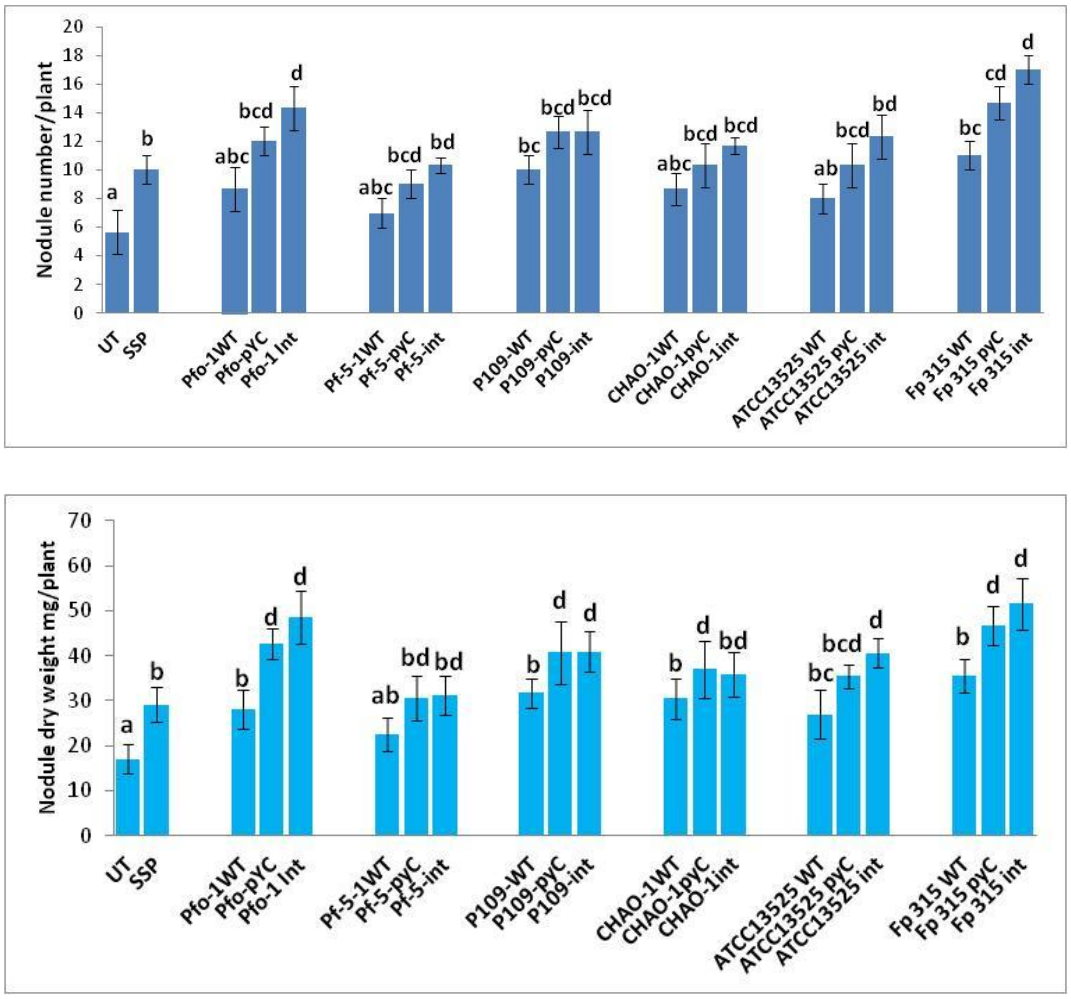

Figure 6.10: Effect of *P. fluorescens* genomic integrants on nodule number and dry weight of mung bean (*Vigna radiata*) at 45 Days after sowing. Columns labeled with the same letter represents non significantly different means ($p<0.05$) after ANOVA

6.3.2.3 Enzyme activities

To determine the effect of *P. fluorescens* genomic integrant treatment on the antioxidant status of mung bean plant, the specific activities of antioxidant enzyme **Superoxide Dismutase (**SOD), **Catalase**, **Guaiacol Peroxidase** (POX) and **Ascorbate peroxidase** (APX) were monitored at 45 days after emergence under P limiting condition. In addition, **Acid Phosphatase** (APase) and **Nitrate Reductase** (NR) activities were also determined to monitor the biochemical basis of P and N status. Significant changes in NR, APase and SOD activities were observed among all the treatments with no alterations in catalase, APX and POX activities (**Fig. 6.11 B-D**).

Significant reduction in SOD activities were observed in SSP control (2.1 fold), PfO-1 wild type and transgenics (~ 1.7 fold), Fp315(pYC) (1.88 fold) and Fp315(Int) (2.06 fold), CHAO-1 (pYC) (1.77) fold, CHAO-1 (Int) (2.04 fold). No alteration in SOD activities observed in p109 strains and CHAO-1 WT and Fp315 WT strains as compared to the uninoculated conrol (**Fig.6.11 A)**. Nitrate reductase activity was found to be repressed in uninoculated control which is 3.45 fold less as compared to the SSP control. Mung bean inoculated with all the *P. fluorescens* PfO-1 (int), Pf-5 (Int) and Fp315 (Int) showed highly significant increase in NR activity as compared to the uninoculated control. Except ATCC13525 WT and Fp315 WT all other wild type strains did not show significant improvement of NR activity (**Fig. 6.11 E**).

The APase activity of all the *yc* plasmid transformants and genomic integrant strains inoculated seedlings was significantly higher than uninoculated control. The wild type culture of CHAO-1 and Fp315 showed an increase by 2.17 fold and 2.2 fold, respectively, in APase activity as compared to the uninoculated control. The highest APase activity was found in Fp315 (Int) which is 3.6 fold and 1.46 fold higher as compared to the uninoculated and SSP control, respectively. PfO-1(Int) also showed a higher (1.4 fold).APase activity compared to the SSP control.

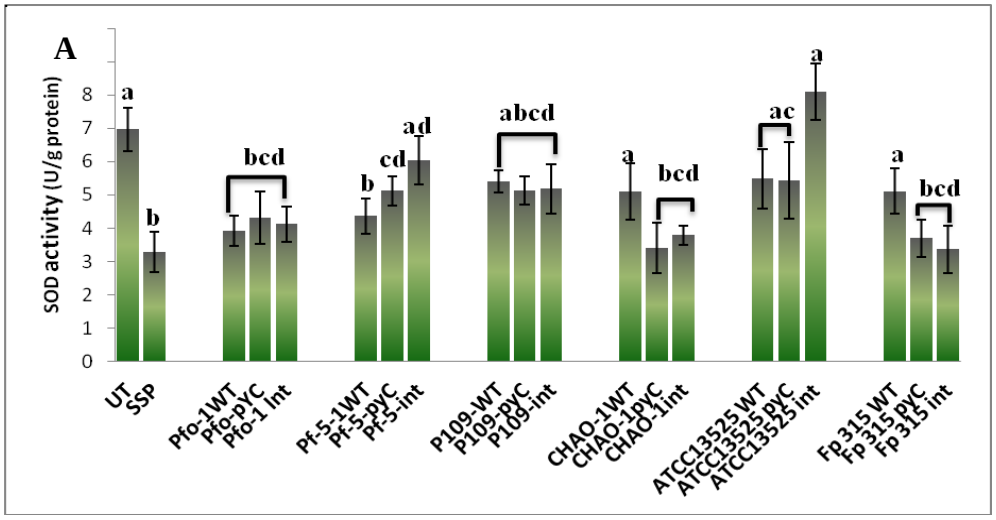
A
SOD activity (U/g protein)
a
b
bcd
b
cd
ad
abcd
a
bcd
ac
a
a
bcd
UT
SSP
Pfo-1WT
Pfo-pyC
Pfo-1 Int
Pf-5-1WT
Pf-5-pyC
Pf-5-int
P109-WT
P109-pyC
P109-int
CHAO-1WT
CHAO-1pyC
CHAO-1int
ATCC13525 WT
ATCC13525 pyC
ATCC13525 int
Fp 315 WT
Fp 315 pyC
Fp 315 int

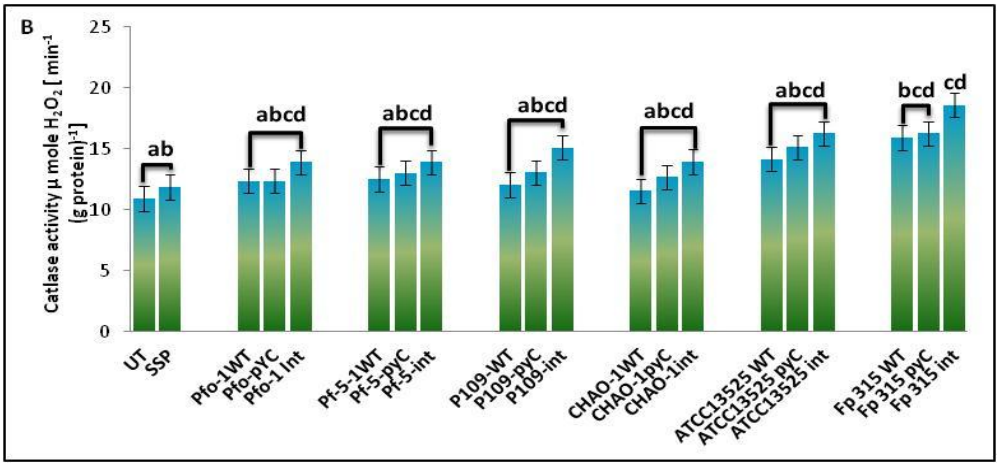
B
Catlase activity µ mole H_2O_2 [min^{-1} (g protein)$^{-1}$]
ab
abcd
abcd
abcd
abcd
abcd
bcd
cd
UT
SSP
Pfo-1WT
Pfo-pyC
Pfo-1 Int
Pf-5-1WT
Pf-5-pyC
Pf-5-int
P109-WT
P109-pyC
P109-int
CHAO-1WT
CHAO-1pyC
CHAO-1int
ATCC13525 WT
ATCC13525 pyC
ATCC13525 int
Fp 315 WT
Fp 315 pyC
Fp 315 int

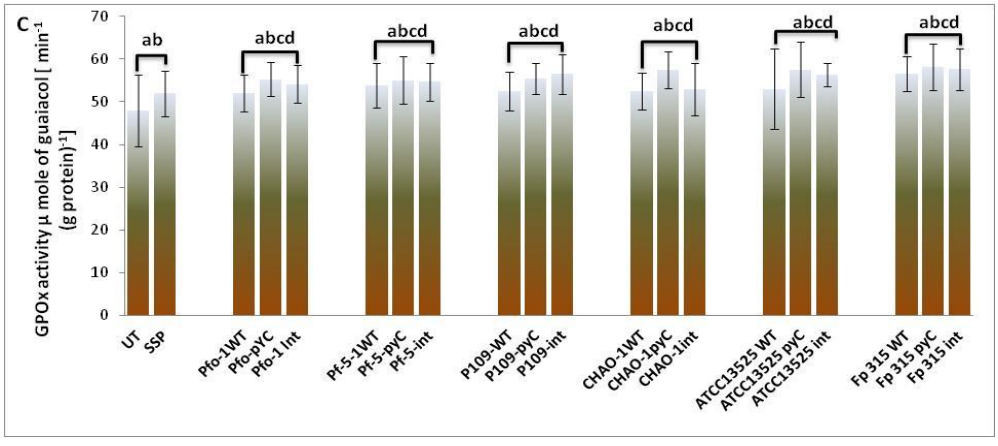
C
GPOx activity µ mole of guaiacol [min^{-1} (g protein)$^{-1}$]
ab
abcd
abcd
abcd
abcd
abcd
abcd
UT
SSP
Pfo-1WT
Pfo-pyC
Pfo-1 Int
Pf-5-1WT
Pf-5-pyC
Pf-5-int
P109-WT
P109-pyC
P109-int
CHAO-1WT
CHAO-1pyC
CHAO-1int
ATCC13525 WT
ATCC13525 pyC
ATCC13525 int
Fp 315 WT
Fp 315 pyC
Fp 315 int

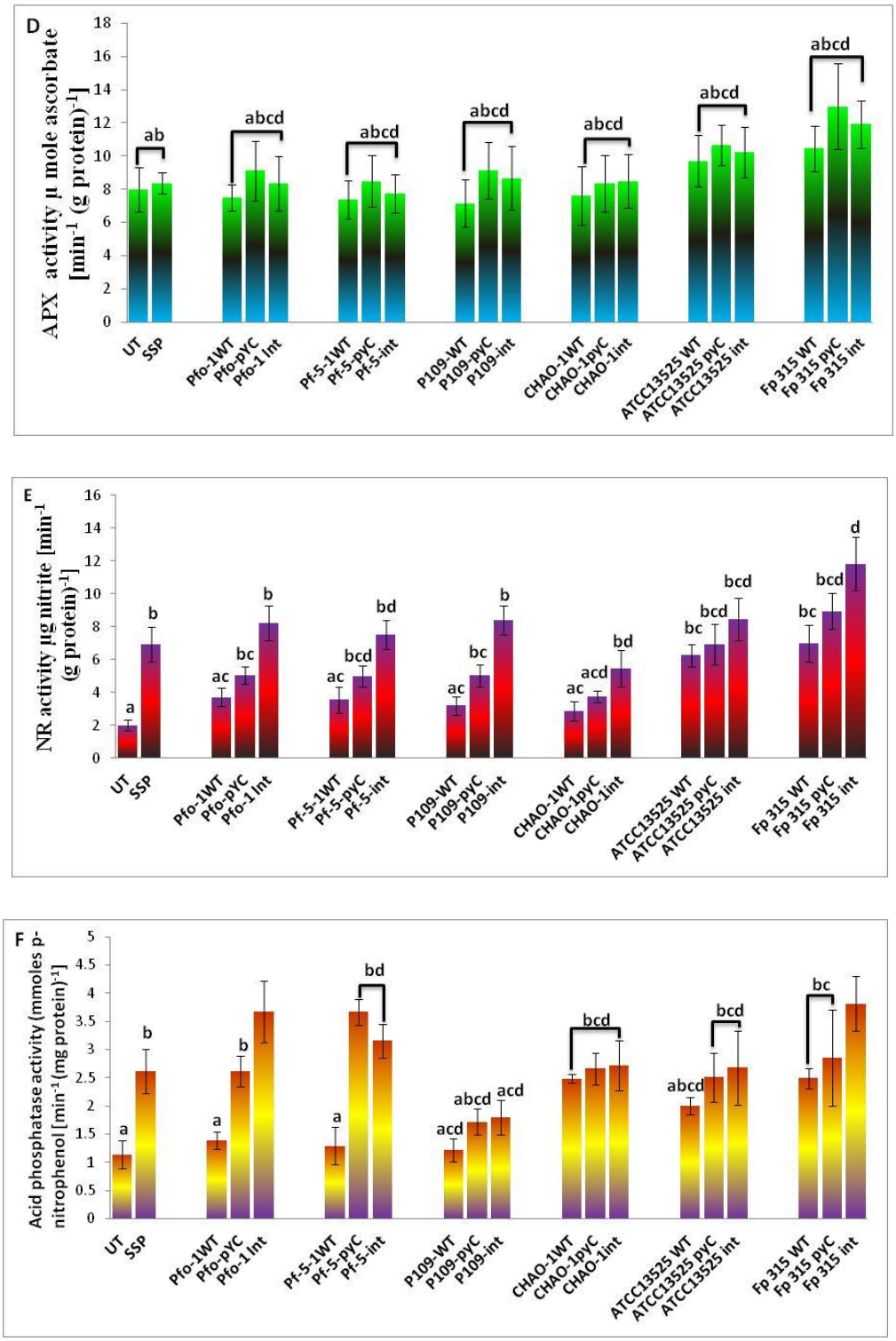

Figure 6.11: Effect of *P. fluorescens* genomic integrants on enzyme activities of mung bean (*Vigna radiata*) at 45 Days after sowing. Columns labeled with the same letter represents non significantly different means ($p<0.05$) after ANOVA

6.3.2.4 P content in shoot and root

Significant increase in root P content was observed in both plasmid transformants and genomic integrant of ATCC13525 and CHAO-1 and genomic integrants of PfO-1 and Fp315. Highest root P content was observed in Fp315(Int) which is even more than SSP control (**Fig.6.12**).

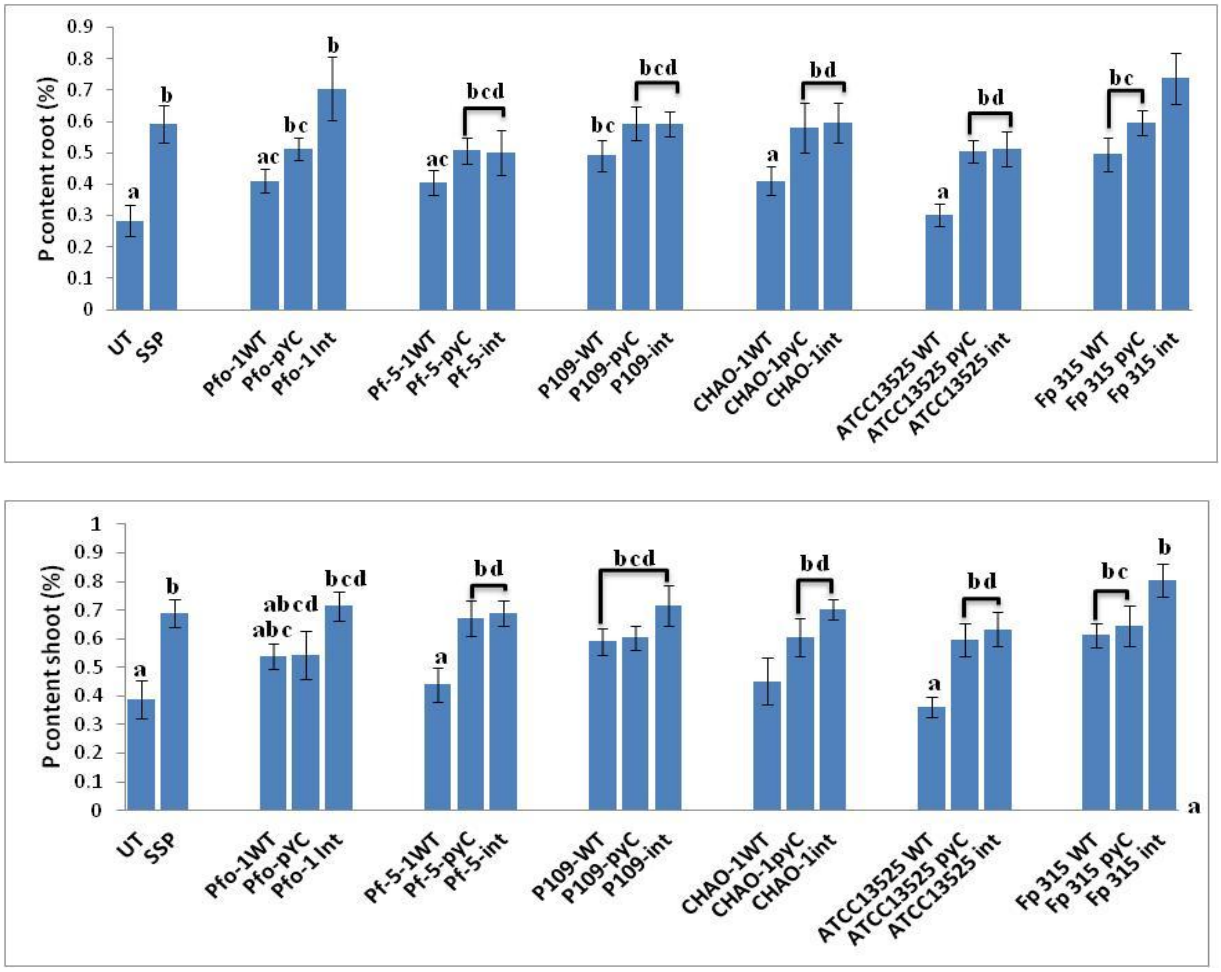

Figure 6.12: Effect of *P. fluorescens* genomic integrants on P content of root and shoot of mung bean (*Vigna radiata*) at 45 Days after sowing. Columns labeled with the same letter represents non significantly different means ($p<0.05$) after ANOVA

6.3.2.5 Available Soil P

Inoculation with PfO-1, Pf-5 and Fp315 increased soluble P as compared to the uninoculated control. The wild type strains of ACCC13525, CHAO-1 and P109 did not result in increase soil Pi.

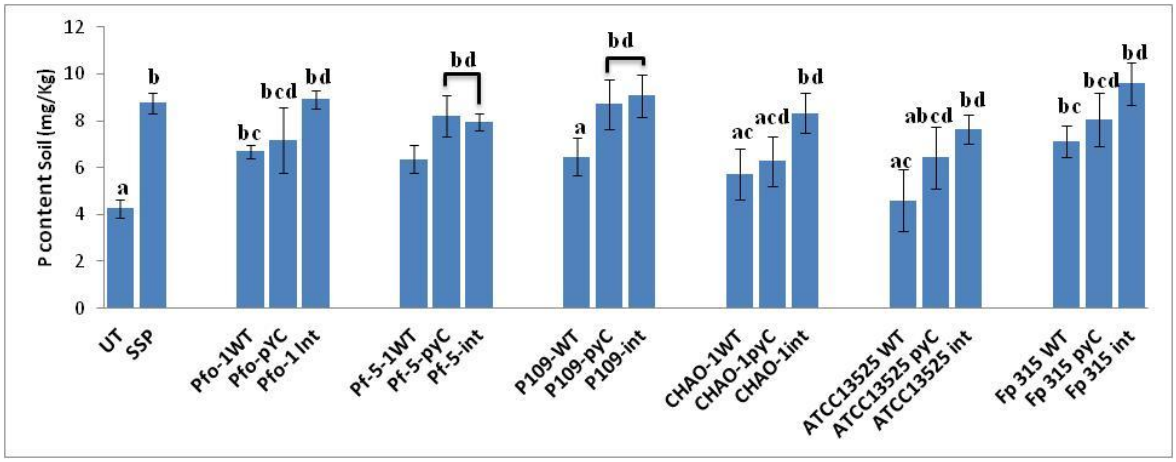

Figure 6.13:. Effect of *P. fluorescens* genomic integrants on available soil phosphorous of mung bean (*Vigna radiata*) at 45 Days after sowing. Columns labeled with the same letter represents non significantly different means ($p<0.05$) after ANOVA

6.4 Discussion

The present work describes the effect of *yc* genomic integration on MPS ability of fluorescent pseudomonads including natural isolates on plan growth promotion of mung bean (*Vigna radiata* GM4) in phosphate deficient soil under controlled environment of green house. P solubilization index of transgenic *P. fluorescens* PfO-1 on PVK agar medium was in the order of WT≤ Gm< YF<YC≤ YCInt and gave phenotype in TRP medium containing 75mM tris HCl and 75 mM glucose, demonstrating the improved functionality of the *yc* operon genomic integration. Among PSMs, only few *Bacillus* strains solubilize mineral phosphates via citric acid secretion. But higher citric acid secretion has been demonstrated in MPS fungi belonging to *Aspergillus* and *Penicillium* spp. (Khan et al., 2006). Genetic modification strategy was investigated in diverse fluorescent pseudomonads including *P. fluorescens* PfO-1, Pf-5, CHAO-1, ATCC13525, P109, and Fp315. All these

pseudomonads are noted for their metabolic diversity and are being investigated extensively for use in applications such as bioremediation of various organic compounds viz., styrene, TNT and, polycyclic aromatic hydrocarbons, and biocontrol of pathogens in agriculture (CHAO-1, Pf-5, and PfO-1). These *P. fluorescens* strains, protect plant roots against soil born pathogens such as *Fusarium* or *Pythium*, as well as phytophagous nematodes through induce systemic resistance in the host plant, outcompete pathogenic soil microbes by siderophores giving a competitive advantage at scavenging for iron, produce compounds antagonistic to other soil microbes, such as phenazine-type antibiotics, secondary metabolite 2,4-diacetylphloroglucinol (2,4-DAPG) and/or hydrogen cyanide. All strains are also known for plant growth promotion to varying extent in different host plants (Ref). *P. fluorescens* P109 and Fp315 are wheat rhizospheric isolates with poor P solubilizers. Such bacteria would be really advantageous if possess efficient MPS ability along with potent biocontrol abilities, thereby serve the current demand for multipurpose biofertilizers (Vessey et al., 2003; Vassilev et al., 2006). Our laboratory results showed improvement of MPS ability in all the strains genomic integrant as compared to wild type strain The MPS phenotype in both the unbuffered and Tris HCl buffered media can be correlated with increase in gluconic and citric acid and the amount of Pi release except P109 strain. The wild type strain of P109 showed higher amount of Pi release as compared to the transgenic strain.

Genetically modified fluorescent pseudomonad strains were tested for growth response of mung bean in phosphate deficient soil condition in controlled environment of green house. All the transgenic strains showed enhancement of all plant growth parameters (leaf number, plant height and dry weight, nodule number, and dry weight) and remarkably at par with the SSP control. *P. fluorescens* ATCC13525 wild type strain showed no significant enhancement in growth promotion compared to the untreated control and growth promotion of other wild type strain was at par or less than the SSP control. The effect of genomic integration of *yc* operon in the bacteria clearly increased the nodule number and dry weight more than native strains and in case of PfO-1 and Fp315, increase was even better than SSP control. Improvement in nodulaion due to inoculation of P solubilizers was also reported in chick pea and other leguminous plant (Tang et al., 2001). Enhanced

nodulation after inoculation of the strain suggested an increase in available P for the plant as leguminous plant require high amount of P for nodule formation and mainainance of high rate of bacterial activity inside the nodule (Leidi et al., 2000; Zaman et al., 2007). The increase dry matter accumulation following inoculation of PSM correlated to increased nodulation, increased shoot and root length and increased number of leaves per plant. The P content of shoot was increased after inoculation with *P fluorescens* strains. Similar results obtained in barley and chick pea when grown in soil treated with insoluble phosphate and PSM *Mesorrhizobium mediterraneum* PECA21 where the P content was significantly increased by 100 and 125%, respectively as compared to control (Peix et al., 2001).

Present study showed the decrease in SOD activity but not in catalase and total peroxidase activities after inoculation with *P. fluorescens* PfO-1 WT and transgenic strain of Fp315, CHAO-1 and Pf-5. Inoculation of PGPR reported to reduce oxidative stress in plants. Abiotic stress conditions cause an increase in ROS formation such as superoxide radical (O^{2-}), hydrogen peroxide, and hydroxyl radicals (OH) at the cellular level (Sgherri and others 2000; Hemavathi and others 2010). Al toxicity and P deficiency both increased SOD and POD activities in maize and rice plants (Tewari et al, 2004; Sharma and Dubey, 2007). Bacterial inoculation benefits plant physiology and growth under abiotic stress conditions including nutrient deficiency (Carmen et al., 2011). Induction of antioxidant enzymes (catalase. SOD, APX, GR and POX) is involved in the alleviation of salinity stress in lettuce plants inoculated with PGPR strains (Bianco & Defez, 2009; Kohler et al., 2010). In contrast, PGPR inoculated plants showed significantly lower activity of antioxidant enzymes as compared to uninoculated plants (Omar et al.,2009; Sandhya et al. 2010). Significant increase of catalase and peroxidase activities is found in salt-stressed leaves of two barley cultivars differing in salinity tolerance after inoculation with *Azospirillum brasilense* (Omar et al., 2009). In contrast, the mRNA expression of SOD CAT, DHAR, GR and APX in bacteria-inoculated considerably increased in plants grown under stress conditions when compared with that of noninoculated stressed plants (Gururani et al 2012).

Plant growth promotion has been associated with the solubilization and increased uptake of phosphate. In the present study, phosphorus use efficiency of mung bean and soil quality were improved after PGPR application as indicated by increased APase activities and soil Pi content. APase induction and nitrate reductase repression is a significant adaptive response under Pi limited condition. Simultaneous exudation of organic acids and APase could increase both P solubility, by releasing bound organic phosphates and its mineralization by increasing the rate of hydrolytic cleavage (George et al., 2002). In addition, nitrate reductase is found to be repressed by Pi starvation, indicating that nitrogen assimilation is repressed under Pi depletion (Wu et al., 2003; Gniazdowska and Rychter, 2000). In the present study, significant enhancement of nitrate reductase activity was observed after inoculation with *P. fluorescens* genomic integrants as compared to the uninoculated plants grown under Pi limited condition. In bean (*Phaseolus vulgaris*), Pi deprivation leads to increased root nitrate accumulation and suppresses shoot nitrate accumulation, possibly by repressing nitrate reductase activity and nitrate transport from roots to shoots. A similar alteration in nitrate contents was observed in wild-type rice plants under Pi starvation conditions, indicating that rice also represses nitrate assimilation during Pi starvation. (Gniazdowska and Rychter, 2000; Hu et al., 2011).

Summarizing, present study demonstrates significant improvement in mung bean growth by transgenic *P. fluorescens.* Another important feature of the present study, the plant inoculation experiments were carried with the genomic integrants in soils without supplementation of rock phosphate. Thus, these bacteria appear to provided mung bean P derived from soil (alkaline vertisol) phosphate. All treatments, showed a consistent increase in growth response to the same level as the SSP control or in some cases even better. Further, improvement in some growth parameters was better in genomic integrants than plasmid transformants. In conclusion, the present study demonstrates that the genetic modifications of diverse fluorescent pseudomonads have similar effects in the central metabolism leading to secretion of citric acid to similar level.

SUMMARY

Summary

Phosphate solubilizing bacteria release P from inorganic complexes by the secretion of wide range of low molecular weight organic acids. P solubilization potential of these bacteria varies based on the amount and nature of organic acid produced. Citric, oxalic, and gluconic acids are the product of central carbon metabolism. Fluorescent pseudomonads show myriads of catabolic diversity in their carbon metabolism. The amount of the organic acid secretion may differ between members of the same genus and sometimes between strains of the same species (Vyas and Gulati 2009; Buch et al. 2010; Archana et al. 2012). Moreover, organic acid secretion in the rhizosphere depends not only on the metabolic potential of the organism but also on the plant physiology as complex set of interactions mediated many compounds including the root exudates as the major C source. The nature of root exudates varies from plant to plant and composed of a complex mixture of several nutrients in low amount. Therefore, it is difficult to predict the organic acid secretion by rhizobacteria which may also vary with plant physiology. Hence, to develop an efficient P biofertilizer with the potential plant growth promoting properties for multiple host systems and diverse eco habitats, the present study was an effort to understand the following aspects: (i) to develop a potential genetic modification strategy to increase the MPS ability of plant growth promoting fluorescent pseudomonads; (ii) to understand *in vitro* metabolic effects of genetic modification on different strains of *P. fluorescens* including rhizospheric isolates; and (iii) to determine the consistency and performance of genetically modified strains in alkaline vertisol soils.

Chapter 3-4 demonstrates the construction of *P. fluorescens* PfO-1 strain harbouring *E. coli* NADH insensitive citrate synthase and *S. tphimurium* sodium citrate transporter (*yc*) operon under *lac* promoter in broad host range plasmid pUCPM18 containing gentamycin resistance. The recombinant plasmid complemented the *cs* mutant phenotype of *E. coli* W620 and citrate transporter mutant phenotype of *E. coli* DH5α when grown on M9 minimal medium without glutamate and in Koser citrate broth respectively. This indicates the expression of respective genes. The expression of yc operon resulted in increased CS activity with a simultaneous increase in citric acid accumulation as well as secretion as compared to the wild type, vector control and strain harbouring only wild type citrate

synthase. The high amount of intracellular citric acid accumulation (~50mM) had no deleterious effect on cell growth given in

Table 1: Comparative effects of overexpression of *yc* operon in *P. fluorescens* PfO-1 grown under M9 minimal medium containing 100 mM glucose as a carbon source

Parameters	WT	pGm	pAB7	pYF	pYC
CS activity	-	No change	2.97 fold increase	5.6 fold increase	4.7 fold increase
Intracellular citric acid	-	No change	2.3 fold increase	5.7 fold increase	5.1 fold increase
Extracellular citric acid	-	10 fold increase	170 fold increase	320 fold increase	533 fold increase
Gluconic acid	-	1.7 fold increase	2.7 fold increase	6.6 fold increase	6.7 fold increase
Acetic acid	-	1.2 fold increase	1.97 fold increase	2.9 fold increase	4.8 fold increase
Pyruvic acid	-	1.26 fold decrease	1.87 fold decrease	2.8 fold decrease	1.8 fold decrease
Growth rate	-	No change	No change	No change	No change
Glucose consumed	-	1.35 fold increase	No change	No change	1.24 fold decrease
Biomass yield	-	1.33 fold increase	1.58 fold increase	3.16 fold increase	2.58 fold increase
G6PDH	-	1.7 fold increase	1.8 fold increase	1.4 fold increase	1.46 fold increase
PYC	-	1.1 fold increase	1.96 fold increase	2.4 fold increase	4.9 fold increase
ICDH	-	No change	No change	No change	No change
ICL	-	No change	No change	No change	No change
GDH	-	1.44 fold increase	1.65 fold increase	2.1 fold increase	1.6 fold increase

The MPS ability in terms of P solubilization index in PVK agar medium was in the order of WT≤Gm<pAB7<pYF<pYC clearly indicating the enhanced effect of both NADH insensitive citrate synthase and citrate transporter over wild type citrate synthase in terms of citric acid secretion. The distribution of glucose between two catabolic pathways: GDH mediated extracellular direct oxidation pathway and intracellular phosphorylative pathway involving active glucose uptake followed by the action of glucokinase and G-6-PDH are responsible for MPS ability of pseudomonads. Higher amount of total glucose utilized and less glucose consumption in *P. fluorescens* PfO-1 (pYC) strain compared to the control correlated with enhanced gluconic acid production and MPS ability. The strain when tested under P limiting condition in buffered TRP medium also showed significant enhancement in MPS phenotype.

The main objective of the present study was to design a stable and broad host range expression system for enhancing citric acid secretion which could provide MPS ability in fluorescent pseudomonads and other PGPR. Considering the stability of the established genetic modification and to test the efficacy in multiple host system the 5th chapter describes the effect of *yc* operon integration into the genome of 6 different *P. fluorescens* strains PfO-1, Pf-5, CHAO-1, ATCC13525 including wheat rhizospheric isolates P109 and Fp315. All these strains are known for bioremediation and biocontrol activities. *P. fluorescens* P109 and Fp315 are reported to possess poor P solubilizing ability. A systematic study was carried out to determine the effects of genomic integration in TRP broth medium and compare with the wild type and plasmid transformants of *yc* operon. MPS phenotype and Pi release of the genomic integrants of all strains were better than the wild type and plasmid bearing strains (**Table 2**). Overexpression of genes using multicopy plasmids can severely burden the host cell by alteration of the energy status of the cell as the resources are diverted towards recombinant protein synthesis and maintenance of the multicopy plasmid and hence overall productivity could be compromised. Therefore, genomic integration results in better effects.

Table 2: Comparative effects of overexpression of *yc* operon plasmid transformants and genomic integrants in *P. fluorescens* PfO-1 and Fp315 grown under TRP minimal medium containing 75 mM glucose as a carbon source.

Parameters	PfO-1		Fp315	
	pYC	pYCInt	pYC	pYCInt
CS activity	2.64 fold increase	3.17fold increase	3.4 fold increase	2.65 fold increase
Intracellular citric acid	5.6 fold increase	4.4 fold increase	5.2 fold increase	4.7 fold increase
Extracellular citric acid	60 fold increase	53 fold increase	77.2 fold increase	80.5 fold increase
Gluconic acid	1.4 fold increase	1.57 fold increase	1.3 fold increase	1.99 fold increase
Acetic acid	UD	UD	UD	UD
Pyruvic acid	UD	UD	UD	UD
Pi release	2 fold increase	2.2 fold increase	2.1 fold increase	2.85 fold increase
Growth rate	No change	No change	No change	1.9 fold increase
Glucose consumed	1.2 fold decrease	1.6 fold decrease	2 fold decrease	1.7 fold decrease
Biomass yield	2.3 fold increase	3.4 fold increase	4.1 fold increase	4.8 fold increase
G6PDH	2 fold decrease	2.1 fold decrease	1.8 fold decrease	1.6 fold decrease
PYC	5.1 fold increase	4.9 fold increase	1.45 fold increase	1.6 fold increase
ICDH	No change	No change	No change	No change
ICL	No change	No change	No change	No change
GDH	1.6 fold increase	2.2 fold increase	1.8 fold decrease	1.6 fold decrease

All parameters are compared with the respective wild type strain

Chapter 6 also describes the effect of genomic integration on growth promotion ability of mung bean plants in alkaline vertisol soil without supplememntation of rock phosphate in green house conditions. All treatments on an average showed a consistent increase in growth to similar extent as the SSP control or in some cases even better. Further, genomic integrants performed better in some parameters than the strain bearing the operon in the plasmid.

In conclusion, the present study illustrates a novel genetic engineering approach of enhancing citric acid secretion and MPS ability by genomic integration of NADH insensitive *E. coli* cs and *S. tphimurium* sodium citrate transporter operon constructed under *lac* promoter in metabolically distinct fluorescent pseudomonads. Genomic integration appears to be a better strategy than plasmid based expression which creates a milestone for getting stable expression system in metabolic engineering studies. Further, genomic integration of yc operon led to enhanced plant growth promotion under P limitation and without supplementation of external rock phosphate by fluorescent pseudomonads. Out of all *P. fluorescens* strain tested, the overall performance of PfO-1 and Fp315 genomic integrants was found to be the best in terms of MPS ability in laboratory condition as well as growth promotion of mung bean in green house. Future prospective will be to test the efficacy of these strains in field condition with multiple host plant under different environmental condition to determine their consistency of P supplementation and other plant growth promotion abilities in agricultural field conditions.

BIBLIOGRAPHY

Bibliography

Aeron, A., Kumar, S., Pandey, P. & Maheshwari, D. K. (2011). Emerging Role of Plant Growth Promoting Rhizobacteria in Agrobiology. *Bacteria in Agrobiology: Crop Ecosystems. (Lakeland)* (D. K. Maheshwari, Ed.). Berlin, Heidelberg: Springer Berlin Heidelberg.

Ajikumar, P. K., Xiao, W. H., Tyo, K. E. J., Wang, Y., Simeon, F., Leonard, E., Mucha, O., Phon, T. H., Pfeifer, B., Stephanopoulos, G. (2010). Isoprenoid pathway optimization for taxol precursor overproduction in *Escherichia coli. Science* **330**, 70-74.

Akhtar, A., Robab, H. M. I. Sharf, A. & Sharf, R. (2012). Plant growth promoting Rhizobacteria : An overview (**2012)**. *J. Nat. Prod. Plant Resour* **2 (1),** 19-31.

Akinterinwa, O. et al. (2008). Metabolic engineering for bioproduction of sugar alcohols. *Curr. Opin. Biotechnol*. **19**, 461–467.

Amarger, N. (2002). Genetically modified bacteria in agriculture. *Biochimie* **84**, 1061–1072.

Ames, B. N. (1966). Assay of inorganic phosphate, total phosphate and phosphatases. *Methods Enzymol* **8**, 115–118.

Anne, M., Ruffing & Rachel-Ruizhen, Chen. (2011). Citrate Stimulates Oligosaccharide Synthesis in Metabolically Engineered *Agrobacterium* sp. *Appl Biochem Biotechnol* **164**, 851–866. DOI 10.1007/s12010-011-9179-1.

Anoop, V. M., Basu, U., McCammon, M.T., McAlister-Henn, L., Taylor, G. J. (2003) Modulation of citrate metabolism alters aluminum tolerance in yeast and transgenic canola overexpressing a mitochondrial citrate synthase. *Plant Physiol* **132**, 2205–2217.

Anthony, J. R., Anthony, L. C., Nowroozi, F., Kwon, G., Newman, J. D. and Keasling, J. D. (2009). Optimization of the mevalonate-based isoprenoid biosynthetic pathway in

Escherichia coli for production of the anti-malarial drug precursor amorpha-4, 11-diene. *Metab Eng* **11,** 13-19.

Aoshima, M., Ishii, M., Yamagishi, A., Oshima, T. & Igarashi, Y. (2003). Metabolic characteristics of an isocitrate dehydrogenase defective derivative of Escherichia coli BL21(DE3). *Biotechnol Bioeng* **84**, 732–737.

Arcand, M. M. & Schneider, K. I. M. D. (2006). Plant- and microbial-based mechanisms to improve the agronomic effectiveness of phosphate rock : a review. *Anais Da Academia rasileira De Ciencias* **78**, 791-807.

Archana, G., Buch, A. & Kumar, G. N. (2012). Microorganisms in Sustainable Agriculture and Biotechnology. *Metabolic Engineering* (T. Satyanarayana & B. N. Johri, Eds.). Dordrecht: Springer Netherlands.

Asadollahi, M. A., Maury, J., Schalk, M., Clark, A. and Nielsen, J. (2010). Enhancement of farnesyl diphosphate pool as direct precursor of sesquiterpenes through metabolic engineering of the mevalonate pathway in *Saccharomyces cerevisiae.Biotechnol Bioeng* **106**, 86-96.

Atsumi, S. and Liao, J. C. (2008). Metabolic engineering for advanced biofuels production from Escherichia coli. *Curr. Opin. Biotechnol.* **19**,414–419.

Babu-Khan, S., Yeo, T. C., Martin, W. L., Duron, M. R., Rogers, R. D. and Goldstein, A. H. (1995). Cloning of a mineral phosphate- solubilizing gene from *Pseudomonas cepacia. Appl Environ Microbiol* **61**,972–978.

Bailey, J. E. (1991). Toward a science of metabolic engineering. *Science* **252**, 1668-1675.

Balbas, P., and Bolivar, F. (1990). Design and construction of expression plasmid vectors in *Escherichia coli. Methods in Enzymology* (D. D. Goeddel, Ed.), Academic Press, San Diego. 14-37

Baldazzi V, Ropers D, Markowicz Y, Kahn D, Geiselmann J, de Jong H. (2010). The carbon assimilation network in *Escherichia coli* is densely connected and largely sign-determined by directions of metabolic fluxes. *PLoS Comput Biol,* **6(6),** e1000812.

Barone, P., Rosellini, D., Lafayette, P., Bouton, J., Veronesi, F. & Parrott, W. (2008). Bacterial citrate synthase expression and soil aluminum tolerance in transgenic alfalfa. *Plant cell reports* **27**, 893-901.

Barth, P. T., N. Datta, R. W. Hedges, and N. J. Grinter (1976). Transposition of a deoxyribonucleíc acid sequence encoding trimethoprim and streptomycin resistances from R483 to other replicons. *J. Bacteriol***. 125**, 800-810.

Basu, A., Apte, S. K. and Phale, P. S. (2006). Preferential utilization of aromatic compounds

Becker J., Zelder, O., Häfner, S., Schröder, H., Wittmann, C. (2011). From zero to hero design-based systems metabolic engineering of *Corynebacterium glutamicum* for l-lysine production. *Metab Eng* **13**:159–168.

Becker, J., Klopprogge, C., Schröder, H. & Wittmann, C. (2009). Metabolic engineering of the tricarboxylic acid cycle for improved lysine production by *Corynebacterium glutamicum*. *Applied and environmental microbiology* **75**, 7866–9.

Becker, J., Zelder, O., Häfner, S., Schröder, H. and Wittmann, C. (2011). From zero to hero-Designbased systems metabolic engineering of *Corynebacterium glutamicum* for L-lysine production. *Metab Eng* **13**, 159–168.

Bhayana, V., and H. W. Duckworth. (1984). Amino acid sequence of Escherichia coli citrate synthase. *Biochemistry* **23**, 2900-2905.

Birnbaum, S., and Bailey, J. E. (1991). Plasmid presence changes the relative levels of many host cell proteins and ribosome components in recombinant *Escherichia coli*. *Biotechnol. Bioeng.* **37**, 736_745.

Bisen, P., Sanodiya, B., Thakur, G., Baghel, R., Prasad, G. (2010). Biodiesel production with special emphasis on lipase-catalyzed transesterification. *Biotechnol Lett* **32**, 1019–1030.

Blankschien, M. D., Clomburg, J. and Gonzalez, R. (2010). Metabolic engineering of Escherichia coli for the production of succinate from glycerol. *Metab Eng* **12**, 409-419.

Blenke, H. M., Ludwig, H., Mäder, U. and Hecker, M-J. (2003). Transcriptional profiling of gene expression in response to glucose in *Bacillus subtilis*: regulation of the central metabolic pathways. *Metab Eng* **5**, 133–149.

Blenke, H. M., Reif, I., Commichau, F. M., Detsch, C., Wacker, I., Ludwig, H. and Stülke, J. (2006). Regulation of citB expression in *Bacillus subtilis*: integration of multiple metabolic signals in the citrate pool and by the general nitrogen regulatory system. *Arch Microbiol*, **185**, 136–146.

Boorsma, A., Michel, E. van der Rest, Lolkema, Jukes S., Konings, W. N. (1996). Secondary Transporters for Citrate and the Mg^{2+} -Citrate Complex in Bacillus subtilis are Homologous Proteins. *J.Bacteriol* **178**, 6216–6222.

Brahmaprakash, G. P. & Sahu, P. K. (2012). Biofertilizers for Sustainability. *Journal of the Indian Institute of Science* **92**.

Buch, A. D., Archana, G. & Kumar, G. N. (2009a). Enhanced citric acid biosynthesis in Pseudomonas fluorescens ATCC 13525 by overexpression of the Escherichia coli citrate synthase gene. *Microbiology (Reading, England)* **155**, 2620–9.

Buch, A. D., Archana, G. & Naresh Kumar, G. (2010b). Broad-host-range plasmid-mediated metabolic perturbations in Pseudomonas fluorescens 13525. *Applied microbiology and biotechnology* **88**, 209–18.

Buch, A., Archana, G. & Naresh Kumar, G. (2009b). Metabolic channeling of glucose towards gluconate in phosphate-solubilizing Pseudomonas aeruginosa P4 under phosphorus deficiency. *Research in microbiology* **159**, 635–42.

Buch, A., Archana, G. & Naresh Kumar, G. (2010a). Heterologous expression of phosphoenolpyruvate carboxylase enhances the phosphate solubilizing ability of fluorescent pseudomonads by altering the glucose catabolism to improve biomass yield. *Bioresource technology* **101**, 679–87.

Burgstaller, W. & Schinner, F. (1993). Leaching of metals by fungi. *J Biotechnol* **27**, 91–116.

Burgstaller, W. (2006). Thermodynamic boundary conditions suggest that a passive transport step suffices for citrate excretion in *Aspergillus* and *Penicillium*. *Microbiology (Reading, England)* **152**, 887–93.

Carmen, B. & Roberto, D. (2006). Soil Bacteria Support and Protect Plants Against Abiotic Stresses. *Management.*

Chartrain, M. et al. (2000). Metabolic engineering and directed evolution for the production of pharmaceuticals. *Curr. Opin. Biotechnol*. **11**, 209–214.

Chavarría, M., Kleijn, R. J., Sauer, U., Pflüger-grau, K. & Lorenzo, V. D. (2012). Regulatory Tasks of the Phosphoenolpyruvate-Phosphotransferase System of *Pseudomonas putida* in Central Carbon Metabolism. *Metabolism Clinical And Experimental* **3**, 1-9.

Chen, Y. P., Rekha, P. D., Arun, A. B., Shen, F. T., Lai and W. A., Young, C. C.(2006). Phosphate solubilizing bacteria from subtropical soil and their tricalcium phosphate solubilizing abilities. *Applied Soil Ecology*, **34** (Suppl 1): 33-41.

Chen, Y.-F., Li, L.-Q., Xu, Q., Kong, Y.-H., Wang, H. & Wu, W.-H. (2009). The WRKY6 transcription factor modulates PHOSPHATE1 expression in response to low Pi stress in Arabidopsis. *The Plant cell* **21**, 3554-66.

Childers, D. L., Corman, J., Edwards, M. & Elser, J. J. (2011). Sustainability Challenges of Phosphorus and Food: Solutions from Closing the Human Phosphorus Cycle. *BioScience* **61**, 117–124.

Choi, K.-H. & Schweizer, H. P. (2006). mini-Tn7 insertion in bacteria with single attTn7 sites: example Pseudomonas aeruginosa. *Nature protocols* **1**, 153-61.

Choi, K.-H. (2009). Applications of Transposon-Based Gene Delivery System in Bacteria. *Journal of Microbiology and Biotechnology* **19**, 217-228.

Choi, Y. J., Bourque, D., Morel, L., Groleau, D. & Mı, C. B. (2006). Multicopy Integration and Expression of Heterologous Genes in Methylobacterium extorquens ATCC 55366 . *Society* **72**, 753-759.

Chou, C. P. (2007). Engineering cell physiology to enhance recombinant protein production in *Escherichia coli. Appl Microbiol Biotechnol* **76**, 521–532. doi:10.1007/s00253-007-1039-0.

Coling, G., Mitchell and P. D. J., Weitzman (1986). Molecular Size Diversity of Citrate Synthases from *Pseudomonas species Journal of' General Microbiology* **132**, 737-742.

Craig, N. L. (1989). Transposon Tn7. D. E. Berg and M. M. Howe (eds.), *Mobile DNA*.Chapter 7, 211-225.American Society for Microbiology, Washington,DC.

Curran, K. & Alper, H. S. (2012). Expanding the chemical palate of cells by combining systems biology and metabolic engineering. *Metabolic engineering* **14**, 289-97).

David, J. Stokell., Lynda, J. Donald.,, Robert Maurus., Nham, T. Nguyen, Gillian Sadler. ,Kajal Choudhary, Philip, G. Hultin., Gary,. D. Brayer, and Harry, W. Duckworth. (2003). Probing the Roles of Key Residues in the Unique Regulatory NADH Binding Site of Type II Citrate Synthase of *Escherichia coli, The Journal of Biological Chemistry* **278**, (37), 35435–35443.

de Leij, F. A. A. M., Thomas, C. E., Bailey, M. J. , Whipps, J. M., Lynch and J. M. (1998). Effect of insertion site and metabolic load on the environmental fitness of a genetically modified Pseudomonas fluorescens isolate. *Appl Environ Microbiol* **64**, 2634–2638.

del Castillo, T., Ramos, J. L., Rodríguez-Herva, J. J., Fuhrer, T., Sauer, U. and Duque, E. (2007). Convergent peripheral pathways catalyze initial glucose catabolism in *Pseudomonas putida*: Genomic and flux analysis. *J. Bacteriol.* **189**(14), 5142-5152.

Dhamankar, H. and Prather, K. L. J. (2011). Microbial chemical factories: recent advances in pathway engineering for synthesis of value added chemicals. *Current Opinion in Structural Biology* **21,** 488–494.

Dharmadi, Y., Murarka, A. and Gonzalez, R. (2006). Anaerobic fermentation of glycerol by Escherichia coli: A new platform for metabolic engineering. *Biotechnology & Bioengeering* **94**, 821–829.

Dimroth, P. (1987). Sodium Ion Transport Decarboxylases and Other Aspects of Sodium Ion Cycling in Bacteria. *Microbiology* **51**, 320–340.

Donald, L. J., and H. W. Duckworth. (1987). Expression and base sequence of the citrate synthase gene of *Acinetobacter anitratum. Biochem. Cell Biol*. **65**, 930-938.

Duan, Y. X., Chen, T., Chen, X. and Zhao, X. M. (2010). Overexpression of glucose-6-phosphate dehydrogenase enhances riboflavin production in *Bacillus subtilis*. *Appl Microbiol Biotechnol* **85**, 1907–1914.

Duckworth, H. W., and Tong, E. K. (1976). *Biochemistry **15***, 108-114.

Dutta, S. & Podile, A. R. (2010). Plant growth promoting rhizobacteria (PGPR): the bugs to debug the root zone. *Critical reviews in microbiology* **36**, 232–44.

Frankel, D.G. (1996). Glycolysis. In: *Escherichia coli* and *Salmonella tiphymurium*: Cellular and Molecular Biology. 2nd edition. Edited by Neidhardt, F.C. ASM Press, Washington, DC, 189–196.

Fuhrer, T., Fischer E. and Sauer, U. (2005). Experimental identification and quantification of glucose metabolism in seven bacterial species. J. Bacteriol.**187**, 1581–1590.

Fujita, Y. (2009). Carbon Catabolite Control of the Metabolic Network in *Bacillus subtilis*. *Bioscience, Biotechnology, and Biochemistry* **73**, 245–259.

Furukawa, J., Yamaji, N., Wang, H., Mitani, N., Murata, Y., Sato, K., Katsuhara, M., Takeda, K. & Ma, J. F. (2007). An aluminum-activated citrate transporter in barley. *Plant & cell physiology* **48**, 1081–91.

Gallmetzer, M. & Burgstaller, W. (2001). Citrate efflux in glucoselimited and glucose-sufficient chemostat culture of Penicillium simplicissimum. *Antonie van Leeuwenhoek* **79**, 81–87.

Glick, B. R. (1995). Metabolic load and heterologous gene expression. *Biotechnol Adv* **13**, 247–261. doi:10.1016/0734-9750(95)00004-A.

Goldstein, A. H., Braverman, K. E. and Osorio, N. (1999). Evidence for mutualism between a plant growing in a phosphatelimited desert environment and a mineral phosphate solubilizing (MPS) rhizobacteria. *FEMS Microbiol. Ecol.* **30**, 295–300.

Goldstein, A. H. and Liu, S-T. (1987). Molecular cloning and regulation of a mineral phosphate solubilizing gene from Erwinia herbicola. *Bio/Technology* **5**, 72–74.

Goldstein, A. H. & Krishnaraj, P. U. (2007). Phosphate solubilizing microorganisms vs . phosphate mobilizing microorganisms : What separates a phenotype from a trait ? E. Vela,´ zquez and C. Rodrı´guez-Barrueco (eds.), First International Meeting on Microbial Phosphate Solubilization, 203–213.

Goldstein, A. H. (1986). Bacterial mineral phosphate solubilization: Historical perspective and future prospects. *Am J. Alt.Agric*. **1**, 57–65.

Goldstein, A. H. (1995). Recent progress in understanding the molecular genetics and biochemistry of calcium phosphate solubilization by gram negative bacteria. *Biol. Agric. Hortic*. **12**, 185–193.

Goosen, N., Horsman, H. P., Huinen, R. G. and van de Putte, P. (1989). *Acinetobacter calcoaceticus* genes involved in biosynthesis of the coenzyme pyrrolo-quinoline-quinone nucleotide sequence and expression in *Escherichia coli* K-12. *J. Bacteriol*. **171,** 447–455.

Görke, B. & Stülke, J. (2008). Carbon catabolite repression in bacteria: many ways to make the most out of nutrients. *Nature reviews Microbiology* **6**, 613–24.

Gringauz, E., K. A. Orle, C. S. Waddell, and N. L. Craig (1988). Recognition of Escherichia coli attTn7 by transposon Tn7: Lack of specific sequence requirements at the point of Tn7 insertion. *J. Bacteriol*. **170**, 2832-2840.

Gururani, M. A., Upadhyaya, C. P., Baskar, V., Venkatesh, J., Nookaraju, A. & Park, S. W. (2012). Plant Growth-Promoting Rhizobacteria Enhance Abiotic Stress Tolerance in Solanum tuberosum Through Inducing Changes in the Expression of ROS-Scavenging Enzymes and Improved Photosynthetic Performance. *Journal of Plant Growth Regulation.*

Gyaneshwar, P., Naresh Kumar, G., Parekh, L. J. & Poole, P. S. **(2002**). Role of soil microorganisms in improving P nutrition of plants. *Plant Soil* **245**, 83–93.

Gyaneshwar, P., Parekh, L. J., Archana, G., Poole, P. S., Collins, M. D., Hutson, R.A. and Naresh Kumar, G. (1999) Involvement of a phosphate starvation inducible glucose dehydrogenase in soil phosphate solubilization by *Enterobacter asburiae*. *FEMS Microbiol. Lett*. **177**, 223-229.

Hamel, R. D. and Appanna, V. D. (2001). Modulation of TCA cycle enzymes and aluminum stress in *Pseudomonas fluorescens*. *J. Inorg. Biochem*. **87**(1-2), 1-8.

Han, H. S. & Lee, K. D. (2005). Plant Growth Promoting Rhizobacteria Effect on Antioxidant Status , Photosynthesis , Mineral Uptake and Growth of Lettuce under Soil Salinity. *Stress: The International Journal on the Biology of Stress* **1**, 210-215.

Han, S. H., Kim, C. H., Lee, J. H., Park, J. Y., Cho, S. M., Park, S. K. , Kim, K. Y., Krishnan, H. B. and Kim, Y. C. (2008). Inactivation of *pqq* genes of *Enterobacter intermedium* 60–2Greduces antifungal activity and induction of systemic resistance. *FEMS Microbiol. Lett.* **282**, 140–146.

Hansen, E. H., Moller, B. L., Kock, G. R., Bunner, C. M., Kristensen, C., Jensen, O. R., Okkels, F. T., Olsen, C. E., Motawia, M. S. Hansen, J. (2009). De novo biosynthesis of vanillin in fission yeast Schizosaccharomyces pombe) and Baker's yeast (*Saccharomyces cerevisiae*).*Appl Environ Microbiol* **75,** 2765-2774.

Hansen, E. J. and Juni, E. (1974). Two routes for synthesis of phosphoenolpyruvate from C4-dicarboxylic acids in *Escherichia coli. Biochem. Biophys. Res. Commun.* **59,** 1204–1210.

Higa, A. I., E. Massarini, and J. J. Cazzulo. (1978). Purification and some properties of the citrate synthase from a marine Pseudomonas. *Can. J. Microbiol*. **24**, 215-221.

Hilda, R. and Fraga, R. (1999). Phosphate solubilizing bacteria and their role in plant growth promotion. *Biotechnol. Adv.* **17**, 319–359.

Hodgson D. A. (2000). Primary metabolism and its control in streptomycetes: a most unusual group of bacteria**.** *Adv Microb Physiol* **42,** 47–238.

Holguin, G.,Glick, B. R. (2001). ExpressionoftheACCdeaminase gene from Enterobacter cloacae UW4 in Azospirillum brasilense. *MicrobialEcol* **4**, 281–8.

Inui, M., Suda, M., Okino, S., Nonaka, H., Puskas, L. G., Vertes, A. A. and Yukawa, H. (2007). Transcriptional profiling of Corynebacterium glutamicum metabolism during organic acid production under oxygen deprivation conditions. *Microbiology* **153**, 2491–2504.

Ishiguro, N., H. Izawa, M. Shinagawa, T. Shimamoto, and T. Tsuchiya.(1992). Cloning and nucleotide sequence of the gene (*citC*) encoding a citrate carrier from several *Salmonella* serovars. *J. Biol. Chem*. **267:**9559–9564.

Iuchi, S., Cole, S. T. and Lin, E. C. (1990). Multiple regulatory elements for the glpA operon encoding anaerobic glycerol-3-phosphate dehydrogenase and the glpD operon encoding aerobic glycerol-3-phosphate dehydrogenase in Escherichia coli: further characterization of respiratory control. *J Bacteriol* **172**, 179–184.

James Elser, Elena Bennett. (2011). A broken biogeochemical cycle. *Nature* **478**, 29-31.

Jiang, L., Althoff, E. A., Clemente, F. R., Doyle, L., Rothlisberger, D., Zanghellini, A., Gallaher, J. L., Betker, J. L., Tanaka, F., BarbasIII, C. F., Hilvert, D., Houk, K. N. and Stoddard, B. L., Baker,D. (2008). De novo computational designofretro-aldol enzymes. *Science* **319**,138 7–1391.

Joardar, V., et al. (2005). Whole-genome sequence analysis of *Pseudomonas syringae pv. Phaseolicola* 1448A reveals divergence among pathovars in genes involved in virulence and transposition. *J. Bacteriol*. **187** (18), 6488-6498

Jones, K. L., Kim, S.-won & Keasling, J. D. (2000). Low-Copy Plasmids can Perform as Well as or Better Than High-Copy Plasmids for Metabolic Engineering of Bacteria. *Metabolic Engineering* **338**.

Julie, A. Francois, Courtney, M., Starks, Sasitorn, Sivanuntakorn, Hong, Jiang, Aaron, E. Ransome, Jeong-Won, Nam.,, Charles Z., Constantine, T. and Joseph Kappock (2006), Structure of a NADH-Insensitive Hexameric Citrate Synthase that Resists Acid Inactivation *Biochemistry* **45**, 13487-13499.

Kadir, T. A. .A, Mannan, A. A., Kierzek, A. M., McFadden, J. and Shimizy, K. (2010). Modeling and simulation of the main metabolism in *Escherichia coli* and its several single-gene knockout mutants with experimental verification. *Microb Cell Fact* **9**:88.

Kästner, C. N. & Dimroth, P. (2000). The Na + -dependent citrate carrier of Klebsiella pneumoniae : high-level expression and site-directed mutagenesis of asparagine-185 and glutamate-194. 67-73.

Kathleen A., Curran and Hal, S., Alper (2012). Expanding the chemical palate of cells by combining systems biology and metabolic engineering. *Metabolic Engineering* **14**, 289–297.

Khan, A. A., Jilani, G., Akhtar, M. S., Saqlan, S. M. & Rasheed, M. (2009). Phosphorus Solubilizing Bacteria: Occurrence, Mechanisms and their Role in Crop Production. *Agriculture* **1**, 48–58.

Khan, M. S., Zaidi, A. & Wani, P. A. (2007). Role of phosphatesolubilizing microorganisms in sustainable agriculture – a review. *Agron Sustain Dev* **27**, 29–43.

Khan, M. S., Zaidi, A. & Wani, P. A. (2009). Role of Phosphate Solubilizing Microorganisms in Sustainable Agriculture – A Review. *Sustainable Agriculture*, DOI 10.1007/978-90-481-2666-8-34.

Khan, M. S., Zaidi, A. and Wani, P. A. (2006). Role of phosphate-solubilizing microorganisms in sustainable agriculture–A review. *Agron. Sustain. Dev*. **26**, 1-15.

Kim, Y. M., Cho, H. S., Jung, G. Y. and Park, J. M. (2011). Engineering the pentose phosphate pathway to improve hydrogen yield in recombinant *Escherichia coli*. *Biotechnol Bioeng* **108**, 2941–2946.

Koch, B., Jensen, L. E. & Nybroe, O. (2001). A panel of Tn7-based vectors for insertion of the gfp marker gene or for delivery of cloned DNA into Gram-negative bacteria at a neutral chromosomal site. *Journal of Microbiological Methods.*

Koffas, M. A. G., Jung, G. Y., Aon, J. C. and Stephanopoulos, G. (2002). Effect of pyruvate carboxylase overexpression on the physiology of *Corynobacterium glutamicum*. *Appl Environ Microbiol* **68**:5422–5428.

Konings, W. N., J. S. Lolkema and B. Poolman. (1995). The generation of metabolic energy by solute transport. Arch. Microbiol. **164,** 235–242.

Koyama, H., Kawamura, A., Kihar, T., Hara, T., Takita, E. and Shibata D (2000) Overexpression of mitochondrial citrate synthase in Arabidopsis thaliana improved growth on a phosphorus limited soil. *Plant Cell Physiol* **41**,1030–1037.

Koyama, H., Takita, E., Kawamura, A., Hara, T. and Shibata, D. (1999) Overexpression of mitochondrial citrate synthase gene improves the growth of carrot cells in Al-phosphate medium. *Plant Cell Physiol* **40**, 482–488.

Kuo, H.-F. & Chiou, T.-J. (2011). The role of microRNAs in phosphorus deficiency signaling. *Plant physiology* **156**, 1016-24.

Lambertsen, L., Sternberg, C. & Molin, S. (2004). Mini-Tn7 transposons for site-specific tagging of bacteria with fluorescent proteins. *Environmental microbiology* **6**, 726-32.

Lee, D. G., Urbach, J. M., Wu, G., Liberati, N. T., Feinbaum, R. L., Miyata, S., Diggins, L. T., He, J., Saucier, M., Deziel, E., Friedman, L., Li, L., Grills, G., Montgomery, K., Kucherlapati, R., Rahme, L.G. and Ausubel, F. M. (2006). Genomic analysis reveals that *Pseudomonas aeruginosa* virulence is combinatorial. *Genome Biol*. **7**(10), R90.

Lee, E. G., Yoon, S. H., Das, A., Lee, S. H,, Li, C., Kim, J. Y., Choi, M. S., Oh, D. K. and Kim, S. W. (2009). Directing vanillin production from ferulic acid by increased acetyl-CoA consumption in recombinant *Escherichia coli*. *Biotechnol Bioeng* **102 (**13.), 200-208.

Lee, K. H. et al. (2007). Systems metabolic engineering of *Escherichia coli* for Lthreonine production. *Mol. Syst. Biol*. **3**, 149.

Lee, S. J. et al. (2006). Genome-based metabolic engineering of Mannheimia succiniciproducens for succinic acid production. *Appl. Environ. Microbiol*.**72**, 1939–1948.

Lee, S. Y. and Papoutsakis, E. T. (1999). *Metabolic Engineering*. Marcel Dekker

Lee, S. Y. et al. (2005). Systems biotechnology for strain improvement. *Trends Biotechnol*.**23**, 349–358.

Lessie, T. G. and Phibbs, P. V. Jr. (1984). Alternative pathways of carbohydrate utilization in pseudomonads. *Annu. Rev. Microbiol*. **38**, 359–388.

Li, H. & Pajor, a M. (2002). Functional characterization of CitM, the Mg2+-citrate transporter. *The Journal of membrane biology* **185**, 9-16.

Li, R., Townsend, C. A. (2006). Rational strain improvement for enhanced clavulanic acid production by genetic engineering. *Metab Eng* **8,** 240–252.

Lichtenstein, C. and S. Brenner (1981). Site-specific properties of Tn7 transposition into the *E. coli* chromosome. *Mol. Gen. Genet*. **183** , 380-387.

Liu ST, Lee LY, Tai CY, Hung CH, Chang YS, Wolfram JH, Rogers R and Goldstein AH (1992). Cloning of an *Erwinia herbicola* gene necessary for gluconic acid production and enhanced mineral phosphate solubilization in *Escherichia coli* HB101 nucleotide sequence and probable involvement in biosynthesis of the coenzyme pyrroloquinoline quinine. *J. Bacteriol*. **174**, 5814–5819

Liu, T. S., Lee, L. Y., Tai, C. Y., Hung, C. H., Chang, Y. S., Wolfram, J. H., Rogers, R. and Goldstein, A. H. (1992). Cloning of an *Erwinia herbicola* gene necessary for gluconic acid production and enhanced mineral phosphate solubilization in *Escherichia coli HB101*: Nucleotide sequence and probable involvement in biosynthesis of the coenzyme pyrroloquinoline quinone. *J Bacteriol* **174**, 5814–9.

Lolkema, J. S., H. Enquist, and M. E. van der Rest. (1994). Transport of citrate catalyzed by the sodium-dependent citrate carrier of *Klebsiella pneumonia* is obligatory coupled to the transport of two sodium ions. *Eur.J. Biochem*. **220,** 469–475.

Luesink, E. J., van Herpen, R. E., Grossiord, B. P., Kuipers, O. P. and de Vos W. M. (1998). Transcriptional activation of the glycolytic *las* operon and catabolite repression of the *gal* operon in *Lactococcus lactis* are mediated by the catabolite control protein CcpA. *Mol Microbiol,* **30:**789–798.

Lugtenberg, B. and Kamilova, F. (2009). Plantgrowth- promoting rhizobacteria. Annu. Rev. Microbiol. 63, 541–556.

M. do Vale Barreto Figueiredo, Seldin, L., Araujo, F. F. and Mariano R.L.R. (2010). Plant Growth and Health Promoting Bacteria. *Growth (Lakeland)* **18**, 21–44 (D. K. Maheshwari, Ed.). Berlin, Heidelberg: Springer Berlin Heidelberg.

MacGregor, C. H., Wolff, J. A., Arora, S. K., Hylemon, P. B. and Phibbs. P. V. (1992) Catabolite repression control in *Pseudomonas aeruginosa*. , *Pseudomonas molecular biology and biotechnology*. American Society for Microbiology, Washington, D.C. E. Galli, S. Silver, and B. Witholt (ed.), 198–206.

Martin, C. H, Nielsen, D. R., Solomon, K. V. and Prather, K. L. J. (2009). Synthetic metabolism: engineering biology at the protein and pathway scales. *Chem Biol* **16**:277.

Martin, R., Beat R., Katharina, Noh., Wolfgang, W., Sauer,U. and Zamboni N., (2012).Collisional Fragmentation of Central Carbon Metabolites in LC-MS/MS Increases Precision of 13C Metabolic Flux Analysis. *Biotechnology and Bioengineering* **109**,(3)

Martínez-gómez, K. *et al.* (2012). New insights into *Escherichia coli* metabolism : carbon scavenging, acetate metabolism and carbon recycling responses during growth on glycerol. *Microbial Cell Factories* **11,** 1-21.

Marty-Teysset, C., C. Posthuma, J. S. Lolkema, P. Schmitt, C. Divies, and W. N. Konings. (1996). Proton motive force generation by citrolactic fermentation in *Leuconostoc esenteroides*. *J. Bacteriol*. **178,** 2178–2185.

Massarini, E., and J. J. Cazzulo. (1975). Two forms of citrate synthase in a marine pseudomonad. *FEBS Lett.* **57**, 134-138.

Max Chavarría, A., Roelco, J., Kleijn,B., Sauer, U., Katharina, Pflüger-Grau, B. and Víctor de Lorenzoa (2012). Regulatory Tasks of the Phosphoenolpyruvate-Phosphotransferase System of *Pseudomonas putida* in Central Carbon Metabolism. *Mbio.*

Misra, H. S., Rajpurohit, Y. S. & Khairnar, N. P. (2012). Pyrroloquinoline-quinone and its versatile roles in biological processes. *Journal of Biosciences* **37**, 313-325.

Mlakar, T. and Legiša, M. (2006). Citrate inhibition-resistant form of 6-Phosphofructo-1-Kinase from *Aspergillus niger*. *Appl. Environ. Microbiol*. **72**(7)**,** 4515–4521.

Moon, T. S., Dueber, J. E., Shiue, E. and Prather, K. L. J. (2010). Use of modular,synthetic scaffolds for improved production of glucaric acid in engineered *E. coli*. *Metab Eng* **12**,298.

Morrissey, J. P., Walsh, O Donnell, U. F. A., Moenne-Loccoz, Y. and O_Gara, F. (2002). Exploitation of genetically modified inoculants for industrial ecology applications. *Antonie van Leeuwenhoek* **81**, 599–606.

Nelson, K. E., et al. (2002). Complete genome sequence and comparative analysis of the metabolically versatile *Pseudomonas putida* KT2440. *Environ. Microbiol*.**4** (12), 799-808

Ner, S. S., V. Bhayana, A. W. Bell, I. G. Giles, H. W.Duckworth, and D. P. Bloxham. (1983). Complete sequence of the gltA gene encoding citrate synthase in *Escherichia coli*. *Biochemistry* **22**, 5243-5249.

Nešvera, J. & Pátek, M. (2011). Tools for genetic manipulations in Corynebacterium glutamicum and their applications. *Applied microbiology and biotechnology* **90**, 1641-54.

Netik, A., Torres, N. V., Riol, J.-M. & Kubicek, C. P. (1997). Uptake and export of citric acid by Aspergillus niger is reciprocally regulated by manganese ions. *Biochim Biophys Acta* **1326**, 287–294.

Nielsen, J. (1997). Physiological engineering. In Physiological Engineering Aspects of Penicillium chrysogenum. Nielsen, J., ed., *World Scientific*, 23–62,

Nielsen, J. (2011). Transcriptional control of metabolic fluxes. *Mol Syst Biol* **7**, 478.

Nogales, J., Palssøn B. O. and Thiele, I. (2008). A genome-scale metabolic reconstruction of *Pseudomonas putida* KT2440: iJN746 as a cell factory. *BMC Syst. Biol*. **2**:79.

O'Connor, M., Peifer, M., and Bender, W. (1989). Construction of large DNA segments in *Escherichia coli. Science* **244**, 1307_1312.

Oh, M. K., Liao, J. C. (2000). Gene expression profiling by DNA microarrays and metabolic fluxes in *Escherichia coli. Biotechnol Prog* **16**, 278–286.

Ohkama-Ohtsu, N. & Wasaki, J. (2010). Recent progress in plant nutrition research: cross-talk between nutrients, plant physiology and soil microorganisms. *Plant & cell physiology* **51**, 1255-64.

Ow, D. S. W., Nissom, P. M., Philp, R., Oh. S. K. W., Yap, M. G. S. (2006). Global transcriptional analysis of metabolic burden due to plasmid maintenance in Escherichia coli DH5 during batch fermentation. Enzyme Microb Technol **39**, 391–398. doi:10.1016/j.enzmictec.2005.11.048.

Papagianni, M. & Avramidis, N. (2011).Lactococcus lactis as a cell factory: a twofold increase in phosphofructokinase activity results in a proportional increase in specific rates of glucose uptake and lactate formation. *Enzyme and microbial technology* **49**, 197-202.

Papagianni, M. & Avramidis, N. **(2012).** Engineering the central pathways in Lactococcus lactis: functional expression of the phosphofructokinase (pfk) and alternative oxidase (aox1) genes from Aspergillus niger in Lactococcus lactis facilitates improved carbon conversion rates under oxidizing c. *Enzyme and microbial technology* **51**, 125-30.

Papagianni, M. (2012). Recent advances in engineering the central carbon metabolism of industrially important bacteria. *Microbial cell factories* **11**, 50.

Papagianni, M., Avramidis, N. and Filiousis, G. (2007). Glycolysis and the regulation of glucose transport in Lactococcus lactis spp. lactis in batch and fed-batch culture**.** *Microb Cell Fact* **6**.

Park, J. H. and Lee, S. Y. (2008). Towards systems metabolic engineering of microorganisms for amino acid production. *Curr. Opin. Biotechnol*. **19,** 454–460

Park, J. H. et al. (2007). Metabolic engineering of Escherichia coli for the production of L-valine based on transcriptome analysis and in silico gene knockout simulation. *Proc. Natl. Acad. Sci.* U. S. A. **104**, 7797–7802.

Park, J. H. et al. (2007). Metabolic engineering of Escherichia coli for the production of L-valine based on transcriptome analysis and in silico gene knockout simulation. *Proc. Natl. Acad. Sci.* U. S. A. **104**, 7797–7802.

Park, J. H. et al. (2008). Application of systems biology for bioprocess development. *Trends Biotechnol.* **26**, 404–412.

Park, S.-J., Mccabe, J., Turana, J. & Gunsalus, R. P. (1994). Regulation of the citrate synthase (*gltA*) gene of *Escherichia coli* in response to anaerobiosis and carbon supply: role of the arcA gene product. *J Bacteriol* **176**, 5086–5092.

Peters, J. E. & Craig, N. L. (2001). Tn7 : Smarter Than we thought. *Cell* **2**, 806-814.

Plaxton, W. C. & Tran, H. T. (2011). Metabolic adaptations of phosphate-starved plants. *Plant physiology* **156**, 1006-15.

Prather, K. L. J. and Martin, C. H. (2008). De novo biosynthetic pathways:rational design of microbial chemical factories. *Curr Opin Biotechnol* **19**:468.

Preston, G. M. (2004). Plant perceptions of plant growth-promoting *Pseudomonas*. *Phil.Trans. R. Soc.* Lond. B. **359**, 907–918.

Puchalka, J., et al. (2008). Genome-scale reconstruction and analysis of the *Pseudomonas putida* KT2440 metabolic network facilitates applications in biotechnology. *PLoS Comput.* Biol. **4**:e1000210.

Qian, Z. G., Xia, X. X. and Lee, S. Y. (2009). Metabolic engineering of Escherichia coli for the production of putrescine: a four carbon diamine. *Biotechnol Bioeng* **104**, 651-662.

Qian, Z. G., Xia, X. X. and Lee, S. Y. (2011). Metabolic engineering of Escherichia coli for the production of cadaverine: a five carbon diamine.*Biotechnol Bioeng* **108**:93-103.

Raab, A. M., Gebhardt, G., Bolotina, N., Weuster-Botz, D. and Lang, C. (2010). Metabolic engineering of Saccharomyces cerevisiae for the biotechnological production of succinic acid. *Metab Eng* **12**, 518-525..

Ramos, A., B. Poolman, H. Santos, J. S. Lolkema, and W. N. Konings. (1994).Uniport of anionic citrate and proton consumption in *Leuconostoc oenos*. *J.Bacteriol*. **176:**4899–4905.

Ramos, C., L. Mølbak and S. Molin (2000). Bacterial activity in the rhizosphere analyzed at the single-cell level by monitoring ribosome contents and synthesis rates. *Appl. Environ. Microbiol*. **66**, 801-809.

Rampioni, G., Leoni, L., Pietrangeli, B. & Zennaro, E. (2008). The interplay of StyR and IHF regulates substrate-dependent induction and carbon catabolite repression of styrene catabolism genes in *Pseudomonas fluorescens* ST. *BMC Microbiol* **8:** 92.

Richardson, A. E. & Simpson, R. J. (2011). Soil microorganisms mediating phosphorus availability update on microbial phosphorus. *Plant physiology* **156**, 989–96.

Robert Maurus, Nham T. Nguyen, David J. Stokell, Ayeda Ayed, Philip G. Hultin, Harry W. Duckworth and Gary D. Brayer.(2003). Insights into the evolution of allosteric properties: the NADH binding site of hexameric type II Citrate Synthases**.** *Biochemistry* **42**, 5555-5565.

Rodríguez, H., Fraga, R., Gonzalez, T. & Bashan, Y. (2006). Genetics of phosphate solubilization and its potential applications for improving plant growth-promoting bacteria. *Plant and Soil* **287**, 15–21.

Rodríguez, H., Fraga, R., Gonzalez, T. and Bashan, Y. (2006). Genetics of phosphate solubilization and its potential applications for improving plant growth-promoting bacteria. *Plant and Soil* **287**(1-2), 15-21.

Rogers, M., N. Ekaterinaki, E. Nimmo, and D. Sherratt (1986). Analysis of Tn7 transposition. *Mol. Gen. Genet*. **205**, 550-556.

Rojo, F. (2010). Carbon catabolite repression in Pseudomonas : optimizing metabolic versatility and interactions with the environment. *FEMS microbiology reviews* **34**, 658–84.

Roos, W. & Slavik, J. (1987). Intracellular pH topography of Penicillium cyclopium protoplasts. Maintenance of delta pH by both passive and active mechanisms. *Biochim Biophys Acta* **899,** 67–75.

Rozkov, A., Avignone-Rossa, C. A., Ert, P. F., Jones, P., O'Kennedy, R. D.,Smith ,J. J., Dale, J. W., Bushell, M. E. (2004) Characterization of the metabolic burden on *Escherichia coli* DH1 cells imposed by the presence of a plasmid containing a gene therapy sequence. *Biotechnol Bioeng* **88**, 909–915. doi:10.1002/bit.20327.

Ruijter, G. J. G., Kubicek, C. P. & Visser, J. (2002). Production of organic acids by fungi. In *The Mycota*l., *Industrial Applications.* Edited by H. D. Osiewacz. Berlin: Springer. **X** ,213–230.

Ryan, P. R., Tyerman, S. D., Sasaki, T., Furuichi, T., Yamamoto, Y., Zhang, W. H. & Delhaize, E. (2011). The identification of aluminium-resistance genes provides opportunities for enhancing crop production on acid soils. *Journal of experimental botany* **62**, 9-20.

Ryu, Y.-G., Butler, M. J., Chater, K. F. & Lee, K. J. (2006). Engineering of primary carbohydrate metabolism for increased production of actinorhodin in Streptomyces coelicolor. *Applied and environmental microbiology* **72**, 7132–9.

Saharan, B. S. & Nehra, V. (2011). Plant Growth Promoting Rhizobacteria : A Critical Review. *Life Sciences* **2011**, 1–30.

Sambrook, J. & Russell, D. W. (2001). Molecular Cloning: a Laboratory Manual, 3rd edn. Cold Spring Harbor, NY: Cold Spring Harbor Laboratory.

Sarma, M. V. R. K., Saharan, K., Prakash, A., Bisaria, V. S. & Sahai, V. (2009). Application of fluorescent Pseudomonads Inoculant Formulations on *Vigna mungo* through Field Trial. *Engineering and Technology*.

Sashidhar, B. and Podile, A. R. (2010). Mineral phosphate solubilization by rhizosphere bacteria and scope for manipulation of the direct oxidation pathway involving glucose dehydrogenase. *J. Appl. Microbiol*. **109,** 1–12.

Sauer, U., and Eikmanns, B. (2005). The PEP-pyruvate-oxaloacetate node as the switch point for carbon flux distribution in bacteria. *FEMS Microbiol Rev*, **29**:765.

Sauer, U., Cameron, D. C. and Bailey, J. E. (1998). Metabolic capacity of *Bacillus subtilis* for the production of purine nucleosides, riboflavin, and folic acid. *Biotechnol Bioeng* **59**, 227–238.

Sauer, U., Hatzimanikatis, V., Bailey, J. E., Hochuli ,M., Szyperski, T. and Wüthrich, K. (1997). Metabolicfluxes in riboflavin-producing *Bacillus subtilis*. *Nature Biotechnol*, 15:448–452.

Schleissner, C., Reglero, A. and Luengo, J. M. (1997). Catabolism of D-glucose by *Pseudomonas putida* U occurs via extracellular transformation into D-gluconic acid and induction of a specific gluconate transport system. *Microbiol.* **143**, 1595-1603.

Schmidt-Eisenlohr, H. and Baron, C. (2003). The competitiveness of Pseudomonas chlororaphis carrying pJP4 is reduced in the Arabidopsis thaliana rhizosphere. *Appl Environ Microbiol* **69**, 1827–1831. doi:10.1128/AEM.69.3.1827-1831.2003.

Sharma, V., Archana, G. & Kumar, G. N. (2011). Plasmid load adversely affects growth and gluconic acid secretion ability of mineral phosphate- solubilizing rhizospheric bacterium Enterobacter asburiae PSI3 under P limited conditions. *Microbiological Research* **166**, 36–46. Elsevier.

Shiloach, J. and Rinas, U. (2009). Glucose and acetate metabolism in *E. coli*- System level analysis and biotechnological applications in protein production processes. *Systems Biology*

and Biotechnology of Escherichia coli. Edited by Lee SY. Dordrecht: Springer Science and Bussiness Media B.V, 377–400.

Sonenshein A. L. (2007). Control of key metabolic intersections in Bacillus subtilis. *Nat. Rev. Microbiol*. **5**, 917-927**.**

Srivastava, S., Kausalya, M. T., Archana, G., Rupela, O. P. & Naresh Kumar, G. (2006). Efficacy of organic acid secreting bacteria in solubilization of rock phosphate in acidic alfisols. In First International Meeting on Microbial Phosphate Solubilization. Series:Developments in Plant and Soil Sciences, Edited by E. Velazquez & C. Rodriguez-Barrueco. Berlin: Springer **102**, 117–124.

Stephanopoulos, G., Aristodou, A. and Nielsen. J. (1998). *Metabolic engineering*. London, UK: Academic Press.

Stover, C. K. et al. (2000). Complete genome sequence of *Pseudomonas aeruginosa* PA01, an opportunistic pathogen. *Nature* **406**, 959-964

Swanson, B. L., Hager, P., Phibbs, P. V. Jr., Ochsner, U., Vasil, M. L. and Hamood, A. N. (2000). Characterization of the 2-ketogluconate utilization operon in *Pseudomonas aeruginosa* PAO1. *Mol. Microbiol*. **37**(3), 561-573.

Tian-rong, G. U. O., Peng-cheng, Y. A. O., Zi-dong, Z. H., Jiang-jia, W. A. N. G. & Mei, W. A. N. G. (2012). Devolvement of Antioxidative Defense System in Rice Growing Seedlings Exposed to Aluminum Toxicity and Phosphorus Deficiency. *Changes* **19**.

Trantas, E., Panopoulos, N. and Ververidis, F. (2009). Metabolic engineering of the complete pathway leading to heterologous biosynthesis of various flavonoids and stilbenoids in Saccharomyces cerevisiae. *Metab Eng* **11**, 355-366.

Tseng, H. C., Harwell, C., Martin, C. and Prather, K. (**2010).** Biosynthesis of chiral 3-hydroxyvalerate from single propionate-unrelated carbon sources in metabolically engineered *E. coli*. *Microb Cell Factories* **9**:96.

Tseng, H. C., Martin, C. H., Nielsen, D. R. and Prather, K. L. (2009). Metabolic engineering of Escherichia coli for enhanced production of (R)- and (S)-3-hydroxybutyrate. *Appl Environ Microbio,* **75**, 3137-3145.

van der Rest, M. E., T. Abee, D. Molenaar, and W. N. Konings. (1991). Mechanism and energetics of a citrate transport system of *Klebsiella pneumoniae*. *Eur. J. Biochem*. **195:**71–77.

Van Dijken, J. P. and Quayle, J. R. (1977). Fructose metabolism in four *Pseudomonas* species. *Arch. Microbiol*. **114**:281–286.

Van Straaten P. (2002). Rocks for Crops: Agrominerals of sub-Saharan Africa. Nairobi, Kenya: ICRAF, 338.

Van Vuuren, D. P., Bouwman, a. F. & Beusen, a. H. W. (2010). Phosphorus demand for the 1970–2100 period: A scenario analysis of resource depletion. *Global Environmental Change* **20**, 428–439. Elsevier Ltd.

Vassilev, N., Eichler-Löbermann, B. & Vassileva, M. (2012). Stress-tolerant P-solubilizing microorganisms. *Applied microbiology and biotechnology* 851-859.

Vassilev, N., Vassileva, M. & Nikolaeva, I. (2006). Simultaneous P-solubilizing and biocontrol activity of microorganisms: potentials and future trends. *Applied microbiology and biotechnology* **71**, 137-44.

Vassilev, N., Vassileva, M. (2003). Biotechnological solubilization of rock phosphate on media containing agro-industrial wastes. *Appl.Microbiol. Biotechnol*. **61**, 435–440.

Vasudevan, P. and Briggs, M. (2008). Biodiesel production−current state of the art and challenges. *J Ind Microbiol Biotechnol* **35**, 421–430.

Velázquez F, di Bartolo I, de Lorenzo V. 2004. Genetic evidence that catabolites of the Entner Doudoroff pathway signalCsource repression of the sigma54 *Pu* promoter of *Pseudomonas putida*. *J. Bacteriol*. **186**, 8267–8275.

Vind, J., Sorensen, M. A., Rasmussen, M. D., and Pedersen, S. (1993). Synthesis of proteins in Escherichia coli is limited by the concentration of free ribosomes. *J. Mol. Biol.* **231**, 678_688.

Viveros –Martinez, O., Jorquera, M. A., Crowley, D. E., Gajardo, G. & Mora, M. L. (2010). Mechanism and practical consideration involved in plant growth promotion **10**, 293–319.

Vogler, A. P, S. Trentmann, J. W. Lengeler (1989). Alternative route for biosynthesis of amino sugars in Escherichia coli K-12 mutants by means of a catabolic isomerase. *J. Bacteriol*. **171**, 6586-6592.

Wang, Z., Chen, T., Ma, X., Shen, Z. and Zhao, X. (2011). Enhancement of riboflavin production with *Bacillus subtilis* by expression and site-directed mutagenesis of *zwf* and *gnd* gene from *Corynebacterium glutamicum*. *Biores Technol* **102**, 3934–3940.

Wang, Z., Xiang, L., Shao, J., Węgrzyn, A., Węgrzyn, G. (2006) Effects of the presence of ColE1 plasmid DNA in Escherichia coli on the host cell metabolism. *Microb Cell Fact* **5**, 34. doi:10.1186/1475-2859-5-34.

Warner, J. B., Krom, B. P., Magni, C., Konings, W. I. L. N., Lolkema, J. S., Al, W. E. T. & Acteriol, J. B. (2000). Catabolite Repression and Induction of the Mg 2ℯ -Citrate Transporter CitM of *Bacillus subtilis*. *Society* **182**, 6099-6105.

Weissenborn, D. L., Wittekindt, N., Larson, T.J. (1992). Structure and regulation of the *glp*FK operon encoding glycerol diffusion facilitator and glycerol kinase of *Escherichia coli* K-12. J *Biol Chem* **267**:6122–6131.

Weitzman, P. D. J. (1981). *Ad*V. *Microbiol. Physiol.* ***22***, 185-244.

Weitzman, P. D. J., and M. W. Danson. (1976). Citrate synthase. *Curr. Top. Cell. Regul.* **10**, 161-204.

Wendisch,, V. F. et al. (2006). Metabolic engineering of Escherichia coli and Corynebacterium glutamicum for biotechnological production of organic acids and amino acids. *Curr. Opin. Microbiol.* **9**, 268–274.

Williams, S. G., Greenwood, J. A. and Jones, C. W. (1996). Physiological and biochemical changes accompanying the loss of mucoidy by *Pseudomonas aeruginosa*. *Microbiol.* **142,** 881-888.

Wittmann, C. (2010). Analysis and Engineering of Metabolic Pathway Fluxes in *Corynebacterium glutamicum*. 21-49, doi:10.1007/10.

Wittmann, C. (2010). Analysis and Engineering of Metabolic Pathway Fluxes in Corynebacterium glutamicum 21–49.

Wood, H.G. and Utter, M.F. (1965). The role of CO2 fixation in metabolism. *Essays Biochem*. **1**, 1–27.

Xia, X. X., Qian, Z. G., Ki, C. S., Park, Y. H., Kaplan, D. L. and Lee, S. Y. (2010). Native-sized recombinant spider silk protein produced in metabolically engineered *Escherichia coli* results in a strong fiber. *Proc Natl Acad Sci* U S A **107**, 14059-14063.

Yadav, V. G., de Mey, M., Lim, C. G., Ajikumar, P. K. and Stephanopoulos, G. (2012). The future of metabolic engineering and synthetic biology: towards a systematic practice. *Metab Eng*. **14**(3), 233-41.

Yamamoto, H. & Murata, M. (2000). The CitST two-component system regulates the expression of the Mg-citrate transporter in Bacillus subtilis. *Molecular Microbiology* **37**, 898-912.

Yang, J., Kloepper, J. W. & Ryu, C.-min. **(2010).** Rhizosphere bacteria help plants tolerate abiotic stress. *Trends in Plant Science* 1-4.

Yang, X. Y., Yang, J. L., Zhou, Y., Pineros, M., Kochian, L. V., Li, G. X., Zheng, S. J**. (2011).** A de novo synthesis citrate transporter, VuMATE, implicates in Al-activated citrate efflux in rice bean (*Vigna umbellata*) root apex. *Plant Cell and.*

Yanping, Zhang., Yan, Zhu., Yang, Zhu. and Yin, Li.The (2009). Importance of engineering physiological functionality into microbes. *Trends in Biotechnology* **27**(12), 664-672, doi:10.1016/j.tibtech.2009.08.006.

Young, E. and Alper, H. (2010). Synthetic biology: tools to design, build, and optimize cellular processes. *J. Biomed. Biotechnol*. **2010**, 130-781.

Yu, C., Cao, Y., Zou, H. and Xian, M. (2011). Metabolic engineering of *Escherichia coli* for biotechnological production of high-value organic acids and alcohols. *Appl Microbiol Biotechnol* **89**,573–583.

Zaldivar, J., Nielsen, J. and Olsson, L. (2001). Fuel ethanol production from lignocellulose: a challenge for metabolic engineering and process integration. *Appl Microbiol Biotechnol* **56**, 17–34.

Zastrow, M. L., Peacock, A. F. A., Stuckey, J. A. and Pecoraro, V. L. (2012). Hydrolytic catalysis and structural stabilization in a designed metalloprotein. *Nat. Chem*. **4**, 118–123**.**

Zhang, F., Rodriguez, S. and Keasling, J. D. (2011). Metabolic engineering of microbial pathways for advanced biofuels production. *Curr Opin Biotechnol* **22**, 775-783.

Zhu, Y., Chen, X., Chen, T., Shi and S,. Zhao, X. (2006). Over-expression of glucose dehydrogenase improves cell growth and riboflavin production in *Bacillus subtilis*. *Biotechnol Lett*, **28**, 1667–1672.

APPENDIX

Two factorial completely randomized design (CRD) analysis

Set No 7.1: No of nodules/plant

```
      ************************************
      *    ANALYSIS OF VARIANCE TABLE    *
      ************************************

-------------------------------------------------------------------------
Source        D.F.       S.S.      M.S.         F-cal      Significance.
-------------------------------------------------------------------------
Factor A       5        113.07       22.61        17.90       .00000
Factor B       4        679.15       169.79       134.42      .00000
Factor A X B   20       109.96       5.50         4.35        .00000
Error          60       75.79        1.26
-------------------------------------------------------------------------
Total          89       977.97
-------------------------------------------------------------------------

      ******************************************
      * T W O   W A Y   M E A N   T A B L E *
      ******************************************

-------------------------------------------------------------------------
Factors      B( 1 )     B( 2 )     B( 3 )     B( 4 )     B( 5 )
         Mean for A
-------------------------------------------------------------------------
A( 1 )        6.000     10.000     10.000     13.000     16.000
            11.000
A( 2 )        6.000     10.000      8.000     10.000     11.000
             9.000
A( 3 )        6.000     10.000     11.000     14.000     14.000
            11.000
```

A(4) 6.000 10.000 10.000 9.283 12.000
9.457
A(5) 6.000 10.000 9.000 12.000 14.000
10.200
A(6) 6.000 10.000 12.000 16.000 18.000
12.400

Mean for B 6.000 10.000 10.000 12.381 14.167

****
* TABLES OF SEM, SED, AND C.D. *
****

Factors	C.D.	SE(d)	SE(m)
Factor (A)	0.8211	0.4104	0.2902
Factor (B)	0.7495	0.3746	0.2649
Factor (A X B)	1.836	0.9176	0.6489

Set No 7.2. Nodule dry wt. mg/plant

****
* ANALYSIS OF VARIANCE TABLE *
****

Source	D.F.	S.S.	M.S.	F-cal	Significance.
Factor A	5	1035.85	207.17	15.27	.00000
Factor B	4	6609.45	1652.36	121.78	.00000
Factor A X B	20	1098.95	54.95	4.05	.00001
Error	60	814.12	13.57		

Total 89 9558.36

****

* TWO WAY MEAN TABLE *

****

Factors B(1) B(2) B(3) B(4) B(5)
Mean for A

A(1) 17.500 29.000 30.320 46.000 49.000
34.364

A(2) 17.500 29.000 23.320 31.260 33.345
26.885

A(3) 17.500 29.000 32.342 41.420 42.448
32.542

A(4) 17.500 29.000 31.080 25.950 36.384
27.983

A(5) 17.500 29.000 27.288 35.990 42.060
30.368

A(6) 17.500 29.000 36.920 47.000 52.000
36.484

Mean for B 17.500 29.000 30.212 37.937 42.540

****

* TABLES OF SEM, SED, AND C.D. *

****

Factors C.D. SE(d) SE(m)

Factor (A) 2.6911 1.3450 0.9511

Factor (B) 2.4566 1.2279 0.8682

Factor (A X B) 6.017 3.0076 2.1267

Set No 7. 3 No. of leaves/plant

****

* ANALYSIS OF VARIANCE TABLE *

****

Source D.F. S.S. M.S. F-cal Significance.

Factor A 5 63.09 12.62 3.81 .00458

Factor B 4 1367.81 341.95 103.35 .00000

Factor A X B 20 102.61 5.13 1.55 .09765

Error 60 198.52 3.31

Total 89 1732.04

****

* T W O W A Y M E A N T A B L E *

****

Factors B(1) B(2) B(3) B(4) B(5)

Mean for A

A(1) 9.000 19.000 15.000 19.000 20.000

16.400

A(2) 9.000 19.000 14.000 18.000 18.000

15.600

A(3) 9.000 19.000 16.000 20.000 20.000

16.800

A(4) 9.000 19.000 15.000 13.950 20.000

15.390

A(5) 9.000 19.000 11.000 17.000 18.000

14.800

A(6) 9.000 19.000 17.000 20.000 21.000

17.200

Mean for B 9.000 19.000 14.667 17.992 19.500

****

* TABLES OF SEM, SED, AND C.D. *

****

Factors	C.D.	SE(d)	SE(m)
Factor (A)	1.3289	0.6642	0.4697
Factor (B)	1.2131	0.6063	0.4287
Factor (A X B)	N.S.	1.4852	1.0502

Set No 7. 4 Root length (cm)

****

* ANALYSIS OF VARIANCE TABLE *

****

Source	D.F.	S.S.	M.S.	F-cal	Significance.
Factor A	5	199.61	39.92	5.33	.00041
Factor B	4	3130.91	782.73	104.46	.00000
Factor A X B	20	296.86	14.84	1.98	.02194

Error 60 449.59 7.49

Total 89 4076.97

****

* T W O W A Y M E A N T A B L E *

****

Factors B(1) B(2) B(3) B(4) B(5)
Mean for A

A(1) 13.260 28.090 22.350 27.830 32.900
24.886

A(2) 13.260 28.090 21.620 26.340 26.290
23.120

A(3) 13.260 28.090 23.540 29.810 28.690
24.678

A(4) 13.260 28.090 21.280 19.897 29.132
22.332

A(5) 13.260 28.090 16.370 25.320 26.530
21.914

A(6) 13.260 28.090 24.950 31.250 32.840
26.078

Mean for B 13.260 28.090 21.685 26.741 29.397

****

* TABLES OF SEM, SED, AND C.D. *

****

Factors	C.D.	SE(d)	SE(m)
Factor (A)	1.9998	0.9995	0.7068
Factor (B)	1.8256	0.9125	0.6452
Factor (A X B)	4.472	2.2350	1.5804

Set No 7.5 Shoot length(cm)

****

* ANALYSIS OF VARIANCE TABLE *

****

Source	D.F.	S.S.	M.S.	F-cal	Significance.
Factor A	5	503.43	100.69	3.61	.00640
Factor B	4	10273.46	2568.36	92.07	.00000
Factor A X B	20	912.10	45.61	1.63	.07369
Error	60	1673.71	27.90		
Total	89	13362.70			

****

* T W O W A Y M E A N T A B L E *

****

Factors	B(1)	B(2)	B(3)	B(4)	B(5)	Mean for A
A(1)	24.750	52.250	41.250	52.250	55.000	45.100
A(2)	24.750	52.250	38.500	49.500	49.500	

42.900

A(3) 24.750 52.250 44.000 55.000 55.000
46.200

A(4) 24.750 52.250 41.250 36.117 55.000
41.873

A(5) 24.750 52.250 30.250 46.750 49.500
40.700

A(6) 24.750 52.250 46.750 55.000 57.750
47.300

Mean for B 24.750 52.250 40.333 49.103 53.625

****

* TABLES OF SEM, SED, AND C.D. *

****

Factors	C.D.	SE(d)	SE(m)
Factor (A)	3.8585	1.9286	1.3637
Factor (B)	3.5223	1.7605	1.2449
Factor (A X B)	N.S.	4.3124	3.0493

Set No 7. 6 Root dry wt. (g/plant)

****

* ANALYSIS OF VARIANCE TABLE *

****

Source	D.F.	S.S.	M.S.	F-cal	Significance.
Factor A	5	0.07	0.01	5.87	.00018
Factor B	4	1.02	0.26	102.37	.00000

Factor A X B 20 0.07 0.00 1.34 .19040

Error 60 0.15 0.00

Total 89 1.32

****

* TWO WAY MEAN TABLE *

****

Factors B(1) B(2) B(3) B(4) B(5)
Mean for A

A(1) 0.244 0.496 0.409 0.532 0.565
0.449

A(2) 0.244 0.496 0.369 0.484 0.520
0.423

A(3) 0.244 0.496 0.362 0.499 0.506
0.422

A(4) 0.244 0.496 0.350 0.499 0.469
0.412

A(5) 0.244 0.496 0.241 0.402 0.451
0.367

A(6) 0.244 0.496 0.376 0.540 0.612
0.454

Mean for B 0.244 0.496 0.351 0.493 0.521

****

* TABLES OF SEM, SED, AND C.D. *

****

Factors	C.D.	SE(d)	SE(m)
Factor (A)	0.0365	0.0183	0.0129
Factor (B)	0.0334	0.0167	0.0118
Factor (A X B)	N.S.	0.0408	0.0289

Set No 7. 7 Shoot dry wt.(g/plant)

****

* ANALYSIS OF VARIANCE TABLE *

****

Source	D.F.	S.S.	M.S.	F-cal	Significance.
Factor A	5	4.81	0.96	3.46	.00819
Factor B	4	114.98	28.75	103.29	.00000
Factor A X B	20	5.04	0.25	0.91	.58164
Error	60	16.70	0.28		
Total	89	141.53			

****

* T W O W A Y M E A N T A B L E *

****

Factors	B(1)	B(2)	B(3)	B(4)	B(5)	Mean for A
A(1)	2.574	5.434	4.290	5.434	5.720	4.690
A(2)	2.574	5.434	4.004	5.148	5.148	

4.462

A(3) 2.574 5.434 4.576 5.720 5.720

4.805

A(4) 2.574 5.434 4.290 4.906 5.720

4.585

A(5) 2.574 5.434 3.146 4.862 5.148

4.233

A(6) 2.574 5.434 4.991 5.720 6.006

4.945

Mean for B 2.574 5.434 4.216 5.298 5.577

****

* TABLES OF SEM, SED, AND C.D. *

****

Factors C.D. SE(d) SE(m)

Factor (A) 0.3854 0.1926 0.1362

Factor (B) 0.3518 0.1758 0.1243

Factor (A X B) N.S. 0.4307 0.3046

Set No 7.8 P content in root(%)

****

* ANALYSIS OF VARIANCE TABLE *

****

Source D.F. S.S. M.S. F-cal Significance.

Factor A 5 0.10 0.02 15.36 .00000

Factor B 4 1.32 0.33 250.83 .00000

Factor A X B 20 0.14 0.01 5.13 .00000

Error 60 0.08 0.00

Total 89 1.64

****

* TWO WAY MEAN TABLE *

****

Factors B(1) B(2) B(3) B(4) B(5)

Mean for A

A(1) 0.257 0.567 0.353 0.547 0.653

0.475

A(2) 0.257 0.567 0.370 0.500 0.467

0.432

A(3) 0.257 0.567 0.510 0.590 0.553

0.495

A(4) 0.257 0.567 0.420 0.597 0.560

0.480

A(5) 0.257 0.567 0.320 0.470 0.503

0.423

A(6) 0.257 0.567 0.513 0.597 0.660

0.519

Mean for B 0.257 0.567 0.414 0.550 0.566

****

* TABLES OF SEM, SED, AND C.D. *

****

Factors	C.D.	SE(d)	SE(m)
Factor (A)	0.0265	0.0133	0.0094
Factor (B)	0.0242	0.0121	0.0086
Factor (A X B)	0.059	0.0297	0.0210

Set No 7.9 P content in shoot(%)

****

* ANALYSIS OF VARIANCE TABLE *

****

Source	D.F.	S.S.	M.S.	F-cal	Significance.
Factor A	5	0.06	0.01	12.05	.00000
Factor B	4	1.06	0.26	283.13	.00000
Factor A X B	20	0.07	0.00	3.52	.00008
Error	60	0.06	0.00		
Total	89	1.23			

****

* T W O W A Y M E A N T A B L E *

****

Factors	B(1)	B(2)	B(3)	B(4)	B(5)	Mean for A
A(1)	0.410	0.690	0.509	0.660	0.702	0.594

A(2)	0.410	0.690	0.522	0.670	0.668
	0.592				
A(3)	0.410	0.690	0.565	0.630	0.696
	0.598				
A(4)	0.410	0.690	0.525	0.565	0.675
	0.573				
A(5)	0.410	0.690	0.403	0.577	0.617
	0.539				
A(6)	0.410	0.690	0.570	0.667	0.763
	0.620				
Mean for B	0.410	0.690	0.516	0.628	0.687

****
* TABLES OF SEM, SED, AND C.D. *
****

Factors	C.D.	SE(d)	SE(m)
Factor (A)	0.0223	0.0112	0.0079
Factor (B)	0.0204	0.0102	0.0072
Factor (A X B)	0.050	0.0249	0.0176

Set No 7.10 Available P content in soil (mg kg^{-1} soil)

****
* ANALYSIS OF VARIANCE TABLE *
****

Source	D.F.	S.S.	M.S.	F-cal	Significance.

Factor A	5	12.64	2.53	20.66	.00000
Factor B	4	297.01	74.25	606.72	.00000
Factor A X B	20	15.73	0.79	6.43	.00000
Error	60	7.34	0.12		
Total	89	332.73			

****
* TWO WAY MEAN TABLE *
****

Factors	B(1)	B(2)	B(3)	B(4)	B(5)	Mean for A
A(1)	4.180	8.783	6.969	8.807	9.320	7.612
A(2)	4.179	8.783	6.502	8.323	8.322	7.222
A(3)	4.179	8.783	7.407	9.280	9.233	7.776
A(4)	4.179	8.783	6.922	7.280	9.272	7.287
A(5)	4.179	8.783	5.099	7.886	8.325	6.855
A(6)	4.179	8.783	7.847	9.299	9.776	7.977
Mean for B	4.179	8.783	6.791	8.479	9.041	

****

* TABLES OF SEM, SED, AND C.D. *

****

Factors	C.D.	SE(d)	SE(m)
Factor (A)	0.2556	0.1277	0.0903
Factor (B)	0.2333	0.1166	0.0825
Factor (A X B)	0.571	0.2856	0.2020

Set No 7.11 SOD(units g^{-1} protein)

****

* ANALYSIS OF VARIANCE TABLE *

****

Source	D.F.	S.S.	M.S.	F-cal	Significance.
Factor A	5	76.05	15.21	226.62	.00000
Factor B	4	140.47	35.12	523.22	.00000
Factor A X B	20	54.73	2.74	40.77	.00000
Error	60	4.03	0.07		
Total	89	275.29			

****

* T W O W A Y M E A N T A B L E *

****

Factors	B(1)	B(2)	B(3)	B(4)	B(5)
Mean for A					

A(1)	3.000	5.300	4.000	4.500	6.000
	4.560				
A(2)	3.000	5.300	4.410	5.477	6.300
	4.897				
A(3)	3.000	5.300	3.650	5.010	5.200
	4.432				
A(4)	3.000	5.300	3.200	3.633	5.700
	4.167				
A(5)	3.000	5.300	6.000	6.333	8.000
	5.727				
A(6)	3.000	5.300	7.800	8.100	10.000
	6.840				

Mean for B	3.000	5.300	4.843	5.509	6.867

****

* TABLES OF SEM, SED, AND C.D. *

****

Factors	C.D.	SE(d)	SE(m)
Factor (A)	0.1893	0.0946	0.0669
Factor (B)	0.1728	0.0864	0.0611
Factor (A X B)	0.423	0.2115	0.1496

Set No 7.12 CAT(µ mol H_2O_2 min^{-1} g^{-1} protein)

****

* ANALYSIS OF VARIANCE TABLE *

****

Source D.F. S.S. M.S. F-cal Significance.

Factor A 5 68.33 13.67 30.54 .00000

Factor B 4 201.25 50.31 112.42 .00000

Factor A X B 20 50.26 2.51 5.61 .00000

Error 60 26.85 0.45

Total 89 346.69

****

* TWO WAY MEAN TABLE *

****

Factors B(1) B(2) B(3) B(4) B(5)

Mean for A

A(1) 11.000 12.000 12.500 13.000 14.000

12.500

A(2) 11.000 12.000 13.167 13.300 13.900

12.673

A(3) 11.000 12.000 12.100 13.600 15.000

12.740

A(4) 11.000 12.000 11.900 12.400 14.200

12.300

A(5) 11.000 12.000 14.400 15.263 16.300

13.793

A(6) 11.000 12.000 15.900 16.920 18.000

14.764

Mean for B 11.000 12.000 13.328 14.081 15.233

****

* TABLES OF SEM, SED, AND C.D. *

****

Factors	C.D.	SE(d)	SE(m)
Factor (A)	0.4887	0.2443	0.1727
Factor (B)	0.4461	0.2230	0.1577
Factor (A X B)	1.093	0.5462	0.3862

Set No 7.13 APX(µmole ascorbate min^{-1} g^{-1} protein)

****

* ANALYSIS OF VARIANCE TABLE *

****

Source	D.F.	S.S.	M.S.	F-cal	Significance.
Factor A	5	62.79	12.56	43.11	.00000
Factor B	4	50.13	12.53	43.03	.00000
Factor A X B	20	47.91	2.40	8.22	.00000
Error	60	17.48	0.29		
Total	89	178.30			

****

* T W O W A Y M E A N T A B L E *

****

Factors	B(1)	B(2)	B(3)	B(4)	B(5)	Mean for A
A(1)	8.000	8.533	7.607	9.113	8.800	8.411
A(2)	8.000	8.533	7.550	8.883	7.800	8.153
A(3)	8.000	8.533	7.200	9.530	8.900	8.433
A(4)	8.000	8.533	8.067	8.300	8.900	8.360
A(5)	8.000	8.533	9.460	11.477	10.800	9.654
A(6)	8.000	8.533	10.867	12.900	11.800	10.420
Mean for B	8.000	8.533	8.458	10.034	9.500	

****
* TABLES OF SEM, SED, AND C.D. *
****

Factors	C.D.	SE(d)	SE(m)
Factor (A)	0.3943	0.1971	0.1393
Factor (B)	0.3599	0.1799	0.1272
Factor (A X B)	0.882	0.4406	0.3116

Set No 7.14 GPOX(µmole guaiacol min^{-1} g^{-1} protein)

****

* ANALYSIS OF VARIANCE TABLE *

****

Source	D.F.	S.S.	M.S.	F-cal	Significance.
Factor A	5	61.37	12.27	11.37	.00000
Factor B	4	843.09	210.77	195.23	.00000
Factor A X B	20	62.86	3.14	2.91	.00073
Error	60	64.78	1.08		
Total	89	1032.09			

****

* T W O W A Y M E A N T A B L E *

****

Factors	B(1)	B(2)	B(3)	B(4)	B(5)	Mean for A
A(1)	48.000	52.000	52.333	55.000	54.000	52.267
A(2)	48.000	52.000	54.600	55.600	55.000	53.040
A(3)	48.000	52.000	52.700	57.200	56.000	53.180
A(4)	48.000	52.000	53.333	56.333	52.800	52.493
A(5)	48.000	52.000	55.000	58.000	56.000	53.800

A(6) 48.000 52.000 56.800 58.667 58.200
54.733

Mean for B 48.000 52.000 54.128 56.800 55.333

****
* TABLES OF SEM, SED, AND C.D. *
****

Factors	C.D.	SE(d)	SE(m)
Factor (A)	0.7591	0.3794	0.2683
Factor (B)	0.6929	0.3463	0.2449
Factor (A X B)	1.697	0.8484	0.5999

Set No 7.15 Acid Phosphatase(mmoles p-nitrophenol g^{-1} protein)

****
* ANALYSIS OF VARIANCE TABLE *
****

Source	D.F.	S.S.	M.S.	F-cal	Significance.
Factor A	5	1.27	0.25	253426.00	.00000
Factor B	4	47.51	11.88	11877760.00	.00000
Factor A X B	20	5.14	0.26	257206.00	.00000
Error	60	0.00	0.00		
Total	89	53.92			

****

* T W O W A Y M E A N T A B L E *

****

Factors	B(1)	B(2)	B(3)	B(4)	B(5)	Mean for A
A(1)	1.320	1.980	1.200	2.600	3.680	2.156
A(2)	1.320	1.980	1.200	2.650	3.160	2.062
A(3)	1.320	1.980	1.180	2.580	2.050	1.822
A(4)	1.320	1.980	1.180	2.610	2.810	1.980
A(5)	1.320	1.980	1.170	2.770	2.790	2.006
A(6)	1.320	1.980	1.150	2.620	3.810	2.176
Mean for B	1.320	1.980	1.180	2.638	3.050	

****

* TABLES OF SEM, SED, AND C.D. *

****

Factors	C.D.	SE(d)	SE(m)
Factor (A)	0.0007	0.0004	0.0003
Factor (B)	0.0007	0.0003	0.0002

Factor (A X B) 0.002 0.0008 0.0006

Set No 7.16 NR(µg nitrite min^{-1} g^{-1} protein)

****

* ANALYSIS OF VARIANCE TABLE *

****

Source D.F. S.S. M.S. F-cal Significance.

Factor A 5 103.14 20.63 112.00 .00000

Factor B 4 394.88 98.72 536.00 .00000

Factor A X B 20 74.23 3.71 20.15 .00000

Error 60 11.05 0.18

Total 89 583.31

****

* TWO WAY MEAN TABLE *

****

Factors B(1) B(2) B(3) B(4) B(5)

Mean for A

A(1) 2.000 6.000 3.660 5.013 8.080

4.951

A(2) 2.000 6.000 3.837 5.117 7.800

4.951

A(3) 2.000 6.000 3.963 5.060 8.280

5.061

A(4)	2.000	6.000	2.910	3.683	5.110
	3.941				
A(5)	2.000	6.000	6.140	7.357	9.900
	6.279				
A(6)	2.000	6.000	7.870	8.823	11.600
	7.259				
Mean for B	2.000	6.000	4.730	5.842	8.462

****

* TABLES OF SEM, SED, AND C.D. *

****

Factors	C.D.	SE(d)	SE(m)
Factor (A)	0.3135	0.1567	0.1108
Factor (B)	0.2862	0.1431	0.1012
Factor (A X B)	0.701	0.3504	0.2478


POSTERS

List of poster presented

Presented a poster in the first Asian PGPR congress held at Hyderabad, India jointly organized by ANGRAU, Hyderabad and Auburn University USA. 21-24 June, 2009.